University of Nottingham

UK | CHINA | MALAYSIA

Development and application of an enhanced lipidomic profiling methods using stable isotope-assisted LC-MS

Malak Ahmad Jaber; MSc

Thesis submitted to the University of Nottingham for the degree of Doctor of philosophy in Pharmacy

September 2019

Abstract

Quantification is a critical step in comprehensive lipidomics studies. Although LC-MS is considered as an available tool for simultaneous detection and quantification of hundreds or thousands of lipid species, the analysed samples are subjected to unwanted variations at multiple stages, including study design, sampling and storage procedures, analytical and data acquisition procedures, that could affect the quality of the results. For targeted lipidomics analysis, these errors can be corrected by the appropriate use of standards. However, for untargeted analysis, it is still problematic to correct the data especially across multiple batches where usually many thousands of closely related lipid species need to be measured in a complex biological matrix.

In this thesis, an approach has been investigated for the first time to correct these variations by adapting an existing normalisation strategy routinely applied in targeted analysis based on standards to untargeted lipidomics studies. Although the cost and availability of authentic synthesised standards limits the practical usefulness of this approach, an alternative *in vivo* isotopic labelling strategy was evaluated. The aim was to present an approach that allows correcting variations introduced during the study and eventually provide a more reliable estimate of lipids in the studied samples.

To find out the source for the generation of labelled standards in complex samples, five different microorganism species were investigated and compared including *E. coli* MG1655, spirulina, *S. cerevisiae* CEN.PK 1137D, *S. cerevisiae* BY4741, and *P. pastoris* NCYC 175. Comparison of the lipid profiles and the efficacy of *in vivo* labelling strategy in these species according to the results revealed that the yeast *P. pastoris* NCYC 175 proved to be the optimum source of isotopically labelled standards leading the way to comprehensive direct and indirect normalisation in quantitative mass spectrometry assays in complex biological samples. After that, the optimum ^{13}C-IS mixture was utilised to develop and validate a novel normalisation approach for untargeted lipidomics studies on plasma samples. An extraction protocol was optimised to ensure maximum efficacy and sensitivity that enabled detection of a higher number of ^{13}C-IS in a reproducible manner. Then, the ^{13}C-IS mixture was used

as an internal standard introduced at the initial stages of samples preparation. From the data presented, the labelled internal standard mixture has shown to be effective in reducing technical and analytical variations introduced during samples preparation, analysis and special situations where the mass spectrometry response starts to fluctuate such as in long analysis time or from day to day that ultimately provides a reliable estimate of those ions.

Subsequently, the developed method was successfully applied to two clinical lipidomic studies. Where for the first one, the method was used to explore the level of intra-tumoral heterogeneity in patients diagnosed with low grade glioma and the results showed a clear distinct lipidomic profile in spatially resolved regions of the tumour and between patients indicating inter- and intra-tumoral heterogeneity that could affect treatment output, survival and quality of life before and after treatment. This highlight the importance of personalised tumour-specific strategies to accommodate these variations. In the second application, the method was applied to study the lipidomic signatures associated in patients diagnosed with diabetes mellitus and to study the effect of an oral supplement of L-carnitine on plasma lipidomic profile on T2DM patients. In conclusion, the developed method highlights the benefit of *in vivo* labelling strategy in the generation of a versatile number of labelled standards that can be used to correct data in untargeted lipidomics efficiently.

Acknowledge

Undertaking this PhD has been a truly life-changing experience for me and it would not have been possible to do without the support and guidance that I received from many people. I wish to convey special acknowledgments to many people for their help in this research. Firstly, I would like to record my gratitude to Dr Dong-hyun Kim and Prof David Barrett for their supervision, help, advice, guidance and patience throughout my PhD program.

I would also like to express my deep and sincere gratitude to Dr Catherine Ortori and Dr Salah Abdelraziq for their advice, supervision, and practical assistance, in particular with the mass spectrometers, data analysis and sample preparation. I wish to thank all members of the Centre for Analytical Biosciences for their help, support, knowledge and warm welcome.

Also I would tank all my friends in Nottingham for being of great support and making life in Nottingham somehow delightful, easy and memorable. I would like to say a heartfelt thank you to my mam, siblings, cousins and every member in my extended family for their continuous encouragement and invaluable support through all the ups and downs of this work.

As well, I would acknowledge my husband, who has been by my side throughout this PhD, living every single minute of it, and without whom, I would not have had the courage to start and finish this journey in the first place, and to my little girl for being such a good little baby and making it possible for me to complete what I started.

Finally, I wish to dedicate this work to my late father, who unfortunately didn't stay in this world long enough to see his daughter become a doctor.

Contents

List of Figures

List of Tables

List of Abbreviations

2-h PG	2-h plasma glucose
5-ALA	5-amino-levulivinic acid
AD	Alzheimer's disease
AGC	Automatic gain control
ATP	Adenosine triphosphate
CACT	Carnitine acylcarnitine translocase
CAD	Coronary artery disease
Cer	Ceramides
CerG1	Glucosylceramides
Ch	Cholesterol
ChE	Cholesteryl esters
CHO	Carbohydrate
CL	Cardiolipins
CNS	Central nervous system
CPT1	Carnitine palmitoyl transferase 1
CPT2	Carnitine palmitoyl transferase 2
CSCs	Cancer stem cells
CV	Coefficient of variation
DG	Diacylglycerols
dhCer	Dihydroceramide
D-IS	Deuterated internal standards
DM	Diabetes mellitus
dMePE	Dimethylphosphatidylethanolamines
ECMDB	*E. coli* metabolome database
EDTA	Ethylenediaminetetraacetic acid
ESI	Electrospray ionisation
FAHFA	Fatty acid esters of hydroxyl fatty acids
FAO	Fatty acid oxidation (FAO)
FDA	Fluorescein diacetate
FDR	False discovery rate
FFA	Free fatty acid
FPG	Fasting plasma glucose
FT-IR	Fourier transform-infrared spectroscopy
GC	Gas chromatography
GDM	Gestational diabetes mellitus
GLUT2	Glucose transporter 2
HbA1C	Haemoglobin A1C
HDL	High-density lipoprotein
HMDB	Human metabolome database
IDF	International diabetes federation

ILCNC	International lipid classification and nomenclature committee
IS	Internal standard
LC	Liquid chromatography
LDL	Low-density lipoprotein
LGG	Low grade glioma
LPA	Lysophosphatidic acids
LPC	Lysophosphatidylcholines
LPE	Lysophosphatidylethanolamines
MALDI	Matrix-assisted laser desorption ionisation
MG	Monoacylglycerols
MS	Mass spectrometry
NMR	Nuclear magnetic resonance
OAHFA	(O-acyl)-ω-hydroxy fatty acids
OGTT	Oral glucose tolerance test
PA	Phosphatidic acids
PAI-1	Plasminogen activator inhibitor type 1
PC	Phosphatidylcholines
PC(O)	Alkylphosphatidylcholine
PCA	Principal component analysis
PDC	Pyruvate dehydrogenase complex
PE	Phosphatidylethanolamines
PG	Phosphatidylglycerols
PI	Phosphatidylinositols
PrI	Propidium iodide
PS	Phosphatidylserines
QA	Quality assurance
QC	Quality control
QMC	Queen's medical centre
RPLC-MS	Reversed-phase liquid chromatography mass spectrometry
RT	Retention time
SM	Sphingomyelins
SO	Sphingosine
SUR1	Sulphonylurea receptor 1
T1DM	Type 1 diabetes mellitus
T2DM	Type 2 diabetes mellitus
TG	Triacylglycerols
TIC	Total ion count
UPLC/MS	Ultra performance liquid chromatography coupled to mass spectrometry
YMDB	Yeast metabolome database

Chapter One

Introduction

1. Introduction

1.1 Importance of lipids

Lipids are a diverse group of naturally existing molecules, including phospholipids, mono-, di- and tri-glycerides, fats, waxes, sterols and fat-soluble vitamins. In general, lipids are considered as amphipathic or hydrophobic small molecules that are produced partially or entirely by carbocation/carbanion-based condensations of isoprene/thioester units, respectively (1, 2). Lipids play several key roles in living organisms especially in energy storage, cellular membrane structure, endocrine actions and in cell signalling and transduction. For example, lipids play a critical role in cell function especially in the formation of the bilayer membrane that acts as a barrier between cells and the outside environment or between internal organelles from the cytoplasm, it is estimated that more than 50% of the mass of cell membranes is composed of lipids (3-5). This lipid barrier helps in maintaining an electrochemical gradient across the membrane and any alteration to its composition will greatly affect its function. For example, the addition of shorter and/or unsaturated fatty acid chains affect the ability of membrane lipids to pack against each other which render the membrane more permeable (4, 6). In addition, lipids play an important role in intracellular membrane transport by the generation of positive or negative curvature. Positive curvature of lipid monolayer is defined by a bulge in the direction of the polar heads and negative curvature is defined by a bulge in the opposite direction (7). Several mechanisms have been proposed to explain the generation of positive or negative curvatures including changes to the membrane lipid composition or by recruiting specialised proteins to the sites of fission and fusion

where lipid head groups serve as an attachment sites for peripheral membrane proteins which are necessary for curvature generation that affects several cell functions such as cell division and intracellular membrane trafficking (5, 8). Moreover, lipids are indispensable compounds in signal transduction between cells (9). Membrane and cytoplasmic lipids can serve as binding sites for cytoplasmic proteins and they can initiate a degradation process that gives rise to cleavage products that act as ligands or substrates for other signalling molecules. These lipids are highly regulated and have an impact on various physiological functions. For example, Ceramide and sphingosine promote apoptosis while sphingosine 1-phosphate stimulate cell growth and inhibit apoptosis. As a result, the role of sphingosine as a messenger of apoptosis is important (10). Many diseases result from aberrant communication between cells and thus the precise balance of signalling lipids and their effects can be employed to discover biomarkers of disease (10-13).

Identification of lipid-related markers in clinical research has the potential for tremendous impact on the diagnosis and prognosis of multiple comorbid conditions (14). It is documented that perturbations in lipid metabolism are associated with several human diseases including diabetes, cancer, atherosclerosis, Alzheimer's and others (15-17). For example, in patients with atherosclerosis, defects in cholesterol and lipid metabolism, especially in the low-density lipoprotein (LDL) receptor, induce a series of biological events that lead to accumulation of plasma lipoproteins in the bloodstream which promotes expression of chemokines and adhesion molecules that promote macrophage apoptosis and necrosis that eventually will provoke a series of cardiovascular events (15, 18-20). Therefore, total blood cholesterol level has been used in assessing the risk of high cholesterol level on the heart function (15). Also, it

was shown that acute elevation in free fatty acid levels in rodents induces muscle insulin resistance within few hours which is comparable to the one caused by prolonged high fat diet-induced insulin resistance which promotes diabetes development (17). In addition, it is believed that a misbalance in lipid levels is associated with the development of Alzheimer's disease (AD) where it was reported that a reduction in phospholipid levels was observed in brain tissues from patients with AD and this could be a result of decreased levels of the phospholipid precursors or/and an increase in phospholipid turnover and metabolism. This reduction in phospholipid level could influence cell viability by reducing stability and permeability of the membrane, which most likely results in cellular dysfunction or cellular death. Also, sphingolipids, which are believed to be abundant in the CNS, play an essential role in signal transmission and even small changes in their levels within the brain might interfere with the neurodegenerative processes including AD, Parkinson's disease and HIV-dementia (16, 21). In cancer research area, metabolic reprogramming is now established and documented in various tumours types (22). Tumour cells must efficiently generate energy and biomass components in order to expand and therefore these cells express flexibility in their metabolic phenotype in order to meet the high energy requirement needed for their growth, proliferation and to withstand harsh tumour environment (23). Since lipids play several key roles in cellular functions and their importance is well-documented in proliferation and growth of cancerous and noncancerous cells, several research groups have inspected lipid alterations in cancerous cells to explore the disease, stratify the patients, discover potential biomarkers and to set up therapeutic strategies through targeting the cancerous cell's lipid metabolism (23, 24). Therefore, monitoring lipid species

could provide a valuable information that could improve our understanding regards different pathological conditions and guide the treatment therapy plan more efficiently.

1.2 Lipid classification

In 2005, a comprehensive classification system for lipids was developed by the International Lipid Classification and Nomenclature Committee (ILCNC) which divides lipids into eight distinct categories (2, 25). Each category is further divided into classes and subclasses. Example for each group and its chemical structure is shown in Figure 1.1.

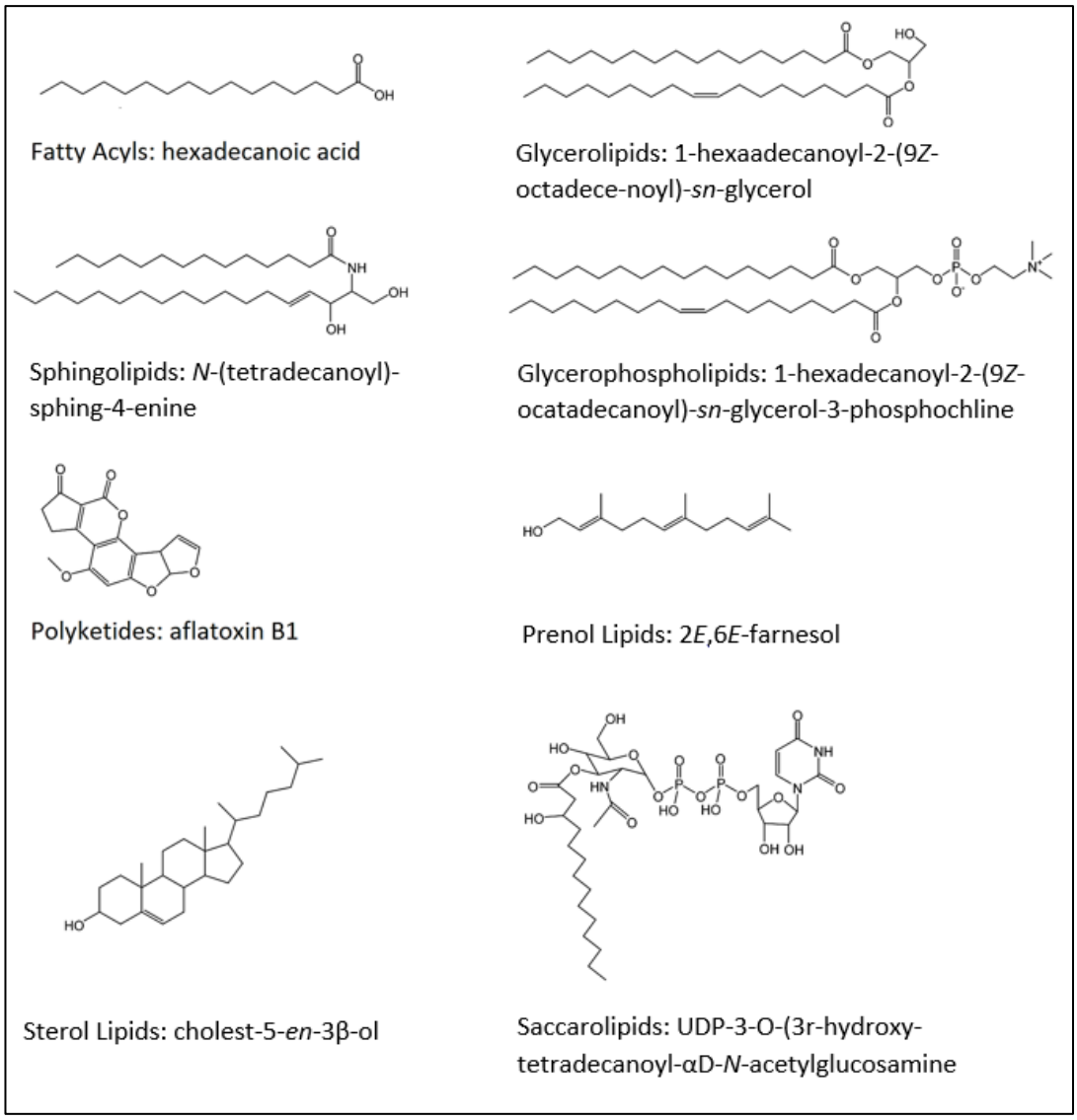

Figure 1.1:Representative structures for the eight lipid categories.

1.3 Lipidomics

The comprehensive examination of a living organism at the molecular level can be categorised into various fields known as the "Omics" cascade which is presented in Figure 1.2. The "Omics" cascade includes: genomics (study of the entire genome), transcriptomics (study of gene expression (mRNA)), proteomics (study of all the proteins expressed) and metabolomics (study of all the metabolites) which collectively help in understanding the biological and biochemical mechanisms in complex systems that occur in response to different perturbations (26).

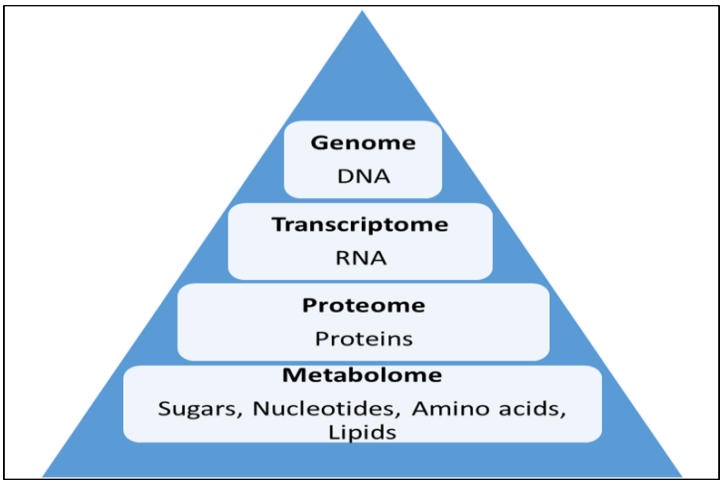

Figure 1.2: The flow of biological information where Lipidomics is considered as a subset within the field of metabolomics.

Metabolomics has been defined as the comprehensive analysis of all metabolites in a biological system (26, 27). Unfortunately, metabolites are much more chemically diverse compared to the 4-letter or the 20- letter codes for genes and proteins respectively (26). However, metabolomics has an advantage over other 'omics' approaches because it can provide a snapshot of cellular response to various perturbations including diseases, toxin exposure, genetic or environmental alterations which can correlate with phenotype (28).

Lipidomics involves the identification and quantification of a variety of lipids and their interaction with each other and it is considered as a subset of the metabolome field (29). Lipids are considered distinct from metabolites and they are treated differently from analytical point view having different physicochemical properties and therefore require different extraction solvents (30). This is because metabolites are distributed over a large range of lipophilicity and hydrophilicity (~40 orders of magnitude on the octanol/water coefficient scale), as is shown in Figure 1.3, and to enhance the extraction efficacy for a wide range of metabolites including polar and nonpolar metabolites, this requires the use of two different extraction step and/or the use of

mixture of extraction solvent (31). Also, within the lipids group itself, the choice of the best extraction solvent depends on the polarity of the lipids to be studied (32). For example, polar lipids (e.g. glycolipids) are more soluble in polar solvents while non-polar lipids (e.g. triacylglycerols) are more soluble in non-polar solvents. Different polarities of various lipid species make it difficult to extract the whole lipidome from biological samples using a single solvent system. In addition, these components are dynamic and present in a wide concentration ranges in the same sample/organism (33, 34). Therefore, suitable combination of organic solvents is essential for lipid analysis.

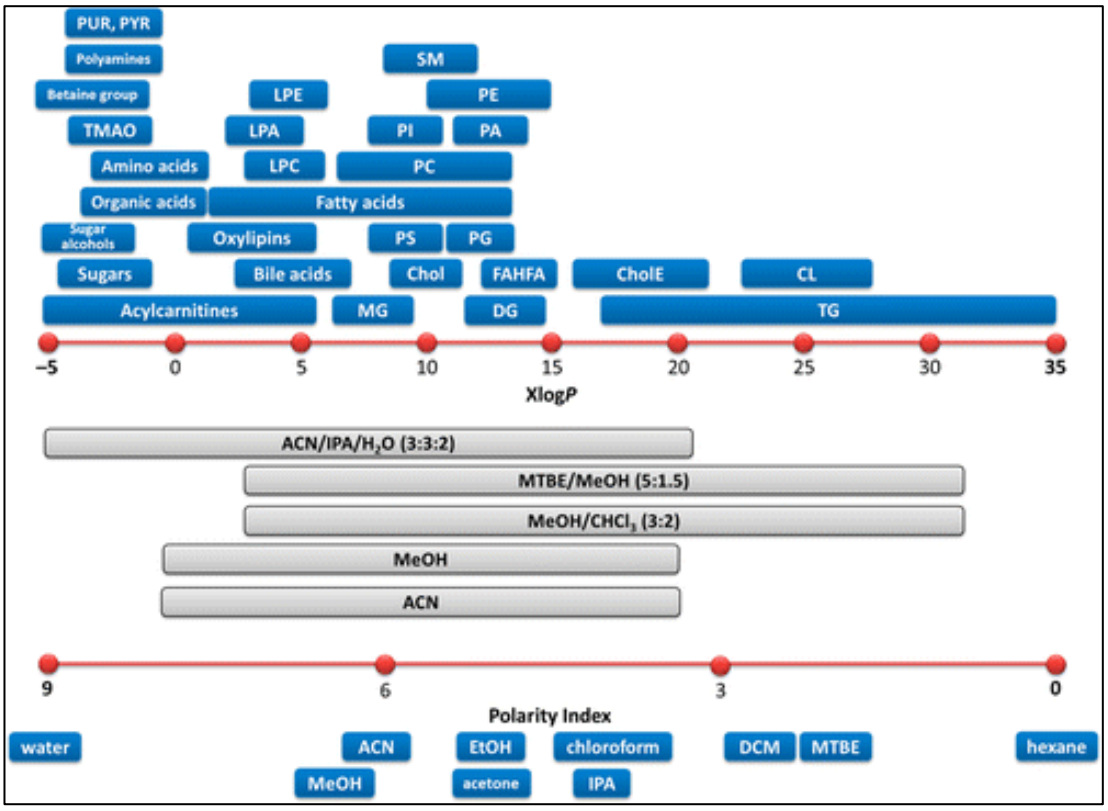

Figure 1.3: Predicted octanol/water partition coefficient (X log P) range of common metabolites in blood plasma and polarity index of different solvents used for sample extraction (31). Legend: Cer, ceramides; Chol, cholesterol; CholE, cholesteryl esters; CL, cardiolipins; DG, diacylglycerols; FAHFA, fatty acid esters of hydroxyl fatty acids; LPA, lysophosphatidic acids; LPC, lysophosphatidylcholines; LPE, lysophosphatidylethanolamines; MG, monoacylglycerols; PA, phosphatidic acids; PC, phosphatidylcholines; PE, phosphatidylethanolamines; PG, phosphatidylglycerols; PI, phosphatidylinositols; PS, phosphatidylserines; PUR, purines; PYR, pyrimidines; SM, sphingomyelins; TG, triacylglycerols; TMAO, trimethylamine N-oxide; ACN, acetonitrile; IPA, isopropanol; H_2O, water; MTBE, methyl tert-butyl ether; MeOH, methanol; $CHCl_3$, chloroform; DCM, dichloromethane; EtOH, ethanol.

1.4 Technical developments in lipidomics

Numerous analytical techniques have been used in metabolomics applications including Fourier transform-infrared (FT-IR) spectroscopy, nuclear magnetic resonance (NMR) spectroscopy and mass spectrometry (MS) but none of these techniques can comprehensively analyse all lipids in a single analysis (26, 33). MS and NMR spectroscopy are two of the most successful techniques for determining the metabolic state of an organism (34). Each of these techniques has its own advantages and disadvantages. NMR is highly selective, reproducible, non-destructive and requires little or no sample preparation. However, NMR suffers from relatively low sensitivity compared to MS. The sensitivity of NMR measurements are within the 10^{-1}–10^{-3}M concentration range, and it could reach as low as 10^{-4}–10^{-5} M while MS is more sensitive to 10^{-18} M (35). However, recently the sensitivity of NMR has been increased greatly by measuring the samples at higher magnetic field strengths but at higher cost (36, 37).For example, increasing the magnetic field in NMR instruments from 7 to 23.5 T, this will enhance the sensitivity and extend the limit of detection from mM range down into the μM range(37). MS is not robust and reproducible as NMR yet, the high sensitivity of MS measurements and its ability to analyse a wide range of molecules due to lower background signals and peaks overlapping especially when coupled to GC or LC system, expand the use of MS in lipid analysis rapidly over the past few years (34, 38, 39).

Three complementary approaches are currently being used in metabolomics studies including lipidomics: targeted, untargeted and semi-targeted (33, 40, 41). The targeted approach is hypothesis-driven, which focuses on identifying and quantifying

a specific set of lipid molecules based on existing knowledge of a biological system whereas the untargeted approach has been used widely to perform global lipid profiling in a biological sample and to discover new biomarkers of disease and cell function. Semi-targeted approach act as an intermediate between the other two approaches, where few hundreds of metabolites are monitored. However, due to the diversity of lipids, lipidomics method development is a complex and challenging area. The development of soft ionisation techniques such as electrospray ionisation (ESI) and matrix-assisted laser desorption ionisation (MALDI) has significantly broadened the range of lipids that can be analysed by MS (42). In lipid analysis, ESI-MS is used more commonly than the other techniques, utilising two different approaches, the shotgun and the liquid chromatography (LC)-MS-approach (43). ESI, initially developed by Fenn in 1989, permits analysing large, non-volatile molecules straightway from the liquid phase without affecting the chemical structures of the analytes (44). The principle of the ESI process is shown in Figure 1.4. The sample enters the ion source of the MS via a capillary tube at normal pressure. Usually, a high voltage (2–5 kV) is applied to the capillary relative to the entrance of the mass spectrometer that provokes an electric gradient along which the charged droplets travel. As they transport, the solvent evaporates and the intensity of the charges as well as the Coulombic repulsion within the droplet increase, which result in dissociation of large droplets into smaller ones. This continues to happen until it ends up with charged individual molecules in the gaseous phase. Then they enter the mass spectrometry for separation and detection based on their mass-to-charge ratio (42, 45).

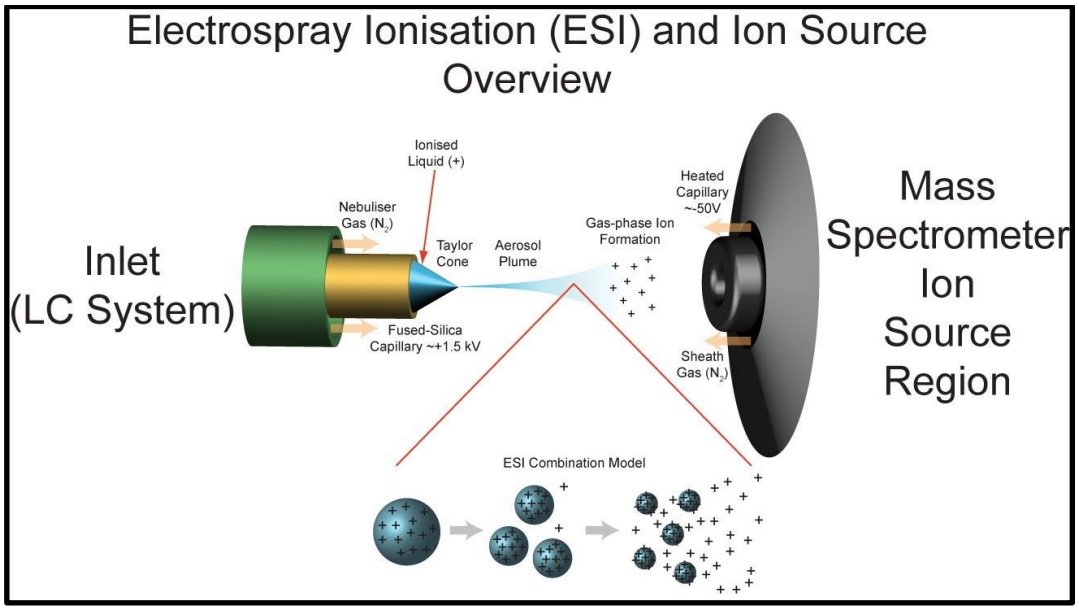

Figure 1.4: Electrospray ionisation mass spectrometry (46).

The ionisation efficiency in MS varies from one lipid class to another (47). For example phosphatidylcholine, lysophosphatidylcholine, phosphatidylethanolamine, and sphingomyelins are detected in positive mode while phosphatidylserine, phosphatidic acid, phosphatidylinositol, phosphatidylglycerol, free fatty acids, phosphatidylethanolamine, and eicosanoids are detected in negative mode (48). Therefore, both modes are required in order to analyse the diverse lipid groups simultaneously with high sensitivity (47). Neutral lipids (e.g., triacylglycerols) which are not easily ionised by ESI, can be seen in the positive mode as an ammonium, lithium, or sodium adducts (48).

The shotgun approach was introduced in 2003 by Han and Gross (45). In this approach, the lipid extract usually without prior purification steps is directly introduced into the MS system without prior separation. Although rapid and efficient analysis of lipid classes and subclasses with high reproducibility can be achieved directly from crude extracts which appropriate for high-throughput and large-scale

studies, overlaps (in term of their m/z) between different molecular species due to the absence of suitable separation methods hinders the identification and quantitation of low abundant species (49). Different separation methods can be used in congection with MS such as LC that can separating mixtures accordance to their physical and chemical propertiest through ravelling across a specific type of column at different rates, leading to different retention times for each compounant of the mixture (50). Moreover, ion suppression limits the use of this technology particularly when some lipid classes are predominant which result in ion suppression of low abundant lipid species (43). Ion suppression is one form of matrix effect that LC-MS suffer from that refer to reduced detector response, or signal:noise (S/N) which hamper thereproducibility and accuracy when measuring trace analytes in complex matrices, such as biological fluids (51, 52). Coupling a separation technology to the MS, like thin layer chromatography, gas or liquid chromatography helps in analysing a full range of phospholipids from a complex mixture which brings lipidomics to practice as well it increases the sensitivity and efficiency of the analysis (53). Combining liquid chromatography (LC) with MS could separate complex lipid extract into individual classes or based on their hydrophobicities, reducing the ion suppression of co-eluting compounds and matrix effects, which can assist in identification of isobaric lipid species where LC-MS based methods typically allow detection of 800–1000 lipids compared to 200–400 lipids using shotgun methods due to higher sensitivity and improved separation of isomeric and isobaric lipids. In addition, retention time based on an LC system provides valuable information for metabolite annotation and makes the identification and quantification more accurate (43, 54-56). However, LC-MS analysis of lipids raises some concerns (57).

First, although LC can reduce interferences and enrich low abundant ions, the high abundant ions will also be enhanced and possibly lead to form lipids aggregate of these ions and thus lose their ionisation efficacy (57). Second**,** introducing different mobile-phase compositions due to gradient elution could introduce variations in ionisation efficiency of lipid ions at different elution times during separation (57). Third, differential loss of lipids after chromatography might occur, which leads to an apparent enrichment in specific lipid species over the others (58). Fourth, the initial mobile phase gradient used in reversed-phase LC analysis can limit solubility of some lipid species that lead to differential apparent ionisation efficiency (57). Fifth, ion suppression or enhancement due to matrix effect can affect quality of the results (59). Lastly, during LC-MS analysis, the sample is subjected to multiple steps, including sample preparation, chromatographic separation, and MS analysis that could lead to experimental variations of different species of lipids in each step. These variations propagate during analysis and have huge influence on the results, especially in the analysis of large batches of samples which takes up to few days of continuous analysis. Therefore, these concerns must be addressed during the analysis.

1.5 Lipid identification

Identification of unknown lipids is still a challenge even with the current techniques, due to extreme complexity of lipid mixture and their structural diversity, including numerous isobaric and isomeric lipids. Lipid identification and the type of structural information per molecule can be achieved at different levels as shown in Figure 1.5.

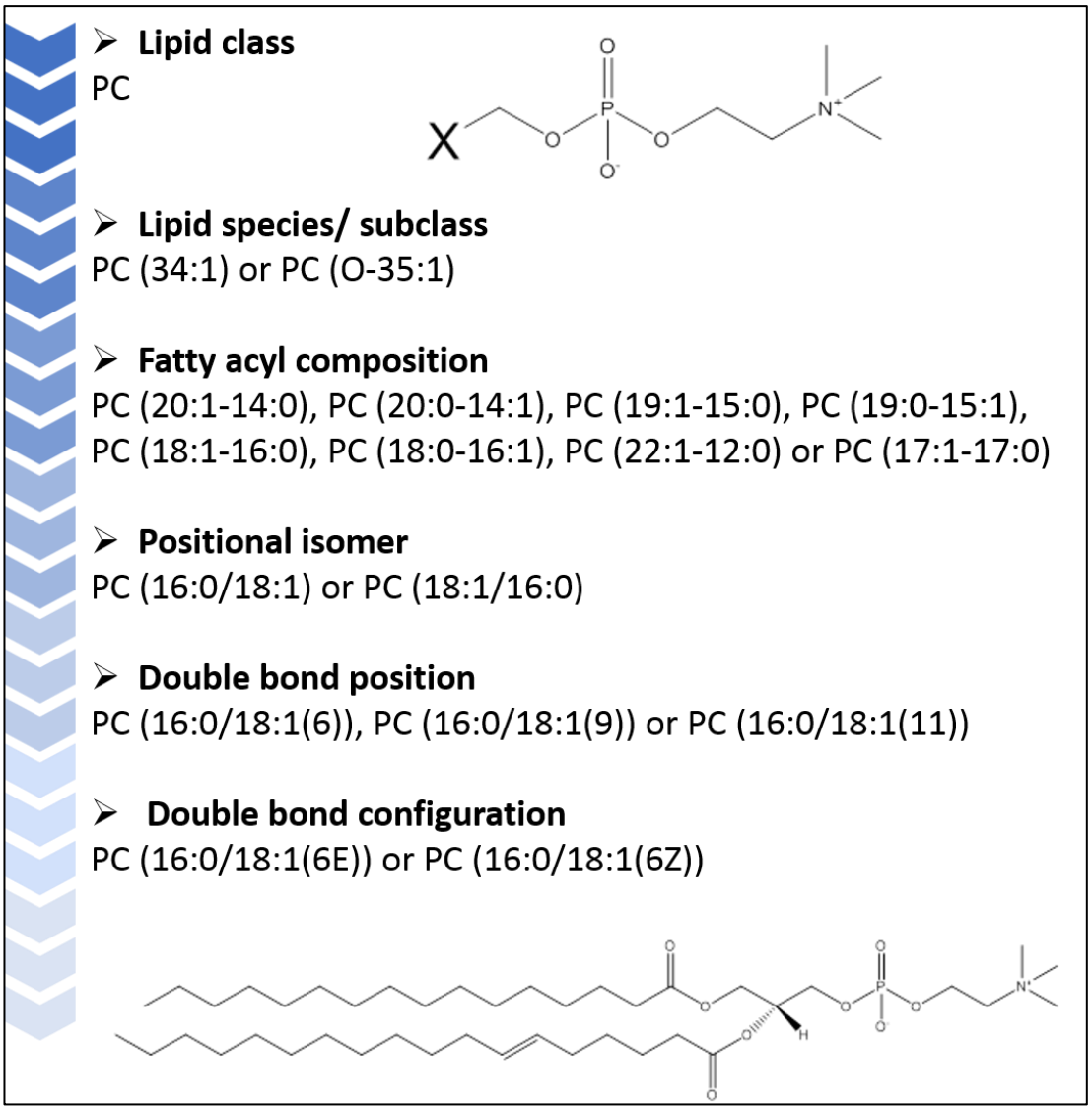

Figure 1.5: Different levels of lipid identification, exemplified by PC (16:0/18:1(6*E*)). More effort and more comprehensive and specific methods are necessary for full structural elucidation of lipid species and accurate identification. Abbriviations: PC: Phosphatidylcholine, The 'O-' prefix is used to indicate the presence of an alkyl ether substituent, The use of *E/Z* designations (as opposed to trans/cis) to define double-bond geometry.

Complete structural elucidation requires several levels of identification including lipid class, total number of carbon atoms and total number of double bonds, total number of carbon atoms and total number of double bonds per acyl chain, location of the double bond and location of each acyl chain in the lipid backbone (60). The main challenges in accurate lipid identification are the accurate fatty acyl composition and the positions of the double bonds which could be more functionally relevant (61). These ultimate desires are not possible by simple MS-only measurements or by using

conventional MS^2 based fragmentation methods. Also, they require the use of more sophisticated techniques such as ozone-induced dissociation, high-energy collision-induced dissociation or multistage fragmentation approaches (60, 62-64).

Researchers in the lipidomics field should not annotate features based on exact mass only as each *m/z* value can represent different lipids ions with different adducts, since the lipidome is diverse and enormous overlap in exact mass is expected between the species (65). Whereas unambiguous lipid identification is achieved only by matching retention time, full scan and product ion spectra with reference standards (66). Putative identification can be made without chemical reference, through matching the retention times (sometimes if the same method and instrument is used), full scan and product ion spectra of that specific peak with entries in different public/commercial spectral databases (67). However, in untargeted studies, manual annotation of all lipid species is unrealistic, therefore researchers usually relied on different software to annotate the lipid species (65). Different software has been developed either based on libraries of fragmentation pattern of experimentally determined or computationally generated (in silico) MS/MS spectrum such as LipidMatch (68), Lipid Data Analyzer (69) LipidBlast (70), LipidSearch (71) and LipidXplorer (72). Although these software decreased time and effort in lipidomic studies, most of them require few optimisation steps, also, to set few parameters in order to decrease the false-identification. Therefore, development of more advanced bioinformatics tools, improved algorithms for processing large-scale data, and more reliable structural annotation are vital to obtain more reliable and comprehensiveness lipid profiling of untargeted lipidomics studies.

1.6 Quantification of lipids

To a chemist, quantification must be very accurate with very limited uncertainty, while for a biochemist, the accuracy is relatively loose since many uncertainties in the analysis are unavoidably and some are inherent by the method of analysis (73). In LC-MS analysis, the goal of quantification is to measure the absolute or the relative abundance of the studied species in the sample of interest. Absolute quantification determines the mass levels of individual lipid species while relative quantification measures the pattern changes of lipid species in the sample (73). For absolute quantification, a calibration curve should be prepared and analysed simultaneously with the sample of interest under identical experimental conditions, whereas for large-scale targeted studies or untargeted studies this is not feasible. In addition, the major obstacle in metabolite quantification is that the metabolite's signal intensity is not linear in MS analysis and it depends on different factors; such as concentration, chemical structure and matrix (59, 74-77). Therefore, a normalisation method must be applied to correct these variations and to obtain a reliable result, where the quantity of the studied species is measured relative to an internal standard or to another relative metabolite or factor.

1.7 Research-practical considerations in lipidomics

1.7.1 Sample type, time and storage

It is estimated that up to 46% of laboratory errors arise due to errors in preanalytical stages (78). Therefore, standardisation and improvement of preanalytical process is a prerequisite in lipidomics. Different factors can affect the experimental design of clinical lipidomics studies (i.e. age, gender, exercise, diet, fasting state, general health

condition, sample time, storage and others) (56, 78-80). Some of the key factors, and their effects on lipid analysis are listed in Table 1.1. It is important that these factors are considered and addressed in both at early stages during experiment planning and at the interpretation of the results. Ideally, lipidomic studies should be conducted within relatively homogeneous groups to reduce the effect of these factors as much as possible to obtain accurate and reliable clinical results (56).

Table 1.1: Summary of some of the key factors and their effects on lipid analysis that should be considered at preanalytical stages in lipidomics studies.

factor	Remarks	Reference
Age	High level of TGs were found in elderly females.	(81)
Gender	Over 70% have been shown to be significantly associated with gender where ChE, TG, Cer, GM and LPC were higher in males while SM, THC and PS were higher in females.	(82, 83)
Diet	Large and variable effects. An increase in PUFAs level was observed upon healthy diet intake with whole grain products and fish. Cholesterol and LDL were significantly lower in vegetarians compared to omnivores. Cer, LPC and DG were decreased upon fatty fish uptake whereas ChE and long-chain TG were increased upon lean fish intake.	(84-87)
Exercise	Changes in metabolite profiles after 30 min cycling exercise that returned to the original profile after 2 h.	(88)
Sampling time	Large effect where it is estimated that 13% of lipids (mostly DGs and TGs) exhibited circadian oscillations around the late afternoon. Also, the metabolite concentrations had a higher variability after morning meal compared to the evening meal.	(89-93)
Anticoagulants	Large effect on most of the detected lipids. EDTA can introduce interfering peaks while citrate can mask endogenous analyte, therefore, the use of lithium heparin is recommended.	(28, 94)
Stability of the lipids	The LPCs levels increase significantly after storage of plasma for more than 24 h at room temperature.	(95, 96)
Freeze–thaw cycles	Maximum two cycles recommended. It is estimated that up to 37% variability were seen in HDL and LDL cholesterol level could result from a single freeze-thaw cycle.	(97)

Abbreviations: EDTA; ethylenediaminetetraacetic acid, LPC; lysophosphatidylcholine, GM; ganglioside, THC; trihexosylceramide, HDL; high-density lipoprotein cholesterol, LDL; low-density lipoprotein cholesterol,TGs: triacylglycerols, PUFAs; poly unsaturated fatty acids..

1.7.2 Sample preparation

Sample preparation has a key impact on the quality, as well as, the sample throughput in lipidomics (56). It is an important step to separate lipids of interest from other biological substances like proteins, sugars or other small molecules that may compromise the efficacy of the analysis. The ideal protocol implanted for sample preparation should be simple, reproducible, able to extract as much as possible of the lipids, able to remove protein efficiently, cheap and feasible, especially, for large scale studies (14). Liquid-liquid extraction is one of the most commonly used protocols for sample preparation. Protocol relies on the use of chloroform-methanol mixture such as Folch (98) and Bligh and Dyer (99) extraction methods have been widely applied in untargeted analysis of lipids. Several studies compared different sample preparation protocols, yet, the results have not always been consistent (100-102). Therefore, the selection of the protocol remains dependent on the physicochemical properties of the target lipids, the origin of the sample and its lipid composition. Thus, different protocols have been tailored towards extraction of specific groups of lipids for targeted analysis or modified global lipid extraction for specific samples (103, 104).

1.7.3 Quality control

Various instrumental variation in LC-MS analysis such as analytical drifts, alteration in ionisation efficiency and gradual changes in column performance in addition to others might arise, especially, in large scale studies. Therefore, in order to reduce bias and improve the reliability of the analysis, the samples are prepared and analysed in a random order. Moreover, different types of quality assurance (QA) and quality control (QC) samples are analysed together with the samples (14, 105, 106). Some of

the QA and QC samples are listed in Table 1.2. Although for targeted analysis a defined inclusion and exclusion criteria for such samples are defined but for untargeted analysis, there is no definitive recommendation currently agreed upon for all samples, and therefore these criteria used in a study usually should be reported in publications, and public data sources (105, 107).

Table 1.2: Quality assurance and quality control samples for lipidomic studies.

Sample	Use (why?)
Blank samples	Could reveal problems due to impurities in the solvents, contamination of the separations system or carryover contaminants. (blank signal greater than a predefined threshold, greater than a percentage of the average signal from the complete biological dataset or more than 20% of LLOQ due to carryover are removed from the analysis).
Solution of authentic chemical standards, not in a biological matrix.	To assess instrumental accuracy and precision. (the acceptance criteria for the used IS compared to the predefined parameters are: mass error of 5 ppm, RT error of < 2%, peak area equal to ± 10% of the predefined peak area and symmetrical peak shape).
Extraction blank	To remove signals derived from non-biological source during samples preparation. (blank signal greater than a predefined threshold, or greater than a percentage of the average signal from the complete biological dataset are removed from the analysis).
Pooled QC sample	To condition the analytical platform prior to analysis, to measure precision, to correct systematic measurement bias and in some cases to correct batch to batch variations. (an average of 5 to 10 injection of QC need to equilibrate the platform and in order to assess the precision of the measurement a total number of QC samples should be 5% of unknown samples or at least six samples per run whichever number is greater while higher number of QC injections needed to be acquired to correct variations within and between batches).
Internal standards added to each sample	To monitor systematic fluctuations over time during analysis.

1.7.4 Normalisation

LC-MS is a versatile technique that helps in identifying and quantifying analytes of interest in a biological matrix. However, the signal intensity of most of the detected species does not correspond to the concentration of the component in the sample. This is due to the large number of factors that can influence the absolute MS response, which are difficult to control including the ionisation technique and polarity, extraction technique, degradation of the analytes during sample preparation and others (108, 109). It is difficult to specify the exact reason for such an effect and normally the observed final effect is due to a combination of several factors (110-113). Therefore, the metabolomics/lipidomics data must be normalised before making any statistical interpretation or drawing any conclusions (114). The main objective of normalisation is to reduce systematic and random bias as much as possible so that only biologically relevant signals are present in the data. Sample normalisation can be either addressed before or after sample acquisition (114). In target analysis where relatively, few metabolites are monitored, errors introduced during samples preparation and analysis can only be controlled through the incorporation of IS into the analytical procedure or by calibration standards to eliminate such effects (115). However, for untargeted analysis where hundreds of metabolites are monitored or for untargeted analysis, the incorporation of such IS is problematic due to the limited availability of such representative IS, their high cost or when the identity of the analytes are unknown (116). Several other normalisation methods have been introduced in the literature and can be employed in lipidomic studies, however, selection of the most suitable normalisation method relies on several parameters (i.e. the nature of the biological sample, convenience, accuracy

of the normalisation method as well as the speed and the cost of performing the selected method). Though, some methods are generic while others are only viable to specific biological media such as normalising the urine samples to their creatinine level (117).

Two main approaches can be used for normalisation of a set of data; either the statistical models or the use of single or multiple standards (118). The statistical models normalise each sample by specific scaling factor such as the median, mean and sum of intensities of the entire chromatogram (total ion count (TIC)) or by the height or the peak area of the highest peak (118-120). This approach assumes that any increase in metabolites intensity is compensated by a decrease in others, and the mean/median of the intensity will be the same per sample. However, this is not true in practice, due to the sample nature itself and the fact that metabolites are largely affected by the environment and they do not have self-averaging property (121, 122). For example, the lipidomics profiles of two different mouse liver samples, obese model and a lean wild-type, were recorded using ultra performance liquid chromatography coupled to mass spectrometry (UPLC/MS), the results are shown in Figure 1.6. Similar levels of phospholipids were found in both types of mice, but the amount of triacylglycerols was increased in the obese mouse. If the data were normalised according to total ion signal this lead to a conclusion that the phospholipids level is decreased while the triacylglycerols level is slightly increased in obese mouse which is not correct (118).

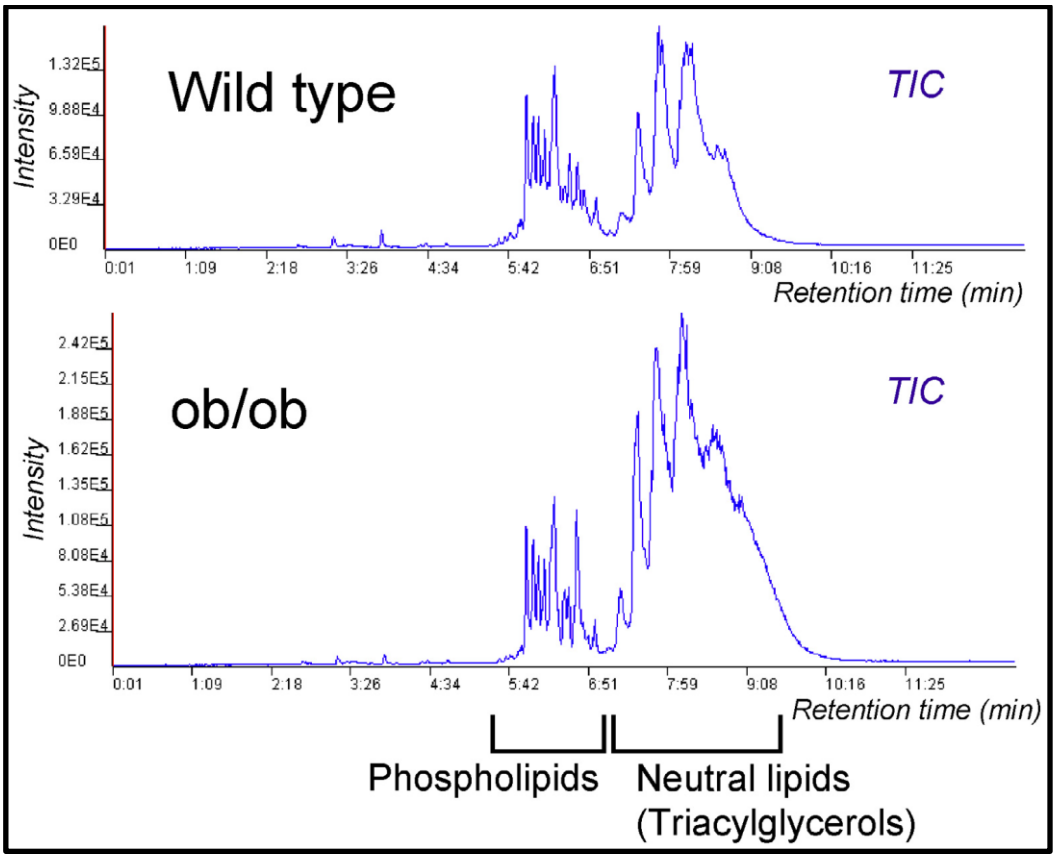

Figure 1.6: Total ion chromatograms from two different mouse phenotypes (118).

Others tried to correct or decrease specific types of systematic errors (i.e. metabolites degradation) or random errors due to inconsistency in LC and MS instrumentation during analysis, especially, in long run in untargeted analysis using different algorithms based on the pooled QC samples interspaced between the biological samples (28, 116). Such algorithms include linear regression (115), LOESS regression (28, 123), regularised cubic spline regression (124), support vector regression (125) and cluster-based regression (126). Also, if these QC samples were drawn from a single homogeneous source and were used across numerous batches, they can be used to correct batch-to-batch variations, where changes in day-to-day instrumental sensitivity can be often observed due to routine and annual maintenance of the instrument (see Figure 1.7) (107, 124).

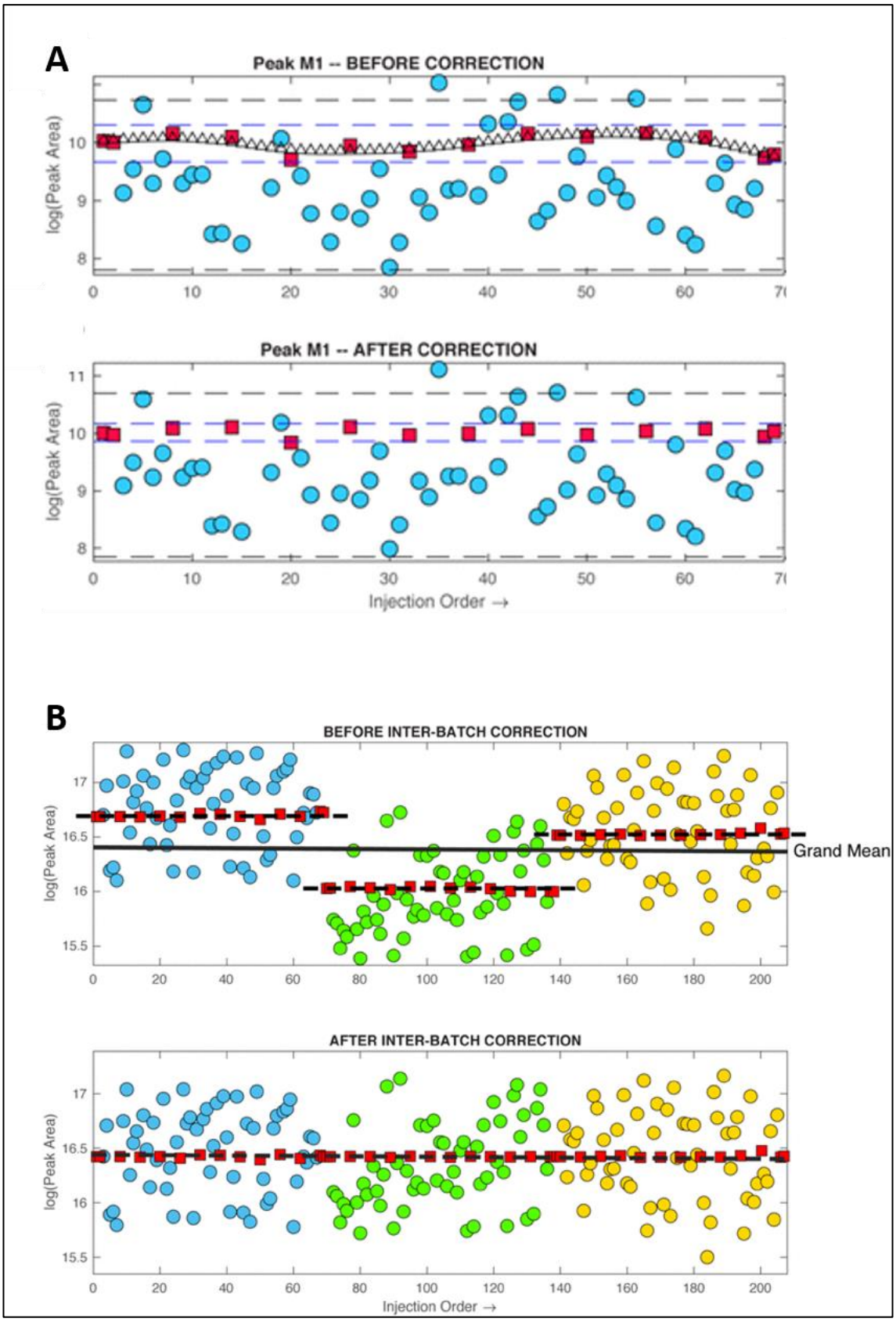

Figure 1.7: For a given metabolite, its measured response is a result of different level of systematic and random variation introduced can be corrected using QC samples (A), While pooled QC samples are used across multiple analytical batches then it is also possible to correct for batch-to-batch variations (B). Red squares are QC samples, blue, green and yellow circles are study samples from batches 1, 2, and 3, respectively (105).

Although each method has its own advantages and drawbacks, no single method is superior over the others. These methods require optimisation of one or more parameters that could determine the degree to which a regression curve fits to the non-linearity in the data and thus overfitting of these parameters could negatively impact the quality of the data (105). Furthermore, these methods require high number of QC samples to be analysed per batch in order to enhance method robustness which could be time consuming. In addition, some of these methods are computationally intensive methods that are not easy to perform and learn by other researcher (123). Most importantly, if one of these methods was applied, it is preferred to use pooled QC derived from the study samples in order to ensure that these QC samples and the used normalisation methods can effectively correct variations introduced during analysis in that specific same sample matrix and to include as much as possible of features (107). As variation introduced by matrix components not similar to the study samples may not represent variation introduced into the data acquired for that study samples and this will affect the normalisation output (107). Also, features were not detected in the QC samples cannot be assessed for repeatability and cannot be normalised by these methods, therefore, this will lead to a loss in the selected features that will be included in any further analysis and consequently loss in metabolic information (28). Likewise, if these QC samples were used for batch-to-batch correction, it is a must to use the same pooled QC samples across different analytical batches and that could be not feasible, especially in large scale studies (28). Furthermore, these methods are considered as post-data acquisition normalisation methods and they cannot correct any variations introduced during sample preparation (105).

1.7.5 Normalisation using labelled internal standards

In this approach data are normalised using standards with similar physicochemical properties of analytes of interest added before or after the extraction process. The lipid species that can be used as standards depend on the targeted species. If accurate quantification was the ultimate goal, a standard that have identical physio-chemo properties to the analytes is preferred as both of them will be subjected to an identical experimental condition starting from sample preparation to analysis (57). In addition, ideally no or very low (less than 1%) overlap between the standards and the endogenous species is a must in the analysis (57). Thus, the ideal internal standard to quantify an analyte of interest is its stable isotope-labelled analogue. Labelled lipids possess the same chemical formula and structure as their unlabeled counterparts and hence they are expected to behave identically during chromatographic separation. However, these isotopologs can be readily differentiated by their mass (*m/z*) (127). Figure 1.8 represents an example of U-^{13}C-labelled and unlabelled PE (30:0), $C_{35}H_{70}NO_8P$ where both have been differentiated based on their masses by the MS but they have been detected at the same retention time.

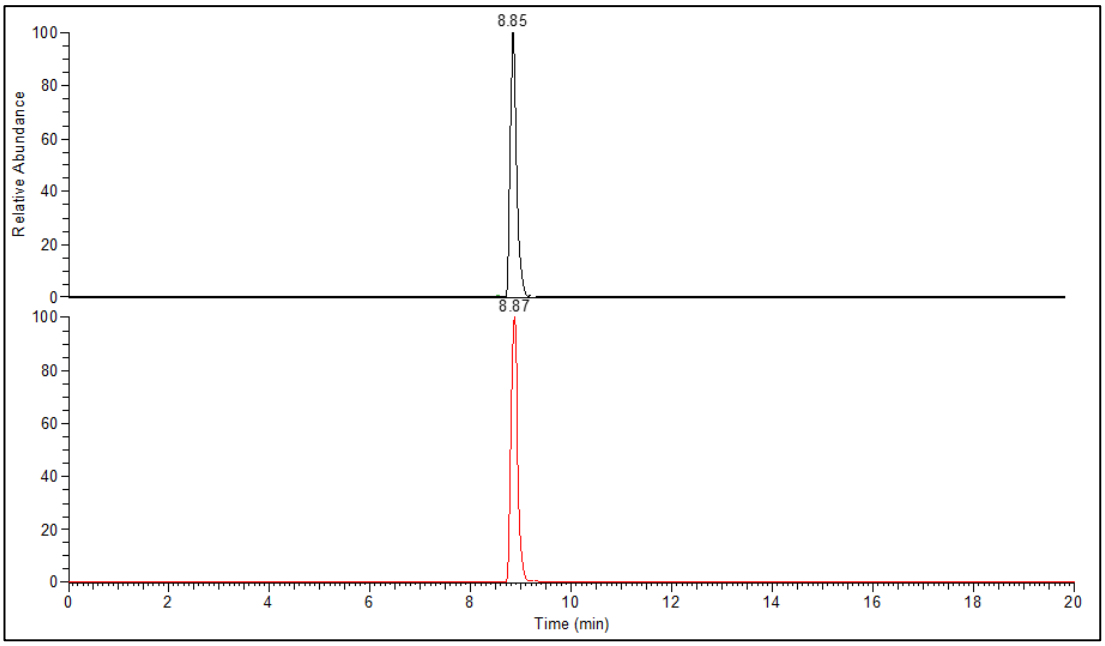

Figure 1.8: Extracted ion chromatograms of the unlabelled naturally abundant, m/z of 662.4766 (black chromatogram) and U-^{13}C-labeled form, m/z of 697.5939 (red chromatogram) of PE (30:0), $C_{35}H_{70}NO_8P$, detected in unlabelled and ^{13}C-labelled *E. coli* MG1566 extract, respectively in the negative mode within a mass error of 5 ppm.

This approach has been wildly used in targeted analysis to obtain the absolute concentration of the studied species either by external or internal standards (128, 129). However, as mentioned before this approach cannot be utilised for large scale targeted studies or for untargeted studies. Therefore, several research groups have been exploring how to adapt this approach to make the most use of these standards in overcoming the diverse variations that could affect the analysis. For example, inclusion of single or multiple IS covering the whole mass range of interest have been utilised for lipid normalisation (130). However, due to the huge diversity of metabolite structures, concentration and composition, it is not practical to assume that all the metabolites/lipids with different masses and different physicochemical properties are subjected to the same amount of variation as the standards (117, 118, 130). In addition, different lipid species could overlap such as ceramides,

diacylglycerols, sphingomyelins, and it is not practical to use the same normalisation factor on these species. Thus, normalisation by retention time could not correct the variations as expected due to matrix specific effects (118).

Others studied the behaviour of different concentrations of different lipid species and they found that at low concentration, lipids from the same class possess approximately have similar response factors (131). This is because the ionisation efficiency of those species relies on the charged head group which is the same in each group (57). Therefore, for better results, at least one standard should be included for each lipid class, this can improve the quality of quantification. However, when various species present in a mixture, it is not practical to include multiple internal standards to normalise each class with various degrees of unsaturation within the same class (132). In addition, non-polar lipid classes that do not have an ionizable head group (cholesterol esters, diacylglycerols, triacylglycerols, etc) do not manifest identical response factors even at low concentration and their response should be determined in advance with respect to their acyl chain length and their degree of unsaturation which complicate the analysis even more (57, 133). Also, the availability of commercial stable isotope-labelled standards and their costs limit the large-scale use of this method (55). Accordingly, an *in vivo* synthesis of U-^{13}C-labelled compounds can be achieved using suitable microorganisms grown in U-labelled substrate-limited culture media (134, 135). As carbon and hydrogen are two of the most abundant atoms in living organisms, they can be replaced by heavy isotope in order to obtain labelled metabolites extract that could serve as IS mixture. However, complete hydrogen replacement using fully deuterated water and nutrients is more expensive, tedious and sometimes, the use of fully deuterated media may not support the

growth of several species while ^{12}C-carbon replacement is easier and less expensive (135, 136).

By sustaining the growth of these organisms on a sole carbon source that could be replaced later with isotopically labelled form, in theory, variety of isotopically labelled metabolites/lipids can be generated from the cells after applying a proper extraction procedure. For many organisms, ^{13}C-labelling can be performed easily and at a reasonable cost (137). For example, ^{13}C-labelled spirulina is already commercially available, while *E. coli* strains are easy to grow on a sole carbon source. Ideally, the source of stable isotopes should be the same as the samples to ensure all relevant metabolites are present. This approach has been widely used for both quantitative analyses in proteomics and metabolomics using ^{15}N- or/and ^{13}C sources and others (129, 137-140). Researchers have been using labelled extract from different organisms such as *E. coli, S. cerevisiae, P. pastoris* and other to normalise a selected number of metabolites which will help them in report their absolute or relative concentrations (129, 134, 141-143). However, a different source of isotopically labelled extract could be used for complex organisms that is difficult to control (127, 143). Table 1.3 lists a summary of few MS metabolomics publications based on *in vivo* labelling strategy.

Table 1.3: A selected list of MS metabolomics publications based on *in vivo* labelling strategy.

Species studied	Source of labelled IS mixture	Source of heavy atom	Comments	Reference
Trypanosoma brucei	*E. coli*	U-^{13}C- glucose	• Hydrophilic compounds • Absolute quantification of 75 intra and extra-cellular metabolites • T. brucei cannot grow on media containing only glucose and it reaches a relatively low cell density when cultivated	(134)
S. cerevisiae CEN.PK113-7D	*S. cerevisiae* CEN.PK113-7D	U-^{13}C- glucose and U-^{13}C-ethanol	• Hydrophilic compounds • Relative quantification of six metabolites • As proof of concept, the application of labelled IS of the studied metabolites for relative quantification eliminate the drawbacks of LC-MS such as ion suppression, nonlinear response and matrix effect. Also, it was able compensate for metabolites loss during sample preparation	(129)
E. coli K-12 strain NCM3722	*E. coli* K-12 strain NCM3722	U-^{13}C- glucose	• Hydrophilic compounds • Absolute quantitation of 60 folate species • Global analysis of intracellular folates in *E. coli* in response to trimethoprim, dihydrofolate reductase inhibitor that leads to net folate oxidation	(128)
E. coli NCM3722	*E. coli* NCM3722	U-^{13}C- glucose	• Hydrophilic compounds • Absolute quantification of 103 intra and extra-cellular metabolites	(144)
maize roots	*E. coli* DH10B and *S. cerevisiae* BRF	U-^{13}C- glucose and U-^{13}C-sodium bicarbonate	• Hydrophilic and hydrophobic compounds • Absolute quantification of 226 metabolites	(145)

Fusarium graminearum	*Fusarium graminearum*	U-^{13}C- glucose	• The IS mixture was used to investigate the impact of Pb treatment on maize root metabolism • Relative quantification of 307 feature pairs in untargeted analysis • The IS mixture enable improvement in precision of workflow and reduces technical variability	(143)
Arabidopsis thaliana	*Arabidopsis thaliana*	$^{13}CO_2$	• Hydrophilic compounds • Relative quantification of 20 selected compounds • The possibility of relative quantification of 643 different pairs of unique elemental compositions in untargeted analysis	(146, 147)
Clostridium autoethanogenum	spirulina	Commercially available U-^{13}C spirulina lyophilised cells	• Hydrophilic compounds • Absolute quantification of 52 metabolites • The IS mixture enable calculation of the absolute concentration of intracellular metabolites detected in *C. autoethanogenum* that was suitable for computational modelling to understand and optimize the active metabolic pathways in gas fermentation	(148)
P. pastoris CBS7435	*P. pastoris* CBS7435	U-^{13}C- glucose	• Hydrophilic compounds • Absolute quantification of 22 amino acids	(149)
P. pastoris	*P. pastoris*	U-^{13}C- glucose	• Hydrophilic compounds • Relative quantification of 34 metabolites • The IS mixture was used to evaluate the recoveries and repeatability during the extraction process and the extract treatment	(140)
P. pastoris	*P. pastoris*	U-^{13}C- glucose	• Lipophilic compounds • Relative quantification of 215 lipid species	(150)

			• Absolute quantification of 20 lipid species from different lipid classes	
human A549 lung cancer cells	*S. cerevisiae* strain S90	U-^{13}C- glucose and $^{15}N_2$-ammonium sulfate	• Relative quantification of 40 compounds	(151)
S. cerevisiae strain YJM789	*S. cerevisiae* strain S90	U-^{13}C- glucose and $^{15}N_2$-ammonium sulfate	• Relative quantification of 44 compounds	(151)
Human plasma	*P. pastoris*	U-^{13}C- glucose	• Lipophilic compounds • Relative quantification of 40 lipid species • absolute quantification of 12 selected lipid species from different lipid classes • 114 labelled lipids IS extracted from *P. pastoris* from the classes of PC, LPC, PE, PI, DG and TG were found to be common with human plasma, hence they are available for compound-specific quantification while another 98 labelled lipids that are not common with human plasma that can be used for quantification-based class or RT	(152)

Although *in vivo* labelling strategy enable the production of a wide variety of stable labelled standards that greatly enhance accuracy and precision of absolute and relative quantification by correction of technical and analytical variations that are difficult to evaluate and compensate, the use of these standards in profiling methods have not been widely explored. In addition, limited work has been applied to global lipid analysis and the applications of these standards into complex biological samples such as human biofluids using LC-MS especially in untargeted studies (153).

1.8 Aims and objectives

Labelled IS are routinely used in targeted studies to correct systematic and random errors that could introduced during the analytical work flow in LC-MS setup. However, due to the complexity of the analysis, the cost and the limited availability of labelled lipid standards this approach have not been applied into untageted lipidomic studies before. Therefore,the aim of this project is to develop a novel method for lipidomic data normalisation using an ideal U-^{13}C-labelled organism extract. Once this proposed normalisation method works effectively and successfully in reducing technical and analytical variation that could be introduced during sample preparation through analysis, it can then be utilised to perform more complex targeted and untargeted lipidomics studies.

The objectives of this project are:

- To select the optimum species for production of stable labelled IS mixture.
    - To investigate which organism that could give a better coverage of different lipid classes. The higher the number of common lipids between the internal standards mixture and the sample will make the internal standards mixture more efficient in normalisation of the sample.
    - To explore the labelling efficiency of the selected species.
- To develop and validate a novel normalisation technique using ^{13}C-labelled extract by monitoring the coefficient of variation (CV) per lipid as the main performance measure for the developed normalisation method.
- To apply the validated normalisation technique to clinical samples, human brain glioma samples and human plasma samples.

Chapter Two

Materials and methods

2. Materials and methods

2. 1 General materials and reagents

Ammonium acetate, acetonitrile, chloroform and Pierce® solution for MS calibration were obtained from Fisher Scientific, Loughborough, UK. Isopropanol was obtained from Acros Organics, New Jersey, USA. Methanol was obtained from VWR chemicals, Pennsylvania, USA. All the organic solvents were of LC-MS grade. Milli-Q water was prepared using Milli-Q water purification system (Millipore, MA, USA).

2.2 Sample preparation

Lipid extraction was performed according to the method of Bligh and Dyer using a mixture of methanol, chloroform and water (the specific amount used of each solvent will be listed in the individual experimental chapters) (99). Samples were vortexed for 10 min at 4^{o}C and centrifuged for 5 min at 13,000 *g*. The non-polar lower layer (mostly chloroform containing the lipids) was collected and transferred to new 2 mL Eppendorf tubes and dried under vacuum at room temperature using Juan evaporator centrifuge (Thermo Scientific, UK). The dried non-polar layer was reconstituted in 100 µL of isopropanol (LC-MS grade). The reconstituted samples were centrifuged again at 13,000 *g* for 10 min at 4^{o}C to remove any insoluble particles. Finally, 80 µL of the supernatant was transferred to a pre-labelled HPLC vial and stored at -80^{o}C until analysis.

2.3 Reversed-phase liquid chromatography mass spectrometry (RPLC-MS)

2.3.1 Chromatography

Chromatographic separation was conducted on ACE Excel 2µm super C18 column (50 × 2.1 mm, pore size 100 Å, Advanced Chromatography Technologies Ltd, Scotland, UK) using a Dionex Ultimate 3000 Series UHPLC system (Thermo Fisher Scientific, USA). Mobile phases used were: (A) acetonitrile:ammonium acetate (40:60, 10 mM final concentration) and (B) isopropanol:acetonitrile:ammonium acetate (80:10:10, 10 mM final concentration). The gradient was as follows: 0 min:30%B, flow rate 300 µL, 2 min: 35% B, flow rate 300 µL, 8 min: 100% B, flow rate 300 µL, 17 min: 100% B, flow rate 500 µL, 18-20 min: 20% B, flow rate 300 µL. Column and autosampler temperature were 45 and 4 ^{o}C respectively. Sample injection volume was 10 µL.

2.3.2 Mass spectrometric conditions

Mass spectrometry was performed on a hybrid quadrupole Orbitrap Q-Exactive^{TM} MS (Thermo Fisher Scientific, Hemel Hempstead, UK) acquiring data in full scan ion mode and tandem MS/MS in both positive and negative modes using an electrospray ionisation (ESI) source. Data were acquired simultaneously in full scan ion mode at m/z 100–1500, resolution 70,000, automatic Gain Control™ (AGC) target 3E6 and maximum ion injection time of 100 ms. Data were acquired tandem MS/MS mode at data-dependent MS/MS scans on top 5 precursor ions per scan, resolution 17,500, Automatic Gain Control™ (AGC) target 1E5, maximum ion injection time 50 ms, scan range 200 to 2,000 *m/z* and electrospray voltage of 4 Kv. The capillary temperature and heater temperature were maintained at 256 and 413 ^{o}C, respectively. Sheath,

auxiliary and sweep gas flow rate (arbitrary unit) were: 48, 11 and 2, respectively. S-lens RF level of 70. Figure 2.1 represents a schematic diagram of the Q-Exactive plus that used in this project.

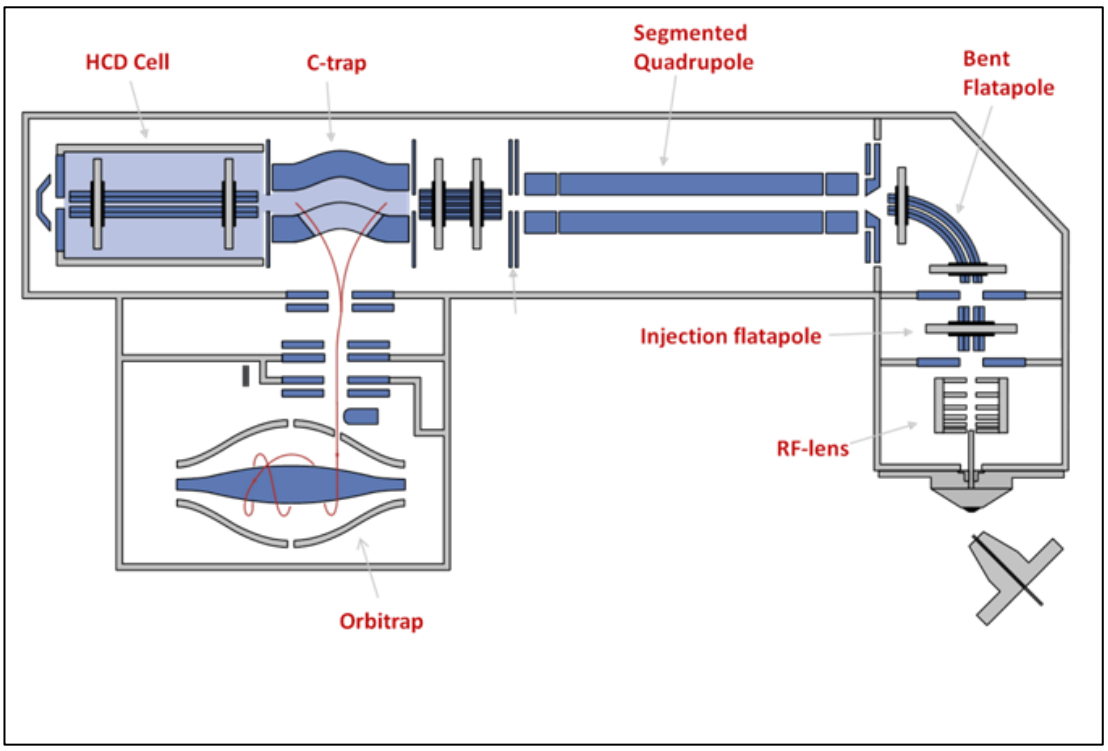

Figure 2.1: A schematic diagram of the Q-Exactive plus system that used in this project (154).

The MS was calibrated using Pierce® solution in both negative and positive ionisation modes and the MS performance was assessed at each run using pooled quality control samples (QC) interspaced between every 3-10 samples based on the total number of analysed samples. The data quality obtained from the LC-MS/MS analysis was assessed by determining the variability (CV%) in the mean peak intensities of all peaks present in QC samples using a metabolomics approach proposed by Want *et al.* (155). A specific dataset was selected when the CV% of peak intensities across at least 70% of the detected features was less than 30%. Figure 2.2 represents an example of RP-LC-MS chromatogram of a human plasma lipid profile and the

expected RT of various lipid classes detected under the chromatographic method prescribed previously.

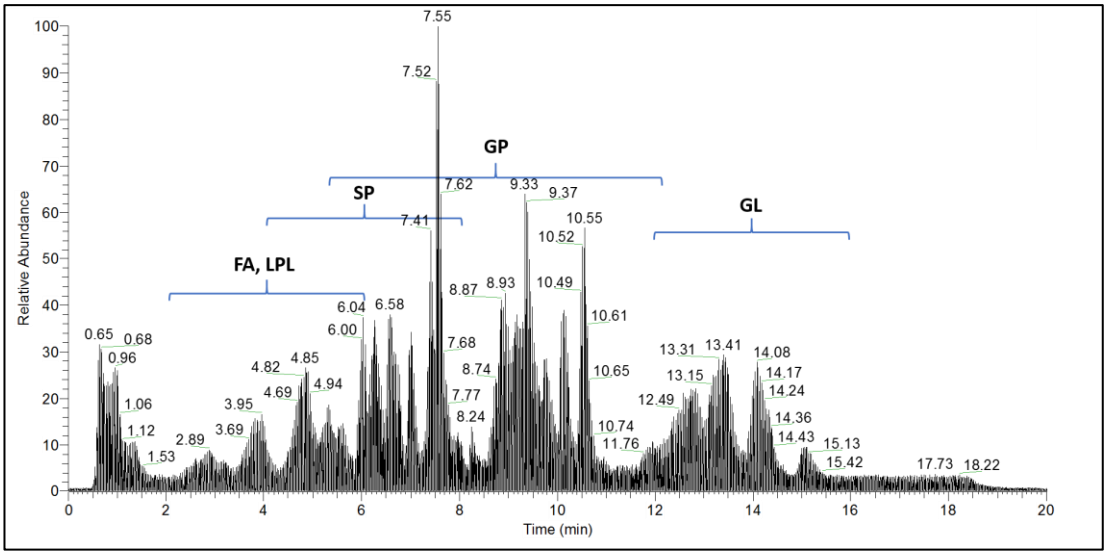

Figure 2.2: An example of RPLC-MS chromatogram in combined mode (positive and negative modes) of a human plasma lipid profile and the expected RT of various lipid classes detected under the chromatographic method prescribed previously. Abbreviation: FA: Fatty Acyls, LPL: Lysophospholipids, SP: Sphingolipids, GP: Glycerophospholipids, GL: Glycerolipids.

2.4 Data processing

2.4.1 Lipid identification

LipidSearch™ 4.1.16 (MitsuiKnowledge Industry, Tokyo, Japan) is a lipid identification software for lipidomics data by comparing their *m/z* and fragmentation patterns with an internal library that contains more than one million lipid ions and their predicted fragment ions from fatty acid chains and head groups. The library contains 19 main lipid classes and 71 subclasses. The software can also be used to align lipid data obtained from multiple LC-MS samples. LipidSearch™ parameters used for lipids identifications and alignment across samples are listed in Tables 2.1 and 2.2.

Table 2.1: LipidSearch™ parameter used for lipid identification.

Search parameter	Settings
Database	Q-Exactive
Search type	Product
Experiment type	LC-MS
Precursor tolerance	5 ppm
Product tolerance	5 ppm
Intensity threshold	1.0%
Execute Quantitation	on
m/z tolerance (quantitation)	−/+ 5.0 ppm
RT range (min.) (quantitation)	−/+ 0.5
Top rank filter	On
Main node filter	Main isomer peak
m-Score threshold	5.0 (1.0)*
c-Score threshold	2.0
FA priority	On
ID Quality Filter	A, B, C and D
Target class	ALL lipid classes
Ion adducts (pos)	H+, Na+ and NH_4+
Ion adducts (neg)	H- and CH_3COO +
S/N	2

*m-Score threshold was selected as 1 when the lipids profile of different species was explored in order to include as much as possible of that species lipidome to get a better comparison between the studied species.

Table 2.2: LipidSearch™ parameters used for alignment.

Search parameter	Settings
Exp type	LC-MS
Alignment Method	mean
R.T. Tolerance	0.5 min
Calculate unassigned peak area	On
Filter type	New filter
Top rank filter	On
Main node filter	Main isomer peak
m-Score threshold	5.0 (1.0) *
ID quality filter	A, B, C and D

*m-Score threshold was selected as 1 when the lipids profile of different species was explored in order to include as much as possible of that species lipidome to get a better comparison between the studied species.

Since the m-Score is calculated based on the number of matches between lipid fragments and library spectra, high number of matches gives high m-scores, which indicates that the identification of lipid species is more reliable. The ID quality filter used in LipidSearch™ also gives an idea about the reliability of the identification. Filter ID of A and B means that the lipid class and fatty acid chains were identified, C: either lipid class or fatty acid chains were identified, while type D identifications is the least reliable identification because it is based only on mass or features such as fragment ions.

2.4.2 Software to assess the labelling pattern

Isotope labelling offers advantages for MS metabolomics in term of metabolites identification and quantification, pathway discovery and flux analysis (127). Different heavy isotopes have been implemented in various metabolomics and proteomics studies including ^{2}H, ^{13}C, ^{15}N, ^{18}O and ^{34}S (156-158). Stable isotopes have the same number of protons, but they differ in mass due to a difference in the number of neutrons. Metabolites that only differ in the isotope composition are called isotopologues (127, 159). Each isotopologue has $\binom{n}{K}$ isotopomers (identical isotopic composition but different position of the isotope atoms within the metabolite), where n represents the number of carbon atoms in the metabolite and k represents the number of carbons that are labelled (159). Isotopologues possess similar physicochemical properties and hence they behave identically under chromatographic separation, but they are easily differentiated by their mass (*m/z*) in MS or NMR. However, isotopomers can only be resolved using specific detection methods that can assign the position of these labelled atoms such as nuclear

magnetic resonance spectroscopy or MS analysis of multiple fragments in tandem mass spectrometry (160-163).

In this project, labelling using carbon heavy atom will be employed to produce stable labelled ISs. A carbon is predominantly found as the light isotope (^{12}C) with natural abundance of 98.89% and the natural abundance of the heavy stable isotope form (^{13}C) is 1.11%. For example, the natural abundance of fully unlabelled metabolite with four carbons is $((98.89\%)^4 = 95.63)$ and $((1.11\%)^4 = 1.52E\text{-}08)$ represents the natural abundance of fully labelled form with (4*1.00335) Da higher than the monoisotopic peak of the fully unlabelled metabolite while (100-(95.63+1.52E-08) = 4.36) represent the natural abundance of partially labelled form of that metabolite (127, 159). Both open sources and commercial software are widely used to identifying and/or quantifying metabolites of interest in data gathered from unlabelled data created by MS-based metabolomics studies including IDEOM (164), mzMatch (165), MZmine (166), XCMS (167) and Progenesis (168). Although some of these software can be used manually to extract information of labelled metabolites, they cannot be used for global analysis of data from labelled metabolomics studies (127). Different tools currently available that can handle labelled MS data including CAMERA (169), MetExtract (170), MAVEN(171), mzMatch-ISO (172) and others (173-176). Advantages and disadvantage of these software are summarised in Table 2.3. The labelling percentage of selected lipids detected in positive mode in labelled extract of *Pichia pastoris* previously identified by LipidSearch™ in unlabelled samples were explored and compared using three different software available in our lab: mzMatch-ISO, Tox-ID, and Xcalibur. mzMatch-ISO is an R tool for isotope-labelling studies that annotates and quantifies mono-isotopic and corresponding isotope-labelled peaks of

metabolites in isotope-labelled LC-MS data. This software generate various plots and tables that describe the labelling pattern in more detail based on the chemical formula provided and the expected RT for the selected metabolites (172). Tox-ID 2.12.57 (Thermo Fisher Scientific, USA) is a semi-automated compound identification tool that used in forensic and clinical laboratory. The software is used to record peak intensity of known mass ions at specific retention times that can be used to calculate ^{13}C-enrichment or labelling percentage manually using equations 2.1 and 2.2, respectively based on accurate mass scans using exact accurate mass error of 5 ppm and RT window of 0.13 min ion threshold of 1.00E+04 that could minimise false negative peak picking. The AUC_U, AUC_P and AUC_L represent the area under the curve (peak area) of unlabelled metabolite, partially labelled metabolites and fully labelled metabolite of interest, respectively.

$$^{13}\mathrm{C} - \text{enrichment } (\%) = \left(\frac{AUC_{\mathrm{L}}}{AUC_{\mathrm{L}} + AUC_{\mathrm{U}}}\right) * 100 \quad \text{....Equation 2.1}$$

$$\text{labelling } (\%) = \left(\frac{AUC_{L}}{AUC_{\mathrm{L}} + AUC_{\mathrm{P}} + AUC_{U}}\right) * 100 \quad \text{....Equation 2.2}$$

Table 2.3: Advantages and disadvantages of currently available software for labelled metabolomics data analysis (modified after (127)).

Software	Advantages	Disadvantages
mzMatch-ISO	• Uses the standard XCMS peak-picking algorithm to pick peaks and can retrieve missing peaks from raw data • Written in the R statistical software. A single command with well-documented parameters is all that is required to run an analysis • Results include chromatograms and several plots that describe the labelling patterns within replicates and within an experiment • Can work on most biologically relevant isotopes – C, H, N, O and S • Can be used for both targeted and untargeted isotope profiling	• Has a command line interface • Has a steep learning curve
MAVEN	• Robust and easily comprehensible plots to differentiate the labelling patterns between replicates and sample groups within an experiment • The pathway visualizer and isotopic flux animator in this software offer automated inference into biological events detected within a study • A very robust user interface that is easy to understand and operate • Can be used as a tool to quickly inspect the labelling pattern of a given metabolite	• Development of custom algorithms and data integration that would extend the capabilities of the software is challenging for a typical biologist
MetExtract	• Offers a very basic visualisation of the monoisotopic and corresponding isotope peaks • Has a comprehensive user interface that enables custom parameters to be defined	• MetExtract employs a brute force method to extract peaks from mass spectra rather than exploiting other well-established peak-picking algorithms • The basic visualisation of peaks offered is not sufficient in many applications
CAMERA	• Specifically designed for the annotation and evaluation of mass spectral features including isotope peaks, adducts and fragments that co-elute from a chromatographic column. • Written in the R statistical software and is open source. This offers plenty of scope for further extension	• The software provides only a basic visualisation of the light and heavy isotopologue chromatograms • Rapid differentiation and relative quantification of isotope patterns is not currently possible with this software
	• User-friendly and familiar interface in the form of Microsoft® Excel spreadsheets • Very easy to implement once the underlying software is installed	• Designed for the annotation and evaluation of mass spectral features including isotope peaks, adducts and fragments that co-elute from a chromatographic column

IDEOM	• Results in the form of tables that can be easily exported for further statistical analyses	• Cannot directly access raw data to retrieve missing peaks (requires mzMatch-ISO for this function)
iMS2Flux	• Provides a framework for automated isotopologue analysis for large datasets • Focus on validation and correction of MS-derived data and output in format suitable for MFA	• Additional software is required for the initial peak detection and for the final flux analysis • Cannot directly access raw data when performing data checks
FiatFlux†	• ^{13}C-MFA tool that has a convenient user interface • Facilitate FBA • GC–MS based tool	• Works only on ^{13}C-labeled data • Does not work on LC–MS data • Requires predefined steady-state stoichiometric model to predict flux • Cannot perform untargeted metabolomics and trace the route of labelled carbon atoms
^{13}C-Flux2	• Aimed at providing a direct measure of flux in a system being investigated • Provide insights into metabolic pathway activity by comparing flux phenotypes under different environmental conditions and physiological states as well as for a variety of carbon sources • Has been used in numerous ^{13}C-MFA studies • Works on GC–MS, LC–MS and NMR data	• Requires a detailed steady-state stoichiometric model that encompasses the metabolism being studied • Command-line interface • Works only on ^{13}C labelled studies • Cannot perform untargeted metabolomics on labelled data
OpenFlux	• An attempt to make a flexible version of ^{13}C-Flux2 to perform steady-state ^{13}C MFA using mass isotopomer distribution data • Spreadsheet-based user interface	• Not applicable for targeted and/or untargeted metabolomics data analysis and isotope profiling
Tox-ID	• Can be used to search on specific mass or for a screening method for different adducts form	• Semi-automated and can only be used for targeted analysis • Time consuming
Trace Finder	• Quick and easy to use • Report peak area instead of intensity	• Can only work for specific imported database (targeted analysis only)

†These are metabolic-flux analysis tools that require a predefined stable steady-state stoichiometric model of the metabolism to determine the flux. MFA: Metabolic flux analysis; FBA: Flux balance analysis.

The results of two software packages (Tox-ID and mzMatch-ISO) were compared to the manual method (using Xcalibur 2.2: the same software that used to acquire the data) in order to select the software that can reveal the labelling pattern of the identified lipids in the labelled extract more efficiently. Figure 2.3 summarises the labelling percentage of selected lipids detected in positive mode in labelled extract of *Pichia pastoris* using three different software: Tox-ID, mzMatch-ISO, and Xcalibur.

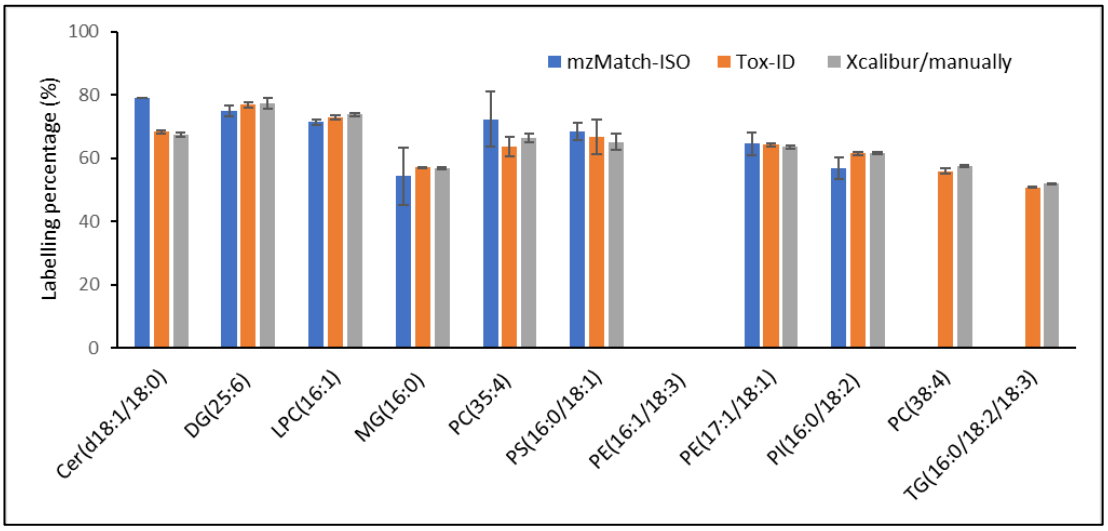

Figure 2.3: The labelling percentage of selected lipids detected in positive mode using three different software.

As shown in Figure 2.3, the labelling percentage results of some lipids using mzMatch-ISO and Tox-ID were comparable with Xcalibur results, however, Tox-ID results were closer to Xcalibur/manual method. In other lipids (e.g. PC (38:4) and TG (16:0/18:2/18:3)) mzMatch-ISO failed to detect the U-^{13}C-labelled mass of these lipids especially for [NH_4^+] adducts, which was reflected on the reported labelling pattern and labelling percentage. Figure 2.4 represents an example of the labelling pattern of PC (38:4) and TG (16:0/18:2/18:3) using the three software. mzMatch-ISO has the potential to be used in various metabolomic studies but the structural complexity of lipids molecules, their relatively high molecular weights and their huge number of

isomers and isobars might affect the quality of mzMatch-ISO's results which makes it difficult to be applicable for lipidomics studies (177).

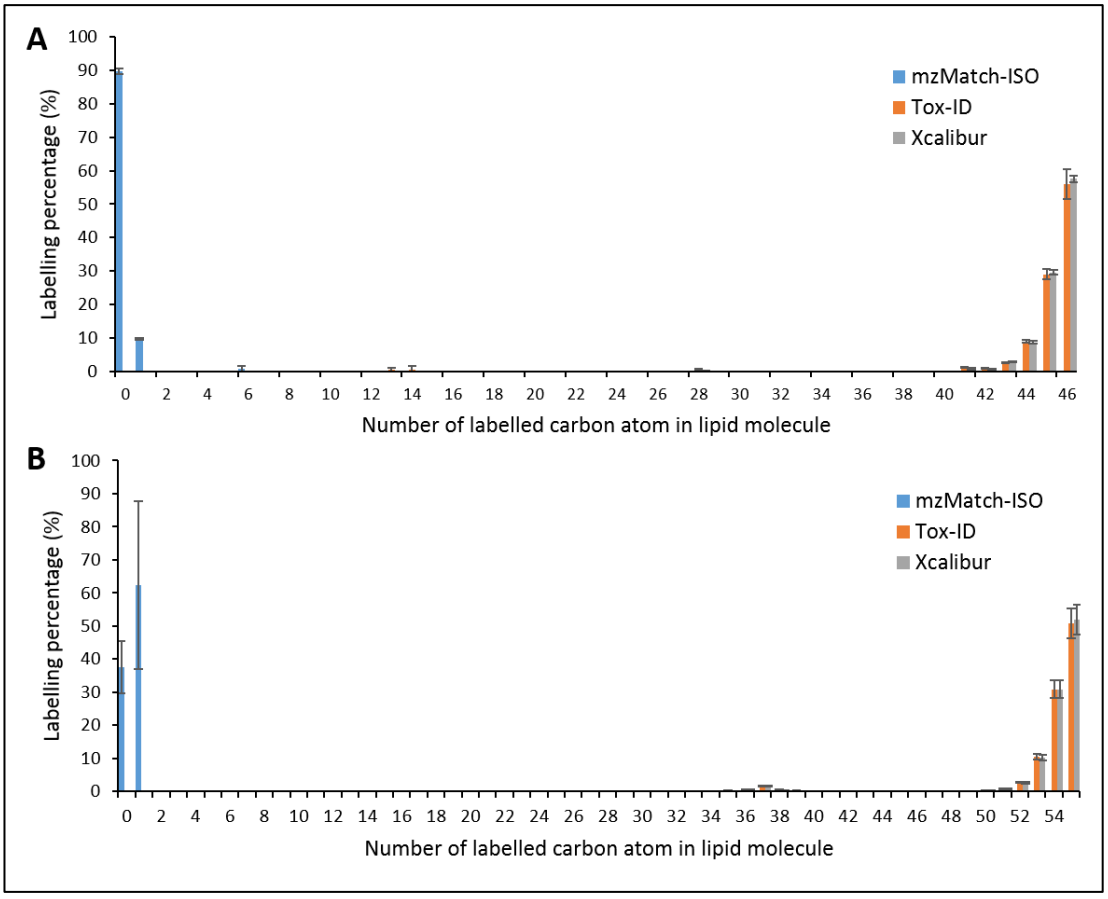

Figure 2.4: The labelling pattern of (A) PC (38:4), $C_{46}H_{85}NO_8P$ and (B) TG (16:0/18:2/18:3), $C_{55}H_{96}O_6$ both detected in positive mode as H^+ and NH_4^+ adducts, respectively in U-^{13}C-labelled *P. pastoris* extract using three different software.

Reporting the whole labelling pattern of a long list of lipids using Tox-ID based on Equation 2.2 is time consuming and since only the intensity of U-^{13}C-labelled lipids are required to normalise unlabelled lipid. Tox-ID will be used to assess the labelling efficacy of our labelling strategy throughout the project by calculating the ^{13}C-

enrichment of the labelled lipid species using Equation 2.1, and only the full labelling pattern of the optimum source of internal standards mixture will be explored.

2.4.3 Normalisation and statistical analysis

Once lipid ion species are identified using LipidSearch™, the *m/z* of the possible U-^{13}C-labelled form of that species can be calculated based on Equation 2.3 corresponding to the previously found accurate monoisotopic masses of the unlabelled endogenous lipid ions and their expected chemical formula. Where m/z_L and m/z_U represent the mass to charge ratio of the fully labelled and fully unlabelled lipid ion respectively, N_C represents the number of carbon atom in that lipid species (without the adduct) and 1.00335 represent the difference in atomic weight of heavy and light carbon atom.

$$m/z_L = m/z_{\mathrm{U}} + (1.00335 * N_C) \ldots . \text{Equation 2.3}$$

After that, a list of the *m/z* of the unlabelled and labelled forms of the identified lipid species alongside their proposed identity and their expected RT was introduced as a database into another software called Trace Finder that was used to integrate and extract peaks areas of (RT, *m/z*) lipid pairs from the LC-MS/MS raw data based on mass error of 5 ppm, RT window of 30 s and S/N of 10. Then, the results were exported to an Excel spreadsheet where the normalisation was done manually by dividing the peak area of the unlabeled form of the lipid ion species by that of its labelled form (if it was detected) or by another labelled lipid ion in the same class or the nearest labelled lipid ions to it (if its labelled form was not detected). The quality of the datasets obtained after normalisation was assessed using univariate (CV%) and multivariate (PCA) approaches.

2.5 Project workflow

To overcome unexpected systematic variations and obtain accurate quantitative lipidomics data, a new LC-MS-based lipid profiling method will be developed using *in vivo* labelling strategy to produce different variety of stable isotopes that can be used as a source of internal standards. First, the optimum source for production of IS mixture that provide more common lipids with complex biological samples and can be efficiently labelled in a simple and cost-efficient way will be explored. Then, the optimum species will be used to generate high quality of large scaled ^{13}C-labelled IS mixture that can be used to demonstrate the ability of these IS mixture to correct various types of systematic variations that can be introduced during sample preparation and analysis in LC-MS setup. After that, the validated method using the optimum IS mixture will be applied in quantitative lipidomic studies in clinical samples to overcome unexpected systematic variations which will lead to more reliable and reproducible results. Figure 2.5 illustrates the general workflow of the project.

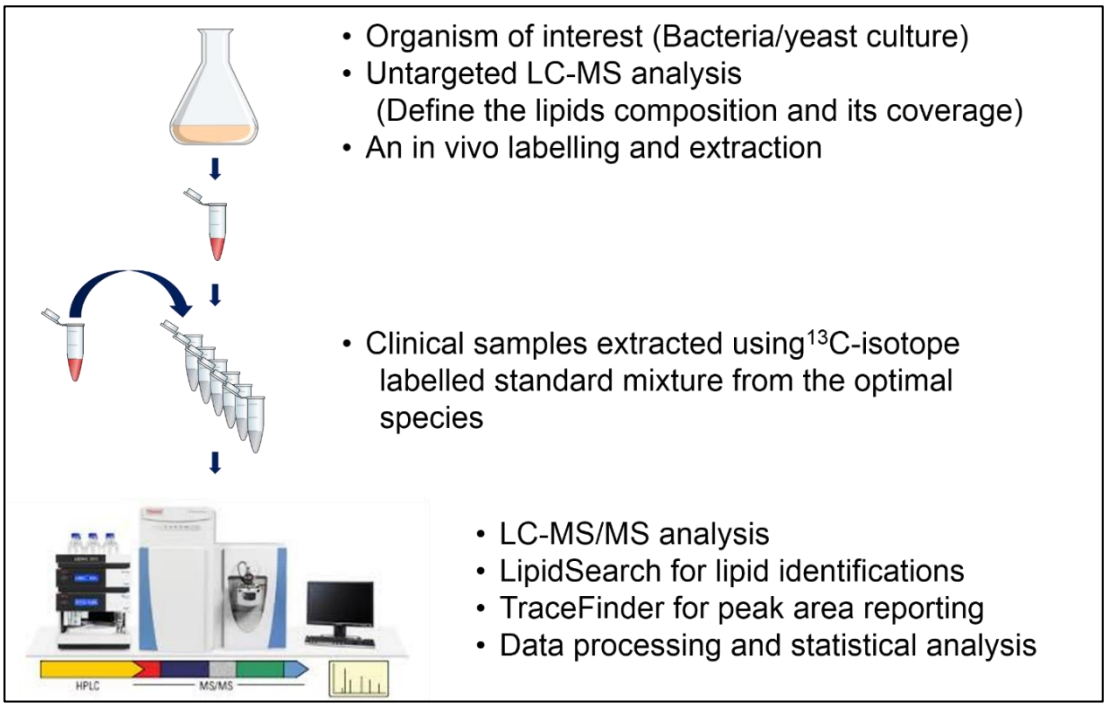

Figure 2.5: Project general workflow.

Chapter Three

Generation of uniformly labelled ^{13}C lipid standards in yeast and bacteria species

3. Generation of uniformly labelled ^{13}C lipid standards in yeast and bacteria species

3.1 Introduction

3.1.1 Why are uniformly isotopically labelled internal standards needed in lipidomics analysis?

Monitoring lipid changes is an essential task in comprehensive lipidomic studies. Lipidomics involves the identification and quantification of a variety of lipids and their interaction with each other or with other enzymes *in vivo* and it is considered as a subset of metabolomics (178). Among the various analytical platforms that can be used for metabolomics/lipidomics applications, LC-MS based platforms provide a valuable tool to monitor lipid changes as well as to identify specific biomarkers which can be used as potential drug targets for pharmaceutical and clinical research (139, 179-183). However, quantification of lipids is extremely challenging due to i) the chemical diversity of lipids, ii) isomeric and isobaric lipids, iii) dynamic range of lipids, and iv) limited stability of some of the studied lipids (69, 150). In addition, the nonlinear responses due to ion suppression and enhancement caused by matrix effect can often result in inaccurate quantification making it difficult to highlight biological and/or clinical significance (55, 110). Furthermore, a key limitation of this technique is the lack of a reliable normalisation method for the structurally diverse lipid species in a biological sample. Therefore, in order to overcome any unexpected systematic variations and obtain more accurate quantitative measurement, normalisation method must be applied to the samples which will lead to more reliable and reproducible results.

Several research groups chemically synthesised a diverse range of isotopically labelled compounds like hormones, steroids and fatty acids (55, 184-186). However, this

approach is laborious, costly, requires high synthetic expertise not always available in metabolomics groups and cannot be used in large-scale metabolomics where a diverse and complex structures of the metabolites are included in the analysis. To overcome these problems researchers are using an *in vivo* labelling strategy where various organisms can be grown on ^{13}C-labelled carbon source to produce a wide range of isotopically labelled intracellular metabolites which can be used as a source of internal standards for accurate quantification.

3.1.2 Microorganisms which have been used to generate uniformly labelled internal standards

Ideally, the same organism being studied should be used to generate ^{13}C-labelled IS mixture in order to cover most of intracellular metabolites. For complex biological samples that cannot be grown on one carbon source where it is difficult to produce high labelling efficacy (187), different organisms can be used as a source of IS mixture. Reviewing the literature, *E. coli* (134, 138, 188), spirulina (189-191), *S. cerevisiae* (129, 138, 192) and *P. pastoris* (140, 150, 193), were found among the most commonly used species to produce IS mixture for quantitative analysis in proteomics and metabolomics studies. The labelled extract produced using these species either were used in quantitative analysis to study the metabolome of that specific species that used to generate the IS mixture itself or as IS in metabolomics studies to quantify (either absolute or relative quantification) of indigenous metabolites detected in other species or nonbiological samples. In addition, these labelled extracts could be used in flux experiments (134), metabolic pathway exploring (194), elemental formula annotation of different metabolites (195).

E. coli is a Gram-negative, rod shaped bacterium that is found in the lower intestines of mammals (196). It is one of the most intensively studied prokaryotes and has been considered as a "model organism" for studying numerous essential processes. *E. coli* can be rapidly and easily grown as it has simple nutritional needs and fast growth rate that makes it a good organism to use as a source of IS. Previously *E. coli* have been used to generate labelled f metabolites that were used in targeted metabolomics, metabolic-flux analyses or for MS-method improvements. The labelled extract of *E. coli* was used by Kim *et al*. to obtain the absolute concentration of 75 intra and extra-cellular metabolites detected in *Trypanosoma brucei* (134). In 2014 K. Li *et al.* were able to quantify more than 226 metabolites that might be involved in stress response in maize by co-extraction the ^{13}C-labelled cells of *E. coli* and *S. cerevisiae* (138).

Algae *Arthrospira platensis* commonly known as spirulina is grown on ^{15}N or ^{13}C to incorporate stable isotopes into its protein and metabolites. Spirulina is supplied as a ready-to-use powder -unlabelled and labelled whole cell powder by Cambridge Isotope Laboratory. Lyophilised powder of labelled spirulina has been routinely used in proteomics studies (190, 191) but it was newly explored in metabolomics study conducted by our group (189). In this study, the ^{13}C-labelled extract of spirulina powder was used as it is to provide absolute quantification of 43 metabolites found in *Clostridium autoethanogenum* extract to understand and optimize the active metabolic pathways in gas fermentation.

Saccharomyces cerevisiae is the most widely studied eukaryotic organism. It is commonly associated with the brewing and baking industries due to its ability to produce ethanol and carbon dioxide, respectively. In addition, it is one of the most frequently used species in functional proteins production (197). *S. cerevisiae* is a single-budding yeast,

approximately 5–10 µm, can grow both aerobically and anaerobically on a variety of carbon sources. It is easy to handle and to manipulate and possess relatively simple lipidome (197). However, It is believed that their lipid biosynthesis and metabolism are very similar to those of higher eukaryotes with known exceptions (198). It has been widely used as a source of IS to correct variation introduced during analysis. In 2003, Mashego *et al.* reported the ability of ^{13}C-labelled extract of *S. cerevisiae* CEN.PK113-7D in eliminating the nonlinear response of the MS and consequently reducing the experimental error that could happen due to the matrix effect (129). In 2004 Wu *et al.* used the metabolite extract of *S. cerevisiae* CEN.PK cultivated in a fed-batch fermentation on fully U-^{13}C-labelled substrates to study the effect of a glucose pulse on cells in steady-state and transient conditions. They verified that the used IS led to more accurate, precise and robust results in metabolome analysis (192). Vielhauer *et al.* explored the use of *S. cerevisiae* as a source of internal standards in GC–MS based quantification of central carbon metabolism intermediates and he claims that the presented approach will enable more labs to achieve more accurate absolute quantification (199).

Pichia pastoris is a well-known cell factory in biotechnology. *P. pastoris* is an efficient eukaryotic microorganism that can generate similar metabolite/ lipid profiles to mammalian cells (150). Also, its culture can reach a very high cell densities in relatively short time and it can be grown on non-complex media with one carbon source (150). The use of ^{13}C-labelled extract of *P. pastoris* has been recently explored by Neubauer *et al.* in 2012 as a tool to evaluate sample preparation in metabolomics study (140). Then, in 2017 he explored the possibility of using its lipids extract as a reference for compound-specific quantification where he reported that more than 200 lipid species were

identified from the labelled extracts with an excellent ^{13}C-enrichment that can be used as IS for absolute or relative quantification (150).

3.1.3 The requirements for successful generation of isotopically labelled lipids as internal standards

In this project, isotopically labelled IS mixture produced from the optimum species will be applied into complex studies that involve human plasma samples and human brain tissue. The use of these labelled extract as IS in untargeted analysis in clinical biological samples has not been previously explored especially in lipidomics studies except in one recent study (152). In that study, Rampler *et al.* revealed that *in vivo* labelling of *P. pastoris* enable the production of 212 lipid standards from 13 lipid classes that can be applied for compound specific quantification and/or for class/RT specific quantification in complex systems such as human plasma. Also, they were able to improve quantification of 40 lipids from 6 classes (DG, LPE, PC, PE, PI, TG) detected in human plasma (152).

The ideal host system that can be used to generate isotopically labelled IS should have similar metabolome (and lipidome) profiles to mammalian cells or the target samples. in addition, this host system should be rapidly and easily grown under simple nutritional needs to enable simple and complete labelling of most of the metabolites extracted. Also, it is advantageous if it can be grown to a very high cell densities that will increase the product yields of the labelled IS mixture in relatively short time with relatively low cost. As well, it is useful if it has a very stable cell wall enabling longer storage periods and reduce metabolite leaching during sample collection (152).

Although different species were used as a source of labelled IS in various studies and applications, their use have not been widely explored in complex human samples.

Therefore, it is necessary to compare between these species to explore which species can be used to provide a high quality labelled IS mixture that can be employed in quantitative analysis of human samples as it would provide a better measurement of the human adaptation system to external or internal stimuli.

3.2 Objectives

The objectives of this chapter are:

- To compare the lipidome of different species (*E. coli* MG 1655, spirulina, *S. cerevisiae* BY4741, *S. cerevisiae* CEN.PK 113-7D and *P. pastoris NCYC 175*) to find out which one most resembles the human lipidome.
- To study the quality of ^{13}C-enrichment of identified lipids in the studied species.
- To select the optimal source for labelled internal standards mixture.

3.3 Materials and methods

3.3.1 Materials

Table 3.1 summarises the specific materials that were used during this chapter and their sources.

Table 3.1: List of materials used in this chapter.

Material	Supplier
Microorganisms	
E. coli MG1655	kindly provided by Dr Nigel Halliday, The Centre for Biomolecular Sciences, University of Nottingham, UK
Spirulina whole cells (lyophilised powder) unlabelled	Cambridge Isotope Laboratory, USA
Spirulina whole cells (lyophilised powder) (U-^{13}C, 97%)	Cambridge Isotope Laboratory, USA
S. cerevisiae BY4741	kindly provided by Professor Simon Avery, School Biosciences, University of Nottingham, UK
S. cerevisiae CEN.PK 113-7D	EUROSCARF, Germany
P. pastoris NCYC175	National Collection of Yeast Cultures, UK
Medium components	
D-Glucose	Sigma-Aldrich, USA
Bacto™ Agar	Scientific Laboratory Supplies, UK
Yeast extract	OXOID, UK
Peptone	Sigma-Aldrich, USA
M9 Minimal salts	Sigma-Aldrich, USA
Magnesium sulphate heptahydrate	Sigma-Aldrich, USA
Calcium chloride dihydrate	Sigma-Aldrich, USA
Thiamine hydrochloride	Sigma-Aldrich, USA
Propidium iodide	Sigma-Aldrich, USA
Fluorescein diacetate	Sigma-Aldrich, USA
Yeast nitrogen base without amino aci	Formedium, UK
L-Methionine	Formedium, UK
L-Histidine	Formedium, UK
L- Leucine	Formedium, UK
Uracil	Formedium, UK
Complete supplement mixture	Formedium, UK
D-Glucose (U-$^{13}C_6$, 99%)	Cambridge Isotope Laboratory, USA

3.3.2 Species growth condition

In order to prepare the unlabelled extract, the studied species were grown as described below. For preparation of labelled biomass samples, 99% U-^{13}C-glucose was used in minimal media preparation instead of ^{12}C-glucose.

3.3.2.1 *E. coli* MG 1655

A culture of *E. coli* in M9 minimal media was prepared overnight. Then, a known amount of the overnight culture was diluted with 100 mL of M9 minimal media to an optical density (OD_{600}) of 0.1 and grown at 37°C and 122 rpm until it reached the stationary phase. The M9 minimal medium was prepared according to Cold Spring Harbor Protocols (200), which consists of: 100 mL of 5X M9 solution (33.9 g of Na_2HPO_4, 15 g of KH_2PO_4, 5 g of NH_4Cl, 2.5 g of NaCl per litre), 2 mL of 1 M $MgSO_4$, 0.1 mL of 1 M $CaCl_2$, 0.8 mL of 5% thiamine and 20 mL of 20% glucose per litre of sterile water.

3.3.2.2 Spirulina

The unlabelled and labelled form of spirulina was purchased from Cambridge Isotope Laboratory and used as received.

3.3.2.3 *S. cerevisiae* BY4741

A culture of *S. cerevisiae* BY4741 in minimal media was prepared overnight. Then, known amount of the overnight culture was diluted with 100 mL of minimal media to an optical density (OD_{600}) of 0.1 and grown at 30°C and 122 rpm until it reached the stationary phase. The minimal media was prepared according to Verduyn *et al.* (201), which consists of: 5 g/L of $(NH)_2SO_4$, 1 g/L of KH_2PO_4, 0.5 g/L $MgSO_4$, 0.1 g/L of $CaCl_2$, 0.1 g/L of NaCl, 500 µg/L of H_3BO_3, 40 µg/L of $CuSO_4$, 100 µg/L of KI, 200 µg/L of $FeCl_3$, 400 µg/L of $MnSO_4$, 200 µg/L of Na_2MoO_4, 400 µg/L of $ZnSO_4$, 2 µg/L of Biotin, 400 µg/L of calcium pantothenate, 2 µg/L of folic acid, 2000 µg/L of inositol, 400 µg/L of nicotinic acid, 200 µg/L of *p*-aminobenzoic acid, 400 µg/L of pyridoxol hydrochloride, 200 µg/L of riboflavin, 400 µg/L of thiamine hydrochloride. Filter-sterilised essential amino acids were added after heat sterilisation of this medium. Final concentrations of amino acids were: 150

mg/L of methionine, 260 mg/L of leucine, 20 mg/L of uracil, and 60 mg/L of histidine. At the end, known amount of filter-sterilised glucose solution was added to a final concentration of 2%.

3.3.2.4 *S. cerevisiae* CEN.PK 1137D

A culture of *S. cerevisiae* CEN.PK 1137D in minimal media was prepared overnight. Then, known amount of the overnight culture was diluted with 100 mL of minimal media to an optical density (OD_{600}) of 0.1 and grown at 30°C and 122 rpm until it reached the stationary phase. The minimal media was prepared according to Verduyn *et al.* [28], which consists of: 5 g/L of $(NH)_2SO_4$, 1 g/L of KH_2PO_4, 0.5 g/L $MgSO_4$, 0.1 g/L of $CaCl_2$, 0.1 g/L of NaCl, 500 µg/L of H_3BO_3, 40 µg/L of $CuSO_4$, 100 µg/L of KI, 200 µg/L of $FeCl_3$, 400 µg/L of $MnSO_4$, 200 µg/L of Na_2MoO_4, 400 µg/L of $ZnSO_4$, 2 µg/L of Biotin, 400 µg/L of calcium pantothenate, 2 µg/L of folic acid, 2000 µg/L of inositol, 400 µg/L of nicotinic acid, 200 µg/L of *p*-aminobenzoic acid, 400 µg/L of pyridoxol hydrochloride, 200 µg/L of riboflavin, 400 µg/L of thiamine hydrochloride. At the end, known amount of filter-sterilised glucose solution was added to a final concentration of 2%.

3.3.2.5 *P. pastoris* NCYC175

A culture of *P. pastoris* NCYC175 in minimal media was prepared overnight. Then, a known amount of the overnight culture was diluted with 100 mL of minimal media to an optical density (OD_{600}) of 0.1 and grown at 30°C and 122 rpm until it reached the stationary phase. The minimal media was prepared according to Verduyn *et al.* [28], which consists of: 5 g/L of $(NH)_2SO_4$, 1 g/L of KH_2PO_4, 0.5 g/L $MgSO_4$, 0.1 g/L of $CaCl_2$, 0.1 g/L of NaCl, 500 µg/L of H_3BO_3, 40 µg/L of $CuSO_4$, 100 µg/L of KI, 200 µg/L of $FeCl_3$, 400 µg/L of $MnSO_4$, 200 µg/L of Na_2MoO_4, 400 µg/L of $ZnSO_4$, 2 µg/L of Biotin, 400 µg/L of

calcium pantothenate, 2 µg/L of folic acid, 2000 µg/L of inositol, 400 µg/L of nicotinic acid, 200 µg/L of *p*-aminobenzoic acid, 400 µg/L of pyridoxol hydrochloride, 200 µg/L of riboflavin, 400 µg/L of thiamine hydrochloride. At the end, known amount of filter-sterilised glucose solution was added to a final concentration of 2%.

3.3.3 Growth curve

In order to construct a growth curve, a known amount of overnight culture in minimal media was used to inoculate freshly prepared minimal media (as described in section 3.3.2) to OD_{600} 0.1. Then, the growth rate of the studied species were monitored by measuring the OD_{600} every 2 h for 36 h (*n*=3) to confirm the ability of the selected media to maintain the growth of the studied species and to investigate when the cells reach the stationary phase.

3.3.4 Sample extraction

To facilitate the extraction, cellular lipids were extracted according to Bligh and Dyer method (99). Figure 3.1 provides a simple illustration of sample preparation steps. Cell pellets of cellular suspension equivalent to 10 mL at OD_{600} of 1 (for spirulina samples 5 mg of lyophilised powder) were suspended in 2.5 mL methanol and vortexed for 5 min, then 1 mL de-ionised H_2O and 1.25 mL chloroform were added and vortexed for another 5 min at 4°C. Phase separation was induced by the addition of 1.25 mL chloroform and 1.25 mL H_2O. The samples were then centrifuged for 10 min at 13000 *g* and 2 mL of the chloroform phase (lower layer of rich lipids) were dried under vacuum at room temperature. Finally, the dried samples were reconstituted using 200 µL of LC-MS grade isopropanol and stored at 80°C until analysis.

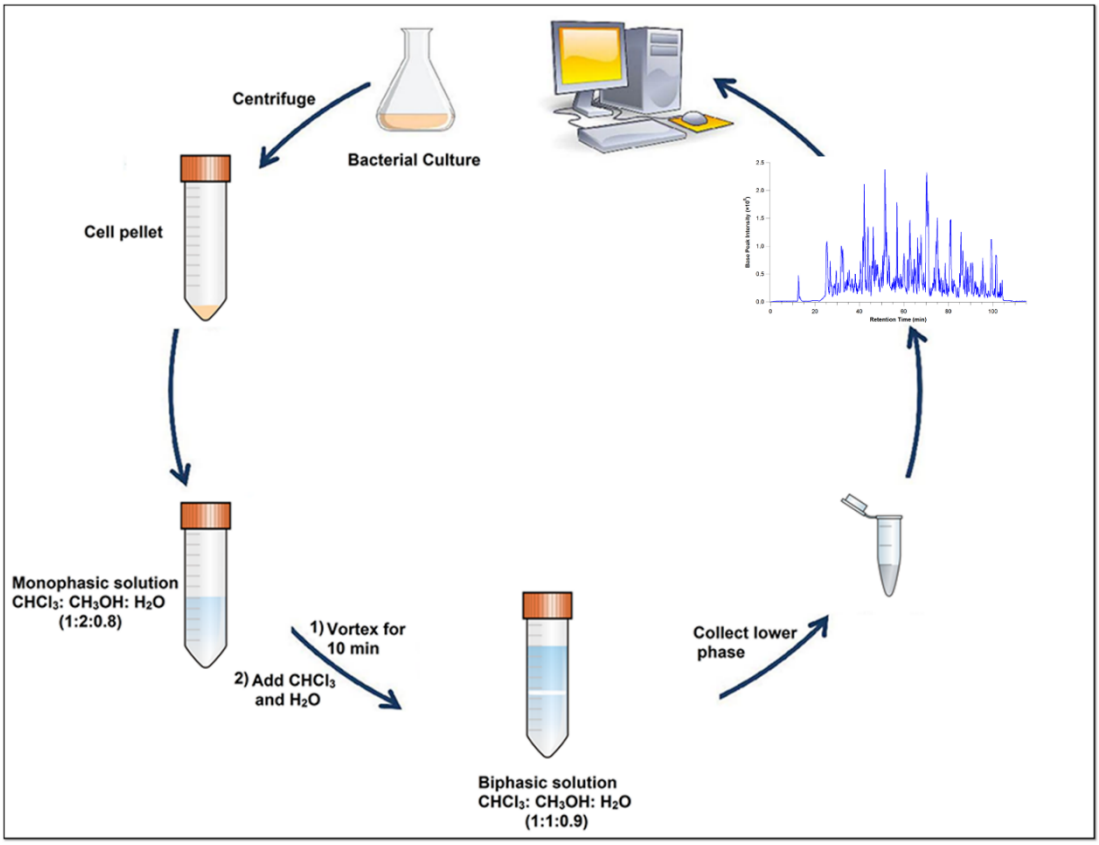

Figure 3.1: A schematic presentation of sample preparation process.

3.3.5 Live/ dead staining assay

To investigate the efficiency of the extraction procedure in lysing the cells, two dyes such as fluorescein diacetate (FDA) and propidium iodide (PrI) were used. FDA is specific for metabolic activity. The molecule itself is not fluorescent, however, live cells hydrolyse it into fluorescent fluorescein that emits green fluorescence. PrI is specific for membrane integrity. When the membrane is damaged, PrI enters the cell and binds to either DNA or RNA, as a result, a red fluorescence is observed. Therefore, three physiological conditions could be distinguished: i) viable cells with the intact membrane (green fluorescence), ii) dead cells (red fluorescence), and iii) injured cells which have a metabolic activity but their membrane is damaged (red and green fluorescence) (202).

Killed samples of yeast cells were prepared as follow: i) heat-killed controls, cell pellets (1 mL of cell culture of OD_{600} 1) were suspend in 1 mL phosphate buffered saline and place loosely capped in 70–80°C water bath for 10 min (used to construct the calibration curve), ii) alcohol-killed controls, cell pellets (1 mL of cell culture of OD_{600} 1) were suspended in 1 mL of 70% isopropyl alcohol and incubated at RT for 60 min, mixed every 15 min (used as positive control).

Cell pellets of live and heat killed samples were suspended in 1 mL of phosphate buffered saline. After that, 300 µL of FDA solution (stock solution of 5 mg/mL in acetone and diluted again to 10 µg/mL) and 15 µL of PrI solution (0.5 mg/mL) were added to the samples and incubated for 30 min at RT. Then, different volumes of the viable: killed cell suspension were mixed to prepare samples of 0, 20, 40, 60, 80 and 100% viability. The samples were analysed by plate reader (TECHAN SPARK10M, Switzerland) and the emitted fluorescent beams were collected at the appropriate wavelength (excitation at 480 nm for both dyes and emission wavelength at 525 and 635 nm for FDA and PrI emission respectively). The data were analysed by dividing the emitted green fluorescence (EF_{FDA}) by the emitted red fluorescence (EF_{PrI}) according to Equation 3.1. This ratio was plotted as $Ratio_{FDA/PI}$ versus percentage of viable cells in the suspension. Linear regression analysis was then performed to calculate the equation that can be used to calculate the viability % of extracted samples.

$$\mathrm{Ratio}_{\mathrm{FDA/PrI}} = \frac{\mathrm{EF}_{\mathrm{FDA}}}{\mathrm{EF}_{\mathrm{PrI}}} \ldots . \text{Equation 3.1}$$

Then, Cell pellet of culture samples (1 mL of OD_{600} ~1) were extracted and when the extract composition was chloroform: methanol: water (1:2:0.8), the samples were centrifuged for 10 min at 13000 *g*, and the liquid phase was discarded. Three replicates

of cell pellets of extracted samples, alcohol-killed controls and live cells were treated as mentioned before and the $Ratio_{FDA/PrI}$ was recorded to assess the efficacy of extraction.

3.3.6 Experimental design

3.3.6.1 Exploring the lipidome of different species

For each studied species, three biological replicates of cell culture at early stationary phase were extracted and analysed as detailed previously in section 3.3.4 and 2.3, respectively. The raw data for LC-MS/MS were acquired and visualised with Xcalibur 2.2 software (Thermo Scientific, Hemel Hempstead, UK). Detailed steps for data processing discussed in section 2.4, where the putative identification of lipid molecules from three replicates were aligned and compared against HMDB. Then the ^{13}C-enrichment of identified lipid ions from the three replicates were studied and evaluated.

3.3.6.2 The optimal source of internal standard mixture

Mixtures of different species extract (selected species only: *E. coli*, *S. cerevisiae* CEN.PK 113-7D and *P. pastoris*) were combined in 1:1 and 1:1:1 ratio to find out what is the possible ideal source/sources of IS in our work that can be used as reference for normalisation in quantitative lipidomics involved with clinical samples.

3.3.6.3 The effect of glucose concentration on lipids level

The growth pattern of *P. pastors* and its lipids level on three different glucose concentrations (0.5, 1, 1.5%) were studied and compared to the recommended glucose level (2%) (203). Three biological replicates of each condition were prepared and the OD at 600 nm were recorded each 2 h for 48 h. Meanwhile, samples at 36 h were taken from

the four conditions (*n*=3) and their extracts were analysed using untargeted LC-MS method described in section 2.3.

3.4 Results and discussion

3.4.1 Comparing the unlabelled and labelled extract of different species

3.4.1.1 *E. coli* MG1655

Comparing the *E. coli* Metabolome Database (ECMDB) (204) and Human Metabolome Database (HMDB) (205) revealed that, 376 species were found common between the two databases under the superclass "Lipids and lipid-like molecules" and "Organic compounds" Kingdom out of 2393 and 17856 found in each database respectively. This may indicate that the *E. coli* could provide a good coverage for human lipids enough to be used as internal standards. In real samples, this number could be different depending on sample type, extraction solvents, analytical methods used and so on. Figure 3.2 shows that the minimal media can support the growth of *E. coli* for at least 36 h and the early stationary phase starts after ~12 h of inoculation, where the samples for analysis can be taken.

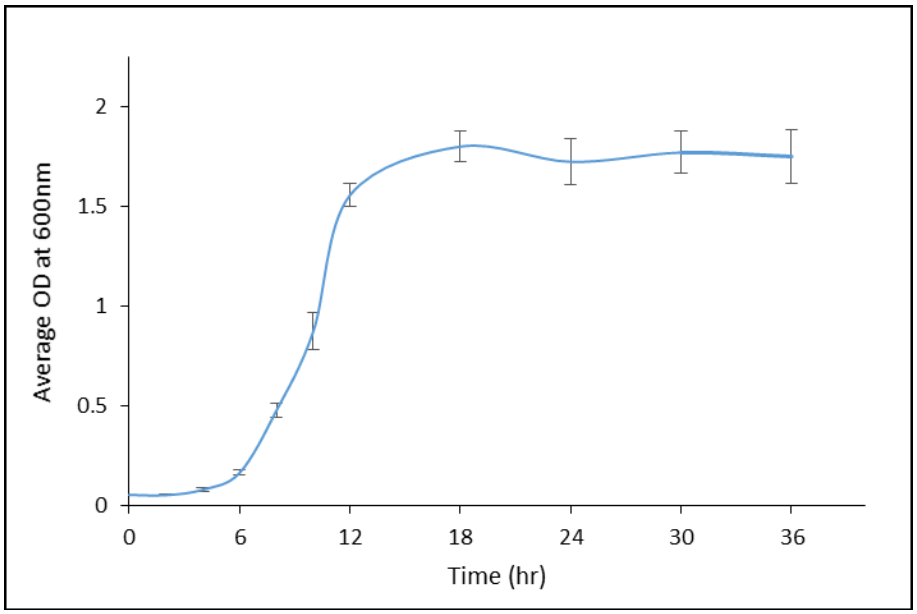

Figure 3.2: Growth curve *E. coli* MG1655 in minimal media (*n*=3). The OD_{600} of the culture was measured every 2 h for 36 h to investigate the growth rate of *E. coli* in minimal media. This media can support *E. coli* growth and the cells enter the stationary phase after ~12 h of inoculation.

After extraction and LC-MS/MS analysis of *E. coli* extract, 241 lipids were putatively identified. Figure 3.3 represents typical total ion chromatograms in ESI negative (A) and positive mode (B), and lipid molecules identified from *E. coli* extract (C). Di-glycerides (DG), phosphatidylethanolamine (PE), monoglycerides (MG) and phosphatidylglycerol (PG) were the most predominant common lipid ions between *E. coli* extract and HMDB. By exploring the phospholipids biosynthesis pathways in *E. coli*, it was found that the major glycerophosphate-based lipids were PE (70%), PG (20%) and cardiolipin (CL) (10%), and this could explain the small diversity of lipids identified in *E. coli* extract (206-208). The ^{13}C-enrichment of identified lipid ions when *E. coli* was grown in minimal media with ^{13}C-labelled glucose presented in Figure 3.4. 69% of lipid ions were efficiently labelled that can be used as IS. High ^{13}C-enrichment (more than 99%) could indicate good labelling efficacy of the studies molecules whearas lower than this percentage could indicate incomplete ^{13}C-labelleing that could affect the normalisation process or

complicate it. Zero ^{13}C-enrichment means that the studied lipid species was not found labelled and it cannot be used as IS in further normalisation steps and this could be for many reasons discussed latter. In theory, extended growth of *E. coli* in uniformly ^{13}C-labeled glucose will lead to complete labelling of many metabolites (192, 209). However, partially labelled forms are also present (6%), primarily due to ^{12}C- contaminant from the inoculum that used to set up an overnight culture (very unlikely) and from ^{12}C-contamination of the labelled glucose (<1%). The rest 36% of ions were not labelled at all or most probably these ions could be miss identified. If some lipids were mistakenly identified, then the expected assigned chemical formula could be wrong and so the number of carbon atoms could be wrong as well. So, their expected calculated fully labelled mass that used to record the presence of labelled lipids will be wrong, therefore those ions will be misguidedly considered as unlabelled. At this point, it seems that *E. coli* could be considered as a source of IS mixture for quantitative lipidomics involved with clinical samples.

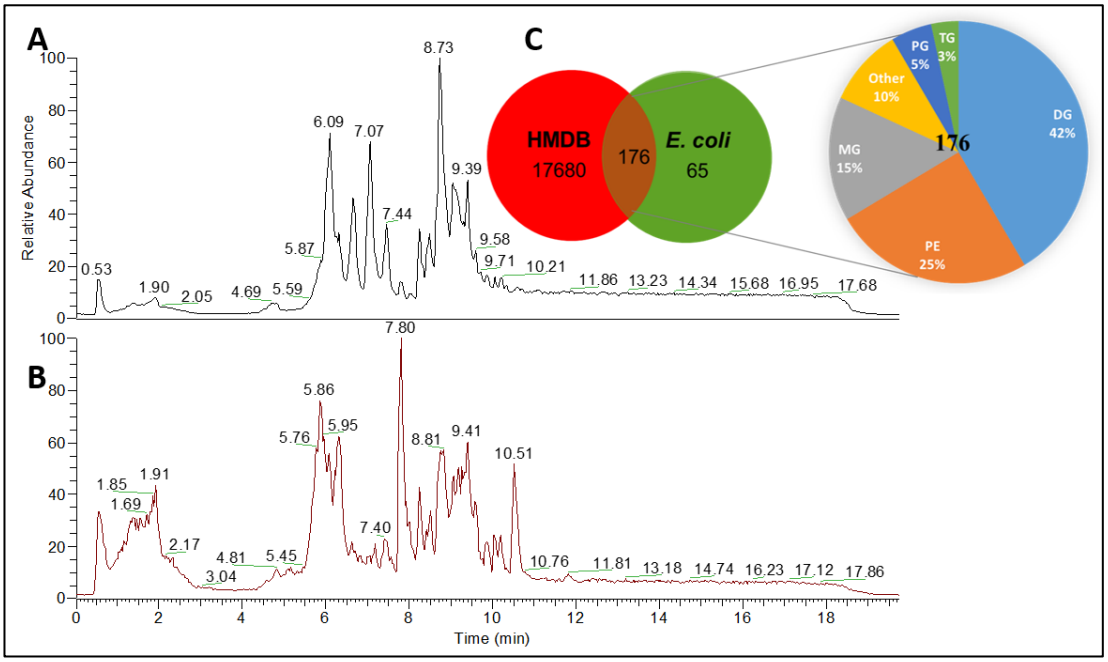

Figure 3.3: An example of total ion chromatogram of *E. coli* extract with ESI in negative (A), positive mode (B) and a pie chart (C) represents the common lipids identified by LipidSearch™ in positive and negative mode from *E. coli* extract and HMDB and their distribution into different lipid classes.

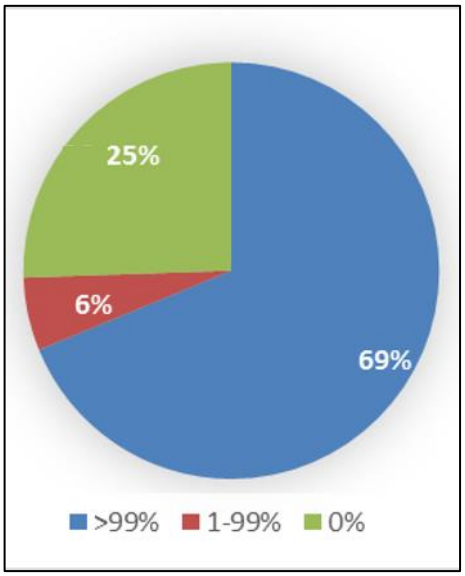

Figure 3.4: Pie chart represents the pattern of ^{13}C-enrichment of detected lipid ions in labelled *E. coli* extract. The blue legend means that 69% (97 ions) of the detected ions their ^{13}C-enrichment more than 99%, the red legend means that 6% (8 ions) of the detected ions their ^{13}C-enrichment between 1 and 99% while the green legend means that 25% (36 ions) of the detected ions the were not labelled and their ^{13}C-enrichment was zero.

3.4.1.2 Spirulina

Figure 3.5 represents an example of total ion chromatograms in ESI negative (A) and positive mode (B), and the lipid molecules identified from spirulina extract (C). TG (32%), PE (27%), DG (25%), PG (14%) and PC (12%) were the most predominant common lipid ions between spirulina extract and HMDB. Comparing the total ion chromatogram of spirulina (Figure 3.5) and *E. coli* (Figure 3.3), a relatively big qualitative difference in the spectra was seen that indicates that spirulina could provide different set of lipids that can be employed as IS. For example, PC were not present in *E. coli*. However, as can be seen in Figure 3.6 which represents the ^{13}C-enrichment of identified lipid ions in ^{13}C-labelled spirulina extract only 40 lipid ions were detected via parameters listed in section 2.4 and only 27 (67%) lipid ions were efficiently labelled. This small number of detected ions could be attributed to the fact that the extracted sample was small (5 mg) and it will be costly if simply more powder was used (1 g of spirulina whole cells (U-^{13}C, 97%) costs £375). Also, ^{13}C-enrichment of commercially available spirulina powders used in our experiment is only 97% and so each lipid has a chance of $(97\%)^n$ of being fully labelled, $(3\%)^n$ will be fully unlabelled and $1-((97\%)^n + (3\%)^n)$ will be partially labelled, where n represents the number of carbon atom in the lipid. Therefore, the probability of one lipid to be fully labelled will be less and the chances of partially labelled forms will be higher compared to the powder of ^{13}C-enrichment of 99%. Although the presence of partially labelled and unlabelled lipids will not hinder either absolute or relative quantification because an equal amount of IS mixture will be added to all samples, it is better to introduce high intensity fully labelled IS mixture as it will be further diluted when extracted with samples of interest. So, the cost and the available isotopic purity of the ^{13}C-labelled powder limit its use as a source of ISs.

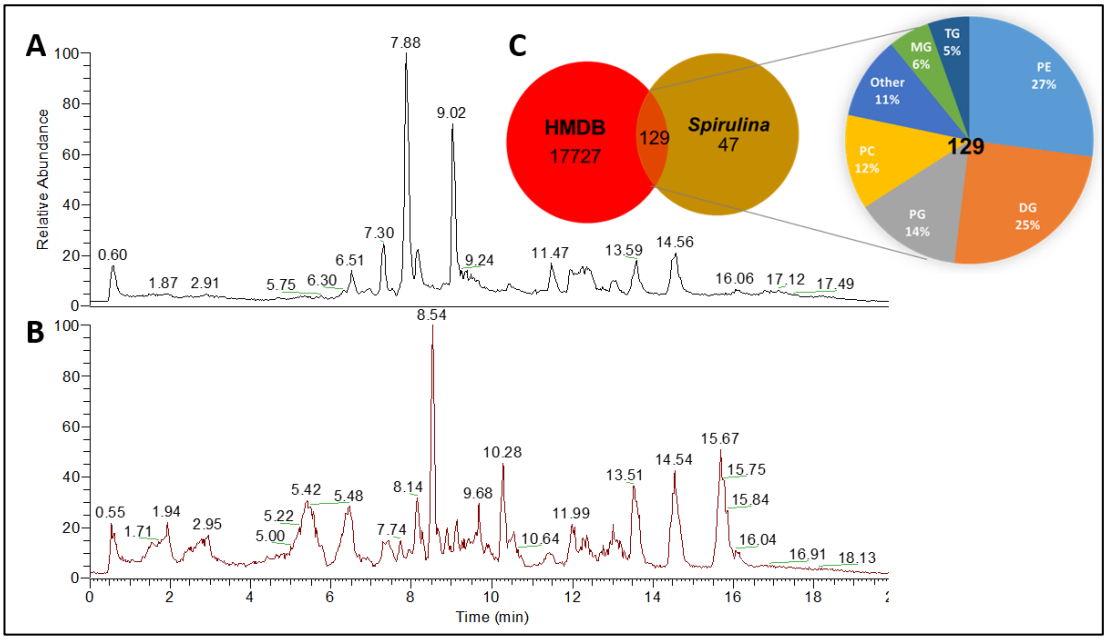

Figure 3.5: An example of total ion chromatogram of spirulina extract with ESI in negative (A), positive mode (B) and a pie chart (C) represents the common lipids identified by LipidSearch™ in positive and negative mode from spirulina extract and HMDB and their distribution into different lipid classes.

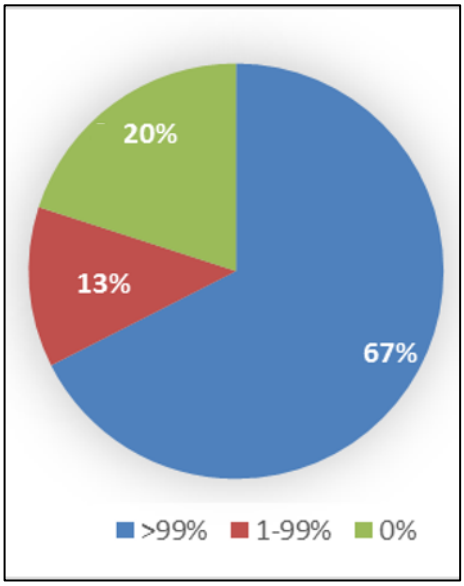

Figure 3.6: Pie chart represents the ^{13}C-enrichment of detected lipid ions in labelled spirulina extract The blue legend means that 67% (27 ions) of the detected ions their ^{13}C-enrichment more than 99%, the red legend means that 13% (5 ions) of the detected ions their ^{13}C-enrichment between 1 and 99% while the green legend means that 20% (8 ions) of the detected ions the were not labelled and their ^{13}C-enrichment was zero.

3.4.1.3 *S. cerevisiae*

Comparing the Yeast Metabolome Database (YMDB) of *S. cerevisiae* and Human Metabolome Database (HMDB) revealed that 845 species were found common between the two databases under the superclass “Lipids and lipid-like molecules” and “Organic compounds” Kingdom out of 2395 and 17856 found in each database respectively (205, 210). This may indicate that the *S. cerevisiae* could provide a good coverage for human lipids enough to be used as IS even better than *E. coli* as it could provide more common lipids with human samples. Although, as mentioned before, in biological samples this number could be different depending on sample type, extraction solvents, analytical methods used and so on. Two strains of *S. cerevisiae* were studied and compared: BY4741 and CEN.PK 1137D. Figure 3.7 shows that the selected media can support the growth of both strains for at least 36 h, where the early stationary phase starts after ~12 h of inoculation, where the samples for analysis can be taken.

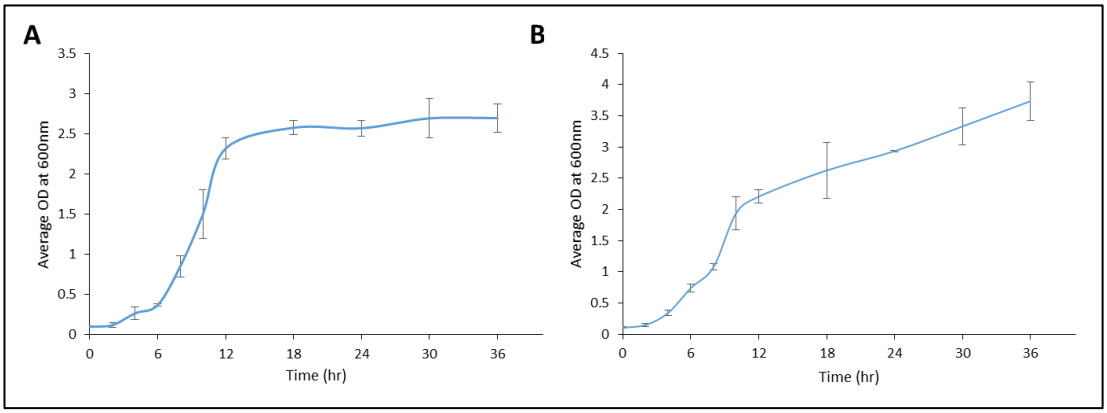

Figure 3.7: Growth curve of *S. cerevisiae* A) BY4741 and B) CEN.PK 113-7D in selected minimal media (*n*=3). The OD_{600} of both cultures was measured every 2 h for 36 h to investigate the growth rate of these species in previously described minimal media. For each strain, the used media can support their growth and the cells enter the stationary phase after ~12 h of inoculation.

By comparing the total ion chromatogram of the two strains in Figure 3.8, a huge difference in the spectra between the two strains can be seen, this could indicate that each strain could provide different set of lipids that can be used as IS. For BY4741 strain

different lipid composition was reported previously because cells were grown at different temperature, different media, different extraction and analysis used, leading to the different composition of lipidome (211). However, different lipid classes can be identified compared to *E. coli* and spirulina such as PS, PI and Cer that can increase the coverage of lipid analysis. Also, when the ^{13}C-enrichment of their detected ions (see Figure 3.9) was compared, both species were able to deliver a good number of fully labelled lipids that can be used as IS. However, the percentage of partially labelled ions in BY4741 strain was high and this could increase the complexity of sample matrix and the chances of ion suppression during analysis. This could be due to more ^{12}C-contaminant introduced during cell growth, for example , ^{12}C-contaminant from the inoculum that used to set up an overnight culture, ^{12}C-contamination of the labelled glucose (<1%), CO_2 fixation and the essential vitamins (unlabelled methionine, leucine, uracil and histidine) present in trace amounts in the medium used to grow *S. cerevisiae* BY474 (192, 209). For example, methionine, leucine and histidine will be degraded and finally converted into acetyl-CoA which is the precursor for fatty acid synthesis and elongation (212). In addition, uracil is used to synthesise uridine monophosphate and eventually they are degraded into urea or β-alanine (213, 214).

S. cerevisiae CEN.PK 1137D is a prototrophic strain that can synthesise its own amino acids so less ^{12}C-contaminant gets introduced into its metabolites/lipids. On the other hand, BY4741 cannot synthesise these amino acids and so they cannot be grown in the same media without these essential amino acids. The unlabelled form of these amino acids was added because the addition of ^{13}C-labelled form will be more expensive. Therefore only CEN.PK 113-7D strain will be considered as a possible source of IS mixture in quantitative untargeted lipidomics for clinical studies.

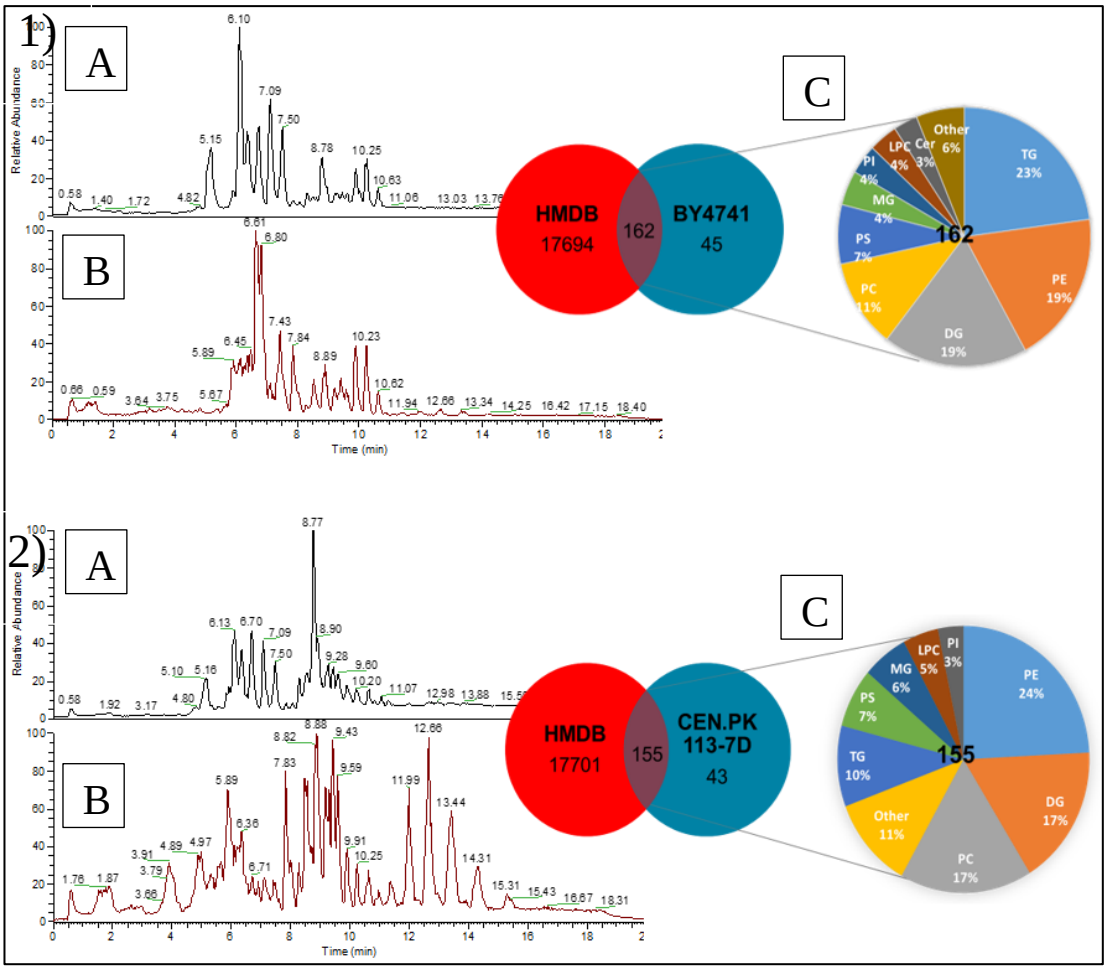

Figure 3.8: An example of total ion chromatogram of *S. cerevisiae* 1) BY4741 and 2) CEN.PK 113-7D extract with ESI in negative (A), positive mode (B) and a pie charts (C) represent the common lipids identified by LipidSearch™ in positive and negative mode from both strains compared to HMDB and their distribution into different lipid classes.

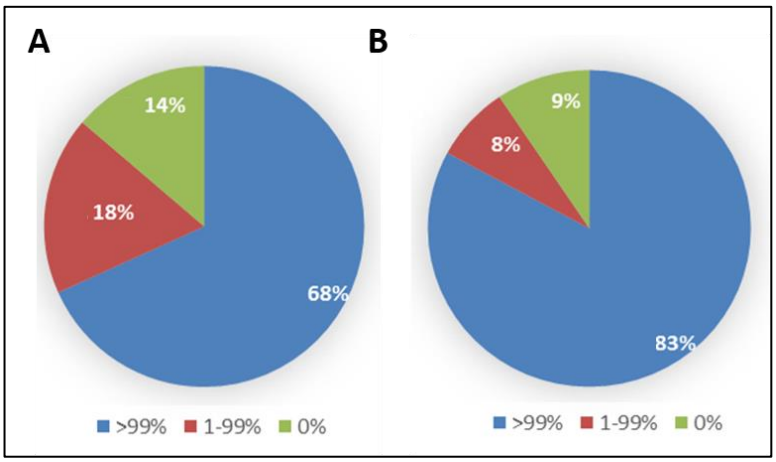

Figure 3.9: Pie charts represent the ^{13}C-enrichment of detected lipid ions in labelled *S. cerevisiae* A) BY4741 and B) CEN.PK 113-7D extract. The blue legend means that 68% (129 ions) and 83% (97 ions) of the detected ions their ^{13}C-enrichment more than 99%, the red legend means that 18% (34 ions) and 8% (9 ions) of the detected ions their ^{13}C-enrichment between 1 and 99% while the green legend means that 14% (26 ions) and 9% (11 ions) of the detected ions the were not labelled and their ^{13}C-enrichment was zero in *S. cerevisiae* BY4741 and CEN.PK 113-7D extract, respectively.

3.4.1.4 *P. pastoris* NCYC 175

As can be seen in Figure 3.10, the selected minimal media supported the growth of *P. pastoris* more than 2 days and the early stationary phase started after ~36 h of inoculation, where the samples for analysis were taken. Also, this species reached a higher OD than *E. coli* or *S. cerevisiae* (OD_{600} at 36 h of inoculation of 1.75, 2.70, 3.73 and 6.81 for *E. coli*, *S. cerevisiae* BY4741, *S. cerevisiae* CEN.PK and in *P. pastoris* respectively) indicating that more cells can be grown and therefore higher amount of lipids/IS mixture can be extracted.

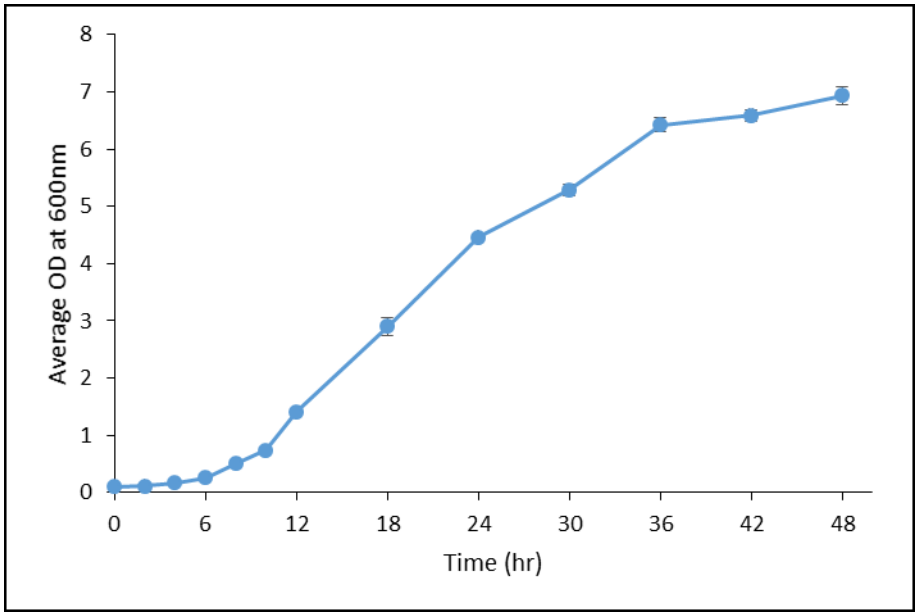

Figure 3.10: Growth curve of *P. pastoris* NCYC175 in selected minimal media (*n*=3). The OD_{600} of the culture was measured every 2 h for 48 h to investigate the growth rate of *P. pastoris* in minimal media. This media can support *P. pastoris* growth and the cells enter the stationary phase after ~36 h of inoculation.

After extraction and LC-MS/MS analysis of *P. pastoris* extract, 440 lipids were putatively identified, and 345 molecules were common with HMDB. Figure 3.11 shows typical total ion chromatograms of the species in ESI negative (A) and positive mode (B), and lipid molecules identified from *P. pastoris* extract (C). TG (32%), DG (15%), PC (14%), PE (11%)

and PS (7%) were the most predominant common lipid ions between *P. pastoris* extract and HMDB similar to previously reported data (150, 215-218). *P. pastoris* is an eukaryotic species that produces similar lipid profiles to mammalian cells and it is believed that it can provide a system that can mimic the eukaryotic lipid biosynthesis pathways better than *S. cerevisiae* (150, 219). TGs represent more than one third of the identified lipids in *P. pastoris* extract and much more than what can be detected in *S. cerevisiae*, and this agrees with previously published data, whereas non-polar lipids such as TG are found to be the major components of lipid droplets present in the yeast when cells are harvested in the early stationary growth phase (215). Since more lipids can be identified from *P. pastoris* compared to *E. coli* and *S. cerevisiae*, this can be advantageous to our work by extending the range of lipids intended to be normalised. Also, more lipids were found to be fully labelled and so more possible IS that can be used for more quantitative untargeted lipidomics associated with clinical samples (see Figure 3.12).

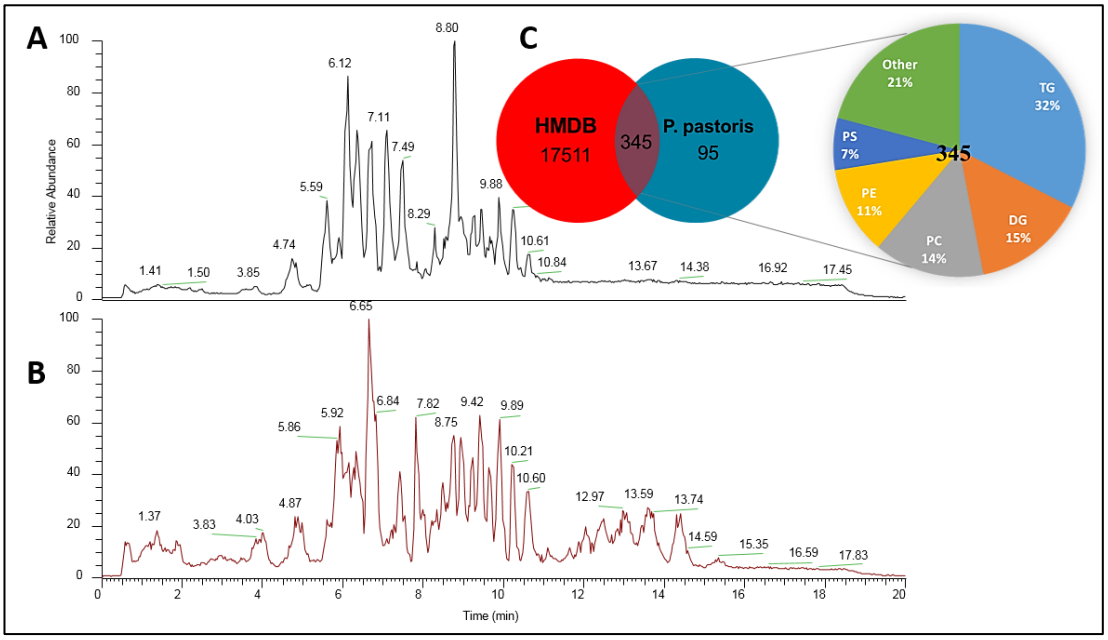

Figure 3.11: Total ion chromatogram of *P. pastoris* extract with ESI in negative (A), positive mode (B) and a pie chart (C) represents the common lipids between the extract and HMDB and their distribution into different lipid classes.

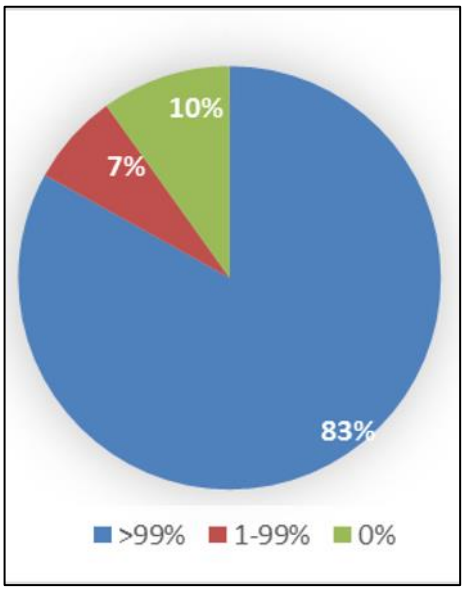

Figure 3.12: Pie chart represents the ^{13}C-enrichment of detected lipid ions in labelled *P. pastoris* extract. The blue legend means that 83% (260 ions) of the detected ions their ^{13}C-enrichment more than 99%, the red legend means that 7% (22 ions) of the detected ions their ^{13}C-enrichment between 1 and 99% while the green legend means that 10% (31 ions) of the detected ions the were not labelled and their ^{13}C-enrichment was zero.

3.4.2 The optimal source of internal standard mixture

Ideally, the same studied species is best to be used as a source of IS to ensure all relevant lipids are included in the analysis. However, for more complex species that cannot grow on one carbon source a combination of different IS source can be ideal as a IS source in order to increase the number of lipids that can be normalised. Among the selected species that showed both best lipid coverage and labelling efficacy (*E. coli* MG1655, *S. cerevisiae* CEN.PK 113-7D and *P. pastoris* NCYC 175), *P. pastoris* is considered as the best source of IS because it produces lipids that overlap more with higher eukaryotic lipidome in comparison to the other two species. However, mixtures of different species were analysed and compared, and their results are summarised in Figure 3.13 and Table 3.2. The lipid class profile of the unlabelled extract of the selected species and different mixtures of these species shown in Figure 3.13 state that each species contains different lipid profile and therefore could provide different set of labelled IS. For example, PE is the major lipid class identified in *E. coli* extract, PE and PC are equally detected in *S. cerevisiae* CEN.PK 113-7D extract while TG is the major lipid class detected in *P. pastoris* extract. Therefore, a mixture of two of these species or more could provide different set of lipids to expand the coverage of human lipids and potentially used as IS after proper labelling. However, although the number of identified lipid ions in the mixture of *P. pastoris* NCYC 175 and *S. cerevisiae* CEN.PK 113-7D extracts and in the mixture of *E. coli* MG1655, *P. pastoris* NCYC 175 and *S. cerevisiae* CEN.PK 113-7D extracts increased compared to the single species extract, the number of detected labelled ions in *P. pastoris* was comparable to other mixture samples. This could be because of the dilution process during samples preparation, ion suppression during analysis as highly abundant ions from different species could suppress co-eluted low abundant ions or because of

the similarity of detected lipids between the samples. It seems that a mixture of *P. pastoris* and *S. cerevisiae* CEN.PK 113-7D extract can provide the highest number of labelled ions but the high cost of growing and co-extracting *S. cerevisiae* CEN.PK 113-7D and *P. pastoris* with the slight increase in the number of labelled lipid ions makes this procedure less worth for a comprehensive source of IS in the future quantitative lipidomics studies. Therefore, *P. pastoris* was selected as an optimal source of IS mixture among the studied species for method validation.

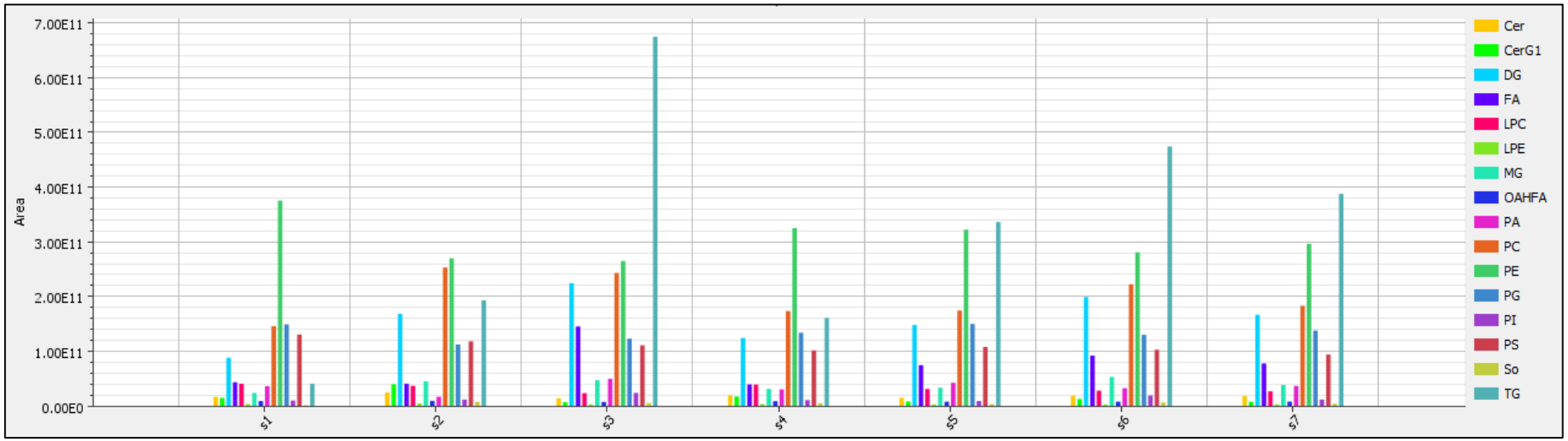

Figure 3.13: Lipid class profiles from *E. coli* MG1655, *S. cerevisiae* CEN.PK 113-7D and *P. pastoris* NCYC 175, and different combinations of these species. Abbreviations: S1- *E. coli* extract, S2- *S. cerevisiae* CEN.PK extract, S3- *P. pastoris* extract, S4- *E. coli* MG1655 and *S. cerevisiae* CEN.PK 113-7D extract mixture, S5- *E. coli* MG1655 and *P. pastoris* NCYC 175 extract mixture, S6- *P. pastoris* NCYC 175 and *S. cerevisiae* CEN.PK 113-7D extract mixture, S7- *E. coli* MG1655, *P. pastoris* NCYC 175 and *S. cerevisiae* CEN.PK 113-7D extract mixture

Table 3.2: Comparison between different mixtures of *E. coli* MG1655, *S. cerevisiae* CEN.PK 113-7D and *P. pastoris* NCYC 175 to find out the optimal source/sources of IS mixture (*n*=3).

Parameters	***E. coli***	***S.cerevisiae* CEN.PK**	***P. pastoris***	**ES***	**EP****	**PS*****	**EPS********
Number of identified lipid ions by LipidSearch™ (mean±SD)	187±2	313±8	401±13	334±3	379±15	409±7	418±8
Numbers of detected ions by Tox-ID (mean±SD)	134±2	253±3	356±3	268±1	325±4	383±24	311±29
Number of lipid ions with ^{13}C-enrichment ≥99% (mean±SD)	121±2	206±6	313±4	223±2	288±4	334±16	279±20

* ES stands for *E. coli* MG1655 and *S. cerevisiae* CEN.PK 113-7D extract mixture.

**EP stands for *E. coli* MG1655 and *P. pastoris* NCYC 175 extract mixture.

***PS stands for *P. pastoris* NCYC 175 and CEN.PK 113-7D extract mixture.

**** EPS stands for *E. coli* MG1655, *P. pastoris* NCYC 175 and *S. cerevisiae* CEN.PK 113-7D extract mixture.

3.4.3 Optimisation and characterisation of the optimal source of IS mixture

3.4.3.1 Optimising ^{13}C-labelled glucose concentration for efficient generation of labelled lipids

It is recommended to grow *P. pastoris* in a culture medium with 2% of the final glucose concentration (203)**.** However, in order to produce a wide range of ^{13}C-labelled lipids in a relatively low cost, the effect of glucose concentration on *P. pastoris* culture was evaluated. Three different glucose concentrations (0.5, 1, 1.5%) were studied and compared to the standard glucose level (2%). Although the cell density is not expected to change the type and amount of labelled lipids that *P. pastoris* can produce, a higher density means more cells and so higher amount of extract can be obtained from the culture. Figure 3.14 shows the growth rates of *P. pastoris* at the different growth conditions. *P. pastoris* was able to grow at 0.5 and 1% of glucose concentration but significantly lower biomasses were obtained. The growth rate and the biomass obtained at 1.5% of glucose concentration were comparable to the recommended condition with 2% of glucose concentration (except at point 36 h).

Also, the levels of 39 lipids identified from different lipid classes were monitored in different conditions, from equal samples collected after 36 h of inoculation and the results are summarised as a heat map in Figure 3.15. The lipids level between samples 1, 1.5 and 2% were comparable and there was no major significant difference between them. However, 8 lipids out of 39, showed a significant difference between samples grown at 0.5% of glucose concentration. A complete evaluation for the reasons behind these effects was not explored here as it is not our main purpose in this project. However, cells grown at different glucose concentrations at 36 h were at the different growth stages (early, mid or late stationary phase) leading to the composition changes

in selected lipids (220-222). Also, there was no significant difference (*p*-value > 0.05) between the samples in term of the total ion count and number of detected features from samples analysed (Table 3.3) when an equal amount (number of cells) were taken. Since the obtained TIC, number of detected features and the level of selected lipids from the extract of cells grown at glucose concentration of 1% were comparable to the extract of cells grown at glucose concertation of 2%, indicating that *P. pastoris* grown at glucose concentration of 1% could provide the same IS mixture as the reference. Although a lower biomass would obtain, the decrease in glucose concentration to half still can maintain an acceptable high growth rate. In conclusion, based on the various experiments, *P. pastoris* which was grown in minimal media with 1% of the final ^{13}C-labelled glucose concentration for 24 h was selected as the best source of internal standards to cover human metabolites. At these conditions, each 200 µL of the labelled *P. pastoris* extract will cost £1.38 which is much lower than buying commercially labelled standards.

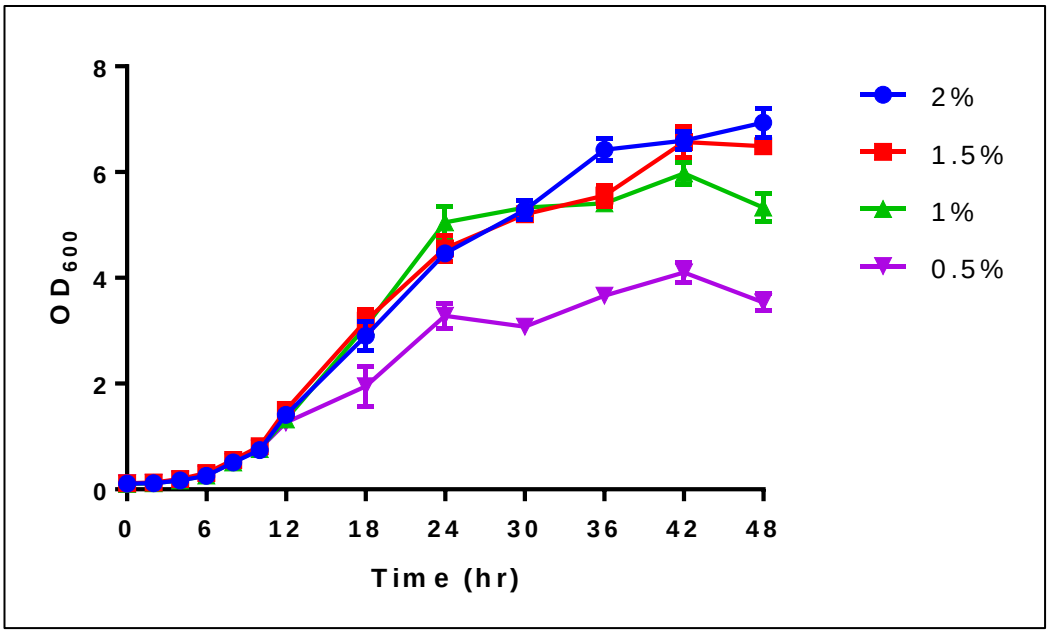

Figure 3.14: The effect of glucose concentration on the growth rate of *P. pastoris* based on the biomass production measured by the optical density at 600 nm (*n*=3).

Figure 3.15: Heatmap representing the effect of glucose concentration on the level of 39 putatively identified lipids detected in *P. pastoris* extract.

Table 3.3: The effect of glucose concentration on TIC and number of detected features in *P. pastoris* extract (*n*=3).

Glucose concentrations (%)	**TIC (mean±SD)**	**Number of detected features (mean±SD)**
2	1.58E12 ± 9.92E10	8622±201
1.5	1.47E12 ± 1.08E10	8761±469
1	1.45E12 ± 4.30E10	8259±127
0.5	1.41E12 ±1.87E10	8233±42

3.4.3.2 Efficacy of cell extraction

Figure 3.16 A and B illustrates the cell viability of *P. pastoris* culture before and after extraction and the calibration curve that used to extract such information, respectively. The figure shows that the yeast cells lose their viability (their cell membrane is disrupted, and their metabolic enzymes are inactive) after extraction. Previous studies used to mechanically disrupt the thick cell wall of the yeast in order to facilitate the extraction of intracellular metabolites and macromolecules (215, 223-225). This was according to previous finding that the cell cycle affects the efficacy of cell disruption where cells in the stationary phase are more resistant to disruption (225, 226). However, the used Bligh and Dyer method was able to break down the cell wall of the yeast and extracting its intracellular lipids which is one of the most critical steps in any metabolomics studies (140).

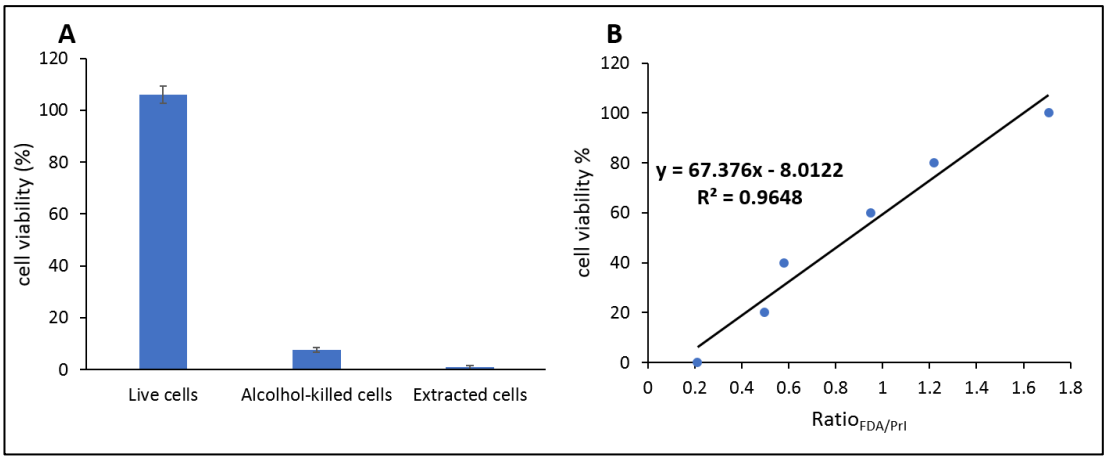

Figure 3.16: A) *P. pastoris* viability before and after extraction and B) the calibration curve that was used to record cell viability of extracted *P. pastoris* cells (n=3). Alcohol-killed cells serve as a positive control.

3.4.3.3 Characterisation of ^{13}C-labelled lipidome derived from *P. pastoris*

357 lipid ions were identified based on accurate fragmentation patterns by LipidSearch™. The detected lipids are fatty acyls (FA, (O-acyl)-ω-hydroxy fatty acids (OAHFA)), glycerolipids (MG, DG, TG), glycerophospholipids (CL, PA, PE, PC, PS, PG, PI, LPC, LPE, dimethylphosphatidylethanolamines (dMePE)), sphingolipids (Cer, glucosylceramides (CerG1), SM, sphingosine (SO)) in accordance to previously reported *P. pastoris* studies (150, 217). Then the fully ^{13}C-labelled lipid ions were assigned by accurate masses of the fully ^{13}C-labelled isotopologue of high-resolution LC-MS/MS data corresponding to the previously found accurate monoisotopic masses of the unlabelled endogenous lipid ions. Comparing MS/MS spectra obtained from unlabelled (Figure 3.17 A) and labelled (Figure 3.17 B) extracts, a mass shifted equivalent to 1.00335 Da increment per carbon atom present in the backbone of identified unlabelled lipid ions.

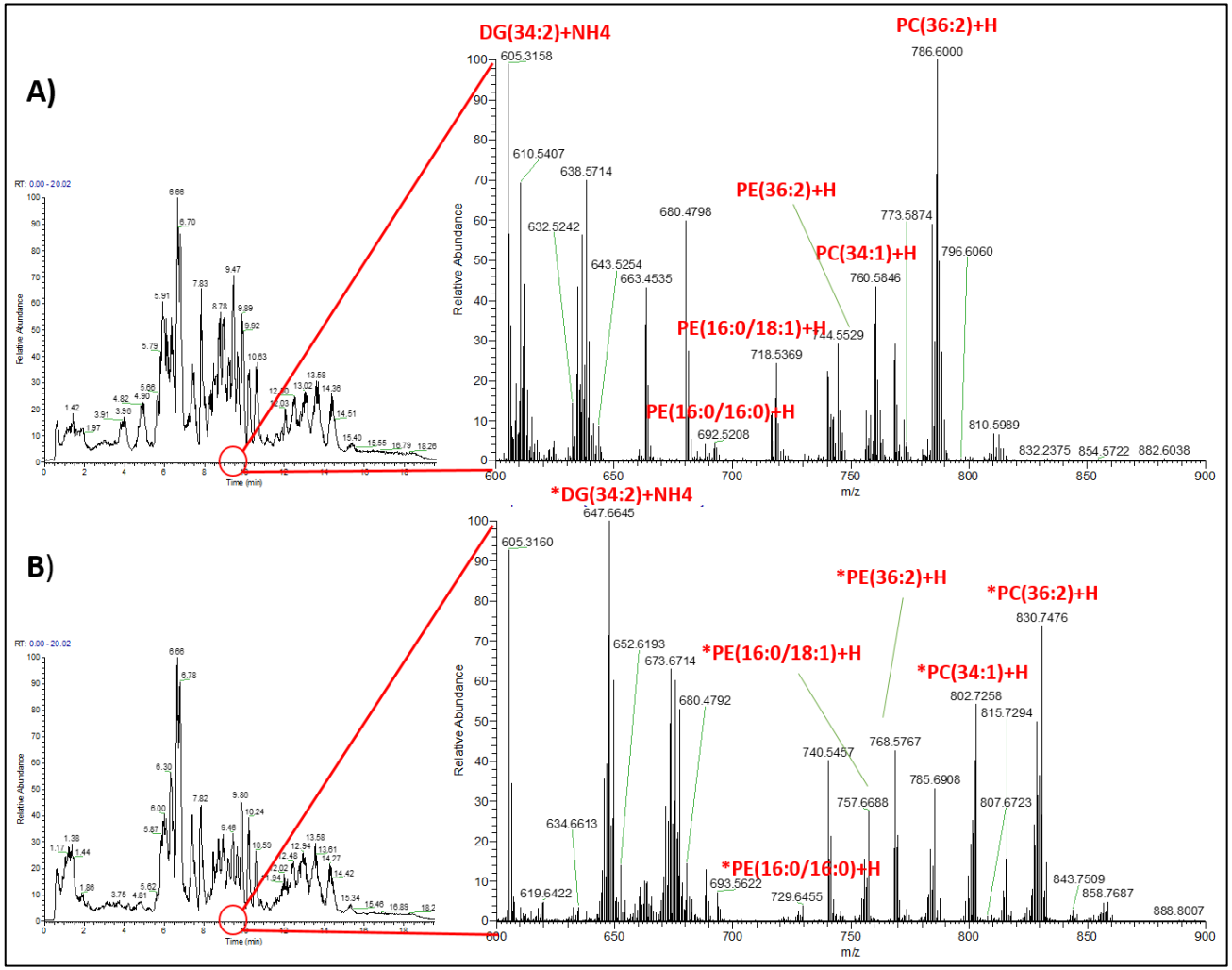

Figure 3.17: Comparison of full scan MS spectra and MS/MS spectra of recorded unlabelled (A) and labelled (B) *P. pastoris* extract in positive mode between 9-10 min within the *m/z* range of 600-900.

In order to assess the ^{13}C-labelling degree of the identified lipids and to understand why some of the identified lipids were not labelled, all isotopologues and their relative abundances were considered. The theoretical masses for these isotopologues were calculated corresponding to the previously found accurate monoisotopic masses of the unlabelled endogenous lipid ions. Then, the full labelling patterns of these identified lipids were evaluated. As expected for an ideal internal standard, retention times of unlabelled lipids and ^{13}C-labelled lipids should match as they share identical physiochemical properties. 246 ions of the labelled ions were detected in *P. pastoris* extract and their retention times were matched with those of the unlabelled ions (within ± 15 s). Furthermore, their detected monoisotopic masses were in excellent agreement with the calculated ^{13}C-masses within a mass error of ± 5 ppm, similar to what have been previously reported by Rampler *et al.* (152). The labelling patterns of these ions revealed an excellent ^{13}C-carbon labelling degree ≥ 98% (see Appendix, Table A.1). Ideally, high ^{13}C-labelling efficiency was expected. Exploring the labelling pattern of identified ions revealed that the other ions were either not labelled or partially labelled. However, this is unlikely because of incomplete labelling rather than incorrect lipid identification. Hence, the assigned number of carbon atom that used to calculate the ^{13}C monoisotopic masses of different isotopologues was wrong. Compound identification is still the bottleneck in LC-MS based metabolomics and lipidomics (227). Employing data dependent mode (MS/MS), the lipid class, fatty acyl-chain length, and the degree of unsaturation can be annotated using LipidSearch™ however, several false positives are still observed (228). Figure 3.18 represents a bar chart explaining the number of lipid ions expected to be accurately identified and misidentified ions based on their labelling pattern. PS is one of the misidentified classes in negative mode in LipidSearch™. Similar

false identifications were reported by Xu L. *et al.* (228). It was revealed that low abundance lipids like PS have a poor chromatographic behaviour and they are integrated from noise or poor peak shapes. Therefore, these lipids cannot be identified or quantified with high confident using the specified parameters that were used in this study. Thus, they suggest increasing the m-score up to 20 and the peak area threshold up to 5.00E06 in order to correctly identify these lipid species. Also, they stated that the m-score which is calculated in the software according to MS/MS fragment matching with its database could be misleading. According to the software developer, the higher the m-score is, the more confident the lipid identifications (229). Here, m-score is related to the number of fragments matched with the database. Therefore, due to the unique fragmentation of each molecular species, lipids that generate few fragments like FA will have a lower m-score compared to lipids that produce more fragments like TG. Therefore, different m-score thresholds should be used for different lipid classes to eliminate this type of unreliable results. Also, they stated that in-source fragmentation inside the Orbitrap and fatty acid dimerisation could be an alternative source to introduce misidentifications especially for dMePE and ChE and OAHFA (228). Hence, IS within mass error of 5 ppm of expected ^{13}C-fully labelled mass detected within RT window of 30 s of unlabelled identified peak will be used for normalisation.

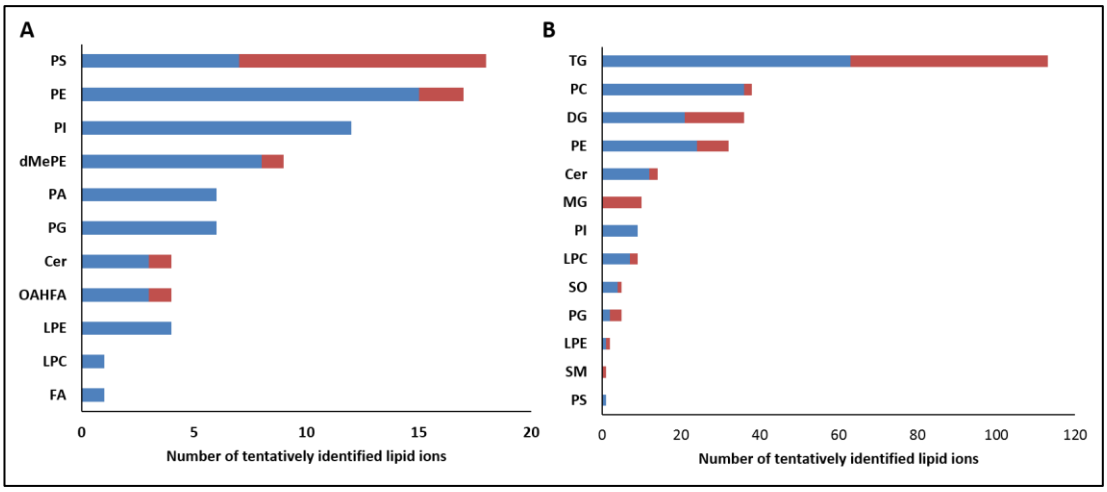

Figure 3.18: A bar chart explaining the number of lipid ions detected in A) negative mode and B) positive mode, expected to be truly identified (coloured in blue) and misidentified (coloured in red) by LipidSearch™ based on their labelling pattern.

3.5 Conclusion

In this chapter, a comparison of lipid profiles and the potential labelling efficacy for five of the most widely used species (*E. coli* MG 1655, spirulina, *S. cerevisiae* BY4741, *S. cerevisiae* CEN.PK 113-7D and *P. pastoris*) as a source of ISs for normalisation in untargeted analysis was presented. It is the first time that a comparison and optimisation of biologically-generated ^{13}C-labelled internal standards have been performed for untargeted lipidomics. It is clearly shown that there is a difference in lipid classes predominant in each species as well as their labelling efficacy. An *in vivo* labelling strategy was used to produce a wide range of isotopically labelled IS, a practical alternative to the expensive route of buying the synthetic form of these ^{13}C-labelled IS. Also, this technique can provide the isotopically labelled forms of different lipids that are not readily available in the market, leading the way toward comprehensive compound-specific normalisation in lipidomics. Although each species could be considered as a valuable source of IS mixture, *P. pastoris* NCYC175 was the optimum source of IS mixture in quantitative analysis in clinical samples, where it can provide more common lipids compatible with known lipids in biologically complex human samples and probably a

higher number of labelled lipids that can be used as IS for normalisation. The use of ^{13}C-labelled *P. pastoris* extract in the proposed normalisation approach will be investigated in the next chapter for its ability to reduce and correct technical/instrumental variations during extraction and analysis.

Chapter Four

Development and validation of an untargeted lipidomics method using ^{13}C-labelled internal standards for normalisation

4. Development and validation of an untargeted lipidomics method using ^{13}C-labelled internal standards for normalisation

4.1 Introduction

In analytical chemistry, measurement of a wide range of analytes in a given sample is never perfect due to measurement errors which can be broken down into two components: systematic and random errors (230). The systematic error generally caused by personal, method or instrumental inaccuracies which makes the mean of a data set differ from the true value. This type of error generally can be minimised or nearly eliminated by applying the proper experimental design. On the other hand, random error has no pattern and it is usually caused by factors that vary from one measurement to another, which makes the data to scatter more around a mean value, random error reasons are unknown and it generally can be reduced but not totally removed (105). However, in successful analysis, the random variance needs to be reduced as much as possible to the point that it is negligible compared to the biological variance (105).

Most MS platforms for metabolomics analysis, especially when coupled to GC or LC, suffer from unwanted variations regards accuracy and precision, batch-to-batch variations, run order effects, and poor reproducibility due to ion suppression/enhancement in ESI, the high dynamic range of metabolite concentrations and their short half-life (231-235). This results in an increase in experimental variation that is not linked to the studied factor and subsequently affects the quality of the data (236). Understanding the causes of these unwanted variations poses a great challenge in metabolomics research especially in the untargeted analysis where it is difficult to evaluate these variations and quantify

them when typically, hundreds or thousands of features are detected. Figure 4.1 represents the growing interest in addressing and correcting these variations in metabolomics/lipidomics studies.

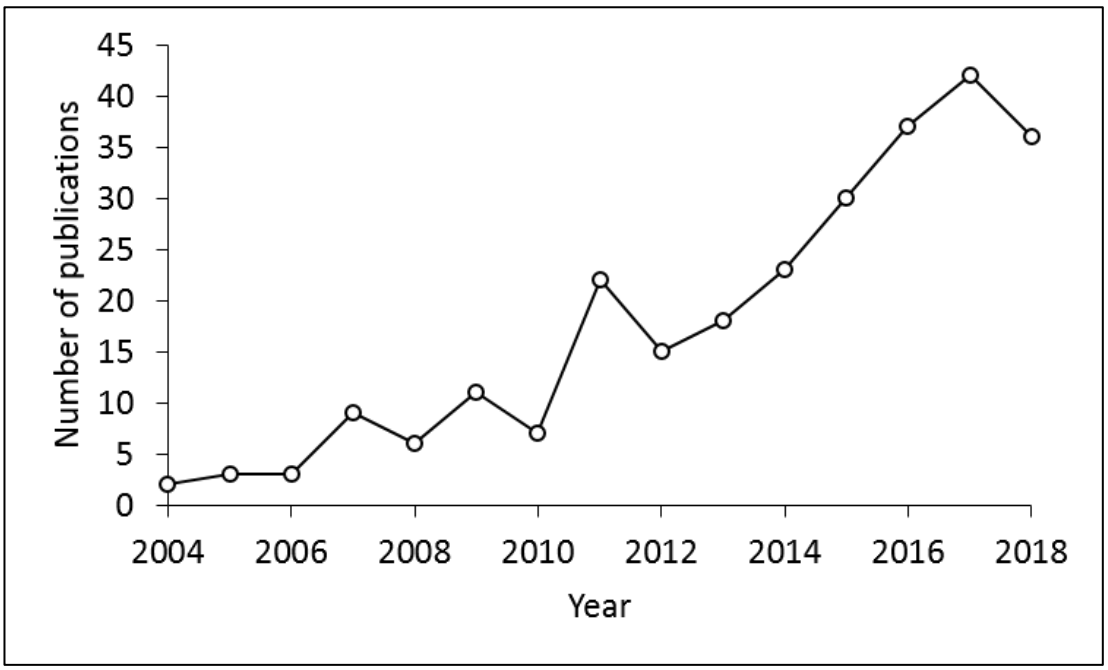

Figure 4.1: Literature survey of published articles that address the need for data normalisation in metabolomics studies. The search query was performed with keywords (normalisation/normalisation) in (metabolomics/lipidomics) from 2004 to 2018 via online analysis tool of Scopus searching platform.

Most types of errors are linked to some type of bias, which usually originates from poor initial experiment design, execution, analysis and interpretation of results and it is one of the main problems in metabolomics experiments (237). With regard to biological biases, samples selection and conditions are very common in metabolomics studies while for analytical biases, sample preparation is the most problematic step (237, 238).

Systematic and random errors are observed in almost every analysis. However, the degree and the direction of these changes depend on the metabolites. Some

metabolites show minimal drift while others drift severely, besides some metabolites show a linear increase in response over time, some show a linear decrease, and many others show a nonlinear change over time. In conclusion, it is advantageous to correct the response of each metabolite avoid or minimize these errors (105).

In targeted studies, obtaining absolute quantification for a specific set of metabolites would provide an accurate estimate of the selected metabolites and compensate for all errors introduced during sample preparation and analysis. The application of an appropriate IS is commonly used to assess and eliminate these variations (128, 231, 236). However, obtaining the absolute concentration of these metabolites using specific calibration curves using IS is difficult, that is because FDA requires at least six calibrator points in the same matrix as the studied samples, covering the quantitation range in every run, this could be very difficult to achieve in metabolomics studies especially when a large number of metabolites is included in the analysis or in large-scale cohort studies (28, 155, 233, 239, 240).

In untargeted studies, it is impossible to provide the absolute concentration of the studied features due to their huge number without prior knowledge of the limits of detection, limits of quantification, and linearity quantifiers (105). In addition, the chemical identities of these features are not known prior to data acquisition and hence it is impossible to use standards and construct a calibration curve for each feature (105). Therefore, as a prerequisite of untargeted studies, a sophisticated experimental design should be employed in order to consider all source of errors including samples' type, source, handling, collection, extraction and storage, method of analysis, data acquisition and data mining (241, 242).

Several normalisation approaches have been utilised to reduce random error in untargeted analysis including application of scaling factors (120, 243, 244), QC samples (124, 245), reference sample (246) or by using an IS or a mixture of IS (115, 118, 129, 140, 247). The increasing interest shown in the scientific literature towards various normalisation methods for untargeted metabolomics, this highlights the significance of this problem, however, it toughens the challenge for the analyst to choose the most appropriate normalisation method (236). However, all of the methods mentioned before except the use of IS are considered as post-acquisition normalisation methods which can correct instrumental variations introduced during analysis. The use of IS can be considered as post- and pre-acquisition normalisation method depending on the time when the IS was added into the samples (105). Therefore, if the IS or the IS mixture was added before sample extraction, it can be used to correct variations introduced from the beginning during sample preparation, storage and all through the analysis. However, In untargeted studies, it is difficult to use only one labelled standard because of the huge diversity of metabolite structures, concentration and composition, in addition it is impractical to assume that all the metabolites with different masses and physicochemical properties are subject to the same amount of variation as the standard (117, 118). Also, in lipidomics studies, different lipid species such as Cer, DG and SM can overlap due to inadequate chromatographic separation, and it is not practical to use the same normalisation factor on these species (118). In addition, non-polar lipid classes that do not have an ionisable head groups (like ChE, DG, TG) do not manifest identical response factors even at low concentration and their response should be determined in advance with respect to their acyl chain length and their degree of unsaturation which make the

analysis even more complicated (57, 133). Therefore, in order to obtain better results, more than one standard should be included in the analysis and preferably one IS for each lipid species or one for each lipid class. However, the cost and the availability of IS limit the use of this approach in untargeted analysis, hence, there has been significant recent interest in generating comprehensive mixtures of isotopically labelled IS *in vivo* to evaluate and correct instrumental variations introduced during samples preparation, storage and analysis (129, 140, 150). However, the ability of these labelled IS to reduce variations in complex biological samples has not been fully evaluated with respect to lipidomics studies.

4.2 Objectives

To evaluate the full capability of the optimised ^{13}C-IS mixture obtained by *in vivo* labelling strategy using *P. pastoris* in correcting various instrumental variations that could arise in untargeted lipidomics studies.

4.3 Materials and methods

4.3.1 Plasma extraction

Extraction was performed according to a modified method of Bligh and Dyer (99). Figure 4.2 represents a schematic presentation of the plasma extraction process.

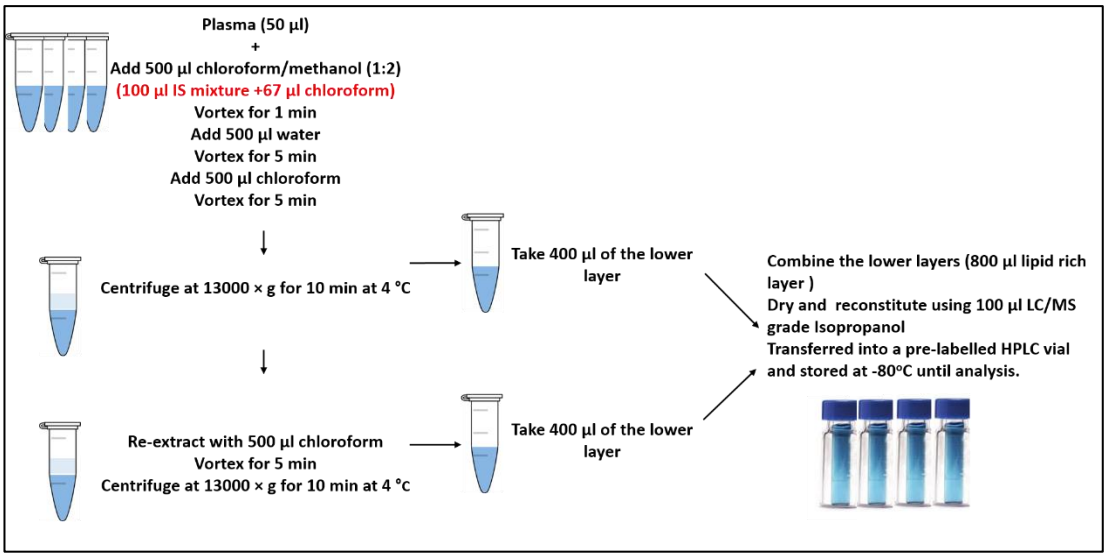

Figure 4.2: Flowchart describing plasma extraction process.

4.3.2 Optimisation of plasma: IS ratio

The amount of IS used is very critical; using too small or very large amount could lead to huge experimental errors and therefore it should be optimised to a certain range. If too little is used, then any small error carried with the IS amount will be amplified and this could results in a large variation of the final results, while if too much is used, this will lead to a matrix effect on endogenous species which will affect the quantification of low abundance species (57). Wang *et al.* proposed that the relative intensity of the added IS to the ion peak that corresponds to the most abundant species in the class should be in the range of 20-500% (57). However, in untargeted analysis with various lipid species with wide dynamic range, it is difficult to estimate the amount of IS that must be used especially when an *in vivo* labelling strategy was used to generate labelled lipid standards. The aim is to choose the lowest amount of "IS mixture" that can provide a higher number of standards with minimal ion suppression that can be considered as a cheaper alternative for commercially available labelled ISs which can be utilised in the high-throughput lipidomic analysis. The unlabelled extract of *P. pastoris* was used instead of the labelled extract to

simplify the analysis and the term “IS mixture” will be used to refer to it. Five ratios of water (50 µL): “IS mixture” were studied: 1:0.2, 1:0.5, 1:1, 1:2 and 1:3. In addition, different amounts of the “IS mixture” were extracted in the presence of plasma (50 µL) to assess the effect of ion suppression during analysis. A list of 166 lipid ions identified and detected previously in all replicates of *P. pastoris* extract, were used to monitor the effect of different dilution ratio. Tox-ID was used to report the intensity of the detected ions based on accurate mass scans with exact mass window (< 5 ppm), RT window (< 0.50 min) and intensity threshold (> 1E4).

4.3.3 Optimisation of SPLASH® amount

The SPLASH® supplied from Avanti® is pre-mixed deuterated internal standards (D-IS) that include all the major lipid classes at ratios relative to human plasma. This mixture provides a lipidomic analytical standard solution for human plasma lipids that can save money and time. According to the company it is supplied in a vial (1 mL after reconstitution with methanol) that is enough for 100 plasma samples (10 µL per sample). List of IS’s present in the solution is shown in Table 4.1. 10 µL of SPLASH® solution was diluted in 90 and 40 µL isopropanol to obtain a dilution of 1:10 and 1:5, respectively, they were then analysed and the signal of the IS’s were compared. Also, the effect of biphasic extraction and inefficient recovery (as described in section 4.3.1 but without the plasma or the IS mixture) on the signal of the IS mixture was studied and compared to the non-extracted SPLASH®.

Table 4.1: List of deuterated compounds present in SPLASH® solution.

Compound name	Chemical formula	Exact mass
PC 15:0-18:1(d7)	$C_{41}H_{73}D_7NO_8P$	752.6054
PE 15:0-18:1(d7)	$C_{38}H_{67}D_7NO_8P$	710.5584
PS 15:0-18:1(d7)	$C_{39}H_{66}D_7NNaO_{10}P$	776.5302
PG 15:0-18:1(d7) (Na Salt)	$C_{39}H_{67}D_7NaO_{10}P$	763.5349
PI 15:0-18:1(d7) (NH_4 Salt)	$C_{42}H_{75}D_7NO_{13}P$	846.5958
PA 15:0-18:1(d7) (Na Salt)	$C_{36}H_{61}D_7NaO_8P$	689.4982
LPC 18:1(d7)	$C_{26}H_{45}D_7NO_7P$	528.3913
LPE 18:1(d7)	$C_{23}H_{39}D_7NO_7P$	486.3444
ChE 18:1(d7)	$C_{45}H_{71}D_7O_2$	657.6434
MG 18:1(d7)	$C_{21}H_{33}D_7O_4$	363.3359
15:0-18:1(d7) DG	$C_{36}H_{61}D_7O_5$	587.5499
15:0-18:1(d7)-15:0 TG	$C_{51}H_{89}D_7O_6$	811.7639
d18:1-18:1(d9) SM	$C_{41}H_{72}D_9N_2O_6P$	737.6388
Cholesterol (d7)	$C_{27}H_{39}D_7O$	393.3981

4.3.4 Experimental design

4.3.4.1 The effect of normalisation by ^{13}C-IS mixture on plasma samples

Plasma samples (50 µL, *n*=6) (three sets of samples were used: human plasma, mouse plasma and pooled human plasma) were extracted in the presence of labelled yeast extract (^{13}C-IS, 100 µL) (1:2 ratio) and of SPLASH® (20 µL) (only in small set of samples due to its high cost). Then all sets of groups were analysed on the Q-Exactive as described previously in section 2.3. Lipid ions in plasma samples extracted without any IS were identified by LipidSearch™ and TF was used to obtain the peak area of the ions (unlabelled, ^{13}C-labelled and deuterated). Although a high mass shift is expected to be introduced by ^{13}C or D-labelling, to ensure that there are no spectral overlays between the selected endogenous unlabelled ions identified in plasma samples and the labelled IS (^{13}C-IS or D-IS from SPLASH® solution) in order to distinguish between the endogenous unlabelled ions and the labelled-IS by the instrument and to ensure that the labelled-IS are absent in the samples of interest to avoid isotopic interferences from the naturally occurring metabolite in the quantification of compounds of interest (248, 249), the following criteria were used:

unlabelled ions detected in three or more replicates from the same group were included in the analysis, average response of unlabelled ion mass in plasma extract over its response in blank samples >10 (S/N=10) and average response of unlabelled ion mass in plasma extract over its response in ^{13}C-IS (or D-IS) extract >10.^{13}C-IS (or D-IS) detected in all replicates were included in the analysis, average response of labelled ion mass in plasma extracted in the presence of ^{13}C-IS (or D-IS) extract over its response in blank samples >10 (S/N >10) and average response of labelled ion mass in plasma extracted in the presence of ^{13}C-IS (or D-IS) extract over its response in plasma extracted without ^{13}C-IS extract >10. Then, these unlabelled identified ions were normalised by TIC, ^{13}C-IS or deuterated lipids and compared to non-normalised data. For normalisation by TIC, the TICs of the samples were calculated from imported data using Xcalibur in positive and negative modes. Ions detected in positive and negative modes were normalised by dividing their peak area by the TIC corresponding to that mode. For normalisation by ^{13}C-IS, lipids ions that their U-^{13}C-labelled form was found in the yeast extract they were normalised by dividing their peak area by the peak area of the labelled form. For the other lipids, which their ^{13}C-labelled form was not found in the yeast extract, a representative IS (the most intense IS) from each lipid class from the common ions were selected and used to normalise ions identified in the same class. For normalisation by SPLASH®, the detected peak area of the D-ions was used to normalise ions detected in the same class. When one lipid class was not detected or was not included in SPLASH® solution, a deuterated ion from other similar class was used for normalisation.

4.3.4.2 The effect of different extraction methods on normalisation by ^{13}C-IS mixture on pooled plasma samples

To test the ability of ^{13}C-IS in reducing variations introduced by different extraction methods, samples were extracted using two methods. The first one (dried samples), the samples were extracted as detailed in section 4.3.1, where the samples were double extracted, their extract was concentrated, and the chloroform was replaced by LC-MS grade isopropanol. The second method (non-dried samples), 50 µL of plasma samples were subjected to single extraction step (using 500 µL chloroform: methanol (1:2) followed by 500 µL water and 500 µL chloroform). After centrifugation, an aliquot of the lower lipophilic phase was mixed with an equal volume of LC-MS grade isopropanol prior to analysis without subsequent evaporation and reconstitution steps. For simplicity, only unlabelled ions that their ^{13}C-labelled form was detected in all replicates were included in the analysis (compound-specific normalisation). To avoid spectral overlays between the selected indigenous unlabelled ions identified in plasma samples and the labelled IS (^{13}C-IS), similar criteria for selection of unlabelled and labelled IS were used as detailed in section 4.3.4.1.

4.3.4.3 The effect of normalisation by ^{13}C-IS in reducing variations introduced during sample preparation and LC-MS analysis on pooled plasma samples

In metabolomics studies, especially in large scale studies, sample preparation could introduce variations between the samples. For example, in one study the plasma metabolome had a distant significant change when the blood was exposed at RT for up to 24 h while no changes were observed when the blood was placed in ice water up to 4 h (250). Therefore, when it is possible, samples analysed in one batch should

be prepared at the same time in order to reduce potential errors observed during sample preparation (28). To test the ability of ^{13}C-IS extract in reducing variations that could be introduced during samples preparation, 101 samples from a pooled human plasma sample were extracted in the presence of ^{13}C-IS extract as detailed in section 4.3.1 and analysed. To ensure that the analysis order does not correlate with sample preparation order, samples were randomised during analysis (28). Then, to test the ability of ^{13}C-IS extract in reducing variations the could be introduced during samples analysis, 230 injections of a pooled extract of human plasma samples extracted in the presence of ^{13}C-IS extract prepared were analysed over more than 77 h. After that, to test the ability of ^{13}C-IS extract in reducing instrumental day to day variations, 15 replicate injections of a pooled extract of human plasma extracted in the presence of ^{13}C-IS extract prepared were analysed on three different days (Day 0, 7 and 14). Three replicates from pooled plasma were extracted without ^{13}C-IS and used for lipid identification. For simplicity, only unlabelled ions that their ^{13}C-labelled form was detected in all replicates were included in the analysis (compound-specific normalisation). To avoid spectral overlays between the selected indigenous unlabelled ions identified in plasma samples and the labelled IS (^{13}C-IS), similar criteria for selection of unlabelled and labelled IS were used as detailed in section 4.3.4.1. Samples were stored at -20°C till analysis.

4.3.4.4 The effect of global ^{13}C-IS normalisation

Previously, for simplicity and ease of calculations, only unlabelled ions detected in 50% or more of the samples and their U-^{13}C-labelled respective form detected in all replicates were normalised and compared. However, to test the ability of ^{13}C-IS

mixture to reduce variations that are introduced during sample analysis globally, all unlabelled ions detected in 50% or more of the samples in long run (when 230 injection of pooled plasma sample were analysed over more than 77 h) were normalised and compared to non-normalised data regardless if the ^{13}C-labelled forms were detected or not.

In that experiment, 423 unlabelled ions were detected in 50% or more of the injections and 100 labelled ions were detected in all samples that can be used for compound-specific normalisation directly or non-compound-specific normalisation (when different ^{13}C-IS is used to normalise unlabelled endogenous ions once the U-^{13}C-labelled form of that ions cannot be detected or cannot be labelled in the yeast extract). These unlabelled ions were normalised by TIC and by ^{13}C-IS as described in section 4.3.4.1. However, for normalisation by ^{13}C-IS, when the U-^{13}C-labelled form of a specific lipid was not detected in all replicates, this lipid was normalised using one of the ^{13}C-IS detected in all replicates either based on RT alone or based on RT taking into account chemical similarity (or class similarity). When ions were normalised by RT, their peak areas were divided by the peak area of nearest ^{13}C-IS detected in that ionisation mode whereas when they were normalised by RT based on chemical similarity, their peak area was divided by the peak area of nearest ^{13}C-IS from the same lipid class detected in that ionisation mode. When no ^{13}C-IS detected in one or more lipid class, unlabelled ions in those classes were normalised by the nearest ^{13}C-IS detected in that ionisation mode.

4.3.5 Method evaluation

The performance was assessed by comparing the CV% across all metabolites and replicates. CV% was calculated in an Excel sheet based on Equation 4.1. where σ is the standard deviation and $\bar{x}$ is the grand mean response of the metabolite (251).

$$\mathrm{CV\%} = \left(\frac{\sigma}{\bar{x}}\right) * 100 \ldots . \text{Equation 4.1}$$

The results were plotted as a whisker plot that facilitates visual comparison of CV% from multiple normalisation datasets where lines represent the lower quartile, median and upper quartile values and the whiskers were used to display the minimum and the maximum value. The data also were visualised by a Histogram of CV% values that can clarify the CV% distribution more clearly. Friedman test, a nonparametric test that compares three or more matched groups was used to assess the difference between different normalisation methods (252, 253). Wilcoxon matched pairs test, a nonparametric test that compares two paired groups (252).

MetaboAnalyst has been used to perform unsupervised principal component analysis (PCA) when applicable to evaluate the similarity between different data sets and to assess the impact of different normalisation on the expected variation in the analysis (254). LC-MS spectral data can be described as a data matrix *X*, containing variables *K* with observation *N* for each variable. In PCA analysis, in order to yield interpretable results, these multidimensional data are projected to a reduced new set of uncorrelated orthogonal variables known as principal components (PCs) while retaining as much information as possible. The data were mean centered, scaled using Parito scaling factor and subjected to log transformation to restore normality.

The primary goal of PCA is to identify patterns or class differences from a multivariate dataset (255, 256) .

4.4 Results and discussion

4.4.1 Optimisation of plasma extraction protocol

Figure 4.3 represents the total ion chromatograms of non-dried and dried samples. A marked difference was seen in the chromatogram especially at early RT (at 1.09 min and between 5-7 min where chloroform and LPC were expected as marked by the red circles in Figure 4.3) that could be due to incompatibility of the chloroform with the used column and mobile phases. This was confirmed by the number of identified ions by parent ion search using LipidSearch™ in both groups, where a higher number of ions were identified in the non-dried sample compared to dried sample (see Table 4.2). Also, this could explain why in dried samples, the significantly higher number (*p*-value 8.09E-06) of ions were identified by product search compared to non-dried samples. It seems that in non-dried samples, due to lipids partition when chloroform moves across the column carrying with it some of the lipids, their intensity at the original RT decreases, and therefore they are no longer identified by LipidSearch™ at the used parameter (S/N of 2). Also, the TICs of the dried samples were higher than those in non-dried samples because of chloroform removal, sample double-extraction and extract concentration that could improve the sensitivity and therefore more ions could be identified. These finding can be supported by untargeted analysis of the samples where more features can be detected with high reproducibility in dried samples compared to non-dried samples. Therefore, to avoid lipid partition and possibly double identification and to improve the sensitivity, plasma samples will be

extracted as detailed in section 4.3.1 to include evaporation and reconstitution stages.

Table 4.2: The effect of chloroform removal on the number of detected features in untargeted analysis and on the number of identified lipid ions by LipidSearch™.

Parameters	Plasma (non-dried)	Plasma (dried)
Number of identified ions by LipidSearch™		
Parent search (***n***=1)	1284	950
Product search (***n***=3) (mean±SD)	312±3	415±5*
Detected features		
Feature detected in all replicates (mean)	8200	9245
Features detected with CV% ≤30 (mean)	75%	82%

*Significantly different (*p*-value 8.09E-06).

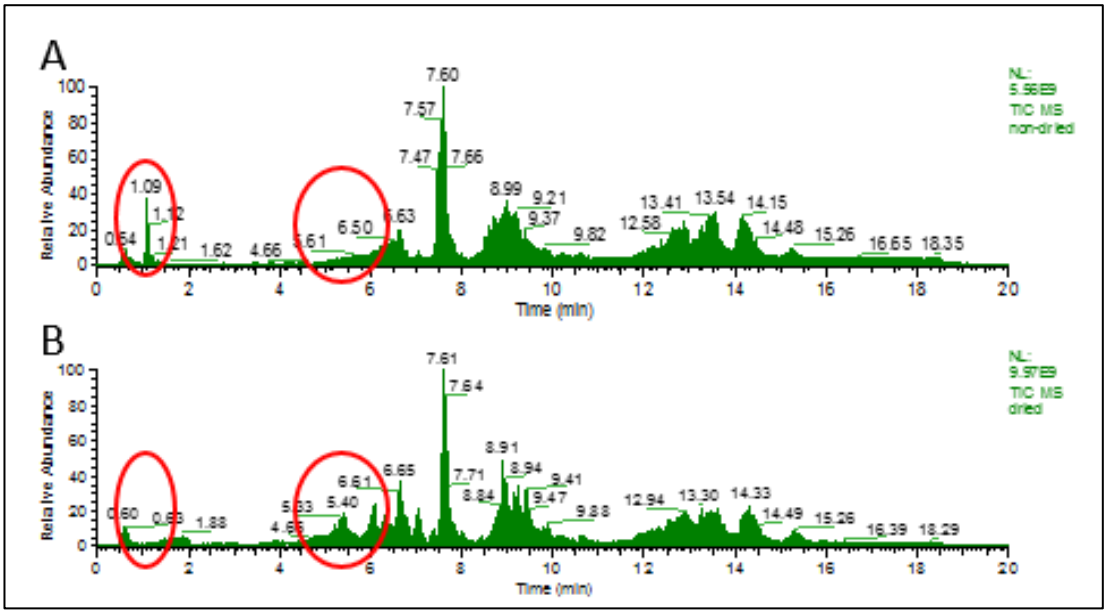

Figure 4.3: The effect of chloroform removal on the total ion chromatogram. A) represents a chromatogram of non-dried human plasma extract. B) represents a chromatogram of a dried human plasma extract. The red circles mark the major difference seen in the chromatogram between the dried and non-dried plasma extract at 1.09 min and between 5-7 min where the chloroform and LPC species were expected to appear respectively.

In addition, a closer look at the list of identified ions in non-dried samples (see appendix, Table A.2), 14 ions (mostly LPC) were detected at ~1.1 min with high intensity. This was not expected as LPC are known to be retained at the used column (ACE Excel 2µm super C18 column, 50 × 2.1 mm, pore size 100 Å, Advanced Chromatography Technologies Ltd, Scotland, UK) and they should be seen later

around 4-6 min. Also, some of these ions were detected with high confidence at different RT. For example, LPC(18:3)+H (*m/z* 518.3241) was detected at 1.14 and 5.39 min (Figure 4.4A) and LPC(20:4)+H (m/z 544.3397) was detected at 1.15 and 4.67 min (Figure 4.4B).

Although lipid isomers could explain this behaviour, the exclusivity of these observations to LPC only and knowing that chloroform is not retained on C18 column excludes this reason. Therefore, these observations could be due to incompatibility of the chloroform with the used column (ACE Excel 2µm super C18 column, 50 × 2.1 mm, pore size 100 Å, Advanced Chromatography Technologies Ltd, Scotland, UK) and mobile phases. As the chloroform carrying the sample moving across the column, the lipids start to partition between isopropanol (mobile phase B) and chloroform. It seems that LPC favour the chloroform and so most of them were eluted at the same time (see Figure 4.4C). Since the time for this process is short, sometimes incomplete partition happens and therefore some of the ions with high intensity retained at different RT and eventually identified by LipidSearch™ again. Also, it seems that this process is variable as it can be seen from the peak area of the identified lipids in three replicates as seen in Figure A.1 in Appendix, which could highly affect any further analysis and normalisation

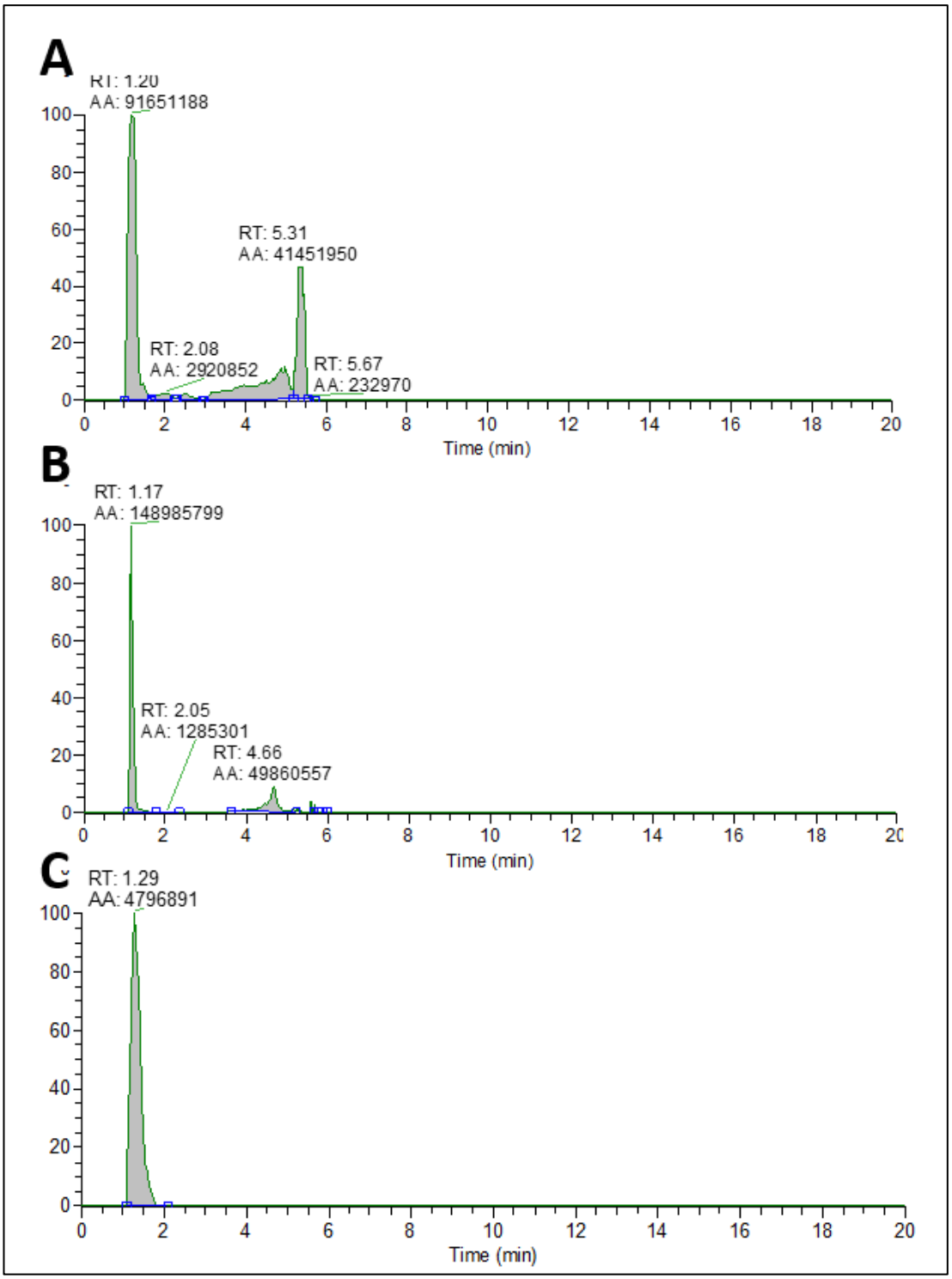

Figure 4.4: The effect of chloroform on the detection of A) LPC(18:3)+H (*m/z* 518.3241), B) LPC(20:4)+H (*m/z* 544.3397) putatively identified by LipidSearch™ in positive mode in plasma extract and C) represents the chloroform peak detected in negative mode (*m/z* 116.9071).

4.4.2 Optimisation of plasma: ^{13}C-IS mixture ratio

Figure 4.5 represents the number of detected ions when a different amount of unlabelled extract was extracted with and without plasma. When "IS mixture" was extracted without plasma (water), the higher the amount used, the more ions can be detected. However, the number of detected ions in samples of 1:2 and 1:3 were similar (*p*-value 0.2909). For "IS mixture" extracted in the presence of plasma, the higher the amount used, the more ions that can be detected. However, there was no significant difference between the number of detected ions from different ratios, fewer ions were detected compared to samples extracted without plasma due to ion suppression from plasma matrix. So, the optimum dilution of the "IS mixture" that is expected to provide a high number of labelled IS's with minimal ion suppression is 1:2 and this optimised ratio was used in subsequent experiments.

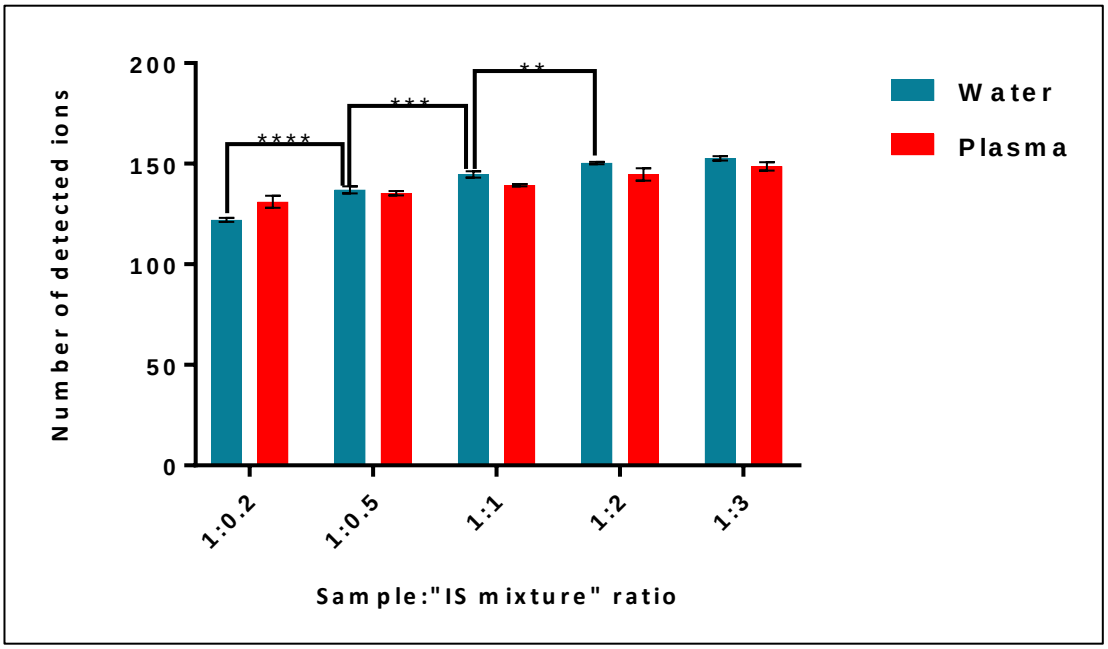

Figure 4.5: The number of detected ions when a different amount of "IS mixture" was extracted with plasma and without plasma (referred to as water) at five dilution ratios (*n*=3). The black stars represent the significant difference in the number of detected ions. (**** *p* <0.0001, *** *p* <0.001, ** *p* <0.01, * *p* <0.05).

4.4.3 Optimisation of SPLASH® mixture addition to plasma

A good signal was obtained from 1:10 dilution, however, when the same amount of SPLASH® was extracted a substantial reduction in signal was observed for all the compounds (see Appendix, Table A.3). Therefore, instead of using 10 µL of the SPLASH® solution as suggested by Avanti®, 20 µL of the solution will be used in order to obtain a good peak of the IS mixture even after extraction. Since there was no reference IS for the D-IS, the matched RT between different adduct in positive and negative mode was used as an indication for the presence of that lipids. Cholesterol adduct was seen at different RT, so no proper conclusion can be withdrawn and therefore it was not used as IS. D-IS masses used for both positive and negative mode are listed in Table 4.3.

Table 4.3:List of internal slandered masses and RT from SPLASH® solution that will be used for normalisation.

Lipid Standard	Adduct	Polarity	*m/z*	RT (min)
ChE 18:1(d_7)	$[M+NH_4]^+$	+	675.6772	14.50
DG 15:0-18:1(d_7)	$[M+NH_4]^+$	+	605.5837	9.70
	$[M-H+CH_3CO_2H]^-$	-	646.5637	9.70
LPC 18:1(d_7)	$[M+H]^+$	+	529.3986	5.61
	$[M-H+CH_3CO_2H]^-$	-	587.4052	5.61
LPE 18:1(d_7)	$[M+H]^+$	+	487.3517	5.74
	$[M-H]^-$	-	485.3371	5.74
MG 18:1(d_7)	$[M+NH_4]^+$	+	381.3697	6.82
	$[M-H+CH_3CO_2H]^-$	-	422.3497	6.82
PA 15:0-18:1(d_7)	$[M+NH_4]^+$	+	685.5500	9.16
	$[M-H]^-$	-	666.5089	9.16
PC 15:0-18:1(d_7)	$[M+H]^+$	+	753.6126	8.99
	$[M-H+CH_3CO_2H]^-$	-	811.6192	8.99
PE 15:0-18:1(d_7)	$[M+H]^+$	+	711.5657	9.04
	$[M-H]^-$	-	709.5511	9.04
PG 15:0-18:1(d_7)	$[M+NH_4]^+$	+	759.5868	8.66
	$[2M-H]^-$	-	1482.099	8.66
PI 15:0-18:1(d_7)	$[M+H]^+$	+	830.5763	8.58
	$[M-H]^-$	-	828.5618	8.57
PS 15:0-18:1(d_7)	$[M+H]^+$	+	755.5555	8.78
	$[M-H]^-$	+	753.5410	8.78
SM d18:1-18:1(d_9)	$[M+H]^+$	+	738.646	8.82
TG 15:0-18:1(d_7)-15:0	$[M+NH_4]^+$	+	829.7977	13.09

4.4.4 Evaluation of ^{13}C-IS mixture for normalisation of lipidomics analysis

4.4.4.1 Evaluation of ^{13}C-IS mixture for normalisation of lipidomics data from human and mouse plasma

Six biologically different human plasma samples were collected from fasting subjects. 392 lipid ions were identified from raw samples using LipidSerach™. 347 ions were detected in all set of groups (the included ion should be detected in three or more of the samples in the same group). 112 ions were found to be common between the plasma samples and the labelled yeast extract where they can be used as IS for compound-specific normalisation or for class normalisation. The assessment of QC samples indicates a stable column and instrumental response during data acquisition since the calculated CV% of 93% of the detected features among the QC samples were less than 30, which indicate a good instrumental reproducibility (155).

Figures 4.6 and 4.7 represent the result of normalisation of 347 ions detected in all set of groups and the compound-specific normalisation of 112 ions that their respective uniformly labelled form was detected in plasma samples extracted in the presence of ^{13}C-IS, respectively. It appears that normalisation by TIC improves the overall response and a lower CV% were obtained for most of the selected ions. However, normalisation by ^{13}C-IS or by SPLASH® had a negative impact on those ions. The reason for such behaviour was not completely understood since many researchers demonstrate the ability of ^{13}C-labelled yeast extract to correct variations during sample preparation and analysis in targeted and untargeted lipidomics studies on plasma samples (140, 150, 152). So, another set of samples were used to evaluate and to confirm why normalisation by ^{13}C-IS or by SPLASH® had a negative impact on CV% of the tested ions.

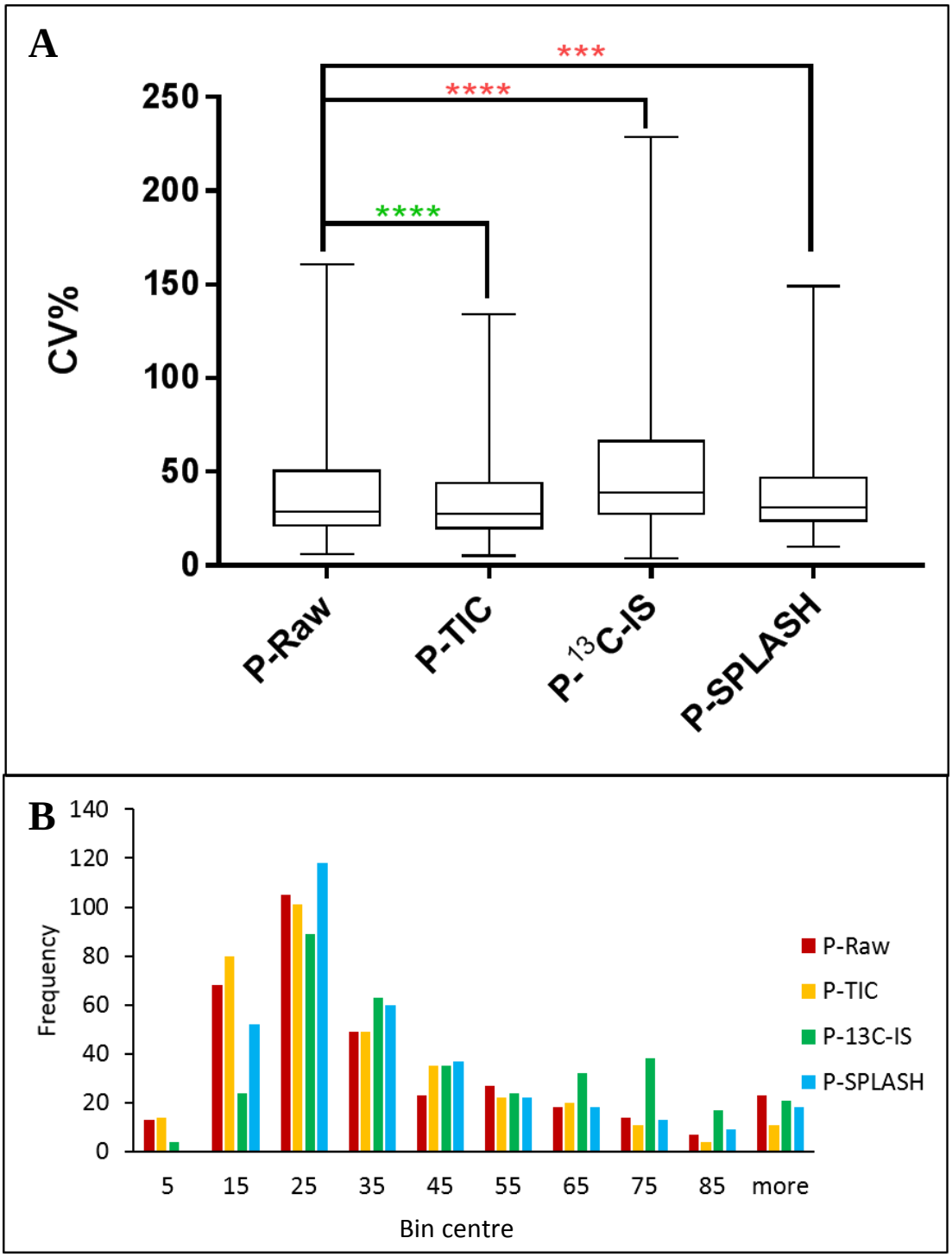

Figure 4.6: Coefficient of variance distributions for different normalisation methods by a whisker plot (A) and by a histogram where the X-axis represents the bin centre of CV% while the Y-axis represents the counts for each bin (Frequency) (B). Data shown are based on human plasma samples (*n*=6) where all 347 lipid ions detected in more than 50% of the samples were normalised by TIC (P-TIC), ^{13}C-IS by compound-specific and non-compound specific normalisation (P-^{13}C-IS) or by SPLASH® solution (P-SPLASH) and compared to raw un-normalised data. (**** p <0.0001, *** p <0.001, ** p <0.01, * p <0.05, where the green colour indicates a reduction in overall CV% while the red colour indicates an increase in overall CV%).

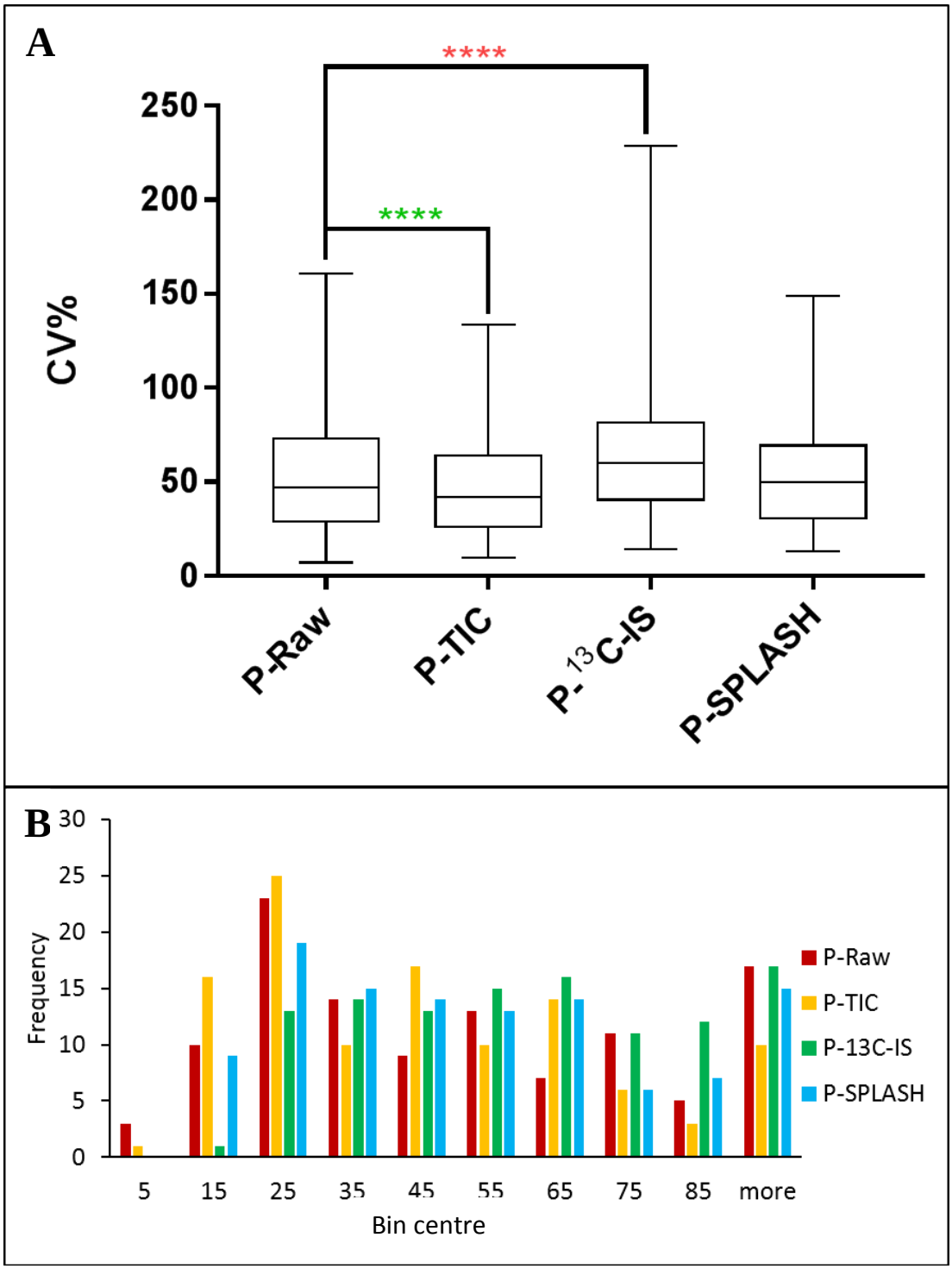

Figure 4.7: Coefficient of variance distributions for different normalisation methods by a whisker plot (A) and by a histogram where the X-axis represents the bin centre of CV% while the Y-axis represents the counts for each bin (Frequency) (B). Data shown are based on human plasma samples (*n*=6) were only common ions between plasma samples and ^{13}C-yeast extract (112 ions) were included in the analysis and normalised by TIC (P-TIC), ^{13}C-IS by compound-specific normalisation (P-^{13}C-IS) or by SPLASH® solution (P-SPLASH) and compared to raw un-normalised data. (**** p <0.0001, *** p <0.001, ** p <0.01, * p <0.05, where the green colour indicates a reduction in overall CV% while the red colour indicates an increase in overall CV%).

In this experiment, six biologically different plasma samples were collected from fasting mice. 415 lipid ions were identified from raw samples. 395 ions were detected in 50% or more in all set of groups. 132 ions were found to be common between the plasma samples and the labelled yeast extract where they can be used as IS for compound-specific normalisation or for class normalisation. The assessment of QC samples indicates a stable column and instrumental response during data acquisition since the calculated CV% of 92% of the detected features among the QC samples were less than 30, which indicate a high instrumental reproducibility (155).

Figures 4.8 and 4.9 represent the result of normalisation of 395 ions detected in all set of groups and the normalisation of 132 ions that their respective uniformly labelled form was detected in plasma samples extracted in the presence of ^{13}C-IS, respectively. It appears that normalisation by TIC improves the overall response and a lower CV% were obtained for most of the selected ions. Compound-specific normalisation by ^{13}C-IS had no observed effect but the overall normalised ions either by compound-specific ^{13}C-IS or by representative ^{13}C-IS had overall a lower CV% compared to raw data while normalisation by SPLASH® had a negative impact on the CV% of those ions.

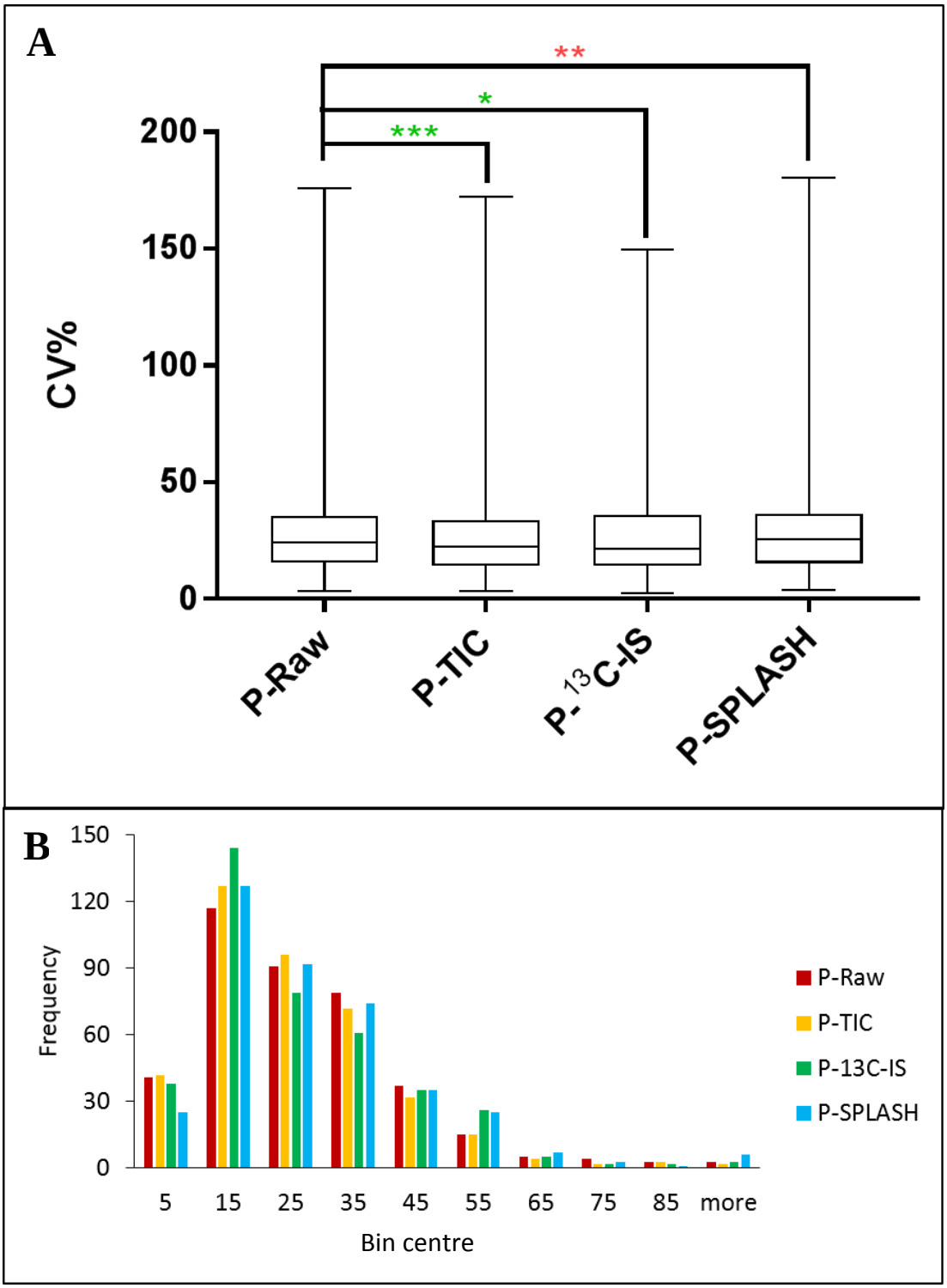

Figure 4.8: Coefficient of variance distributions for different normalisation methods by a whisker plot (A) and by a histogram where the X-axis represents the bin centre of CV% while the Y-axis represents the counts for each bin (Frequency) (B). Data shown are based on mouse plasma samples (*n*=6) where all 395 lipid ions detected in more than 50% of the samples were normalised by TIC (P-TIC), ^{13}C-IS by compound-specific and non-compound specific normalisation (P-^{13}C-IS) or by SPLASH® solution (P-SPLASH) and compared to raw un-normalised data. (**** p <0.0001, *** p <0.001, ** p <0.01, * p <0.05, where the green colour indicates a reduction in overall CV% while the red colour indicates an increase in overall CV%).

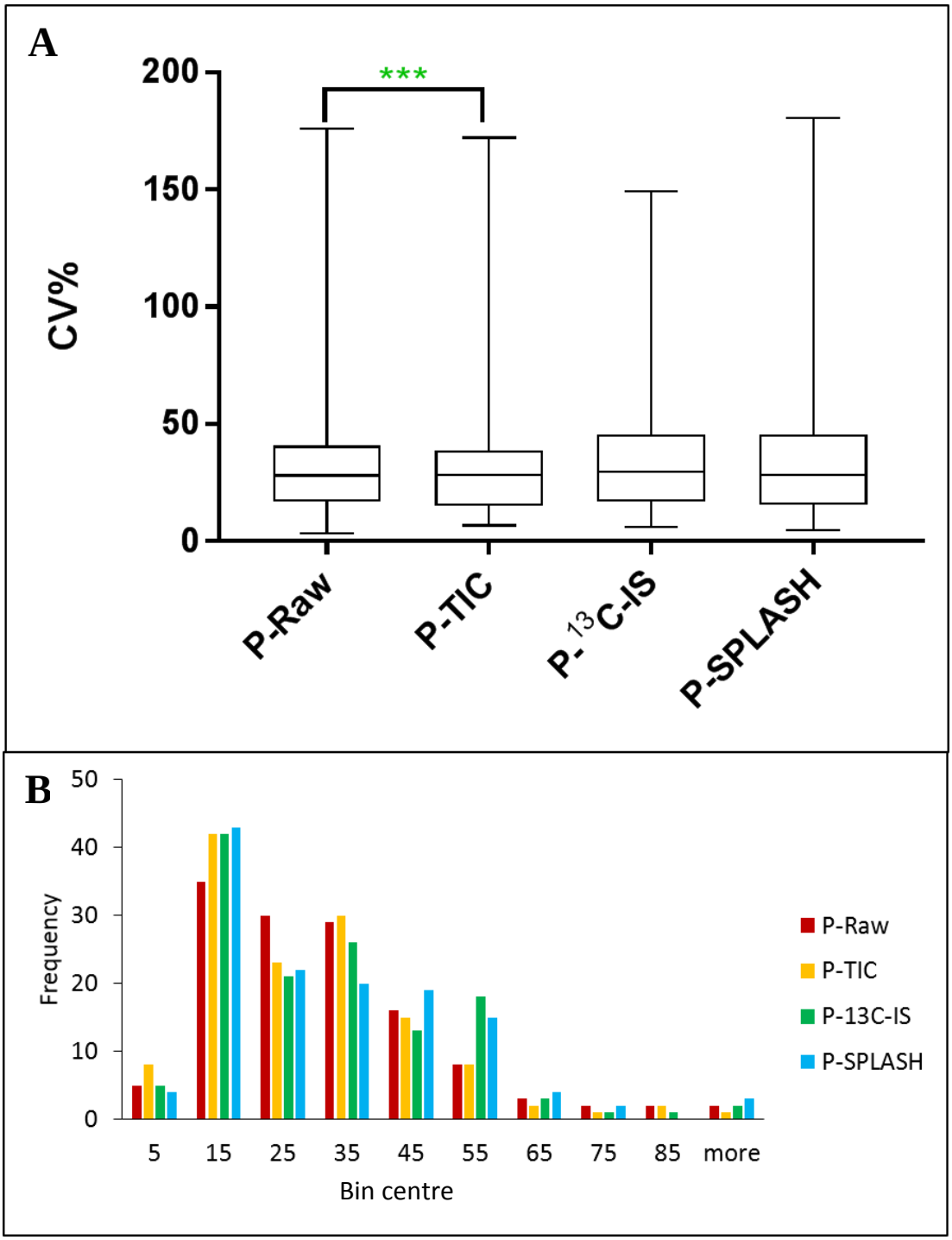

Figure 4.9: Coefficient of variance distributions for different normalisation methods by a whisker plot (A) and by a histogram where the X-axis represents the bin centre of CV% while the Y-axis represents the counts for each bin (Frequency) (B). Data shown are based on mouse plasma samples (*n*=6) were only common ions between plasma samples and ^{13}C-yeast extract (132 ions) were included in the analysis and normalised by TIC (P-TIC), ^{13}C-IS by compound-specific normalisation (P-^{13}C-IS) or by SPLASH® solution (P-SPLASH) and compared to raw un-normalised data. (**** p <0.0001, *** p <0.001, ** p <0.01, * p <0.05, where the green colour indicates a reduction in overall CV% while the red colour indicates an increase in overall CV%).

Having similar physicochemical properties, it is expected that a metabolite and its ^{13}C-labelled counterpart will have the same degree of ion suppression or enhancement if they were analysed under similar conditions. Despite the fact that their levels might change during the analysis, the ratio between the two will be always constant (134, 150, 257). However, it seems that the irregular peak shape of the low abundant labelled form could lead to variation in recorded peak area even after spectral smoothing. In addition, due to the matrix effect, the presence of high abundant co-eluted compounds could interfere with detection of low abundant ions that could affect effective normalisation, especially where ions were normalised by non-identical IS (different ^{13}C-labelled analogues) (59, 258). For example, when TG (16:0/16:0/20:1)+NH_4 was normalised by ^{13}C-IS, the calculated CV% increased from 42 to 99%. The unlabelled and the labelled forms were detected at *m/z* of 878.8149 and 933.9964, respectively at 15.14 min (see Figure 4.10). The low abundant labelled form and its irregular peak shape leading to inconsistent peak integration by TF could be the reason why the CV% increased after normalisation. Also, interference caused by overlapping chromatographical peaks due to possible chemical impurity and/or isotopic interferences from the yeast extract could affect the response of the unlabelled endogenous ions and the IS. This phenomenon known as cross-contribution could affect the normalisation process (259, 260).

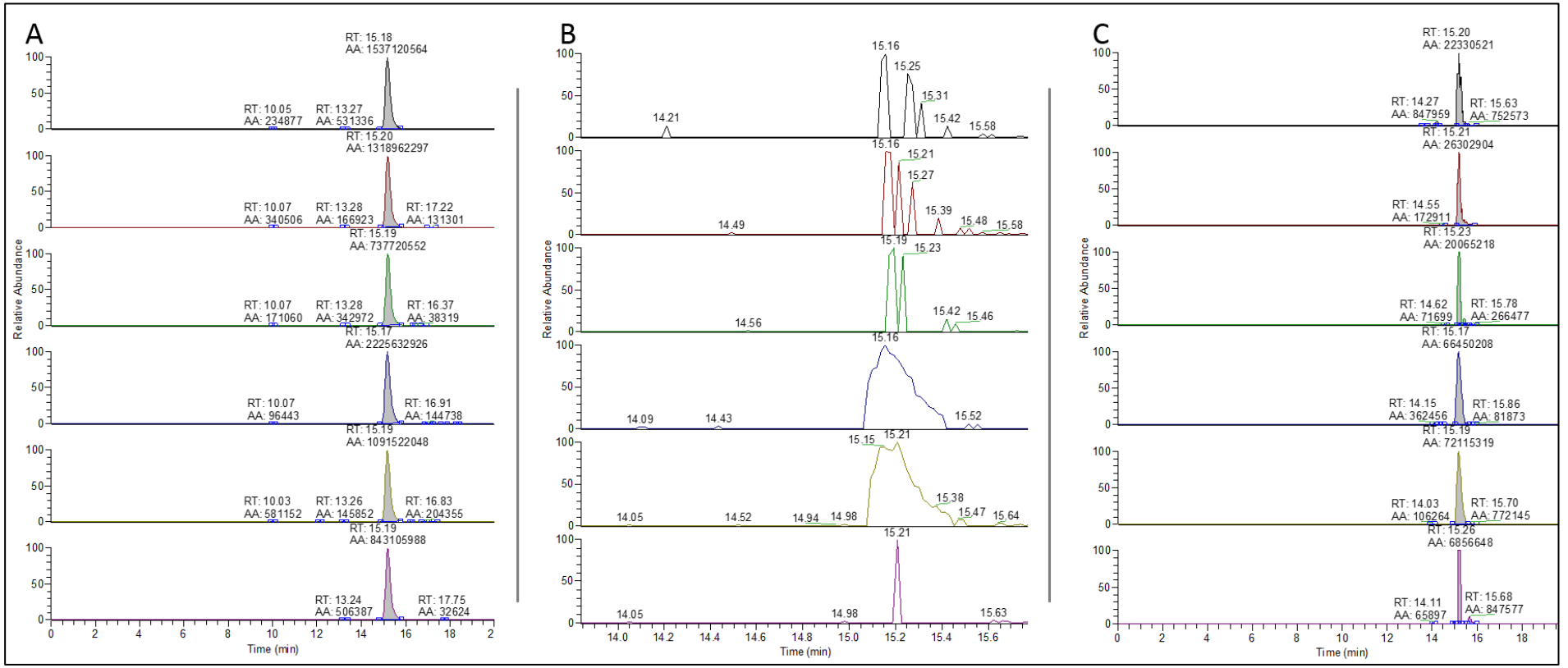

Figure 4.10: Extracted ion chromatograms of A) unlabelled form, B) labelled matched form (unsmoothed peak) and C) labelled matched form (smoothed peak) of TG(16:0/16:0/20:1)+NH_4 detected in plasma samples extracted in the presence of ^{13}C-IS.

In addition, incorrect matching between the labelled form and the unlabeled form of the selected ions could lead to increase the CV% especially when the selected labelled form was from different lipid class as they no longer exhibit similar physicochemical properties (73, 261). For example, when PE (16:0/20:4)+H was normalised by ^{13}C-IS, the calculated CV% increased from 19 to 26%. Peak inspection of both the unlabelled and labelled forms reveals that they were detected at different RT (see Figure 4.11, for the completed extracted ion chromatogram for all replicate refer to Appendix, Figure A.2). The unlabelled form was detected at 8.95 s while the matched labelled form was detected at 8.77 s. Ideally, ^{13}C-labelled form and the unlabelled form analysed at the same chromatographic condition should have the same RT as they possess similar physicochemical properties (257). However, this labelled form is most probably not the labelled form of that unlabelled lipid ions, but it could be mixed with another lipid isomer. Thus, isomers can have different response factor if they belong to different lipid class or does not reflect the level of ion suppression of the unlabelled ions and therefore it could lead to increase in its CV% when it normalised by an isomer. In addition, the false identity of lipid ions reported by LipidSearch™ could lead to a miss-match between unlabelled ions and another isomer or labelled form of different lipids that eventually could affect the normalised CV%.

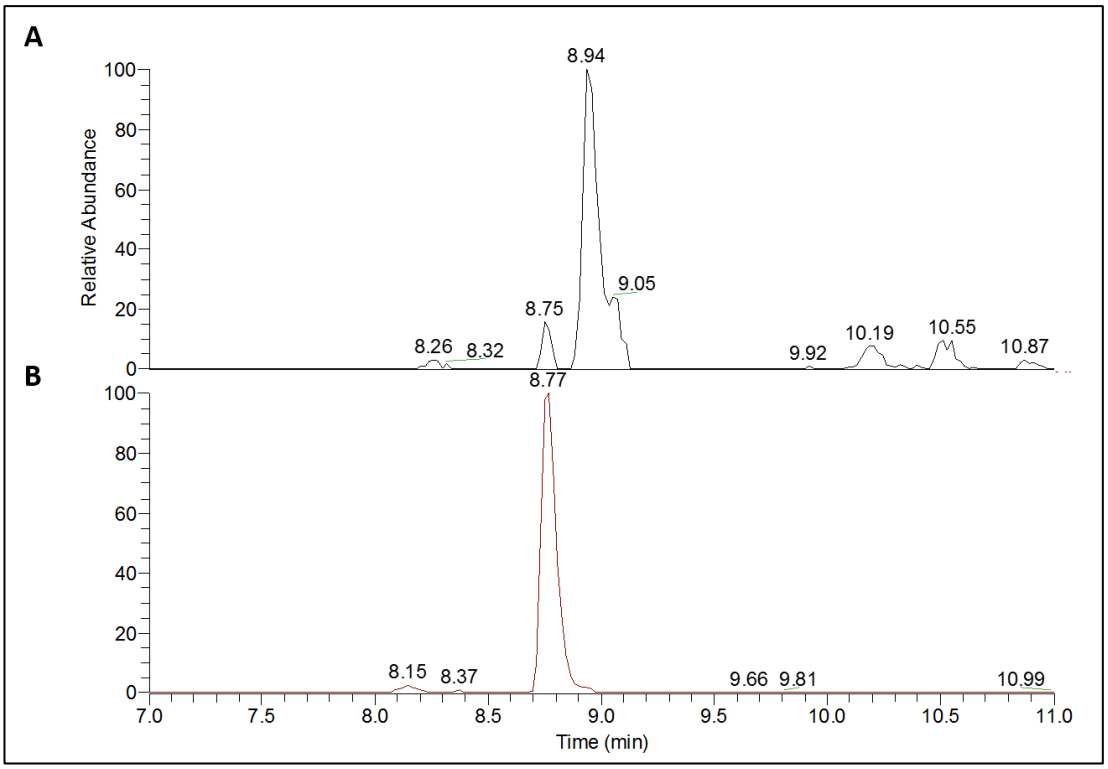

Figure 4.11: Part of the extracted ion chromatogram of A) unlabelled form detected at *m/z* of 740.5236, B) labelled matched form detected at *m/z* of 781.6589 of PE(16:0/20:4)+H detected in mice plasma samples extracted in the presence of ^{13}C-IS.

In both experiments, due to the nature of the samples (samples from biologically different subjects), the calculated CV% in raw data reflects biological variations, such as genetic variations, gender, age, and state of health in addition to analytical and technical variations introduced during sample collection, storage, preparation, analysis and data processing. Since the introduced ^{13}C-IS mixture is expected to correct only analytical and technical variation, the efficacy of the introduced normalisation methods will be further assessed using pooled human plasma where the biological variability between samples are no longer present.

444 lipid ions were identified from a pooled human plasma sample. 404 ions were detected in all set of groups (the included ion was detected in three or more of the samples in the same group). 102 ions were found to be common between the plasma

samples and the labelled yeast extract where they can be used as IS for compound-specific normalisation or for class normalisation. The QC response in this experiment indicates stable column and instrumental response during data acquisition and high system repeatability since the CV% of 89% of the detected features were less than 30 (155).

Figures 4.12 and 4.13 represent the result of normalisation of 404 ions detected in all set of groups and the normalisation of 102 ions that their respective uniformly labelled form was detected in plasma samples extracted in the presence of ^{13}C-IS, respectively. Statistical analysis showed a significant increase in the CV% of selected ions after normalisation by all the methods used. In addition, Figure 4.14A shows that only PE and dMePE normalised by ^{13}C-IS have a marked reduction in their overall CV% after normalisation compared to non-normalised ions (for PE: average CV% dropped from 41.36 to 15.00, *p*-value < 0.0001; for dMePE: average CV% dropped from 59.71 to 48.10, *p*-value 0.0134). Also, as it is shown in Figure 4.14B, ions with good repeatability when they normalised by all methods, their CV% increased. This could be due to the biological nature of the factor used for normalisation due to unavoidable random error in measurement systems according to Philip *et al.* (105, 262) that could propagate the total error. However, the effect of ^{13}C-IS normalisation is seen in ions with higher CV% where the IS were able to decrease the CV% of ions subjected to a high level of variations.

It seems that conducting metabolomics study in a highly controlled reproducible system with stable instrument response and column (C18 columns used for RF-LC-MS studies are considered more robust than other columns such as HILIC (140, 232, 240))

will result in high quality data that does not need any normalisation. In addition, the used column is claimed to provide improved chromatographic performance and stability as claimed by the company (263). So, in the light of these experiments, the effect of ^{13}C-IS normalisation will be evaluated when the LC-MS system is subject to higher analytical variability where the level of random error is expected to increase and affect the quality of the data.

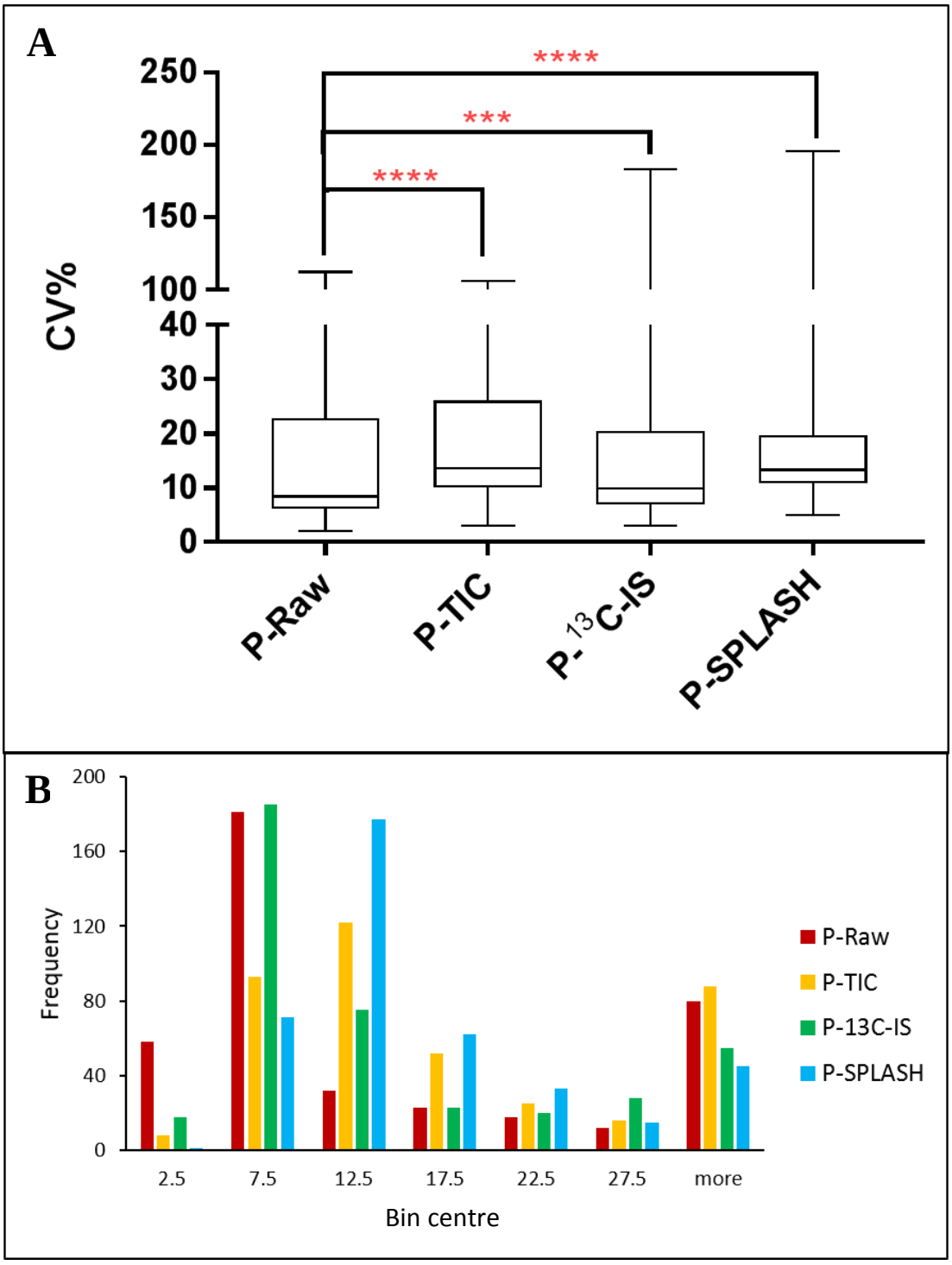

Figure 4.12: Coefficient of variance distributions for different normalisation methods by a whisker plot (A) and by a histogram where the X-axis represents the bin centre of CV% while the Y-axis represents the counts for each bin (Frequency) (B). Data shown are based on pooled human plasma sample from blood bank (*n*=6) where all 404 lipid ions detected in more than 50% of the samples where normalised by TIC (P-TIC), ^{13}C-IS by compound-specific and non-compound specific normalisation (P-^{13}C-IS) or by SPLASH® solution (P-SPLASH) and compared to raw un-normalised data. (**** p <0.0001, *** p <0.001, ** p <0.01, * p <0.05, where the green colour indicates a reduction in overall CV% while the red colour indicates an increase in overall CV%).

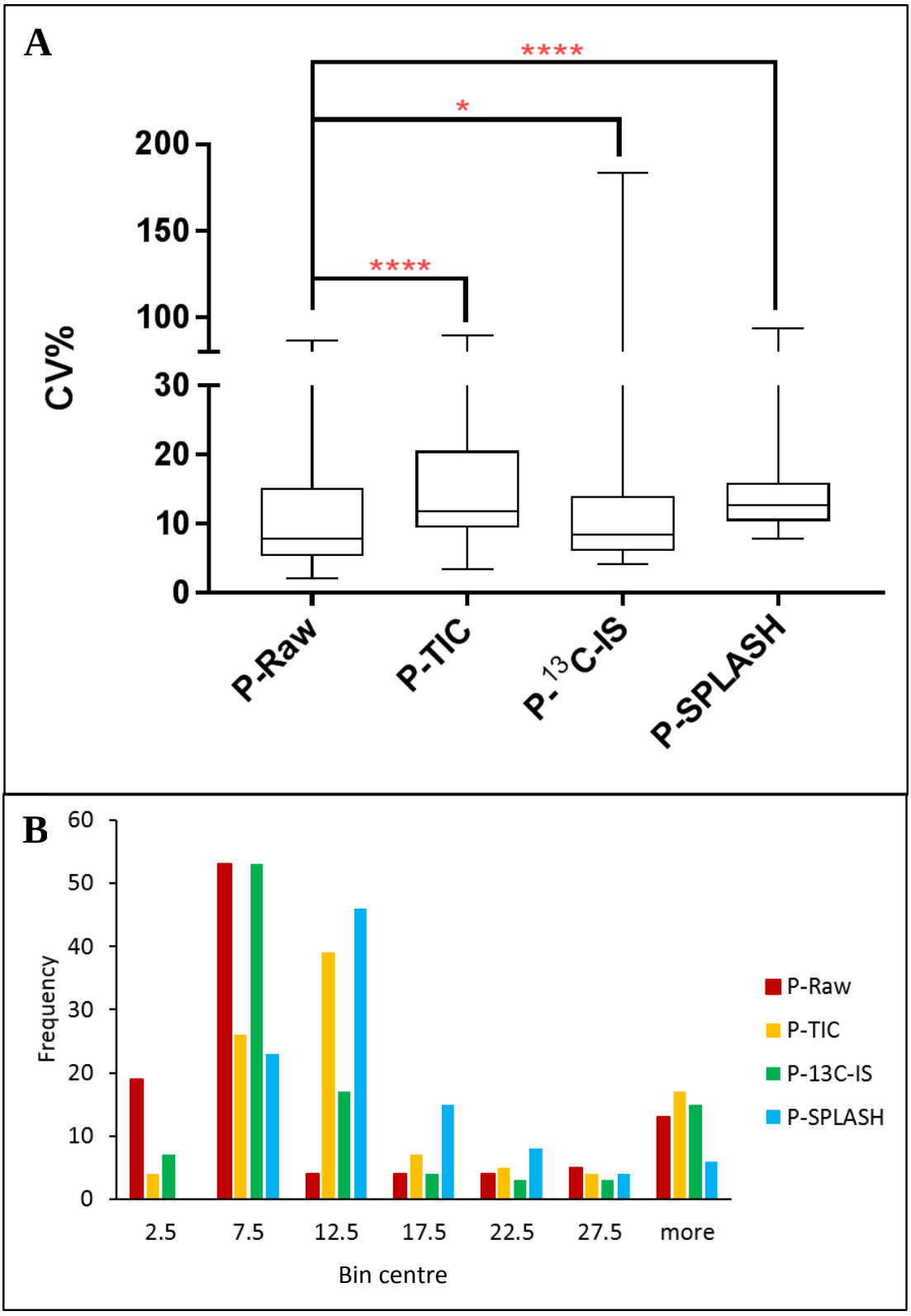

Figure 4.13: Coefficient of variance distributions for different normalisation methods by a whisker plot (A) and by a histogram where the X-axis represents the bin centre of CV% while the Y-axis represents the counts for each bin (Frequency) (B). Data shown are based on pooled human plasma sample from blood bank (*n*=6) where only common ions between plasma samples and ^{13}C-yeast extract (102 ions) where included in the analysis and normalised by TIC (P-TIC), ^{13}C-IS by compound-specific normalisation (P-^{13}C-IS) or by SPLASH® solution (P-SPLASH) and compared to raw un-normalised data. (**** p <0.0001, *** p <0.001, ** p <0.01, * p <0.05, where the green colour indicates a reduction in overall CV% while the red colour indicates an increase in overall CV%).

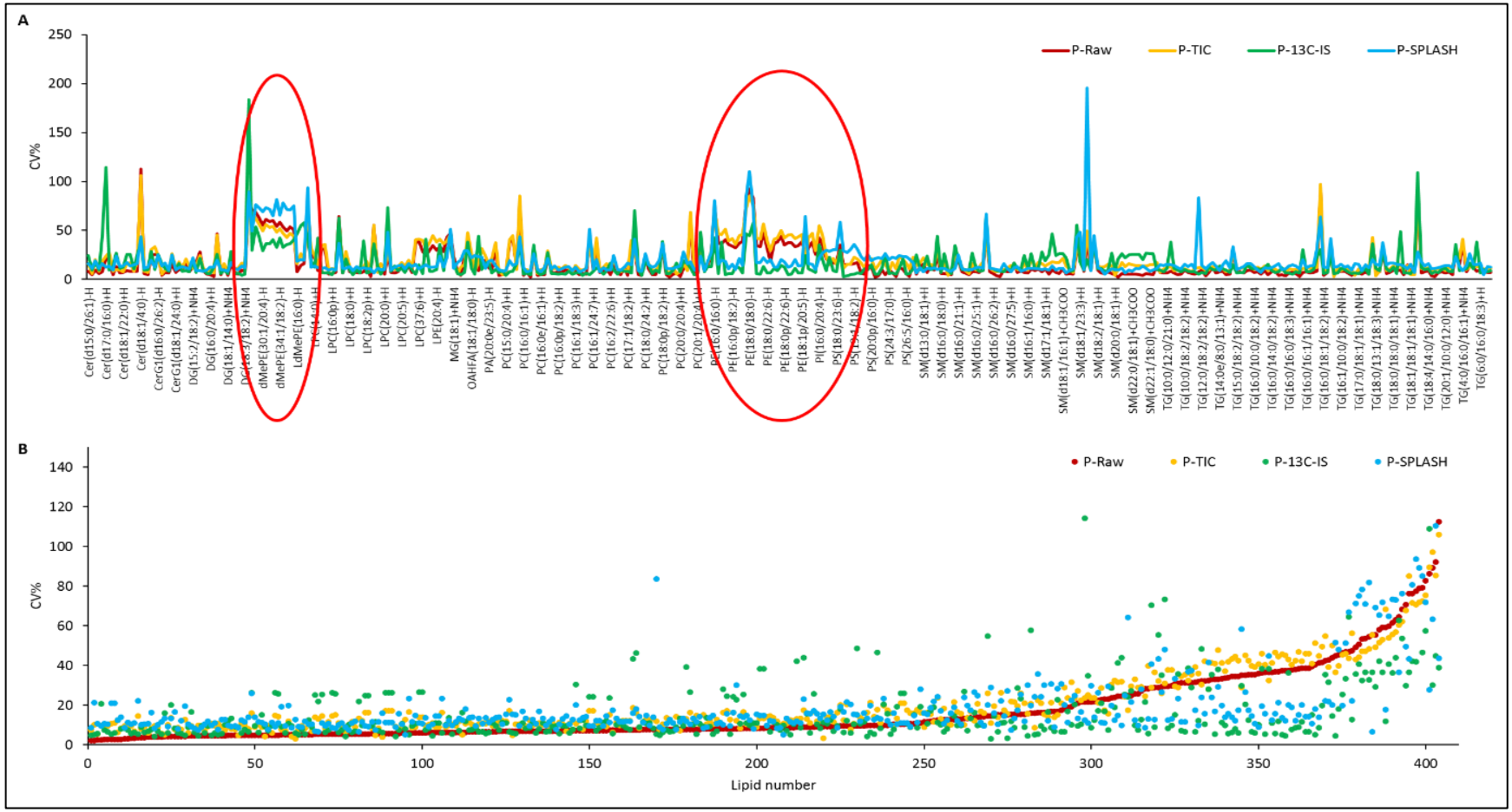

Figure 4.14: The effect of different normalisation methods on the CV% of selected lipid ions when data arranged A) per lipid classes, the red circles highlight when normalisation by ^{13}C-IS reduces the CV% significantly, or B) ascending from low to high CV% (from left to right) based on the raw data CV% values, where normalisation by ^{13}C-IS reduces the CV% significantly when high variability is seen in raw data as seen at the right side of the plot. Data shown are based on pooled human plasma sample from blood bank (*n*=6) where all 404 lipid ions detected in more than 50% of the samples were normalised by TIC (P-TIC), ^{13}C-IS by compound-specific and non-compound specific normalisation (P-^{13}C-IS) or by SPLASH® solution (P-SPLASH) and compared to raw un-normalised data (P-Raw).

4.4.4.2 The effect of different extraction methods on normalisation by ^{13}C-IS mixture on pooled plasma samples

The QC response in this experiment was consistent where the CV% of 85% of the detected features was less than 30%, which indicates a good system repeatability during the analysis for metabolomics/lipidomics studies (155). Due to the nature of the studied samples (single source of plasma), the calculated CV% in raw data reflects variations introduced during sample preparation and analysis only. In non-dried samples, 121 ^{13}C-labelled ions were detected in all replicates and used for compound-specific normalisation whereas, in dried samples, 151 ^{13}C-labelled ions were detected in all replicates and used for compound-specific normalisation. Figure 4.15 represents the normalisation results of the selected ions in non-dried and dried samples. After normalisation, a significant reduction in overall CV% of the selected ions was observed in non-dried samples, while no difference was observed in dried samples. In non-dried samples, the presence of chloroform could introduce more variations as it is not retained on the column and therefore the ^{13}C-IS was able to decrease these variations. Whereas the dried samples were more compatible with the used column and the used method of analysis, as a result, the normalisation was not effective. This was in agreement with our previous normalisation trials, where normalisation had negative or no effect on the CV% of the selected ions in the set of samples where minimal analytical and technical variations are expected.

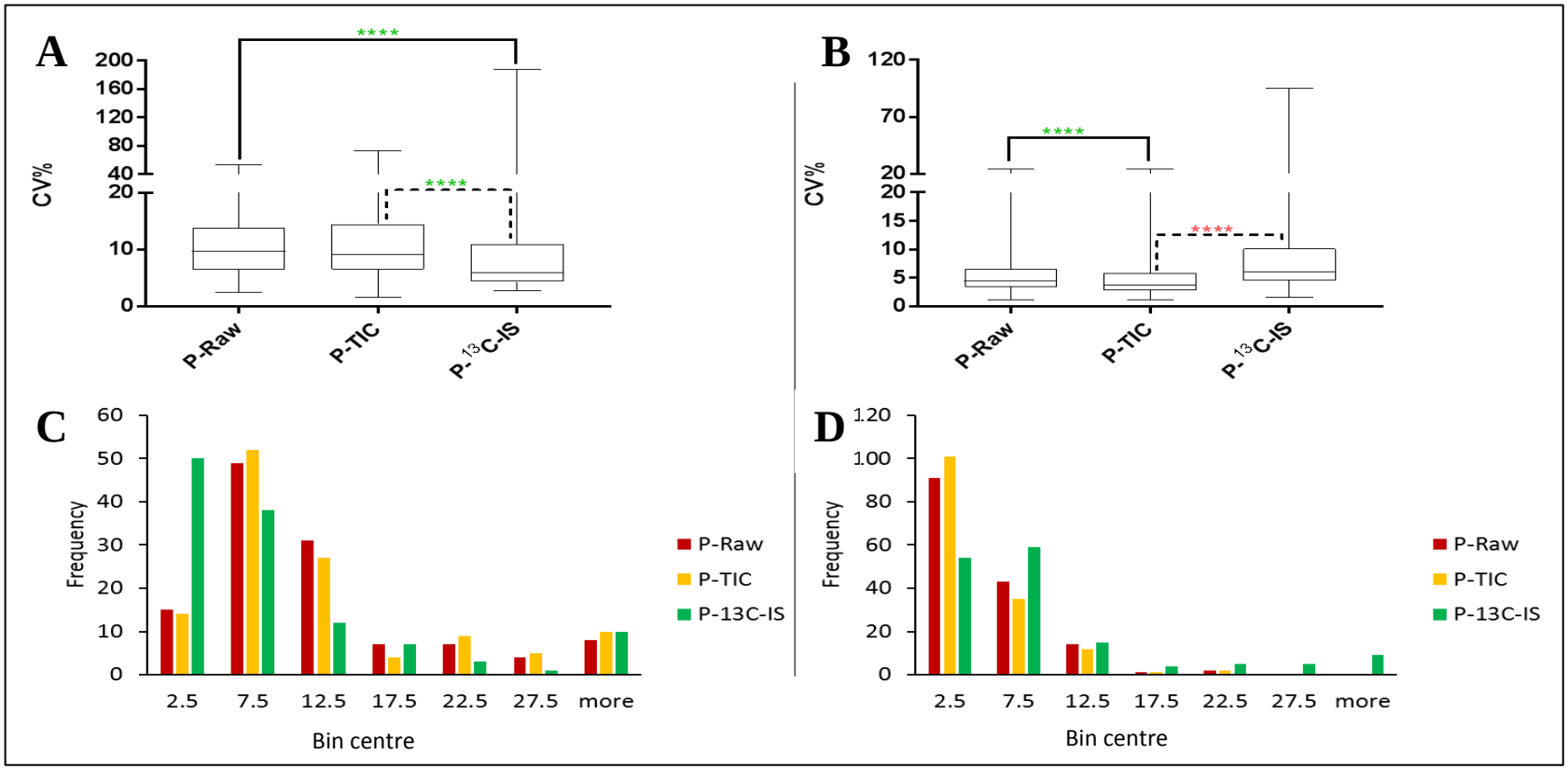

Figure 4.15: Coefficient of variance distributions for different normalisation methods by a whisker plot ((A) and (B)) and by a histogram where the X-axis represents the bin centre of CV% while the Y-axis represents the counts for each bin (Frequency) (C) and (D)) of 121 and 151 lipid ions detected in more than 50% of pooled human plasma from blood bank extracted using two different methods: non-dried samples and dried samples respectively. Data shown discuss the effect of normalisation by TIC (P-TIC) and ^{13}C-IS by compound-specific normalisation (P-^{13}C-IS) on single human plasma sample from blood bank (analytical samples=6) when extracted as detailed in section 4.3.1, where the samples were double extracted, their extract was concentrated, and the chloroform was replaced by LC-MS grade isopropanol (dried samples) and compared to plasma samples subjected to a single extraction step and after that an aliquot of the lower lipophilic phase was mixed with an equal volume of LC-MS grade isopropanol prior to analysis without subsequent evaporation and reconstitution steps (non-dried samples). (**** p <0.0001, *** p <0.001, ** p <0.01, * p <0.05, where the green colour indicates a reduction in overall CV% while the red colour indicates an increase in overall CV%).

To evaluate the effect of chloroform removal and sample concentration, the CV% of unlabelled ions and ^{13}C-labelled ions was studied. 559 unlabelled ions were detected in 50% or more of the samples in plasma extracted alone (condition 1) or in the presence of ^{13}C-IS extract (condition 2). Figure 4.16 represents the effect of drying on the CV% distribution of unlabelled ions. In both conditions, the overall CV% of the selected ions (559 ions) in the dried samples was significantly lower to that in non-dried samples which means dried samples yield more stable ions. This could be because the dried samples are more concentrated and therefore more abundant ions are less subjected to ion suppression during analysis (59, 258) or because the sample solvent is more compatible with the used mobile phase (80% isopropanol) that does not affect the quality of the data unlike incompatible sample solvent as seen before in section 4.4.1.

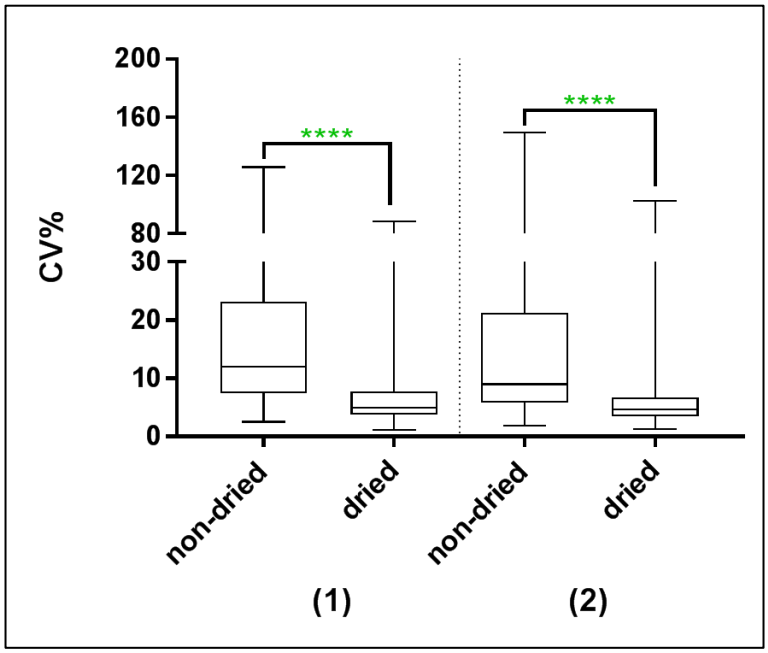

Figure 4.16: The effect of drying on the CV% distribution of 559 unlabelled ions detected in 50% or more in plasma extracted alone (condition 1) or in the presence of ^{13}C-IS extract (condition 2). In all groups, 10 replicates were studied. (**** p <0.0001, *** p <0.001, ** p <0.01, * p <0.05, where the green colour indicates a reduction in overall CV% while the red colour indicates an increase in overall CV%).

In regard to the quality of ^{13}C-IS, Figure 4.17 represents the effect of drying on the CV% distribution of ^{13}C-labelled ions detected in 50% or more in non-dried and dried yeast extract (condition 1), re-extracted yeast extract (condition 2) or in re-extracted yeast extract in the presence of plasma (condition 3) where 156 ^{13}C-labelled ions were detected in all groups. In conditions 1 and 2, the overall CV% of the selected ions in the dried samples was significantly lower to that in non-dried samples, yet in condition 3, there was no statistical difference between the two samples. This could be because the dried samples are more concentrated and therefore more abundant ions are less subjected to ion suppression during analysis or because the sample solvent is more compatible. However, in condition 3, where ^{13}C-IS extract was re-extracted in the presence of plasma, the samples are more concentrated, and the matrix largely affects the ionisation of selected ^{13}C-labelled ion and their CV%. Therefore, the positive effect seen due to drying step is counter by the negative effect of the matrix.

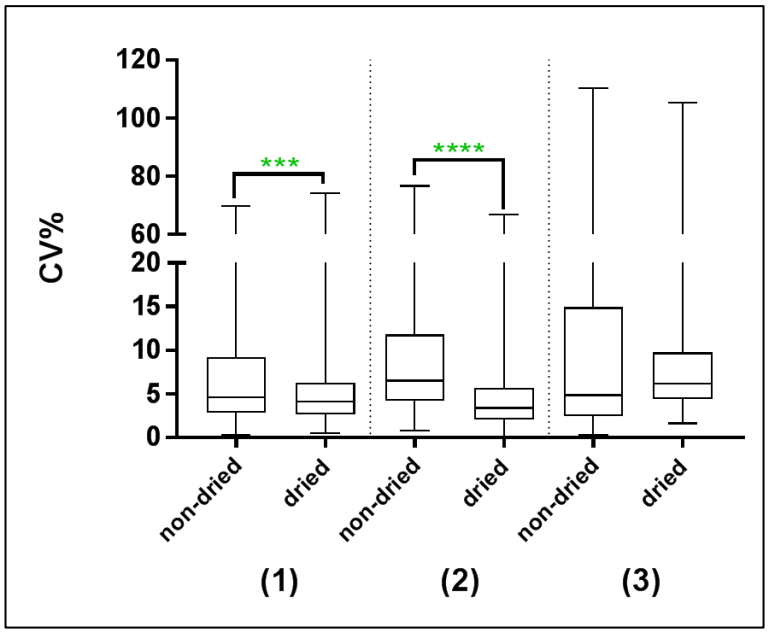

Figure 4.17: The effect of drying on the CV% distribution of 156 ^{13}C-labelled ions detected in 50% or more in non-dried and dried yeast extract (condition 1), re-extracted yeast extract (condition 2) or in re-extracted yeast extract in the presence of plasma (condition 3). In all groups, 3 replicates were studied. (**** p <0.0001, *** p <0.001, ** p <0.01, * p <0.05, where the green colour indicates a reduction in overall CV% while the red colour indicates an increase in overall CV%).

The difference in the drying effect on unlabelled ions (Figure 4.16 (2)) and on ^{13}C-labelled ions (Figure 4.17 (3)) in plasma extracted in the presence of ^{13}C-IS extract could be due to matrix effect. It is believed that the unlabelled ions are more abundant than ^{13}C-labelled ions and therefore the matrix have minimal or no effect on these ions and consequently these ions had significantly lower CV% upon drying. While the matrix had a predominant effect on low abundant ^{13}C-labelled ions and consequently no improvement in CV% of the selected ions was seen upon drying.

Hence, in non-dried samples, it is believed that the presence of chloroform could introduce more variations during analysis that the ^{13}C-IS mixture was able to decrease them. Whereas in dried samples, this source of variation is not introduced into the system and therefore the normalisation was not effective. This in agreement with our previous normalisation experiments discussed in section 4.4.4.1, where

normalisation had negative or no effect on the CV% of the selected ions in the set of samples where minimal analytical and technical variations are expected.

4.4.4.3 The effect of normalisation by ^{13}C-IS in reducing variations introduced during the extraction of a large set of samples

446 ions were identified in the extract of plasma alone. 379 unlabelled ions were detected in 50% or more of the samples in plasma extracted in the presence of ^{13}C-IS extract and 142 labelled ions were present in all samples that can be used for compound-specific normalisation. Figure 4.18 represents the normalisation results of these ions. As shown, ions normalisation by TIC or by ^{13}C-IS had a significant reduction in overall CV% compared to that in raw data. also, ions normalised by ^{13}C-IS had a lower overall CV% compared to ions normalised by TIC but the difference was not significant. This highlight the efficacy of normalisation by ^{13}C-IS mixture in reducing variations that could arise during samples preparation especially when a large number of samples are extracted at the same time.

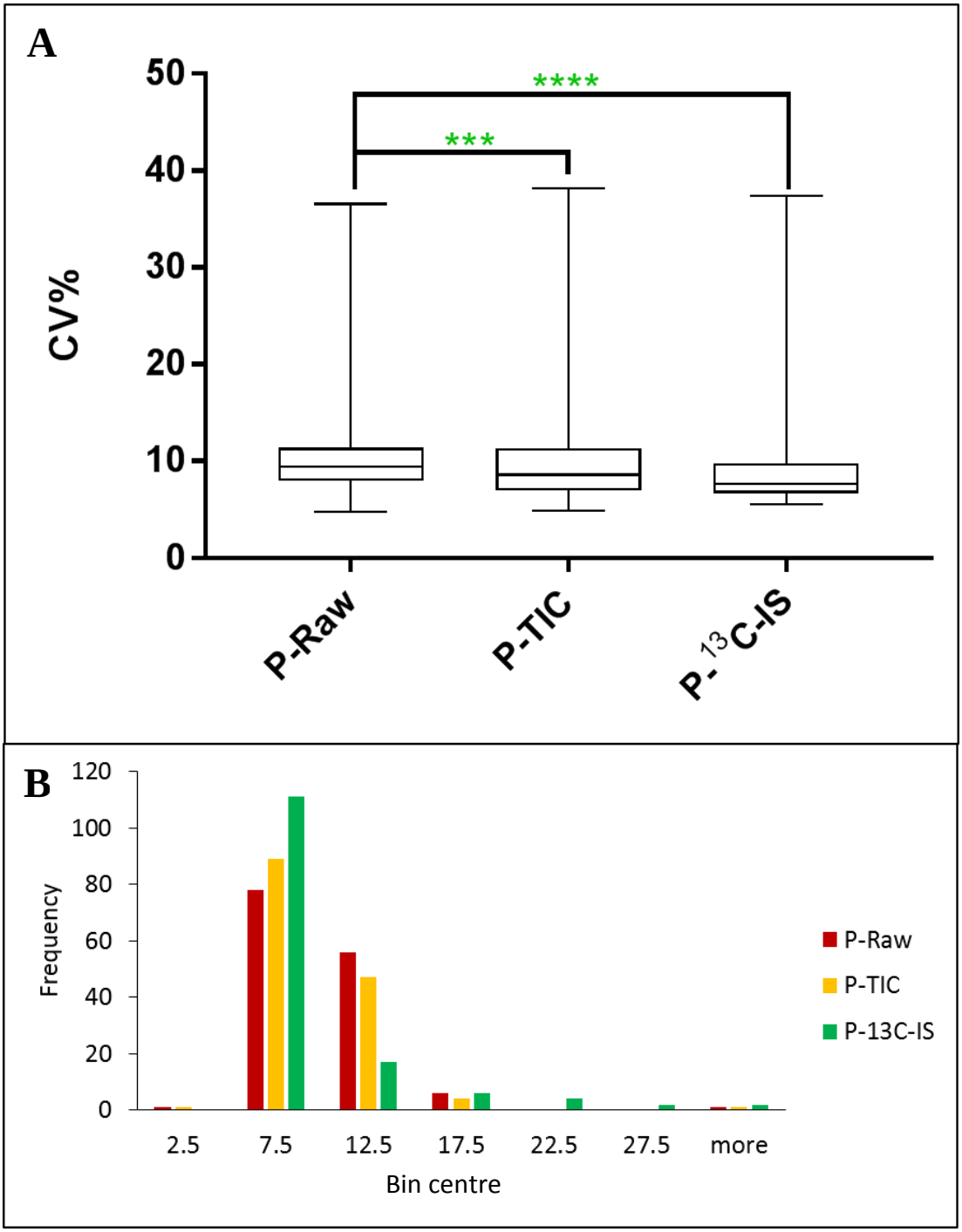

Figure 4.18: Coefficient of variance distributions for different normalisation methods by a whisker plot (A) and by a histogram where the X-axis represents the bin centre of CV% while the Y-axis represents the counts for each bin (Frequency) (B). Data shown are based on pooled human plasma sample from blood bank repeatably extracted (*n*=101) to study the effect of normalisation by ^{13}C-IS in reducing variations introduced during extraction of large set of samples where only common ions between plasma samples and ^{13}C-yeast extract (142 ions) where included in the analysis and normalised by TIC (P-TIC) and by ^{13}C-IS by compound-specific normalisation (P-^{13}C-IS) and compared to raw un-normalised data. (**** p <0.0001, *** p <0.001, ** p <0.01, * p <0.05, where the green colour indicates a reduction in overall CV% while the red colour indicates an increase in overall CV%).

4.4.4.4 The effect of normalisation by ^{13}C-IS in reducing variations introduced during sample analysis over a long analysis time

446 ions were identified in the extract of plasma alone. 423 unlabelled ions were detected in 50% or more of the injections and 100 labelled ions were present in all samples that can be used for compound-specific normalisation. Due to the nature of the studied samples (230 analytical injections of a pooled extract of human plasma samples), the calculated CV% in raw data shown in Figure 4.19, reflects variations introduced during sample analytical variations only. In metabolomics, analysis of a large set of samples for example in cohort studies or samples measured at different time points is a challenge due to analytical drift, where for a given metabolite, time related systematic variation in the reported metabolite response can often be observed (105, 264). This could be due to metabolite instability in the autosampler that could lead to non-enzymatic metabolite conversion (oxidation or hydrolysis) (155), or from changes in chromatography (retention time or peak shape) (116) or interaction of the sample components with the surfaces of the chromatography system and MS instrumentation that could cause a build-up of contaminants that were not effectively removed during analysis (233, 256). In a good experimental design, although randomisation of the sample run order is used to reduce the effect of these variations, it cannot be totally removed or compensated without the use of internal standards (264).

Figures 4.19 and 4.20 represent the normalisation results of the selected ions. Ions normalised by TIC showed a significantly higher overall CV% compared to those in raw data where ions normalised by ^{13}C-IS revealed a significantly lower overall CV%. In Figure 4.20 (1A and 1B), analytical drift in metabolites response can be observed

over time that leads to a clear separation between injections analysed at different days in PCA plot. Similar drift in QC samples was seen in large-scale serum and plasma samples (28) and in urine samples (233) due to sample instability or unexpected instrumental hardware or software errors. Normalisation by TIC was not able to correct these analytical drifts and its reflection on PCA, whereas normalisation by ^{13}C-IS was able to correct these drifts and remove any difference between analysed injections as seen in Figure 4.20 (3A and 3B).

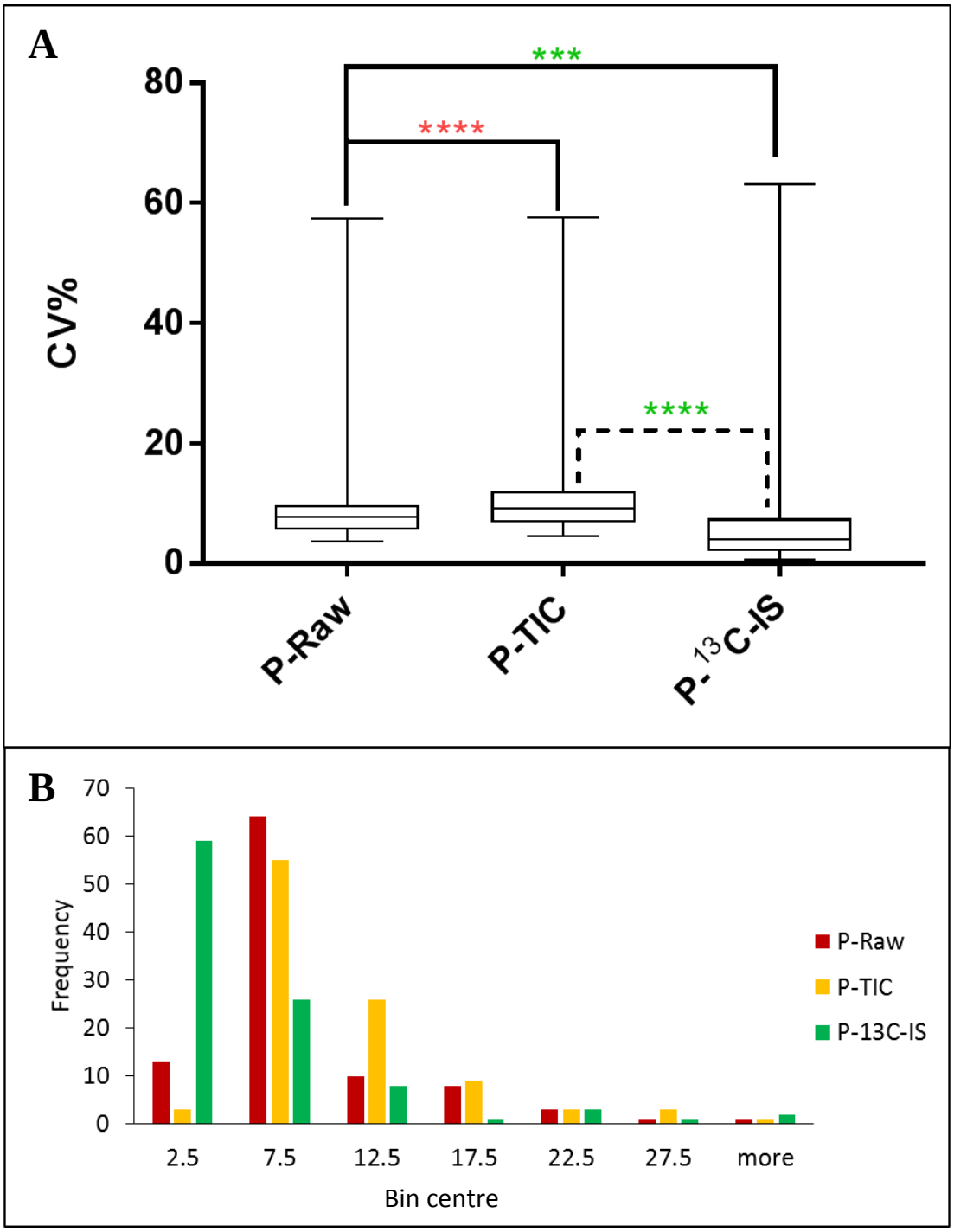

Figure 4.19: Coefficient of variance distributions for different normalisation methods by a whisker plot (A) and by a histogram where the X-axis represents the bin centre of CV% while the Y-axis represents the counts for each bin (Frequency) (B). Data shown are based on pooled human plasma sample from blood bank repeatably injected and analysed (n=230) to study the effect of normalisation by ^{13}C-IS in reducing variations introduced during sample analysis over a long analysis time where only common ions between plasma samples and ^{13}C-yeast extract (100 ions) where included in the analysis and normalised by TIC (P-TIC) and by ^{13}C-IS by compound-specific normalisation (P-^{13}C-IS) and compared to raw un-normalised data. (**** p <0.0001, *** p <0.001, ** p <0.01, * p <0.05, where the green colour indicates a reduction in overall CV% while the red colour indicates an increase in overall CV%).

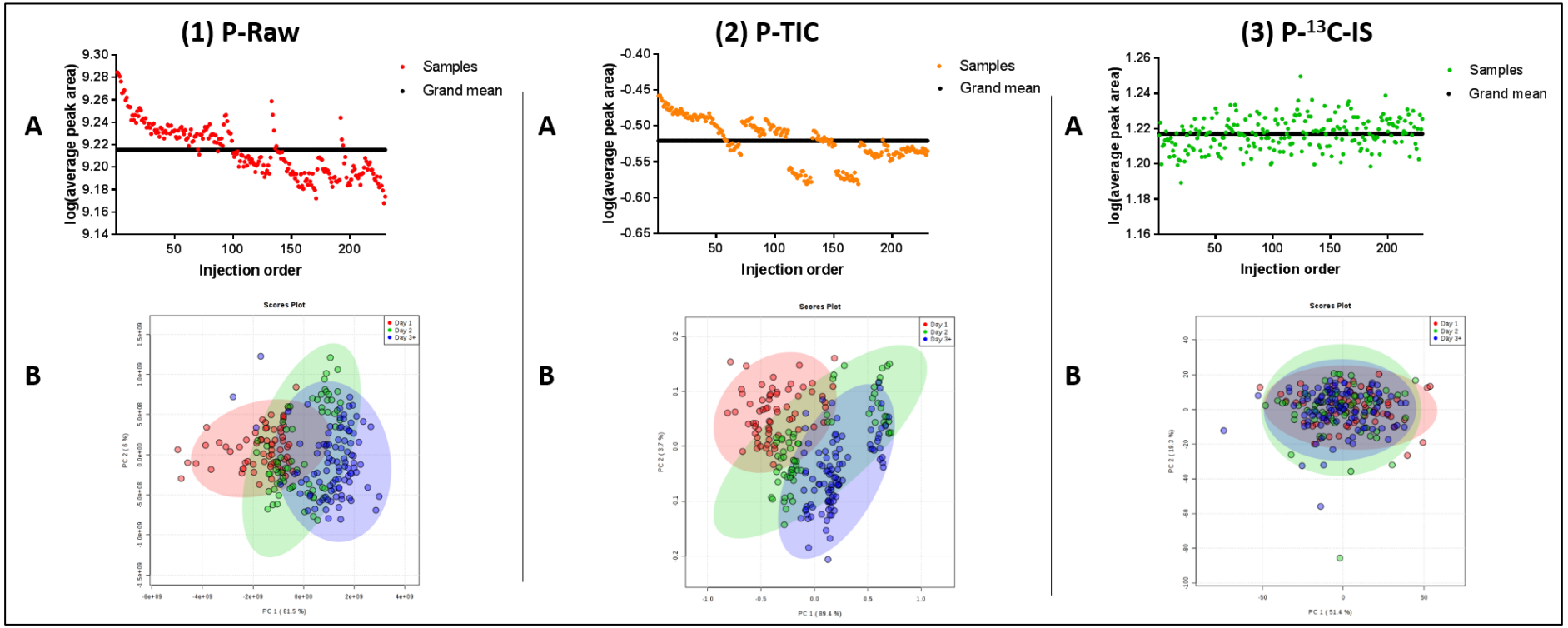

Figure 4.20: The effect of TIC normalisation ((2) P-TIC) and compound-specific normalisation by ^{13}C-IS ((3) P-^{13}C-IS) compared to raw data ((1) P-Raw). The results were visualised as A) log average peak area of the selected ions against injection order and as B) PCA score plots overview. Data shown are based on pooled human plasma sample from blood bank repeatably injected and analysed (*n*=230) to study the effect of normalisation by ^{13}C-IS in reducing variations introduced during sample analysis over a long analysis time where only common ions between plasma samples and ^{13}C-yeast extract (100 ions) where included in the analysis and normalised by TIC (P-TIC) and by ^{13}C-IS by compound-specific normalisation (P-^{13}C-IS) and compared to raw un-normalised data.

4.4.4.5 The effect of normalisation by ^{13}C-IS on human plasma lipidomics data on data acquired on three separate days

446 ions were identified in the extract of plasma alone. 337 unlabelled ions were detected in 50% or more of the injections and 105 labelled ions were present in all samples that can be used for compound-specific normalisation. Assessment of QC samples indicates that good repeatability was obtained during the analysis at each run. Due to the nature of the studied samples, the calculated CV% in raw data shown in Figure 4.21, reflects variations introduced due to batch-to-batch variation. This type of variation arises from sample handling, preparation and storage, MS performance and columns stability over time that collectively affect the results of large-scale studies (233, 246, 256).

Figures 4.21 and 4.22 represent the normalisation results of the selected ions. It appears that ions normalised by TIC had similar overall CV% compared to that in raw data, whereas ions normalised by ^{13}C-IS had a significantly lower overall CV%. Therefore, it reveals that normalisation by ^{13}C-IS was able to decrease day to day variations introduced by the instrument during samples analysis and this can be confirmed by the PCA plot where no grouping in respect to batch variation was seen after normalisation shown in Figure 4.22 (3A). Also, the heat map clearly supports these findings where the intensity of the studied normalised ions shows no trend in ions peak area in respect to the day of analysis as seen in raw data or data normalised by TIC.

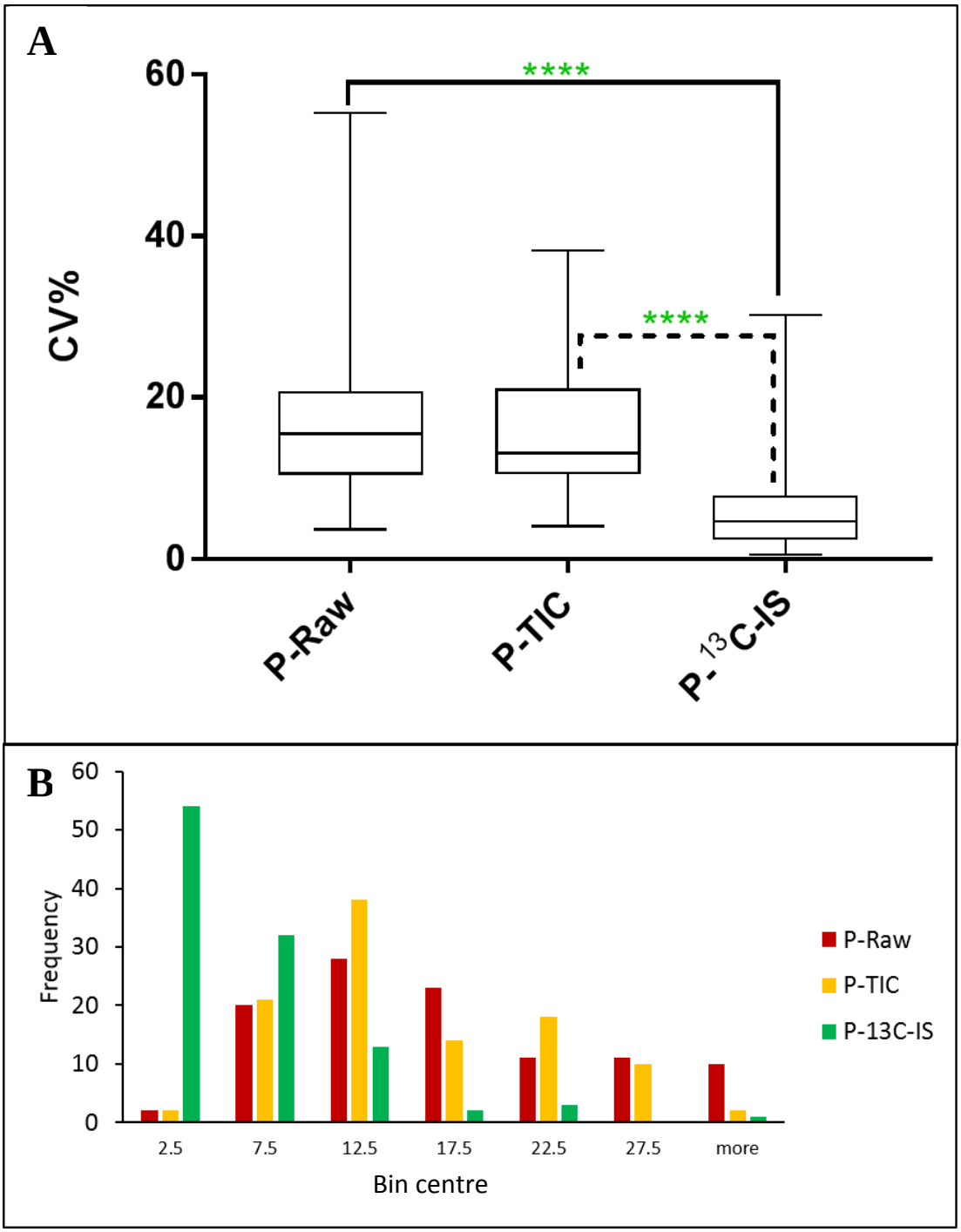

Figure 4.21: Coefficient of variance distributions for different normalisation methods by a whisker plot (A) and by a histogram where the X-axis represents the bin centre of CV% while the Y-axis represents the counts for each bin (Frequency) (B). Data shown are based on pooled human plasma sample from blood bank extracted and analysed (*n*=15) at different days (day 0, day 7 and day 14) to study the effect of normalisation by ^{13}C-IS in reducing variations introduced during sample analysis on three separate days (batch to batch variations) where only common ions between plasma samples and ^{13}C-yeast extract (105 ions) where included in the analysis and normalised by TIC (P-TIC) and by ^{13}C-IS by compound-specific normalisation (P-^{13}C-IS) and compared to raw un-normalised data. (**** p <0.0001, *** p <0.001, ** p <0.01, * p <0.05, where the green colour indicates a reduction in overall CV% while the red colour indicates an increase in overall CV%).

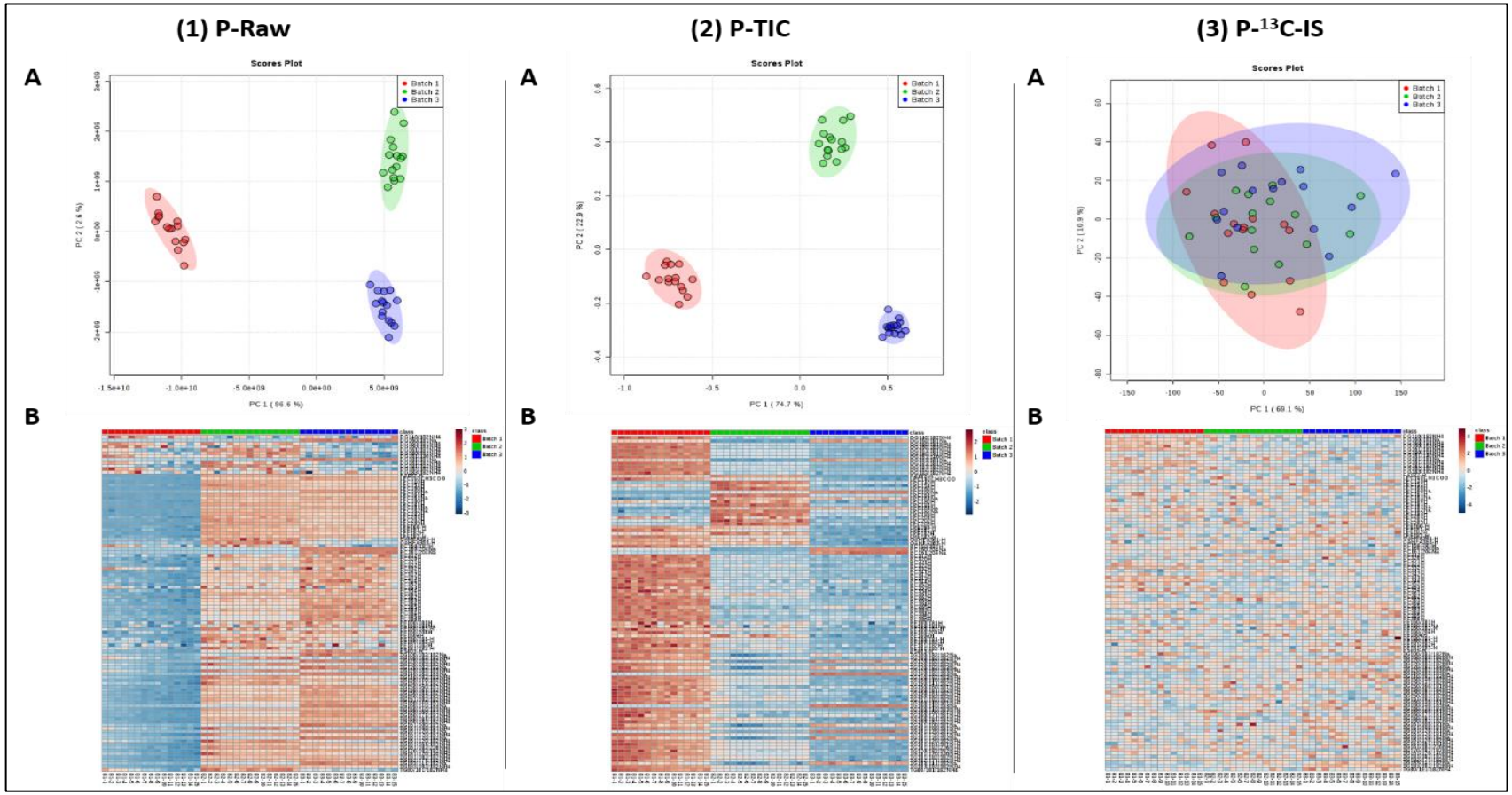

Figure 4.22: The effect of TIC normalisation ((2) P-TIC) and compound-specific normalisation by ^{13}C-IS ((3) P-^{13}C-IS) compared to raw data ((1) P-Raw). The results were visualised as A) PCA score plots overview and as B) heat map where the red, green and blue samples represent samples analysed at day 0, day 7 and at day 14 respectively. Data shown are based on pooled human plasma sample from blood bank extracted and analysed (*n*=15) at different days to study the effect of normalisation by ^{13}C-IS in reducing variations introduced during sample analysis on three separate days (batch to batch variations) where only common ions between plasma samples and ^{13}C-yeast extract (105 ions) where included in the analysis and normalised by TIC (P-TIC) and by ^{13}C-IS by compound-specific normalisation (P-^{13}C-IS) and compared to raw un-normalised data (P-Raw).

4.4.4.6 The effect of global ^{13}C-IS normalisation

Figures 4.23 and 4.24 represent the normalisation results of the selected ions. It appears that overall normalisation by TIC had significantly higher CV% compared to non-normalised data. Also, ions normalised by ^{13}C-IS exhibited different trends. Unexpectedly, ions normalised by ^{13}C-IS based on RT showed a significant reduction in the overall CV% compared to non-normalised data while ions normalised by ^{13}C-IS based on class similarity and RT revealed a non-significant increase in the overall CV%. Ions normalised based on class similarity are expected to have a lower CV% because lipids in the same class are known to have similar response factor as they share the same head group and therefore, they are expected to undergo a similar level of ion suppression during analysis (73, 261). A closer look at the ions that were normalised revealed that 89 ions out of 423, their CV% was increased when normalised based on class similarity compared to when normalised based on RT. A list of these ions is shown in Table 4.4. It shows that SM and TG are the most affected lipids. 62 ions out of 72 identified SM were negatively affected when normalised based on class similarity. Such observation is believed due to false identification by LipidSearch™. Where if the ^{13}C -SM that used as IS to normalise other lipid ions in the same class was not really an SM that will affect the normalisation process since different lipid classes are subjected to a different level of ion suppression (73). The second affected group were TG. TG detected at RT before 10.50 min were negatively affected when normalised based on class similarity by ^{13}C -TG. Similarly, false identification of these early eluted TG could be the reason especially when that the first ^{13}C -TG was detected at RT after 11 min. Also, it could be that the used ^{13}C -TG for normalisation does not reflect the response of these TG with short fatty acyl chain since identical

response factors are not valid for non-polar lipid classes such as TG and SM where the response factors for these species is dependent on fatty-acyl chain length and their degree of unsaturation (73, 261). It has been reported that instrumental response of phospholipid species decreases with increasing acyl chain length, especially at high lipid concentration, while the instrumental response increases with increasing the level of unsaturation of these species (261).

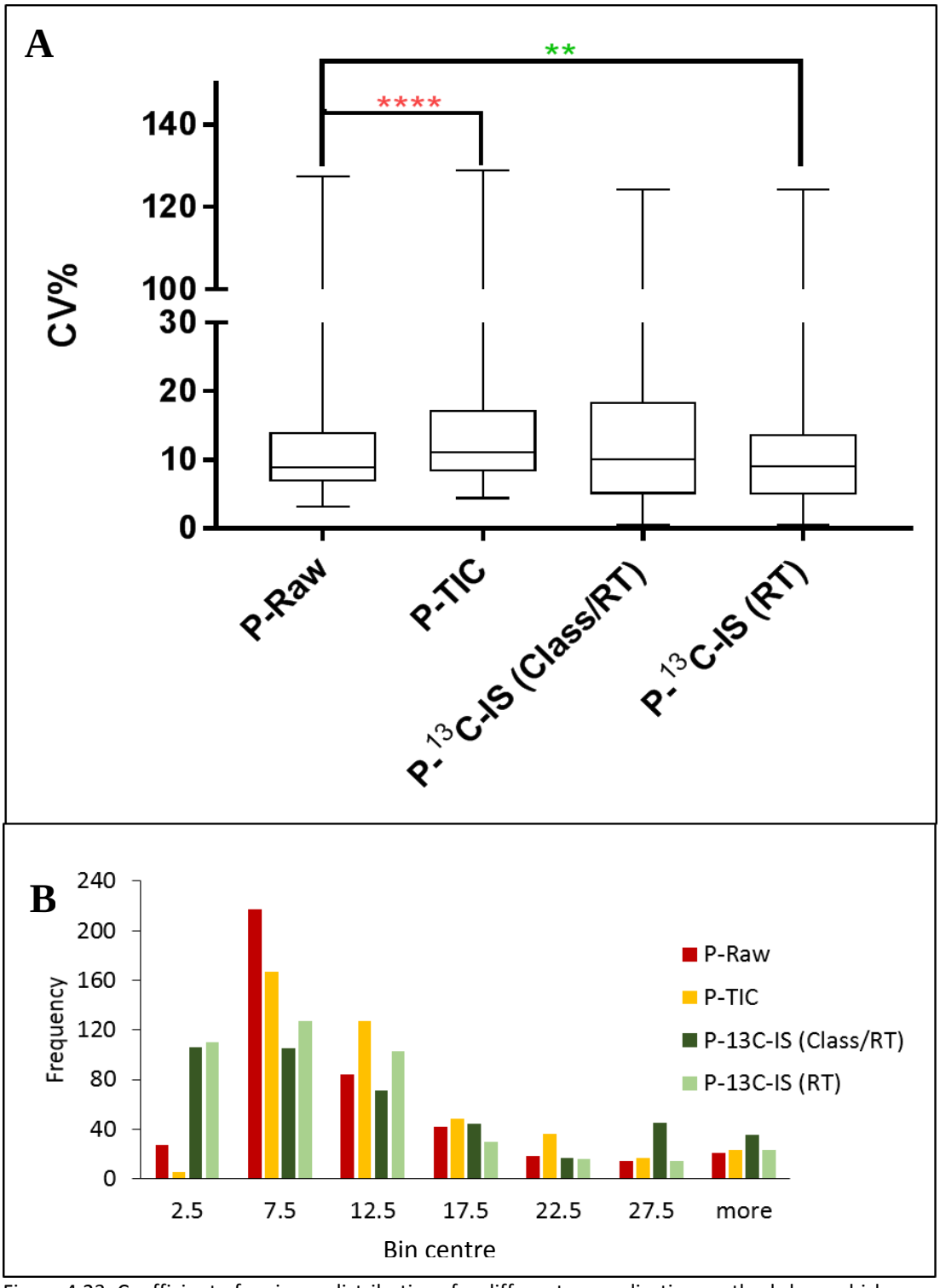

Figure 4.23: Coefficient of variance distributions for different normalisation methods by a whisker plot (A) and by a histogram where the X-axis represents the bin centre of CV% while the Y-axis represents the counts for each bin (Frequency) (B). Data shown are based on pooled human plasma sample from blood bank repeatably injected and analysed (*n*=230) to study the effect of global normalisation by ^{13}C-IS in reducing variations introduced during sample analysis over a long analysis time where all 423 lipid ions detected in more than 50% of the samples where included in the analysis and normalised by TIC (P-TIC) and by ^{13}C-IS by compound-specific normalisation and non-compound specific normalisation either based on RT only (P-^{13}C-IS (RT))or based on RT and chemical similarity (P-^{13}C-IS (class/RT)) and compared to raw un-normalised data (P-Raw). (**** p <0.0001, *** p <0.001, ** p <0.01, * p <0.05, where the green colour indicates a reduction in overall CV% while the red colour indicates an increase in overall CV%).

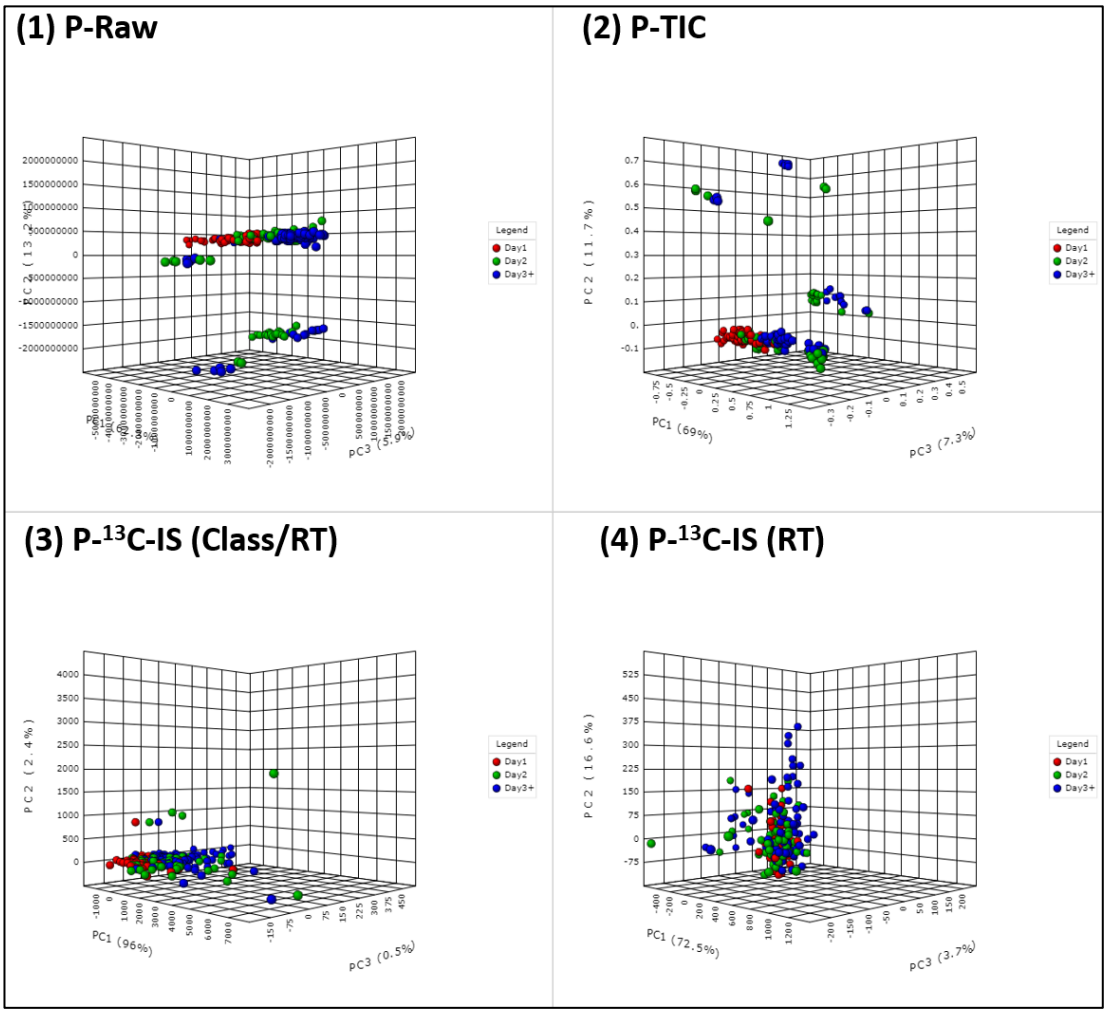

Figure 4.24: The effect of different normalisation methods on the PCA score plots overview. Data shown are based on pooled human plasma samples from blood bank repeatably injected and analysed (*n*=230) to study the effect of global normalisation by ^{13}C-IS in reducing variations introduced during sample analysis over a long analysis time where all 423 lipid ions detected in more than 50% of the samples where included in the analysis and normalised by TIC (P-TIC) and by ^{13}C-IS by compound-specific normalisation and non-compound specific normalisation either based on RT only (P-^{13}C-IS (RT)) or based on RT and chemical similarity (P-^{13}C-IS (class/RT)) and compared to raw un-normalised data (P-Raw).

Table 4.4 : List of 89 ions that have a higher CV% when normalised by ^{13}C-IS based on class similarity compared to when normalised based on RT only.

Lipid ID	Polarity	RT (min)	CV%		Difference in CV%
			Ions normalised based on ^{13}C-IS (Class/RT)	Ions normalised based on ^{13}C-IS (RT)	
SM(d34:1)+H	+	8.75	29.84	1.71	-28.13
SM(d32:1)+H	+	8.34	31.71	4.05	-27.65
SM(d34:2)+H	+	8.43	29.83	2.60	-27.23
SM(d32:2)+H	+	7.98	31.99	5.83	-26.16
SM(d38:1)+H	+	9.47	28.59	2.68	-25.91
SM(d30:1)+H	+	7.76	31.89	6.49	-25.41
SM(d40:2)+H	+	9.49	28.50	3.25	-25.25
SM(d38:2)+H	+	9.15	28.03	3.73	-24.30
SM(d39:1)+H	+	9.64	27.90	3.92	-23.99
SM(d36:3)+H	+	8.54	29.59	5.64	-23.94
SM(d35:1)+H	+	8.91	28.15	4.36	-23.79
SM(d42:1)+H	+	10.17	27.61	3.98	-23.63
SM(d42:3)+H	+	9.71	28.44	5.73	-22.72
SM(d40:1)+H	+	9.80	29.10	6.43	-22.66
SM(d41:1)+H	+	9.98	28.08	5.50	-22.58
SM(d42:2)+H	+	9.79	28.53	6.06	-22.47
SM(d43:2)+H	+	9.99	28.10	5.83	-22.27
SM(d43:1)+H	+	10.31	27.53	6.00	-21.52
TG(33:1)+NH_4	+	6.10	27.53	6.10	-21.43
SM(d42:3)+H	+	9.31	27.04	5.90	-21.14
SM(d18:2/22:2)+H	+	9.51	33.10	12.41	-20.69
SM(d39:2)+H	+	9.26	28.57	7.91	-20.66
SM(d35:2)+H	+	8.52	31.72	11.89	-19.83
SM(d18:1/25:3)+H	+	10.05	28.15	8.42	-19.74
SM(d16:1/25:3)+H	+	9.68	29.34	10.35	-18.98
SM(d16:1/18:3)+H	+	8.37	37.75	18.80	-18.94
SM(d18:1/20:3)+H	+	8.97	33.93	15.11	-18.82
SM(d18:1/24:3)+H	+	9.79	30.07	11.67	-18.40
SM(d45:4)+H	+	10.45	27.85	9.59	-18.26
SM(d18:2/18:3)+H	+	8.45	32.11	13.98	-18.13
SM(d18:1/26:4)+H	+	9.80	29.46	11.66	-17.81
SM(d17:1/26:4)+H	+	9.75	29.55	12.17	-17.38
SM(d36:2)+H	+	8.81	29.36	12.63	-16.73
SM(d45:5)+H	+	9.74	27.41	10.76	-16.65
SM(d36:1)+H	+	9.11	29.35	12.96	-16.39
SM(d18:2/24:3)+H	+	9.52	32.41	16.31	-16.10
SM(d32:2)+CH_3COO	-	7.96	26.26	10.39	-15.87
SM(d18:1/18:3)+H	+	8.81	40.20	25.04	-15.16
SM(d18:1/14:0)+CH_3COO	-	8.34	20.23	6.37	-13.86
SM(d41:2)+H	+	9.68	28.28	14.57	-13.71
SM(d18:1/26:3)+H	+	10.16	32.46	18.78	-13.68
TG(9:0/9:0/15:2)+H	+	6.07	25.14	11.62	-13.51
SM(d44:1)+H	+	10.44	27.15	13.70	-13.45
SM(d33:1)+CH_3COO	-	8.56	18.92	5.67	-13.25
SM(d18:1/16:1)+CH_3COO	-	8.43	18.23	5.24	-12.99
TG(6:0/10:0/17:0)+NH_4	+	6.57	26.41	13.91	-12.50

TG(6:0/10:0/17:0)+H	+	6.56	26.49	14.23	-12.26
SM(d18:1/16:0)+CH_3COO	-	8.76	17.79	5.68	-12.11
SM(d30:1)+CH_3COO	-	7.85	20.94	8.89	-12.04
SM(d18:0/18:3)+CH_3COO	-	8.54	23.08	11.25	-11.83
SM(d36:0)+H	+	9.11	26.52	15.80	-10.72
PC(38:6e)+H	+	9.10	24.19	13.61	-10.57
SM(d18:1/18:1)+CH_3COO	-	8.81	18.12	8.94	-9.19
TG(6:0/16:0/18:2)+NH_4	+	10.54	16.88	7.94	-8.94
TG(4:0/16:0/16:0)+NH_4	+	10.41	17.61	8.73	-8.87
SM(d44:2)+CH_3COO	-	10.14	19.76	12.36	-7.40
SM(d25:0/18:2)+CH_3COO	-	9.90	19.33	12.02	-7.31
SM(d41:1)+CH_3COO	-	9.98	18.56	11.27	-7.30
SM(d42:1)+CH_3COO	-	10.16	18.01	10.89	-7.12
SM(d22:0/20:2)+ CH_3COO	-	9.79	18.34	11.25	-7.09
SM(d43:1)+CH_3COO	-	10.32	19.63	12.55	-7.08
SM(d39:1)+CH_3COO	-	9.65	17.83	10.89	-6.94
SM(d22:0/18:1)+ CH_3COO	-	9.80	18.08	11.15	-6.93
SM(d41:2)+CH_3COO	-	9.69	18.44	11.53	-6.91
SM(d22:0/20:3)+CH_3COO	-	9.70	17.62	11.04	-6.58
SM(d22:1/18:1)+CH_3COO	-	9.47	17.52	11.00	-6.52
SM(d20:0/18:1)+CH_3COO	-	9.47	17.33	10.86	-6.47
TG(6:0/18:1/18:2)+NH_4	+	10.55	15.66	9.82	-5.84
SM(d18:2/26:4)+H	+	9.43	31.33	27.60	-3.73
TG(36:1)+Na	+	5.70	28.58	25.46	-3.12
PC(34:0e)+H	+	9.54	13.54	10.43	-3.10
TG(4:0/16:0/16:0)+Na	+	10.41	20.97	17.88	-3.09
PC(40:2)+H	+	9.87	13.61	10.74	-2.87
PE(18:0/20:4)-H	-	9.25	13.17	10.33	-2.84
PC(44:6e)+H	+	9.81	10.71	7.98	-2.73
PC(42:4p)+H	+	9.73	10.84	8.79	-2.05
SM(d20:0/17:1)+ CH_3COO	-	9.35	15.76	13.78	-1.98
PC(38:3e)+H	+	9.62	16.90	15.25	-1.65
PC(18:0/22:6)+Na	+	9.05	16.36	14.76	-1.60
PC(44:7e)+H	+	9.81	11.94	10.41	-1.53
PE(18:0p/18:2)+H	+	9.45	7.26	5.99	-1.28
ChE(20:5)+NH_4	+	12.88	4.40	3.13	-1.27
TG(6:0/16:0/16:1)+NH_4	+	10.35	14.89	13.72	-1.18
PS(36:0p)-H	-	5.43	9.12	8.09	-1.03
PC(18:2/20:4)+Na	+	8.74	11.01	10.14	-0.87
PS(38:0e)-H	-	6.33	9.81	9.01	-0.81
PE(20:0p/20:4)+H	+	9.49	10.13	9.57	-0.56
PC(37:7)+H	+	8.70	37.18	36.88	-0.30
PE(16:0p/22:4)+H	+	9.36	7.70	7.42	-0.28

4.5 Conclusion

As stated before, metabolites in LC-MS based metabolomics studies can be subjected to a different level of systematic and random errors that are not easy to assess or to correct. The optimal ^{13}C-IS yeast extract has fully demonstrated the effectiveness of these IS mixture in reducing different types of variations introduced at different level in lipid ions response in lipidomics studies during sample preparation and analysis especially in large scale studies where a large number of samples are included that require long analysis time or need to be analysed at different batches as is shown in Figures 4.18 to 4.24 .

Labelled IS-based normalisation methods are superior to other normalisation methods because the data for each sample can be performed independently of other samples in the run. In addition, depending on the timing of adding the IS, different types of variations can be corrected while most of the proposed methods can be considered as post-acquisition correction (105). Although in all previous experiments the assessment of QC samples indicates high quality data that worth exploring, when LC-MS system is subject to higher analytical variability where the level of errors is expected to increase and affect the quality of the data, ions normalised by ^{13}C-IS exhibit an overall lower CV% due to the ability of the IS in correcting errors introduced during samples preparation and analysis. Therefore, the use of ^{13}C-IS mixture can be used to obtain a more accurate estimate of the studied lipids identified in clinical samples.

In addition, normalisation by TIC had a variable response pattern for unknown reasons. However, previous studies suggest that TIC is affected by some biological

factor and does not just account for instrumental variations which can occur with equally probability at any point in the analysis and increase in metabolites intensity is compensated by a decrease in others (246, 265).

The validated proposed normalisation method using stable isotopically labelled IS mixture produced by *in vivo* labelling strategy has shown to be an effective normalisation method in reducing technical and analytical variations that can be introduced at different steps in metabolomics/lipidomics studies. Therefore, the IS mixture can now be used to obtain a more accurate estimate of the lipid identified in clinical samples

Chapter Five

Lipidomic analysis of low-grade glioma in human brain tissue biopsies

5. Lipidomic analysis of low-grade glioma in human brain tissue biopsies

5.1 Introduction

5.1.1 Metabolism in normal cells vs cancerous cells

Normally, cell proliferation is essential for embryogenesis, growth and maintaining proper function of several tissues. Cellular growth, proliferation and death within multicellular organisms depend on the presence of appropriate intracellular and extracellular signals that maintain a balance between cell accumulation and cell death necessary for normal development and tissue homeostasis (266). During cell proliferation, the total biomass of proteins, lipids and nucleic acids are doubled to meet the required nutrients, energy, and biosynthetic activity to duplicate all macromolecular components during each passage through the cell cycle. It is therefore not surprising that metabolic activities in proliferating cells are fundamentally different from those in nonproliferating cells (266-268).

Cancer cells frequently display altered cellular metabolism. These alterations support the increased production of metabolic intermediates required for the synthesis of proteins, nucleic acids and lipids needed for the rapid proliferation (269). Furthermore, these alterations are strongly related to carcinogenesis processes and phenotypes, including transformation, progression, migration and invasion (24). The most prominent alterations are an increase in glucose uptake by aerobic glycolysis, a phenomenon known as the “Warburg effect” (270). Thus extensive aerobic glycolysis has been indicative of aggressive cancer (271). An increase in glutaminolysis has been documented in proliferating cells such as tumour cells especially when energy production from glycolysis is not sufficient (272, 273). Abnormal amino acid and

tricarboxylic acid (TCA) cycle metabolism and other alterations including protein, nucleic acid and lipid biosynthesis, are also enhanced as part of cancer-metabolic reprogramming (269, 274). For example, the pentose phosphate pathway is up-regulated in cancer cells that mediate nucleotides production required for RNA synthesis (275-277). Lipids play many key roles in various cellular functions, such as energy storage, signalling, cell membrane formation, cell-cell interactions in tissues, proliferation, survival, and death (9, 278, 279). Consequently, cancer cells coordinate the activation of lipid anabolic metabolism, membrane formation, production of signalling molecules, and generate adenosine triphosphate (ATP) as an energy source via fatty acid oxidation under energy-deficient conditions (280). Hence there is good reason to study the changes in lipid metabolism in cancer cells and tissues as potential markers of cancer progression or diagnosis.

Various metabolic/lipidomic biomarkers have been assessed to underline their role in diagnosis, in prognostic characterisation and in prediction of therapeutic outcomes. In 2016, Perrotti *et al.* pointed out the potential identified lipid biomarkers in various tumour types. Among the 52 reviewed papers, 65 lipid species or lipid classes which were up or down regulated in the respective sample type have a diagnostic response power and 12 lipid species or lipid class have prognostic response power while only 5 lipid species or lipid class have a predictive value of therapy response in the case of patients receiving neoadjuvant chemotherapy (24). Biomarkers have the potential to improve diagnosis of the disease at early stages, classifying tumoral stages, predicting drug efficacy, contributing to an understanding of drug mechanism of action and may potentially pave the way to personalised care of cancer patients. In spite of significant improvements in cancer diagnoses and

treatments, early detection of cancer through diagnostic, prognostic and predictive metabolic biomarkers remains difficult and requires further investigation (24).

5.1.2 Inter and intra-tumour heterogenicity

Cellular composition of cancer cells and their metabolic activity may vary between patients and/or it may vary within individual tumour regions (281, 282). Intertumoral heterogeneity refers to tumours from different patients whose altered genotype and phenotype are induced by diverse etiological and environmental factors while intratumor heterogeneity refers to genomic and biological variations within a tumour lesion, acquired by tumour cell evolution under diverse microenvironmental selective pressures, linked to different aetiologies (283).

Intra-tumour genetic and metabolic heterogeneity in various cancerous tissue have been documented and proven. Okegawa *et al.* identified metabolic differences within regions of the same tumour in patients with renal cell carcinoma especially in pyruvate metabolism and these findings could improve patient stratification or enlighten personalised therapeutic approaches in human kidney cancer (284). Hensley *et al.* recognised metabolic intra-tumour heterogeneity in patients with non-small cell lung cancer that is related to the perfusion status of the tumour. However, it is unclear whether the change in metabolic activity results from the perfusion status of the tumour or whether the reduced perfusion and altered metabolism are consequences of other factors (285). Gogiashvili *et al.* demonstrated metabolic intra-tumour heterogeneity in patients with breast cancer using ^{1}H NMR spectroscopy, where intra-tumoral variability in the concentration of 32 metabolites across different region of the tumour in three patients was shown (281). In addition, several

groups reported intra-tumoral heterogeneity in glioblastoma patients with different subclones within the tumour that were composed of different populations of cells. Moreover, these subclones exhibited dissimilar drug sensitivities and could use alternative pathways for proliferation (286-289).

Three models have been proposed to explain intra-heterogeneity of a tumour as seen in Figure 5.1: the clonal evolution model, the hierarchical cancer stem cell model and the dynamic or plastic cancer stem cell model. In the clonal evolution model, Peter Nowell proposed that a tumour arises from a single mutated cell that keeps acquiring additional mutations as it progresses and eventually gives rise to additional subpopulations that can further divide and mutate. Then, based on physiological selection pressures conferred by the tumour microenvironment, more aggressive subpopulations are sub-selected over the others based primarily on survival advantage. Thus, this model explains intra-tumour heterogeneity as a result of natural selection. The predominant clones may differ in time and space as different requirements may be present in different areas of the tumour resulting in a complex structure that is further complicated by the application of therapy (276, 290, 291). The hierarchical cancer stem cells model suggests that within a tumour, only a subset of the cells called cancer stem cells (CSCs) possess indefinite self-renewal ability responsible for initiation and maintaining tumour growth, therapy resistance and metastasis. In contrast, the bulk of a tumour consists of rapidly proliferating cells and postmitotic, differentiated cells that cannot self-renew and therefore their contribution to the long-term maintenance of the tumour is negligible. However, this model explains intra-tumour heterogeneity as a result of differences in the stem cells from which they originated (292-295). In the dynamic CSCs, the CSCs phenotype is

much more fluid and de-differentiation of non-CSCs to CSCs can be regulated by external signals and consequently return to the malignant growth cycle (296).

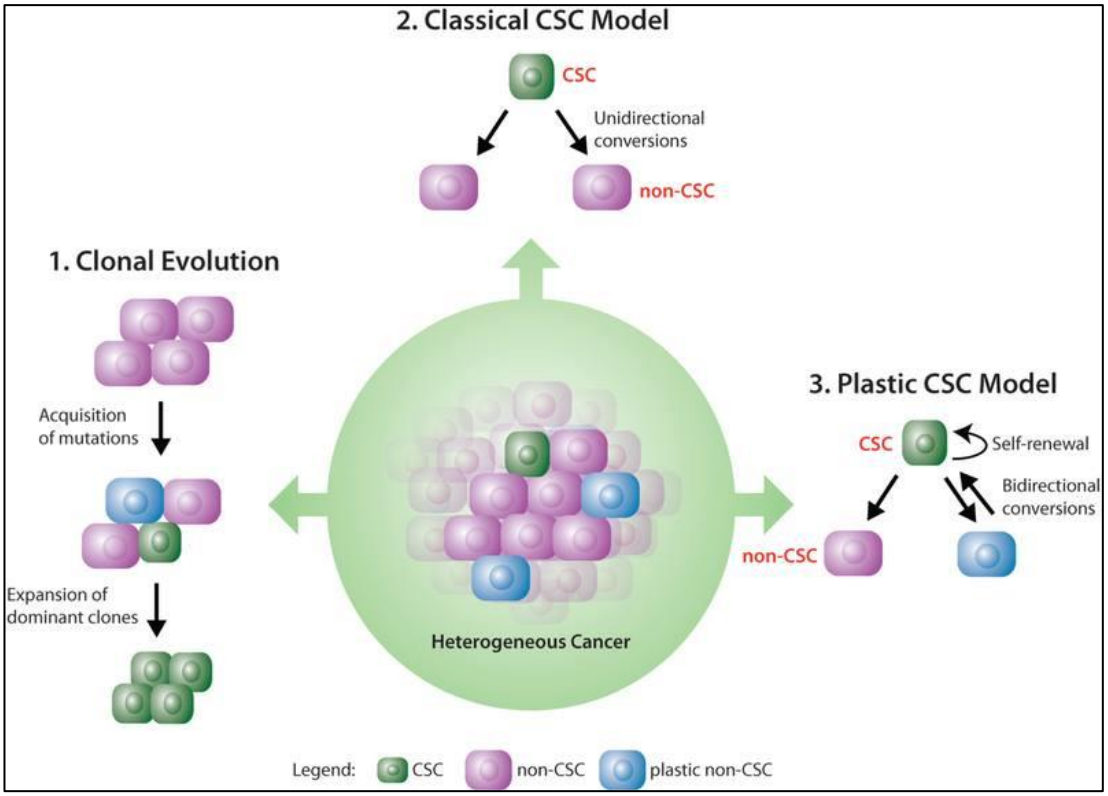

Figure 5.1: Models of tumour heterogeneity, these models are interchangeable and within a particular disease context, all three modes may be present within distinct sub-clonal populations (296). CSC: cancer stem cell.

5.1.3 Clinical implications of intratumor heterogeneity

Intra-tumour heterogeneity and its dynamic nature during the disease development, progression and through treatment, create challenges for the identification of predictive or prognostic biomarkers that could defines clinical outcome as the targeted subclones, or the identified biomarkers may not be readily detectable at diagnosis. This is also a major limitation for therapy choice. For example, targeting one genetic or metabolic pathway based on tumour collected from one region, whilst ignoring prominent dysregulated pathways in other intra-tumour regions, which may

then re-grow the resistant tumour. In addition, samples at primary diagnosis and surgery, represent one molecular snapshot of the cancer and not necessarily the molecular (or metabolic) disease at a later stage when chemotherapy is administered. Thus, bias in sampling could arise in oncologic practice as the therapeutic decision is often made with reference to the primary tumour lesion that is usually diagnosed months or years previously or in cases with patients presented with advanced stage of the disease, from one metastatic site (297-299). This raises important questions. Can clinicians easily discriminate between normal and malignant tissue? Is a single biopsy representative of the whole tumour? Moreover, can these inter and intra-tumoral differences hamper biomarker discovery as multiple sampling from different tumour regions is often impractical?

Furthermore, intra-tumour heterogeneity could affect the treatment success as different subclones of the tumour could have different drug sensitivity. For example, Akio *et al.* showed that the sensitivities of subclones derived from a glioblastoma patient to an inhibitor of epidermal growth factor receptor were dissimilar and could lead to tumorigenesis and therapeutic resistance (286). Similarly, patients diagnosed with chronic myelogenous leukaemia are prone to relapse of the disease due to intra-tumour heterogeneity. Chronic myelogenous leukaemia is caused by the chromosomal translocation that creates a chimeric protein with abnormal kinase activity termed as Bcr-Abl. In these patients, a remarkable response to an inhibitor of Bcr-Abl, imatinib mesylate is observed. However, a significant fraction of these patients suffers from relapse of their disease due to the presence of resistant subclones of leukemic cells which make Bcr-Abl insensitive to inhibition by imatinib. Eventually, the treatment was thought to provide a selective pressure that drives the

expansion of these resistant cells, causing the eventual relapse of the disease (300-303). As a result, intra-tumour heterogeneity can facilitate the adaptation of tumours to different environmental stress that ultimately lead to poor patient outcome in multiple cancer types, including glioblastoma, leukaemia, lung, breast, colon cancer and others (291, 304-307). In addition, it is estimated that only 100 of the estimated 150,000 biomarkers (less than 0.07%) have been qualified and implemented into clinical practice (308). Considering the diversity of intra-tumour heterogeneity, the small population size utilised in cancer diagnostic studies that could affect the statistical power of the study that will ultimately affect implantation of discovered biomarkers into clinic practice (309). Therefore, larger numbers of patients should be screened to determine whether certain markers are more reliable in certain subsets of patients. Thus, understanding the link between inter-tumour and intra-tumour heterogeneity could improve tumour subclassification, treatment stratification and outcome. As a single sample selection could lead to a bias that could lead to inaccurate conclusions, the awareness of the existence of inter and intra-tumoral differences is crucial.

5.1.4 Glioma: aetiology and current treatment

Glioma is an umbrella term used to describe different types of tumours that originate from the glial cells that surround and support neurons in the brain. Glioma includes astrocytes (astrocytoma, anaplastic astrocytoma and glioblastoma), oligodendrocytes, ependymal cells and mixed gliomas (280, 310-312). Gliomas are further classified into grade I, II, III and IV based progressively on the level of malignancy and overall median survival. Grade I gliomas are the least aggressive grade and are related to lesions that have low proliferative potential and can be cured

by surgical procedure, whereas, grade III and IV gliomas are highly malignant and invasive (313, 314). Glioma accounts for ~26% of all primary brain tumours and ~81% of malignant tumours based on studies conducted in the United States between 2011–2015 (315). Grade I and II are considered as low-grade form of the disease with median survival time after surgery between 7-15 years; whereas grade III and IV are classified as high-grade with median survival times after diagnoses of between 3.5-10 years and less 1-2 years, respectively (316). Radical surgery is the first choice for management for low-grade glioma where resection of all visible cancerous tissue followed by radio and/or chemotherapy greatly reduces the risk of subsequent malignant transformation (316). However, it was suggested that due to intra-tumour heterogeneity of these cancer cells, some cells can escape conventional treatments such as chemotherapeutic and radiological treatments and infiltrate into the surrounding normal tissues which complicate their safe removal. In addition, this could explain the invariable relapse and increased incidence of transforming of these low-grade gliomas into a higher and more aggressive grade (317, 318). Complete resection of grade IV glioma (Glioblastoma) guided by the administration of 5-amino-levulivinic acid (5-ALA) (a porphyrin metabolised by cells where the heme synthesis pathway is active, to the fluorescent metabolite protoporphyrin IX) to patients as a drink taken before the surgery, paves the way to more complete resections of the tumour that lead to improved patients overall survival (319). Exploring the metabolic pattern (lipidomic) of these subclones if present, will help in understanding intra-tumour heterogeneity and potentially explain the unavoidable relapse of these tumours and their progression into a higher and more aggressive grade.

5.2 Objectives

The presence of intra-tumour heterogeneity in patients diagnosed with glioma grade II will be explored by assessing lipidomic profiling and intra-tumoral variability of identified lipids from spatially-distinct samples obtained from resected tumour tissue from five patients via an advanced lipidomic profiling method using LC-MS. The study will falsify the hypothesis that there are intra-tumour differences in metabolism in grade II gliomas (low grade glioma (LGG)). If this hypothesis is accepted, this may open research avenues to assess whether one or more sub-populations may ultimately be responsible for progression to grade IV gliomas.

5.3 Materials and methods

5.3.1 Tissue specimens

Glioma tissue samples were collected from five patients with confirmed astrocytoma IDH-1 mutant grade II cancer, treated at the Queen's Medical Centre (QMC) within the UK NHS Trust centre. After surgery, the tissue was snap frozen and stored at –80°C within 10 min. The use of fresh frozen human tissue was approved by the National Research Ethics Service Committee in East Midlands, UK (ethics approval reference 11/EM/0076). Five replicate samples from different locations of the tumour specimens were resected and named A to E. Clinical and pathological characteristics of patients are described in Table 5.1.

Table 5.1: Clinical and Pathological Data from five patients diagnosed with confirmed astrocytoma IDH-1 mutant grade 2 cancer.

Patient code	Sex	Age	Ethnicity	Anatomical brain lobes	Sample location	Sample code
Patient one (LGG 2)	Male	25	White British	Parietal lobe	Superficial	2.1
					Central core	2.2
					Superior	2.3
					Posterior	2.4
Patient two (LGG 5)	Female	37	White British	Left frontal lobe	Superficial	5.1
					Anterior	5.2
					Posterior	5.3
					Central core	5.4
					Inferior	5.5
Patient three (LGG 7)	Female	27	Asian British	Right frontal lobe	Superficial	7.1
					Central core	7.2
					Posterior	7.3
					Anterior	7.4
					Medial	7.5
Patient four (LGG 11)	Female	19	White British	Left frontal lobe	Rim	11.1
					Central core	11.2
					Inferior	11.3
					Lateral	11.4
					Invasive margin	11.5
Patient five (LGG 12)	Male	32	White British	Left frontal lobe	Superficial	12.1
					Anterior	12.2
					Posterior	12.3
					Central core	12.4
					Deep	12.5

5.3.2 Histology

Primary tumour tissue was fixed in 4% paraformaldehyde and 5 µm thickness tissue sections were obtained using a microtome. The tissues were mounted on slides and incubated at 37°C overnight, deparaffinised in xylene and hydrated through decreasing concentrations of ethanol. Then, tissue sections were counter-stained with Harris hematoxylin and Eosin (Surgipath, UK), dehydrated and mounted for microscopic analyses. Histological tests were done only for spatially resolved samples from tumour resected from patients # 1, 2 and 3.

5.3.3 Sample extraction

Samples were extracted for different projects according to Bley and Dyer method (99). Samples were allowed to precool at 4°C, then per 10 mg of tissue, 100 µL of pre-cooled HPLC grade methanol at -20 °C was added, and the tissues were disrupted using a hand-held homogeniser (Bibby Scientific Stuart, SHM1) for 30 s. Then, 300 µL of pre-cooled HPLC grade chloroform at -20 °C was added, and the samples were vortexed for 30 s, followed by administration of 100 µL of pre-cooled deionised water and further vortexed for 30 s. Samples were then centrifuged for 10 min at 13000 x *g* at 4°C to help separate the two phases (upper polar layer and lower nonpolar layer). The polar layer was collected and analysed for a different project and the lower layer (lipid rich layer) was used in this project. 200 µL of the lower layer was mixed with 100 µL of the optimised ^{13}C-IS mixture obtained by an *in vivo* labelling strategy using *P. pastoris*. Then, the samples were dried under vacuum at room temperature and the dried samples were reconstituted using 100 µL of LC-MS grade isopropanol and stored at 80°C until analysis. Another 200 µL of the lower layer of each sample was dried and reconstituted using 100 µL of LC-MS grade isopropanol to investigate if the ^{13}C-IS mixture was able to correct for any analytical variations. The homogeniser was cleaned between two samples using 70% IMS and Chemgene disinfectant solutions. QC samples were prepared by pooling 5 µL from each sample extract.

5.3.4 LC-MS analysis

The LC-MS analysis was carried out as previously described in section 2.3. Five injections of QC sample were analysed at the beginning of the run to condition the column before the analysis, then the samples were analysed in a random order. QC

sample was injected after each ten randomised samples to monitor the repeatability of the LC-MS system.

5.3.5 Lipid identification

Lipid ions were putatively identified based on their fragmentation pattern by LipidSearch^{TM} based on parameters listed in section 2.4.1. The main question was whether the addition of ^{13}C-IS mixture would affect lipid ions identification in the samples of interest, and the aim was to merge the quantification with lipid profiling. Therefore, the number of identified ions of glioma samples extracted from patient # 2 with and without ^{13}C-IS mixture were compared.

5.3.6 Data processing and statistical analysis

Data processing and normalisation was performed as detailed in section 2.4.3. Although a high mass shift is expected to be introduced by ^{13}C-labelling, to ensure that there are no spectral overlays between the selected indigenous unlabelled ions identified in glioma samples and the ^{13}C-IS the following criteria were used: unlabelled ions selection criteria; ions detected in ≥50% of QC samples, average response of unlabelled ion mass in QC samples over its response in blank samples (based on the response of peaks detected at that specific *m/z* at defined RT) >10 and average response of unlabelled ion mass in QC samples over its response in ^{13}C-IS extract >10. For ^{13}C-IS selection; ions detected in all QC samples and their average response in QC samples over their response in blank samples (based on the response of peaks detected at that specific *m/z* at defined RT) >10. Lipid ions detected in QC samples with CV% more than 30 after normalisation were removed from any statistical analysis.

5.4 Results and discussion

5.4.1 Analytical performance and lipidomic data quality

The assessment of QC samples indicates a stable column and instrumental response during data acquisition since the calculated CV% of 77% of the detected features among the QC samples were less than 30, which indicate good instrumental reproducibility (155). This can be further confirmed by the clustering of QC samples closely together in the middle of a PCA scores plot of all samples analysed in this study as shown in Figure 5.2.

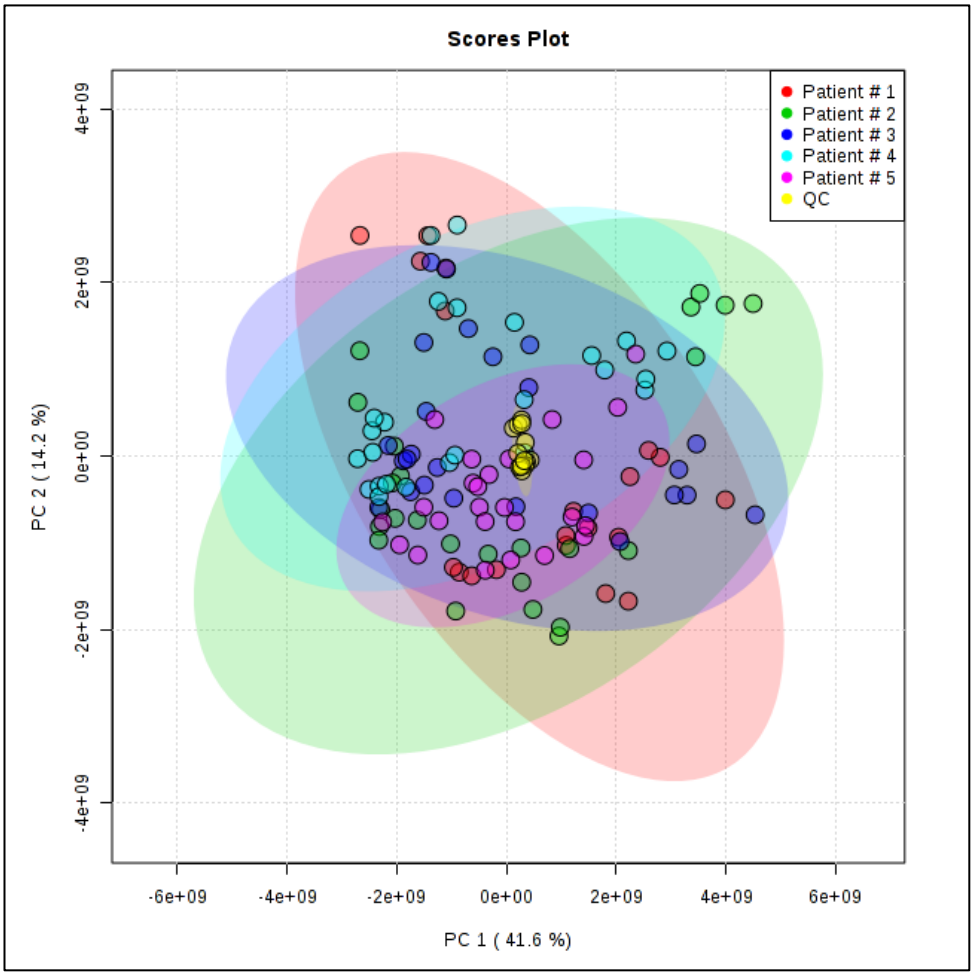

Figure 5.2: PCA plot of all samples analysed in this study where the QC samples are clustered in the middle of the plot. The shaded areas represent "The Hotelling's T ellipse or 95% confidence region" for each group.

5.4.2 Comparison of detected lipids between samples analysed with and without ^{13}C-IS mixture

Figure 5.3 represents the number of identified lipid ions in samples extracted from patient # 1 analysed with and without ^{13}C-IS mixture. On average, 317 lipid ions were putatively identified in samples analysed without ^{13}C-IS mixture in both positive and negative mode while 211 ions were identified in samples analysed with ^{13}C-IS mixture (The number of identified lipid species per sample extracted with and without IS mixture can be seen in Appendix Table A:4) (~33% reduction in number of identified lipid ions). Recent work by Rampler *et al.* has shown similar results, where they observed approximately ~10% decrease in the number of identified lipids in human plasma analysed with ^{13}C-IS mixture from *P. pastoris* (152). This could be attributed to ion suppression due to matrix effects as denser and more complex samples are obtained when ^{13}C-IS mixture is added to the samples as shown in total ion chromatogram and the spectrum of sample 2.1A analysed with and without ^{13}C-IS mixture presented in Figure 5.4. The co-eluted labelled ^{13}C-IS mixture or the unlabelled lipid ions appears to affect the number of unlabelled indigenous lipid ions from glioma samples as the method applied is to perform data-dependent acquisition mode where the most intense five ions per scan are selected and analysed by tandem mass spectrometry and if at certain scans the intensity of labelled ^{13}C-IS was higher than the indigenous ions or the indigenous ions suffered ion suppression, the previously identified ions in samples analysed without ^{13}C-IS will no longer be identified by LipidSearch™ in samples analysed by ^{13}C-IS. Therefore, an additional set of samples analysed without ^{13}C-IS were studied to obtain the highest possible number of identified lipid ions by LipidSearch™ in order to get as much as possible

of information that could effectively reveal intra-tumour heterogeneity in glioma samples.

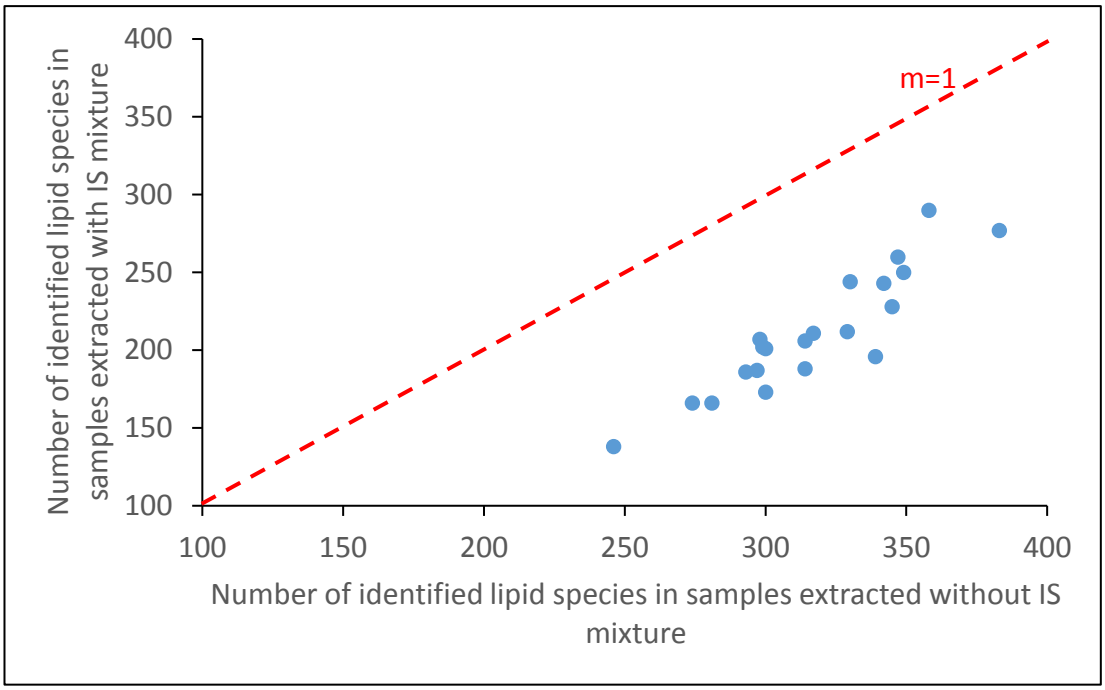

Figure 5.3: Number of identified lipid ions by LipidSearch™ in samples extracted from patient # 1 analysed with and without ^{13}C-IS mixture. The blue dots represent the samples whereas the red dash line repersents the unit line with slope of 1.

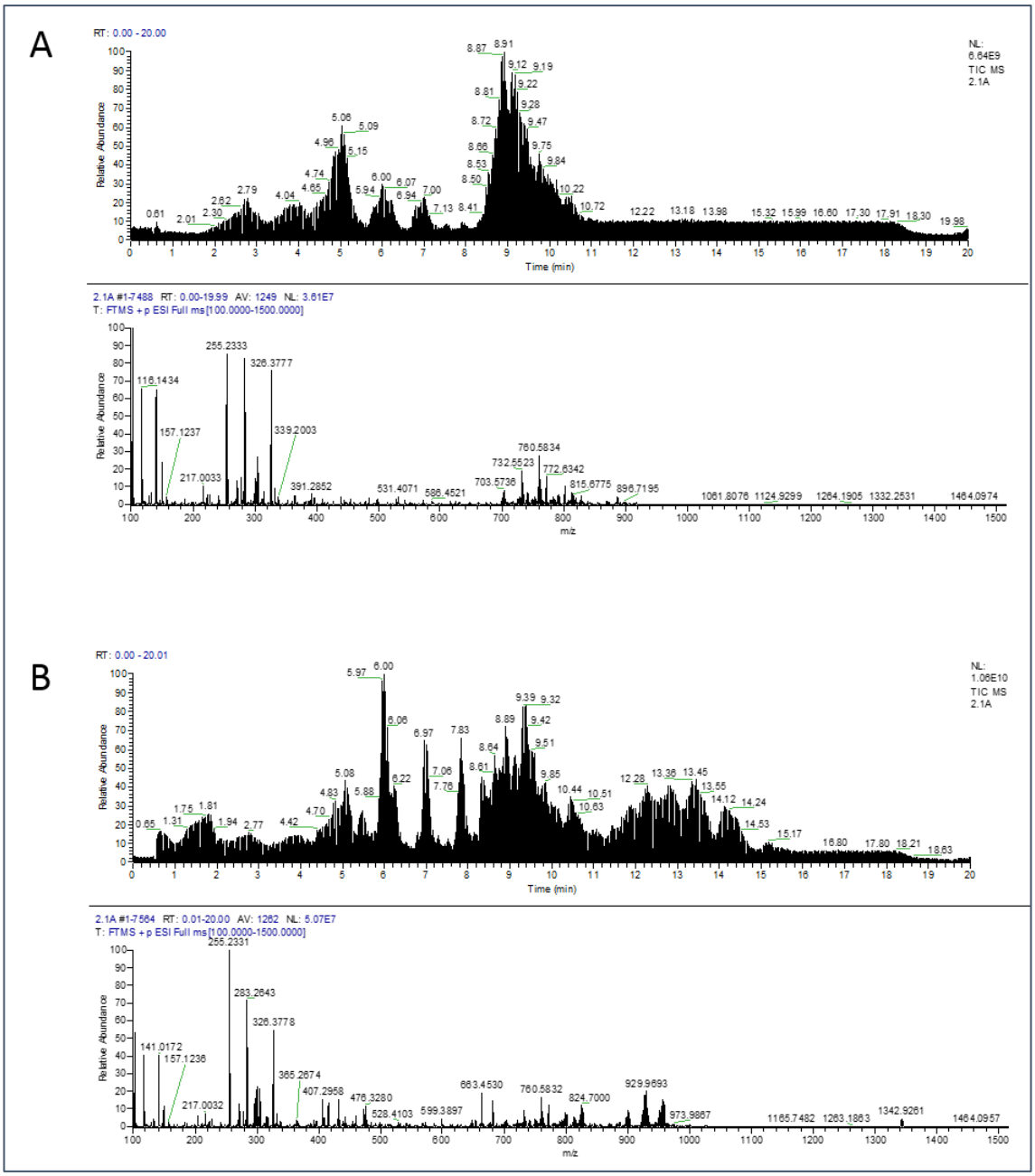

Figure 5.4: Total ion chromatogram and the spectrum of glioma sample extracted from patient # 2 (sample ID 2.1A) analysed without (A) and with (B) ^{13}C-IS mixture.

5.4.3 Normalisation by ^{13}C-IS mixture

As presented in Chapter 4, analysis of large batches of samples is subject to variation in instrumental response due to analytical drift. The addition of ^{13}C-IS mixture was proven to be valuable in correcting or minimising these variations. Since a large set of samples were included in this study (in total, 120 samples from five patients),

compound-specific normalisations were conducted for lipid ions where their respective fully labelled ^{13}C isotopes were detected in all samples. All other identified ions were normalised by one of the selected ^{13}C-IS detected in all samples based on RT. 603 unlabelled ions were detected in 50% or more of the samples. Among these detected ions, the labelled form of 59 ions were detected in all samples that can be used for compound-specific normalisation or to normalise other ions based on RT. The normalisation method was applied to the studied samples and used to investigate Intratumor heterogeneity in glioma biopsy samples in five patents.

5.4.4 Metabolic cluster in glioma samples

This experiment lacks suitable control samples, that is because it is impractical and unethical to take healthy brain tissues from the treated patients due to the location of the studied tumour. As a result, the lipidomic profile in different tumour regions cannot be correlated with the natural healthy state of tissue in normal brain. Therefore, no conclusion can be made on which region can represent more advanced stage of the disease or which region possess similar lipidomic pattern to healthy tissue that could guide the surgeon to define the margin of the tumour more accurately.

Based on the lipidomics data, the lipidome patterns of 120 tumour tissues were separated into two major clusters, Cluster # 1 (C1) and Cluster # 2 (C2) (see Figure 5.5). As shown in Figure 5.4A, Cluster # 2 can be further subdivided into two very closely related sub-clusters C2A and C2B. Relatively high R2 (0.554) and Q2 (0.539) scores were obtained in the proposed OPLS-DA model that indicates a good model and this was used to predict the clusters in the acquired samples. Cluster # 1 (C1) was

characterised by significantly elevated levels of DG, CL and MG while Cluster # 2 (C2) was characterised by significantly elevated levels of LPE, Cer, LPC, OAHFA, SM, dMePE, PE, PG, PC and PS. Table 5.2 represents lipids classes that are statistically different between the two clusters. As a part of anabolic metabolism of cancer cells, the increased cancer cell proliferation induces lipid biosynthesis in order to generate biological membranes. Also, these lipids could provide cancer cells with energy during nutrition and energy deficits, and they might play a more active role in cell transformation and cancer development (269). Since the intensity of identified lipid ions were not compared with the intensity of ions in normal tissue, it is therefore not possible to determine which cluster resembles the normal tissue or which cluster had more predominant changes in its lipid metabolism.

Table 5.2: List of statistically significant lipid classes between Cluster # 1 and 2 observed between spatially separated samples in five patients.

Lipid class	Fold change*	*p*-value	FDR
Lysophosphatidylethanolamine	5.01	1.06E-10	2.99E-10
Ceramide	3.25	2.02E-22	3.43E-21
Lysophosphatidylcholine	2.78	1.94E-9	4.70E-9
(O-acyl)-1-hydroxy fatty acid	2.19	1.0438E-2	1.365E-2
Sphingomyelin	1.78	3.30E-18	1.53E-17
Dimethylphosphatidylethanolamine	1.55	1.4895E-3	2.302E-3
Phosphatidylethanolamine	1.48	1.38E-20	1.18E-19
Phosphatidylglycerol	1.43	2.95E-5	6.27E-5
Phosphatidylcholine	1.34	3.60E-18	1.53E-17
Phosphatidylserine	1.27	8.12E-12	2.76E-11
Diacylglycerol	0.60	1.0079E-3	1.7134E-3
Cardiolipin	0.58	3.3773E-3	4.7845E-3
Monoacylglycerol	0.47	6.7121E-4	1.2678E-3

* Fold change = average response in Cluster # 2/ average response in Cluster # 1.

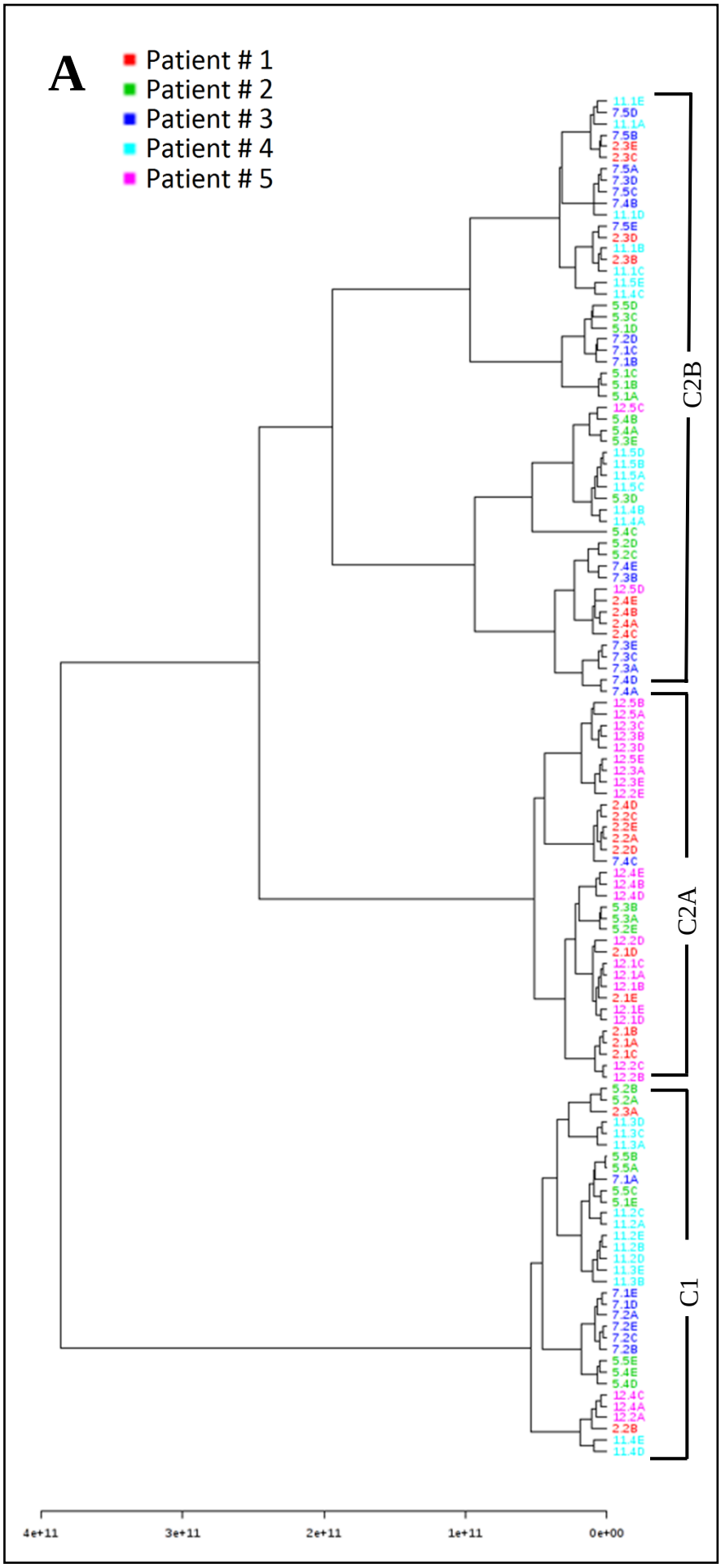
A
Patient # 1
Patient # 2
Patient # 3
Patient # 4
Patient # 5
C2B
C2A
C1
4e+11
3e+11
2e+11
1e+11
0e+00

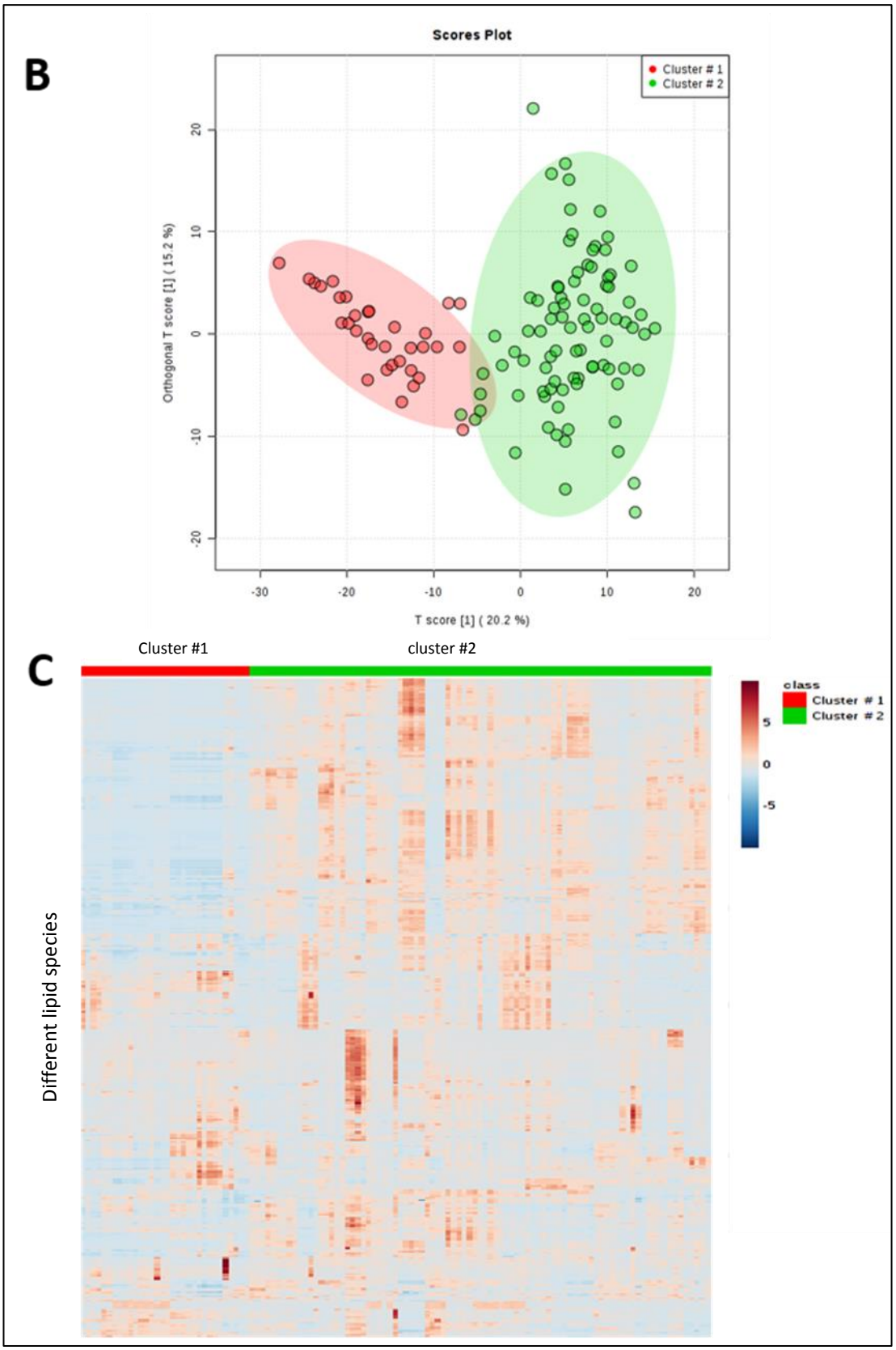

Figure 5.5: Intratumor heterogeneity in glioma samples revealed by lipidomics analysis A) Dendrogram resulting from unsupervised cluster analysis of the studied samples (see previous page), B) OPLS-DA scores plot of the two clusters revealed by hierarchical clustering and C) Heat map of lipidome of the two clusters.

5.4.5 Intra-tumour heterogeneity in glioma samples as revealed by lipidomic analysis

Lipidomic patterns at different tumour sites from five patients were classified into different metabolic clusters, which confirms intra-tumour metabolic heterogeneity. To illustrate the variability of lipid ions levels within each tumour region, the observed intensity was plotted for the separate tissues sampled from each tumour and CV% was calculated for each ion and the total CV% values were plotted as a whisker plot in Figure 5.6. As shown in Figure 5.6A, huge variability was observed within the same tumour as indicated by the high CV% per each patient. Also, the mean of the calculated CV% within each patient were as follows: 63, 80, 66, 79 and 59, respectively for patient # 1 to patient # 5. These results are supported by the PCA plot of identified lipid ions across different spatially resolved tumour samples within the same tumour from five different patients presented in Figure 5.6B where spatially resolved samples from patient # 2 and #4 were more scattered while samples from patient # 1, 3 and 5 are clustered together.

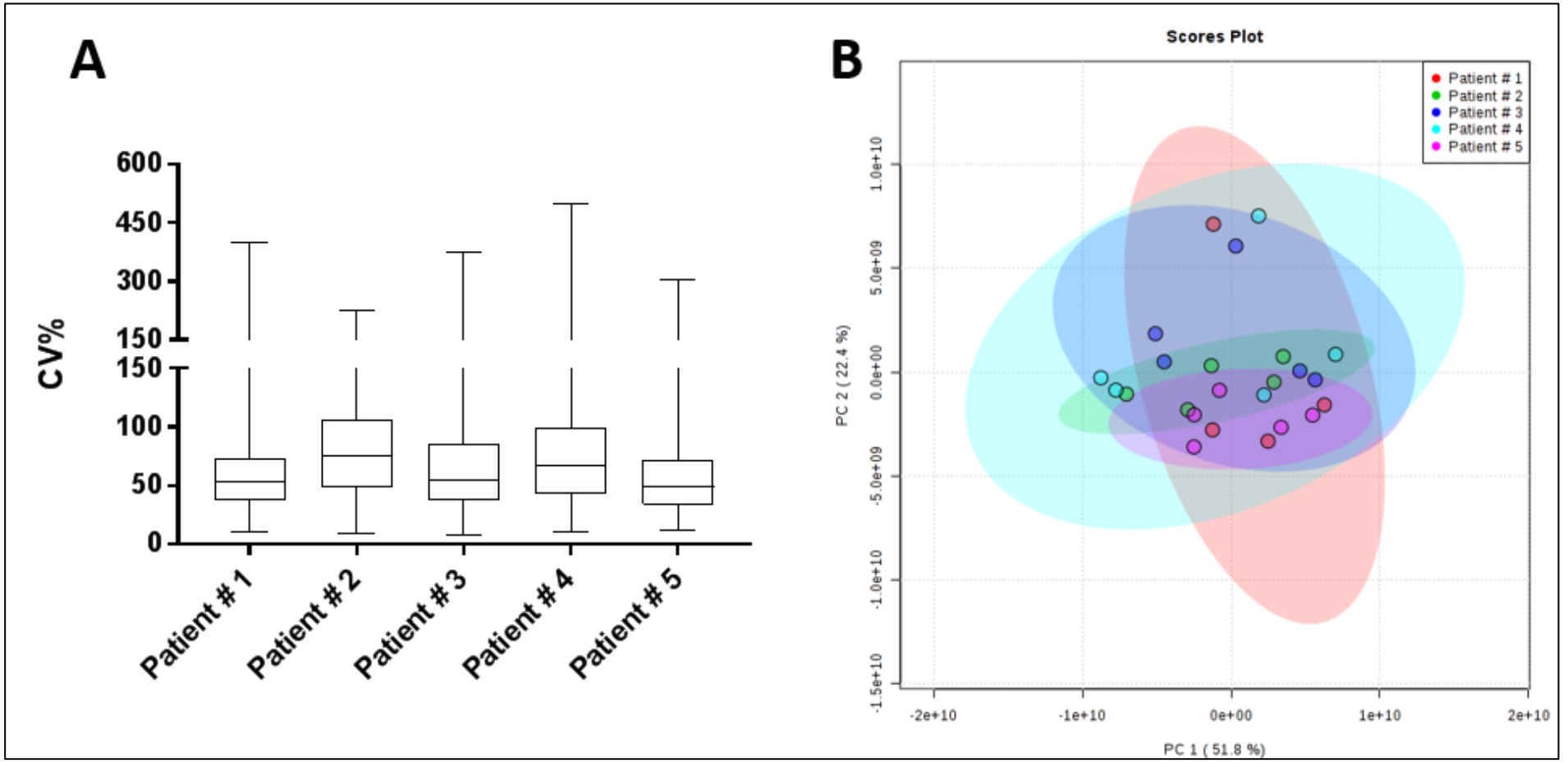

Figure 5.6: Inter and intra-tumour heterogeneity revealed by A) CV% distribution and B) PCA plot of identified lipid ions across different spatially resolved tumour samples within the same tumour from five different patients.

Stained cryosections from the first three patients indicated that histologically they were different (see Figure 5.7). Spatially resolved samples from tumour resected from patient # 1 contained relatively fewer cancerous cells compared to patient # 2 and 3. In addition, the density of these cells differed from one region to another within the same tumour, which could support intra-tumour heterogeneity revealed by the conducted lipidomic study.

Low grade glioma (grade I and II) grow continuously and usually transform to higher grades of glioma ultimately causing progressive disability and premature death (320). A previous study conducted retrospectively on 216 patients diagnosed with LGG who underwent initial resection surgery at University of California, San Francisco between 1989 and 2005, showed that 44% of the patients established an unequivocal increase in tumour size, malignant progression and/or death. Also, they provide clear evidence that greater extent of resection does extend the survival of patients compared with a simple debulking procedure with incomplete resection (321). In addition, intra-tumour heterogeneity in gene expression that controls biological processes such as myelination, cell adhesion and lipid metabolic process was noticed in higher grades of glioma and malignant glioblastoma, which supports our findings (322). Thus, understanding the effect of intra-tumour heterogeneity of these kinds of cancer implanted with a proper experimental design, could lead to a better decision about the treatment plan and could guide the surgeon to what extent should they should resect the tumour and its neighbouring tissue to increase the survival rate with less impairment.

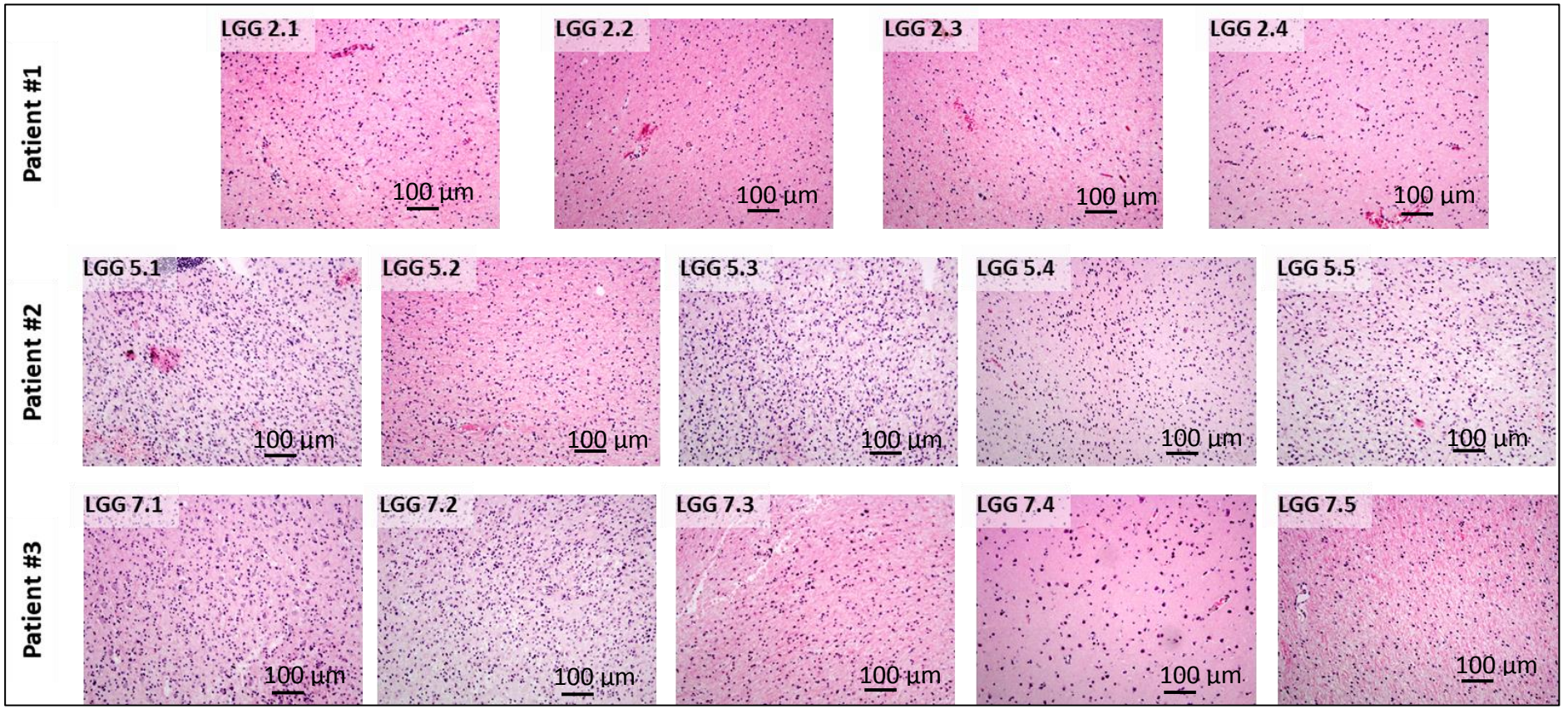

Figure 5.7: Examples of the histology test of Hematoxylin and Eosin (H&E) -stained cryosection of spatially resolved tumour region from three different patients (at 100X magnification) provided by Dr Ruman Rahman, assistant professor of molecular neuro-oncology, faculty of medicine & health sciences at Nottingham University.

5.5 Conclusion

LC-MS analysis of glioma samples using the developed normalisation method was used to study inter and intra-tumour heterogeneity in LGG tumour in five patients. The experimental design of this experiment was not as desired, and some clinical questions cannot be answered by the available set of samples. This was due to the lack of proper control samples and the limited number of patients included in the analysis. The ideal experimental design should include spatially resolved samples from a larger number of patients diagnosed with grade II glioma in order to address the level of inter-tumoral variations which is challenging and difficult to achieve. In addition, proper control samples should be included in the experiment in order to properly correlate intra-tumoral variations in spatially resolved samples. The ideal control samples would be biopsy from healthy region of patients brain however, these kinds of controls are not feasible due to the nature of the samples and their location. Other alternative would be from deceased subjects without previous known conditions that could affect the lipid profile in their brain. Despite these limitations, a clear difference in lipidomic pattern was observed between spatially resolved regions of the tumour indicating intra-tumoral heterogeneity. Also, the degree of intra-tumoral heterogeneity between patients was different that could affect treatment output and therefore personalised tumour-specific strategies should be considered to accommodate such variation to extend progression-free intervals. Inter and intra-tumour heterogeneity suggests that profiling cancer cell phenotypes from single biopsies to guide therapeutic decision making from heterogeneous tumours may prove challenging, especially as heterogeneity could lead to therapeutic resistance or relapse.

Chapter Six

Lipidomic signatures of Type 2 diabetes mellitus in human plasma

6. Lipidomic signatures of Type 2 diabetes mellitus in human plasma

6.1 Introduction

6.1.1 Diabetes mellitus: definition and prevalence

Diabetes mellitus (DM) is a heterogeneous complex metabolic disorder characterised by a high level of blood glucose concentration, abnormalities in protein, carbohydrates and fat metabolism with mineral and electrolyte disruption that are overall collectively linked with an increased risk of different micro and macrovascular diseases (323, 324). Diabetes is considered as an epidemic disorder affecting around 425 million people aged between 20 and 79 years worldwide in 2017 and it is estimated that around 46.5% of diabetic adults are undiagnosed (the symptoms of the syndrome may be subtle and thus may remain undiagnosed) (325). Figure 6.1 represents the number of people diagnosed with diabetes in the world up to 2017 and the expected increment by 2045 as claimed by the International Diabetes Federation (IDF) (326). In the UK, The British Diabetic Association reported that there are 3.8 million people currently diagnosed with diabetes within the UK in 2018 (327). Patients diagnosed with DM can be classified into four groups: type 1 diabetes mellitus (T1DM), type 2 diabetes mellitus (T2DM), gestational diabetes mellitus (GDM) and other specific types of diabetes mellitus due to various known etiologies (328, 329).

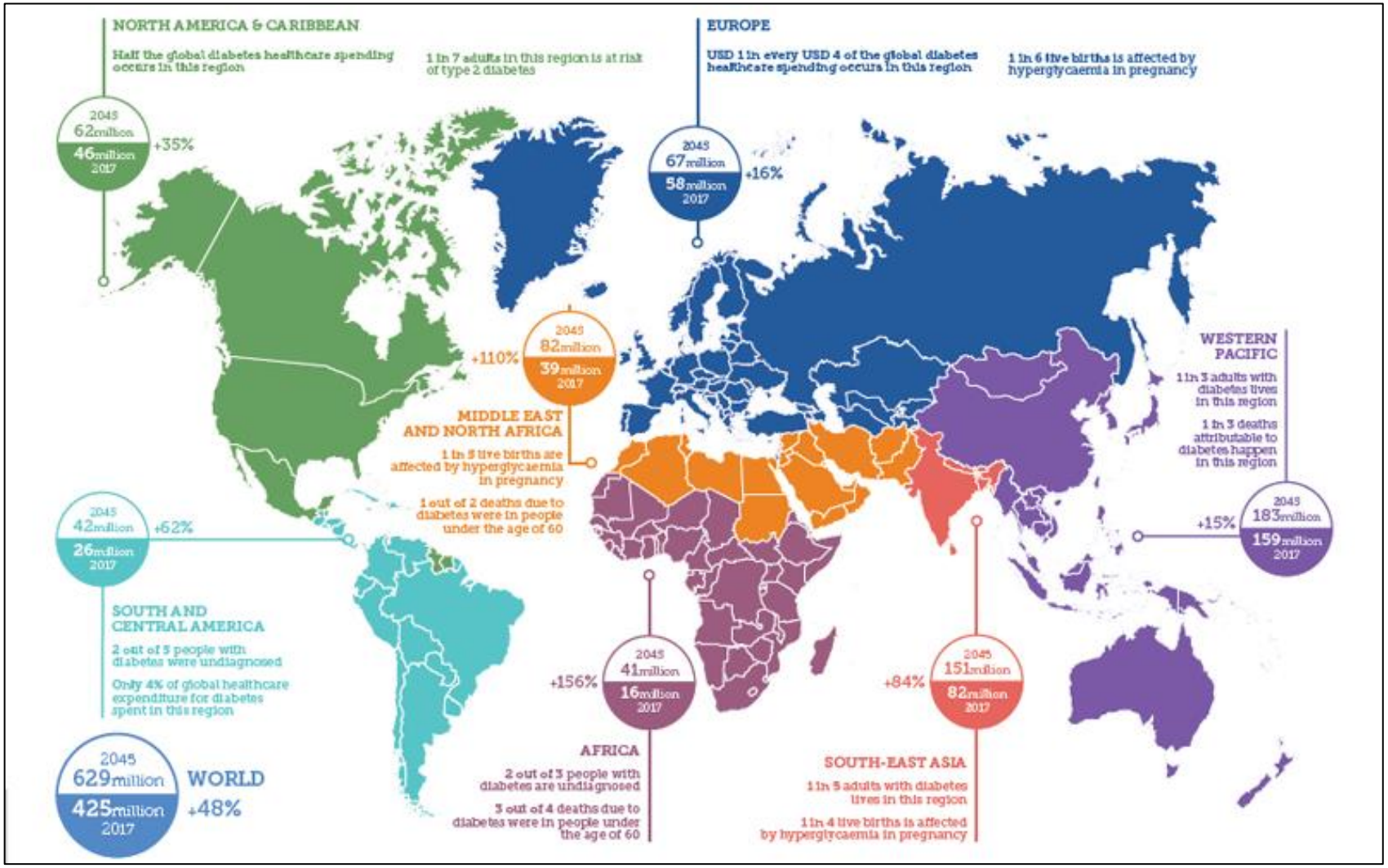

Figure 6.1: Estimated total number of adults (20–79 years) living with DM and the estimated increment by 2045 in the world (326).

6.1.2 Pathophysiology of hyperglycaemia

Upon an increase in glucose concentration in a healthy individual, glucose is taken rapidly by pancreatic β-cells through a hexose transporter called glucose transporter 2 (GLUT2) where it gets phosphorylated by glucokinase. Upon glucose degradation and formation of ATP, the sulfonylurea receptor 1 (SUR1) protein will be activated and that will lead to the closure of the adjacent potassium channel and consequently, calcium channels will open, this triggers the release of insulin (330). Figure 6.2 represents a schematic presentation of how insulin secretion is induced by glucose.

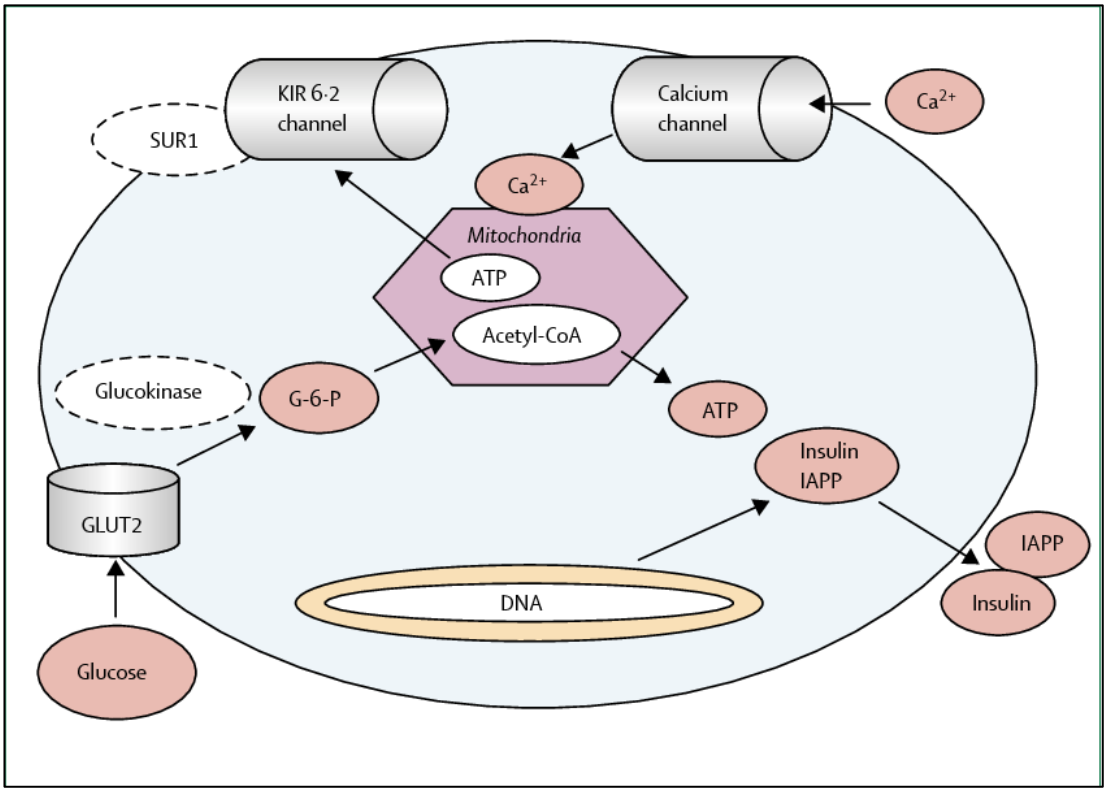

Figure 6.2: Schematic presentation of how glucose induce insulin secretion (330). Abbriveation:, , ATP: Adenosine triphosphate, DNA: Deoxyribonucleic acid, IAPP: Islet amyloid polypeptide, G-6-P: Glucose-6-phosphate, GLUT2: Glucose transporter 2, SUR1: Sulfonylurea receptor 1, KIR 6.2: Inward-rectifier potassium channels.

Insulin is the principal hormone for the regulation of glucose blood level where normal glucose level is maintained by a balance between insulin action and insulin

secretion by β-pancreatic cells (331). As a response to elevated blood glucose level, insulin promotes glucose disappearance by facilitating its uptake into muscles and adipose tissue via GLUT4. Whereas in the liver, insulin inhibits endogenous glucose production by inhibiting glycogenolysis and gluconeogenesis and promote glycogen synthesis in the liver (332). Hepatic and muscular resistant to insulin are associated with hyperglycaemia in T2DM patients (333-336).

Insulin resistant and β-cells dysfunction are strongly associated with several diabetes gene, obesity, inflammation, hyperglycaemia, free fatty acid (FFA) and others through several mechanisms (330). An elevated level of FFA is commonly seen in diabetic patients and in obese individuals, it is known to inhibit insulin stimulated peripheral glucose uptake mechanisms and previously linked to skeletal muscle and liver insulin resistant and considered as a risk factor for developing T2DM (337, 338). The exact mechanism of how FFA mediate insulin resistance is unclear but several mechanisms have been proposed. Firstly, in the hyperglycaemic condition, lipid toxicity (high level of FFA) mediate the decrease in insulin production by opening K channels or by reducing ATP production in β-cells (330, 339-341). Also, it could promote β-cell apoptosis by increasing ceramide synthesis (342-344). Second, as proposed by Randle *et al.* FFA can promote skeletal muscle insulin resistance by impairment of glucose transport activity (GLUT4) (345, 346). Third, high carbon load on the muscle cells due to an increase in FFA drive an increase in fatty acid oxidation (FAO) rate that surpasses that of the TCA cycle, resulting in the accumulation of intramuscular intermediary metabolites, such as fatty acylcarnitine, which may affect insulin sensitivity (347, 348).

6.1.3 Type 2 diabetes mellitus (T2DM)

T2DM accounts for at least 90% of all cases of diabetes and it is characterised by peripheral insulin resistance and consequently, deficiency in insulin secretion due to persistent high demand created by insulin insensitivity and low non-insulin mediated glucose uptake (326, 349). Patients with T2DM exhibit impaired fasting glucose and impaired glucose tolerance and most patients display abdominal obesity which is part of the fat deposition pattern that is linked to insulin resistance (350-352). These patients also experience what is called “insulin resistance syndrome”, which is a cluster of different abnormalities such as hypertension, lipid abnormalities, vascular endothelial dysfunction and atherosclerotic cardiovascular disease due to hyperinsulinemia experienced at the early onset of the disease (353).

T2DM contributes to elevated blood pressure through general types of mechanisms secondary to hyperinsulinemia such as Na^+ retention, increase intracellular Ca^{2+} accumulation, sympathetic nervous system overactivation and increase proliferation of vascular smooth muscle cells via enhanced growth factor activity (353, 354). Several studies showed abnormalities in plasma lipids were correlated to insulin mediated glucose uptake in normal weight and obese healthy non-diabetic subjects as well in patients with T2DM (355-362). These abnormalities include decreased HDL level, increased VLDL level (Hypertriglyceridemia) and to a lesser extent increase in LDL level (Hypercholesterolemia). However, it is not fully known whether the dyslipidaemia is the cause or the result of insulin resistance. In addition, insulin has been well recognised as a risk factor for development of atherosclerosis and coronary artery disease (CAD) independent of plasma lipid levels or blood pressure. This might take place through stimulation of growth factors and connective tissue synthesis,

proliferation of smooth muscle cells, increased cholesterol synthesis and LDL-receptor activity, increased formation decreased removal of atherosclerotic plaque due to increased levels of plasminogen activator inhibitor type 1 (PAI-1) that inhibits fibrinolysis (363, 364). These previous cardiovascular complications considered as the principal cause of morbidity and mortality in addition to its association with kidney complications in patients with diabetes mellitus (365). In summary, it seems that overweight and obesity, sedentary lifestyle characterised as physical inactivity and high dietary intake of carbohydrates, red meat and processed meat and sugar alone or together can be associated with global epidemic widespread T2DM.

DM can be diagnosed either using the fasting plasma glucose (FPG) value where FPG level ≥126 mg/dL (7.0 mmol/L), the 2-h plasma glucose (2-h PG) value after 75-g oral glucose tolerance test (OGTT) where 2-h PG level ≥200 mg/dL (11.1 mmol/L) or by A1C test where A1C level ≥6.5% (48 mmol/mol) (366, 367). The A1C test, also known as haemoglobin A1C, HbA1C or glycated haemoglobin that measures the amount of haemoglobin with attached glucose that is reflected on the average blood glucose levels over the past three months.

6.1.4 Dysregulation of lipid metabolism and its association with T2DM

The association of dyslipidaemia (increased TG and decreased HDL-cholesterol levels) with T2DM has been known for more than two decades (355-362). However, recently researchers have started to globally inspect individual metabolite and lipid species associated with T2DM or with prediabetic individuals. Strong association between dysregulation of lipid metabolism and prediabetic individuals and patients with T2DM was confirmed by plasma profiling of 351 Australian subjects (170 healthy subjects,

64 prediabetic and 117 diagnosed with T2DM using targeted lipidomics and validate their finding on 1076 plasma samples from cohort study designed to explore the genetics origin of cardiovascular disease and its risk factors in extended families of Mexican Americans (368). The plasma lipid profile of individual recognised as prediabetic was similar to the lipid profile for T2DM. However, their lipid profile was different from healthy individuals where approximately 135 out of 259 measured lipid species from different lipid classes such as dihydroceramide (dhCer), Cer, alkylphosphatidylcholine (PC(O)), PE, PI, PG, ChE, DG and TG were significantly associated with T2DM and with prediabetes compared to healthy subjects. In addition, their lipid profile showed a negative association in dhCer and LPC levels whereas dhCer, PE, PG, ChE, DG and TG levels showed a positive association with fasting blood glucose level (FPG) and 2h-post load glucose (2h-PLG) compared to healthy subjects.

6.1.5 Impact of L-carnitine supplementation on glucose metabolism

L-carnitine, 3-hydroxy-4-*N*,*N*,*N*-trimethylaminobutyric acid, is an amino acid derivative. The structural formula of L-carnitine is shown in Figure 6.3. More than 90% of our body reservoir of L-carnitine is stored in muscle cells (369).

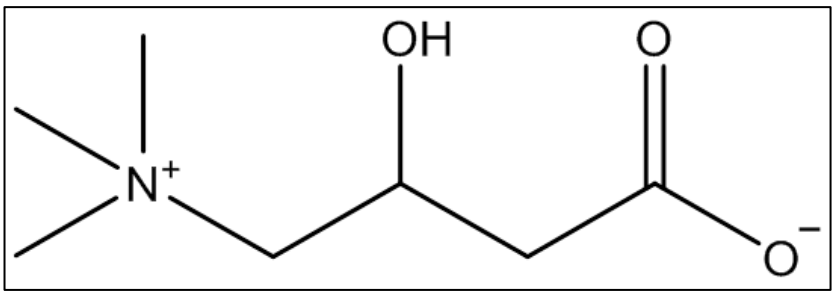

Figure 6.3: Structural formula of L-carnitine.

Free or acyl carnitines play an essential role in the translocation of impermeable long fatty acyl groups from the cytosol into the mitochondrial matrix for subsequent β-oxidation and in buffering excess acetyl groups from a high rate of pyruvate oxidation that outweighs their removal by the tricarboxylic acid cycle as seen in Figure 6.4 (370, 371).

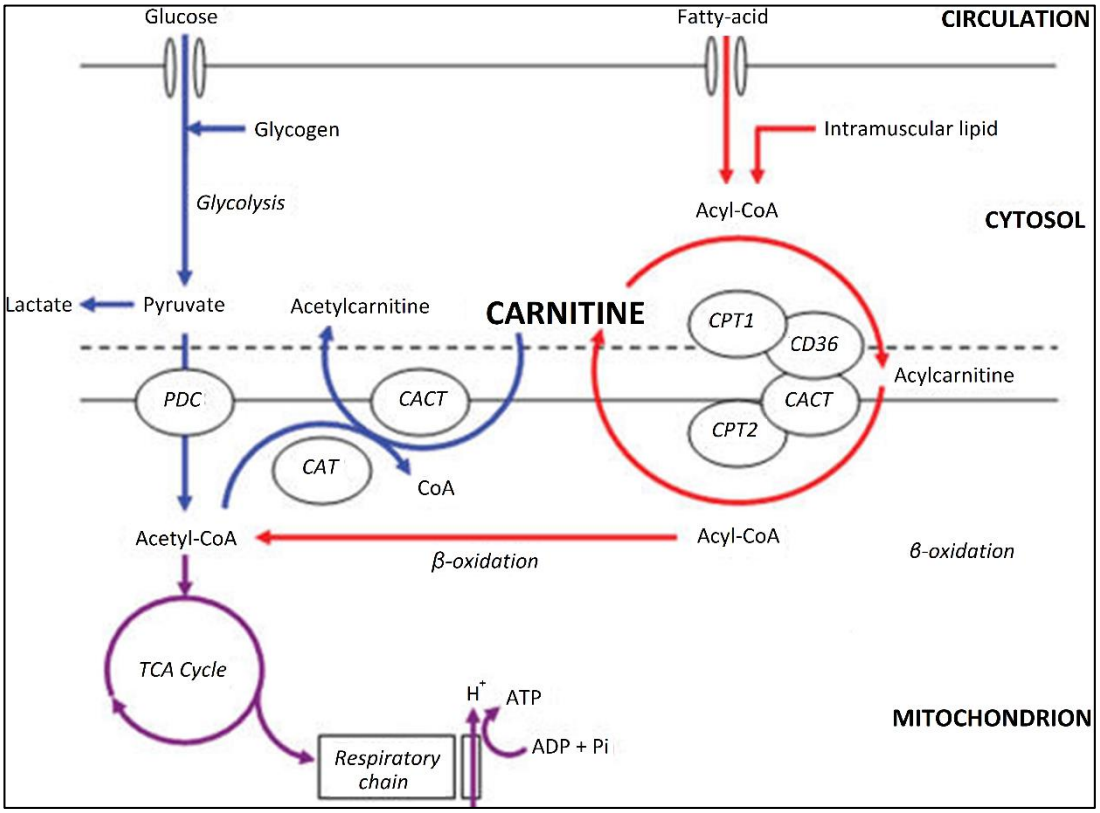

Figure 6.4: The metabolic roles of carnitine in skeletal muscle. The role of carnitine as a shuttle to translocate long-chain fatty acid into the mitochondria is highlighted in red while its role as a buffer for excess production of acetyl-CoA in the mitochondria is highlighted in blue. *Abbreviations:* PDC, pyruvate dehydrogenase complex; TCA, tricarboxylic acid cycle; CAT, carnitine acetyltransferase; CACT, carnitine acylcarnitine translocase; CPT, carnitine palmitoyl transferase; CD36, fatty acid translocase (370).

Carnitine palmitoyl transferase 1 (CPT1), located in the outer membrane of the mitochondria, helps in the formation of acylcarnitine by esterification of carnitine and acyl-CoA (372). Then, a fatty acid translocase called CD36 located in the outer mitochondrial membrane, translocate acylcarnitine from CPT1 to the carnitine acylcarnitine translocase (CACT) located into the mitochondrial inner membrane

(373, 374). That is where simultaneous 1: 1 exchange of acylcarnitine with free intra-mitochondria carnitine is happening. Once inside the mitochondrial matrix, acylcarnitine is trans-esterified back to free carnitine and acyl-CoA via carnitine palmitoyl transferase 2 (CPT2) (375). The intramitochondrial acyl-CoA is then oxidised and cleaved by the β-oxidation pathway to form acetyl-CoA that is a substrate for the TCA cycle (370). The TCA cycle is a series of chemical reactions to release stored energy through the oxidation of acetyl-CoA into ATP and carbon dioxide (376). The other role of carnitine is to buffer excess acetyl groups from the high rate of pyruvate oxidation catalysed by the pyruvate dehydrogenase complex (PDC) and B-oxidation of acyl-CoA that outweighs their removal by the TCA cycle by carnitine acetyltransferase (CAT) (370, 377).

Various studies demonstrated that accumulation of acylcarnitine or low plasma concentration of L-carnitine are associated with insulin resistance and have been related to insulin resistance in diabetic animals and humans (371, 373-375, 378). These findings suggest impairment of entry of fatty acids into mitochondria in diabetic subjects which means that these subjects suffer from a complex oxidation defect (378). Therefore, researchers studied the effect of carnitine supplementation on glucose disposal (379-381). Increased intra muscular free carnitine concentration can decrease intramitochondrial acetyl-CoA/CoA ratio and that increases the activity of pyruvate dehydrogenase complex (PDC) which results in a decrease in glucose plasma concentration (379, 380). Furthermore, it can promote the reduction of cytosolic acetyl-CoA levels by translocation of fatty acyl groups into the mitochondrial matrix for subsequent β-oxidation and that activate the glycolytic pathway and reduces fatty acid availability for lipid synthesis (379). Mixed results were shown in

the literature regards the effect of L-carnitine on plasma lipid profile. For example, Rodrigues *et al.* studied the effect of oral supplement of L-carnitine on lipid metabolism in chronically diabetic rats and he found that short term administration of various amount of L-carnitine (50-200 mg/kg/day) for 1, 3 weeks or (200 mg/kg/day) for 6 weeks showed a decrease in plasma TG level with no effect on plasma cholesterol (382). While Rahbar *et al.* found that after administration of 3 g/ day of L-carnitine to T2DM patients for 12 weeks, a significant reduction in plasma glucose level was observed whereas the TG level was increased (383). He proposed that in diabetic patients, the level of cytoplasmic acetyl-CoA increased due to over-activation of pyruvate dehydrogenase, which is the substrate for the synthesis of malonyl-CoA. Malonyl-CoA is a potent inhibitor of carnitine palmitoyl transferase I (CPT I) that inhibits the effect of L-carnitine in fatty acids translocation into the intramitochondrial and promote TG synthesis (384). Whereas Derosa *et al.* was unable to find any difference in TG, LDL or HDL level in T2DM patients treated by L-carnitine (2g/day) for 6 weeks (385).

6.2 Objectives

In this chapter, global lipidomic analysis of 31 subjects, including nine healthy non-diabetic subject and 22 T2DM patients will be conducted using the developed normalisation method based on LC-MS analysis as described in section 2.4.3. The following aims and objectives were set up for this chapter:

- To confirm the lipidomic difference between healthy nondiabetic subjects and patients diagnosed with T2DM before and after OGTT as shown previously in published research studies.

- To test if the age difference in newly diagnosed T2DM patients influences the patient's plasma lipid profile before and after OGTT.
- To explore the effect of carnitine supplement for six months on T2DM patients based on their plasma lipid profile before and after OGTT.

6.3 Methods

6.3.1 Participant recruitment and grouping

31 subjects including nine healthy individuals and 22 T2DM patients treated at the Queen's Medical Centre within the UK NHS Trust centre submitted written consent forms and were enrolled in the study. The study was approved by the National Research Ethics Service Committee in East Midlands, UK. Initially, all participants were subjected to physical examinations then all participants were given a 2-hour 75 g oral glucose tolerance test. Blood samples were taken at fasting baseline (before OGTT) and after the OGTT. 2 mL of the blood were collected into lithium-heparin containers, and after centrifugation, the isolated plasma samples from all participants before and after the OGTT were collected and stored at –80°C until extraction and further analysis. Clinical and pathological characteristics of patients are described in Table 6.1.

Table 6.1: Baseline characteristics of healthy and T2DM patients enrolled in this study.

parameters	Healthy subjects	T2DM patients
Number	9	22
Gender (male %)	100%	100%
Age in years (average±SD)	46.1±8.7	54.5±8.1
BMI, Kg/m^2	31.1±4.1	29.4±3.8
FPG, mmol/l	4.4±0.4	6.2±1.3
2h-PG, mmol/l	6.6±1.5	11.5±2.7
HbA1c, %	35.9±2.6	48.9±5.4
TG, mmol/l	1.2±0.5	1.5±0.9
Total cholesterol, mmol/l	5.3±1.5	4.5±1.3
LDL, mmol/l	3.5±1.4	2.4±0.9
HDL, mmol/l	1.2±0.3	1.3±0.3
Medication	-	metformin

After that, the diabetic patients were randomised into two groups. One group supplemented with L-carnitine supplements (3 g/day divided into three doses) plus Ensure plus drink for 24 weeks and the other group received a placebo for 24 weeks. It is proved that I.V infusion of L-carnitine accompanied by elevated serum insulin concentration in the presence of hypercarnitinaemia (550–600 μmol/L) or by ingestion of carbohydrate (CHO) and L-carnitine (94 g and 3 g, respectively) up to 24 weeks in healthy volunteers, could increase intramuscular carnitine content by ∼15% and that affects muscle fuel metabolism by increasing fatty acid oxidation and delay muscle glycogen depletion (386, 387). Therefore, in this study, the CHO was replaced by Ensure plus drink; a healthier protein concentrate as a substitute for patients with T2DM that could increase intramuscular carnitine level when accompanied by oral supplements of L-carnitine (3 g/day) for 24 weeks. Clinical and pathological characteristics of the two groups (treatment and placebo) are described in Table 6.2.

Table 6.2: Baseline characteristics of treatment and placebo groups to study the effect of L-carnitine supplement on plasma lipid profile on T2DM patients.

Parameters	**Treatment group**		**Placebo group**	
Number	11		11	
Gender (male %)	100%		100%	
Age in years (average±SD)	53.9±8.9		55.1±7.6	
BMI	29.8±4.3		28.9±3.2	
Medication	metformin		metformin	
	Day 0	**After 24 weeks**	**Day 0**	**After 24 weeks**
FPG, mmol/l	6.3±1.3	6.3±0.5	5.9±0.8	6.2±1.2
2h-PG, mmol/l	10.8±2.2	11.6±3.0	11.2±2.8	12.2±3.7
HbA1c, %	48.8±4.6	49.7±5.3	49.0±6.3	51.9±9.1
TG, mmol/l	1.5±1.1	1.5±0.7	1.4±0.7	1.1±0.6
Total cholesterol, mmol/l	4.9±1.5	4.3±1.6	4.1±1.0	3.7±0.8
LDL, mmol/l	2.5±1.1	2.3±1.3	2.3±0.8	2.0±0.6
HDL, mmol/l	1.5±0.3	1.3±0.3	1.1±0.3	1.1±0.2

6.3.2 Sample extraction analysis

Extraction was performed according to a modified method of Bligh and Dyer as detailed in section 4.3.1 (99). The LC-MS analysis was carried out as previously described in section 2.3. Pooled QC plasma samples were prepared by combining 10 µL of each sample. QC sample was injected to condition the column and after each ten randomised samples to monitor the repeatability of the LC-MS system. Lipid ions were putatively identified based on their fragmentation pattern by LipidSearch™ based on parameters listed in section 2.4.1. Data processing and normalisation were performed as detailed in section 2.4.3. Although a high mass shift is expected to be introduced by ^{13}C-labelling, to ensure that there were no spectral overlays between the selected indigenous unlabelled ions identified in plasma samples and the ^{13}C-IS, ions were selected based on the listed criteria in section 5.3.6, lipid ions with CV% more than 30 across the data set were removed from any further statistical analysis.

6.3.3 Statistical analysis

For lipidomics data analysis, normalised data were subjected to multivariate analysis (OPLS-DA) and univariate analyses (multiple t-test) were performed to extract the lipids demonstrating a significant difference between the studied groups. The *p*-values of the Student's t-test were adjusted using the false discovery rate (FDR) for multiple testing problems (388).

6.4 Results and discussion

6.4.1 Analytical performance and lipidomic data quality

The assessment of QC samples indicates a stable column and instrumental response during data acquisition since the calculated CV% of 76.4% of the detected features

among the QC samples were less than 30%, which indicated a good instrumental reproducibility (155). This was further confirmed by the clustering of QC samples as shown in Figure 6.5. However, during the analysis, the run was interrupted and that can be seen by a closer look at the QC cluster in Figure 6.5, but the assessment of the QC samples indicates a consistent valid response for this batch. In addition, the used ^{13}C-IS mixture is expected to correct these variations as discussed and established before in Chapter 4.

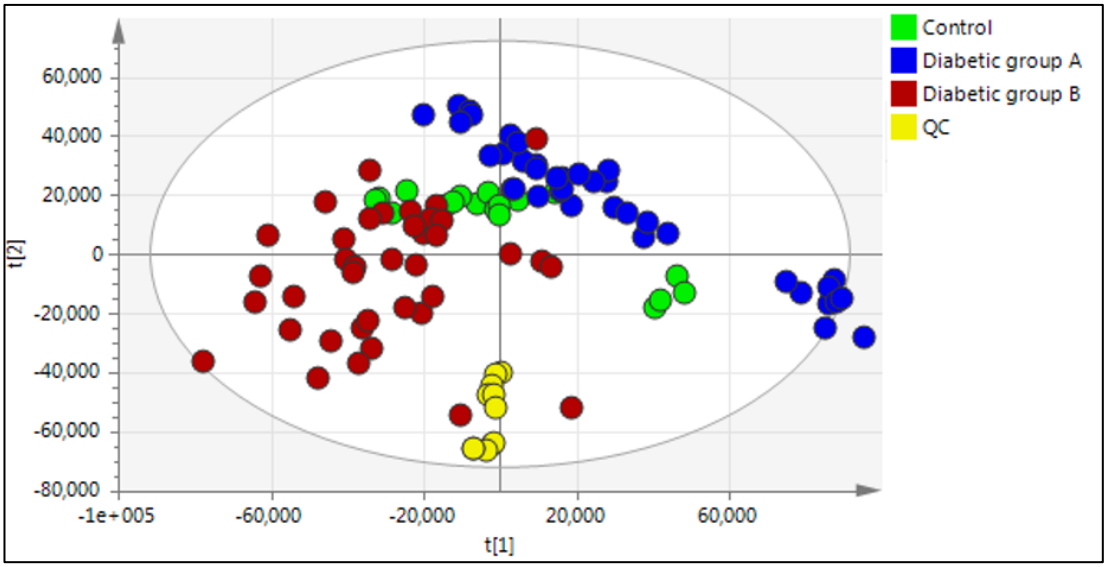

Figure 6.5: PCA plot of all samples analysed in this study where the QC samples are clustered in the middle of the plot.

6.4.2 Lipid ions identification

Figure 6.6 represents the number of identified lipid ions from plasma samples of control group pre and post OGTT extracted with and without ^{13}C-IS mixture. On average, 275 lipid ions were identified in the samples analysed without ^{13}C-IS mixture in both positive and negative mode while 187 ions were identified in samples analysed with ^{13}C-IS mixture (The number of identified lipid species per sample extracted with and without IS mixture can be seen in Appendix Table A.5) (~33%

reduction in the number of identified lipid ions). As presented before in section 5.4.2 and in agreement with Rampler *et al.* findings (217), a significant decrease in the number of identified lipids in human plasma analysed with ^{13}C-IS mixture from *P. pastoris* compared to samples extracted without ^{13}C-IS mixture. This could be attributed to ion suppression due to matrix effects as denser and more complex lipid mixtures would be obtained when ^{13}C-IS mixture is added to the samples as is shown in Figure 6.7.

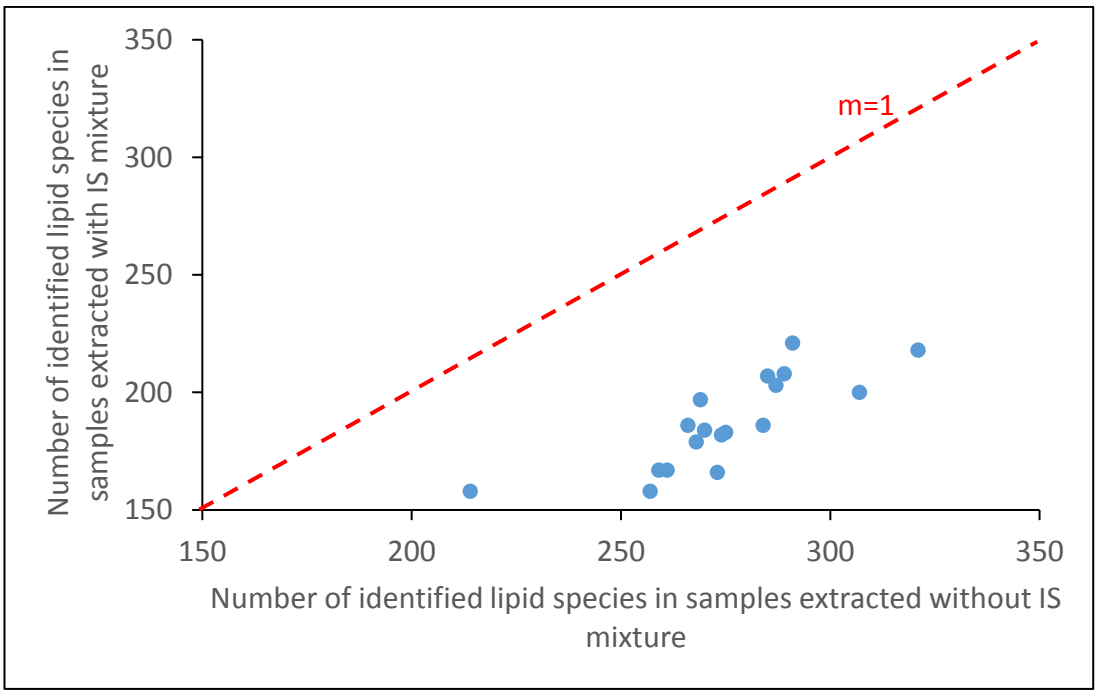

Figure 6.6: Number of identified lipid ions by LipidSearch™ in control plasma samples (nine healthy subjects before and after OGTT) extracted and analysed with and without ^{13}C-IS mixture. The blue dots represent the samples whereas the red dash line repersents the unit line with slope of 1.

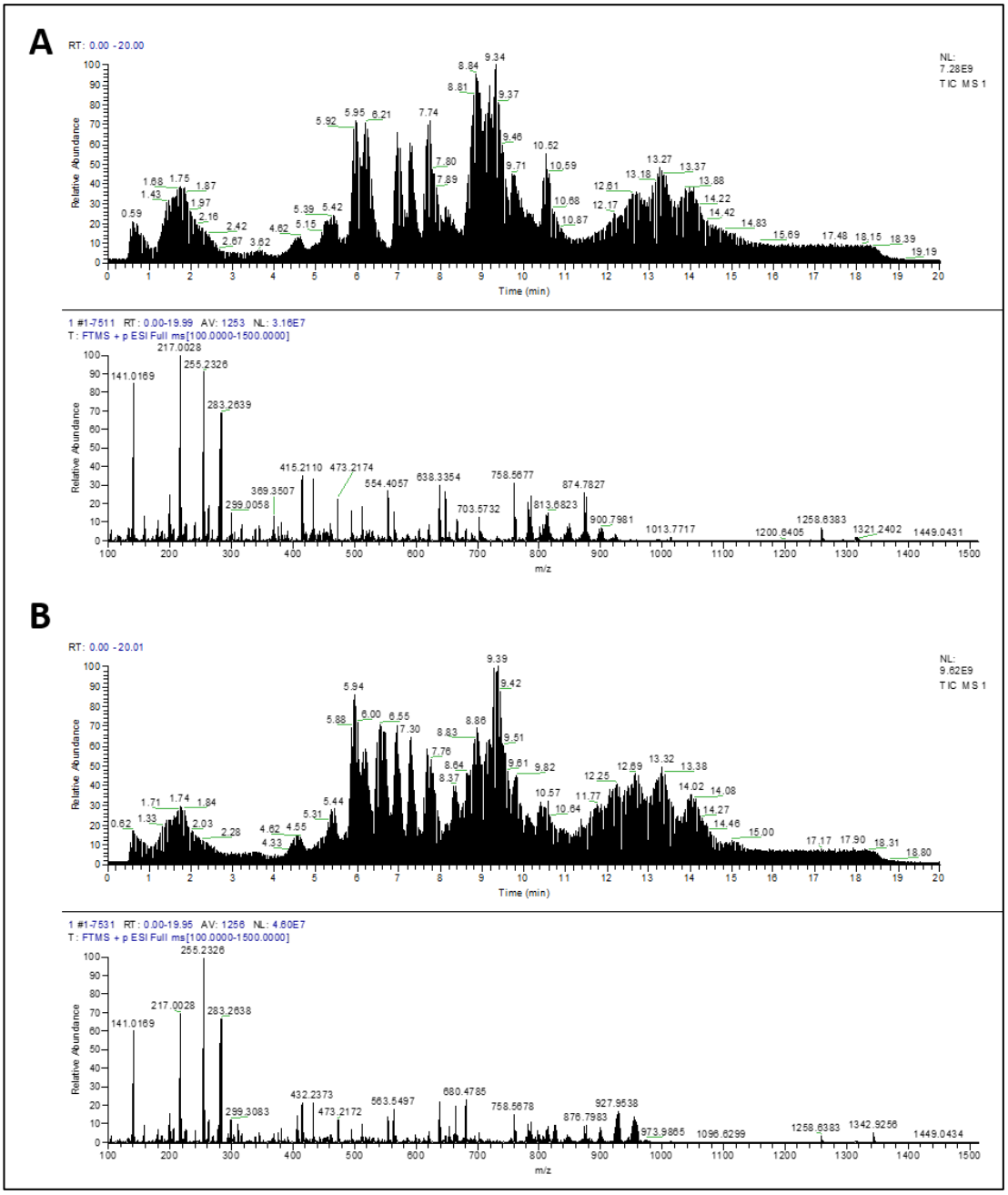

Figure 6.7: Example total ion chromatograms and the spectra of diabetic samples extracted from patient RA2D43 Pre OGTT analysed without (A) and with (B) ^{13}C-IS mixture.

6.4.3 Plasma lipidomic changes in healthy nondiabetic subjects and patients diagnosed with T2DM before and after OGTT

Statistical analysis showed that there was no difference between identified lipid ions between nondiabetic and diabetic subjects based on their pre OGTT lipid profile (nine

non diabetic vs 22 diabetic patients, 357 lipid ions were included in the analysis) or based on their lipid ions fold change after OGTT (nine non diabetic vs 20 diabetic patients, 359 lipid ions were included in the analysis). Both comparisons showed that there was no difference between the two groups as seen in OPLS-DA models in Figure 6.8 A and B respectively. That the Q^2 value shown in Figure 6.8 which describe the goodness of fit of the model is below the normally accepted value of 0.4 and hence the model produced is low quality despite the apparent differences seen in the plot. This was in agreement with the untargeted analysis of all features as well where zero and six features out of 15291 features were statistically different between the two groups based on pre and post OGTT respectively (for OPLS-DA models and scores see Appendix, Figure A.3). However, previous studies had shown that there is a clear association between plasma level profile in patients diagnosed with DM including T2DM patients and in prediabetic individuals (368, 389-392). In addition, Wong *et al.* suggest that inclusion of few plasma lipid markers in classification of individuals at risk of T2DM in addition to conventional classification criteria such as glucose level, BMI, HbA1c and TG level could improve their classification that because these lipid species can capture unobvious smaller signatures of diabetes risk (393). Most of these studies were done on a large scale while in this study fewer samples were included where small changes might be present but not significant and according to the power analysis results seen in Figure 6.9 suggests that any statistical judgment from these samples could be inaccurate and unreliable due to small size per group in this study.

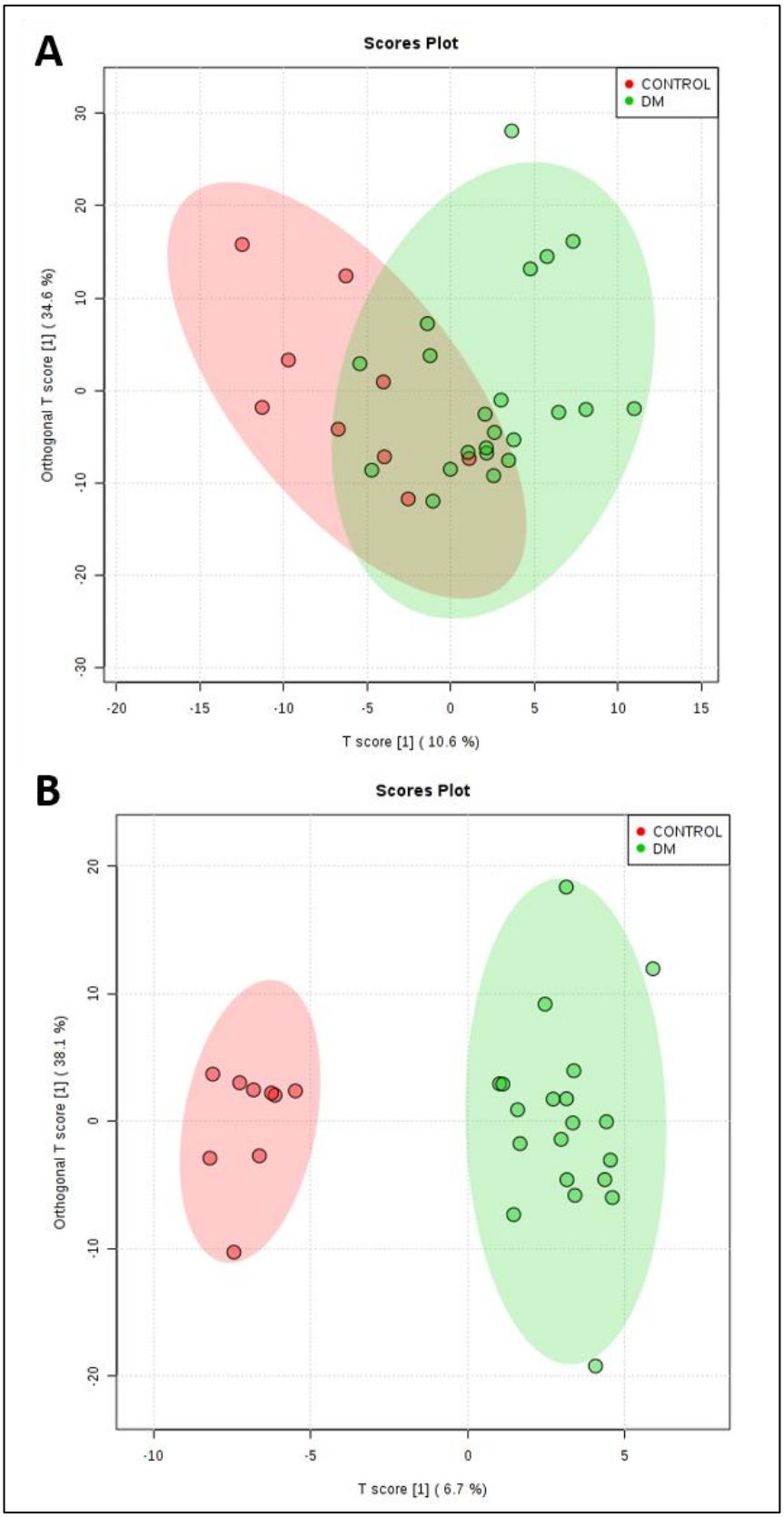

Figure 6.8: OPLS-DA score plots of identified lipid ions extracted from MetaboAnalyst in study of control vs patients diagnosed with T2DM based on A) fasting pre OGTT samples (nine non diabetic vs 22 diabetic patients, 357 lipid ions were included in the analysis, R^2X= 0.106, R^2Y=0.399 and Q^2=0.128) and B) fold change measurement of after OGTT over before OGTT ((nine non diabetic vs 20 diabetic patients, 359 lipid ions were included in the analysis, R^2X= 0.067, R^2Y=0.189 and Q^2=0.101).

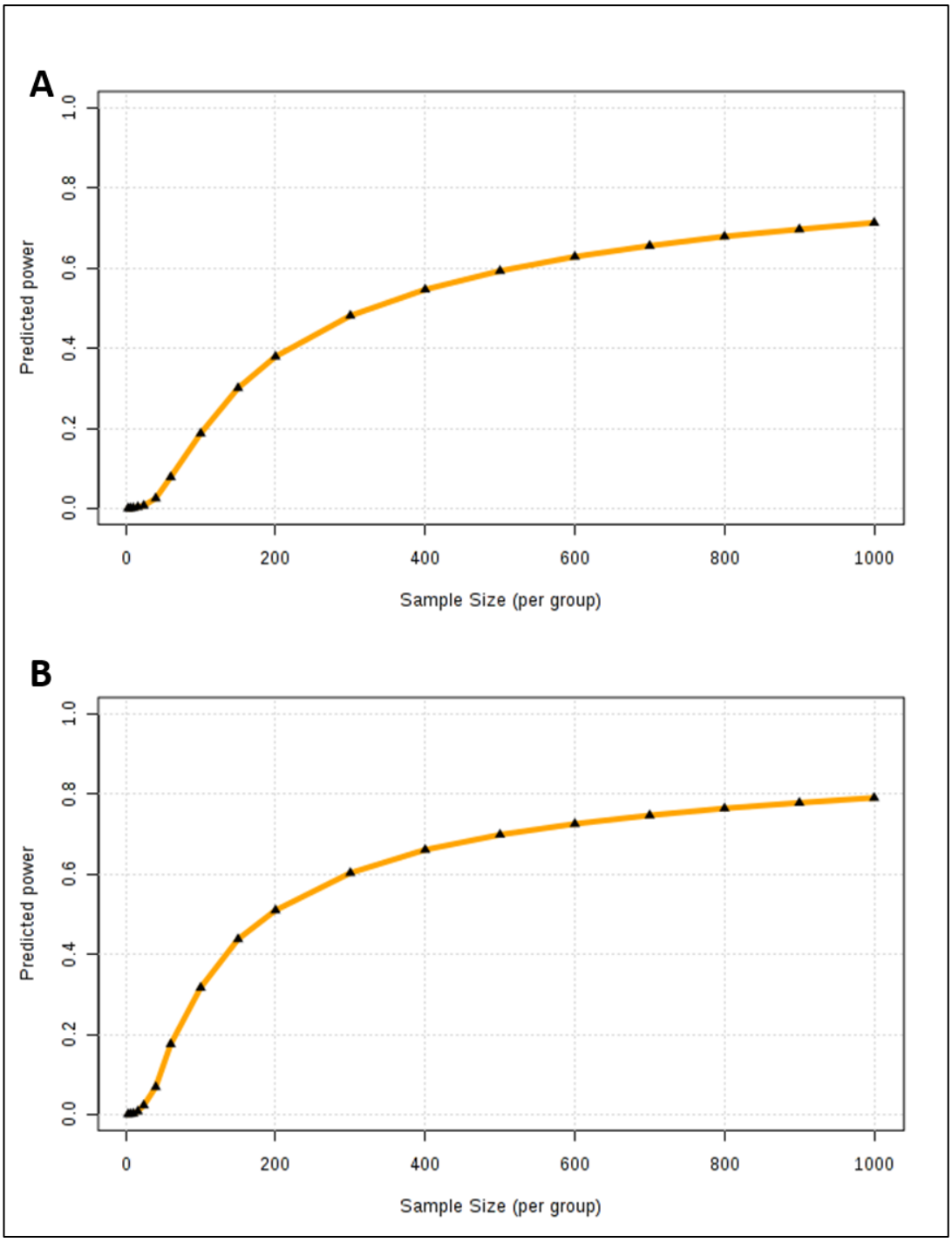

Figure 6.9: Power analysis vs samples size per group with FDR <0.05 extracted from MetaboAnalyst in study of control vs patients diagnosed with T2DM based on A) fasting pre OGTT samples (nine non diabetic vs 22 diabetic patients, 357 lipid ions were included in the analysis) and B) fold change measurement of after OGTT over before OGTT ((nine non diabetic vs 20 diabetic patients, 359 lipid ions were included in the analysis)).

6.4.4 Plasma lipidomic changes in young and old patients diagnosed with T2DM before and after OGTT.

Multiple t. test showed that there was no statistical difference in lipid ions level in identified ions between young (<50 years) and old (>70 years) T2DM patients based on their pre OGTT lipid profile or fold change (after OGTT over before OGTT). In addition, poor OPLS-DA models were obtained as seen in Figure 6.10 A and B. This was in agreement with untargeted analysis of all features as well where no features out of 17342 detected features were statistically different between the two groups and poor model was obtained by multivariate analysis as indicated by the model scores (see Appendix, Figure A.4).

A previous study showed that conventional lipidomic profiles for young (60-75 years, *n*=555) and older T2DM patients (>75 years, *n*=326) were significantly different and in general higher lipids profiles were related to increased cardiovascular mortality in T2DM yet this was not related to the patients age nevertheless the duration of the disease have more pronounced effect (394). Also, another study on patients with T2DM revealed that conventional lipidomic profiles and cardiovascular risk for young (<40 years, *n*=2756 (0.5%)) and older patients (>40 years, *n*=47 163 (99.5%)) were similar. However, in that study, huge differences between group sizes was seen and this could hamper their conclusion (395). These studies could imply that the duration of the disease rather than the patient's age could have more association in relation to a dysregulated lipid profile. Unfortunately, most of the participant in this study were newly diagnosed with T2DM (< 5 years) and therefore, the effect of disease duration cannot be evaluated.

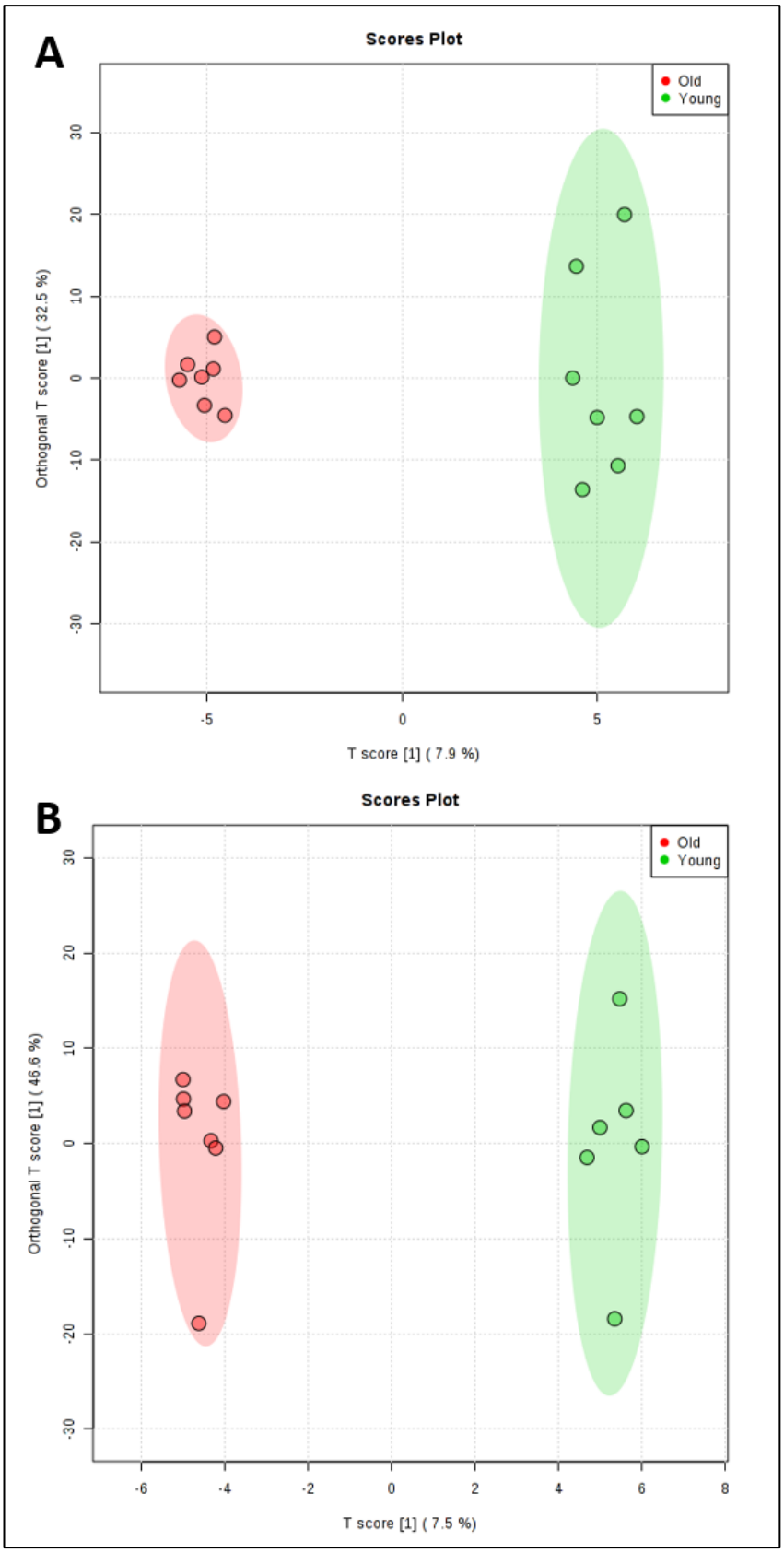

Figure 6.10: OPLS-DA score plots of identified lipid ions extracted from MetaboAnalyst in study of young vs old T2DM patients based on A) fasting pre OGTT samples (seven young vs seven old T2DM patients, 357 lipid ions were included in the analysis, R^2X= 0.079, R^2Y=0.396 and Q^2=0.025) and B) fold change measurement of after OGTT over before OGTT (six young vs seven old T2DM patients, 359 lipid ions were included in the analysis, R^2X= 0.075, R^2Y=0.244 and Q^2=-0.567).

6.4.5 Plasma lipidomic changes in patients diagnosed with T2DM before and after OGTT after carnitine supplement for 24 weeks.

The lipidomic profile of T2DM patients treated with L-carnitine supplement for 24 weeks showed no significant difference in identified lipid ions compared to the placebo group where 377 lipid ions were identified and monitored between the two groups. This was in agreement with supervised (OPLS-DA) statistical analysis of all detected features in untargeted analysis where poor models were obtained when the two groups where analysed simultaneously as seen in Figure 6.11 which represents the OPLS-DA score plot of untargeted analysis models between treated and placebo T2DM patients based on pre OGTT (A) and after OGTT (B), respectively. The OPLS-DA score of the two models indicate that the obtained model was poor, and no clear separation was achieved between the two groups based on their plasma lipidomic profile. This suggests that L-carnitine supplement had no pronounced effect on the plasma lipid profile in the treatment group or the intra-muscular carnitine level was not increased significantly as it was expected. Previous study conducted to study the effect of L-carnitine supplements (1g/day, for 12 weeks) on patients with coronary artery disease stated that there was significant reduction in TG level with no changes in other plasma lipid and they attributed these findings to carnitine antioxidant activity rather than to its ability for lipid lowering effect by translocation of fatty acids into mitochondria and thereby reduces fatty acid available for lipid synthesis (396). In reported literature, L-carnitine supplements had a mixed effect on plasma lipid profiles where it was reported that a lipid-lowering effect of these supplements was observed yet others failed to do so (385, 397-401). Thus, the effect of these supplements on the plasma lipid profile remains unclear. Also, different factors could

play an important role in controlling the effect of these supplements such as the diet and the lifestyle of the enrolled patients that could affect their lipid profile through the study. Unfortunately, intra-muscular carnitine concentration was not measured at the beginning and throughout this study and therefore the exact reason for such effect cannot be explored or investigated. The measurement of L-carnitine concentration in two groups before and after the supplements would make this study more valid and more informative.

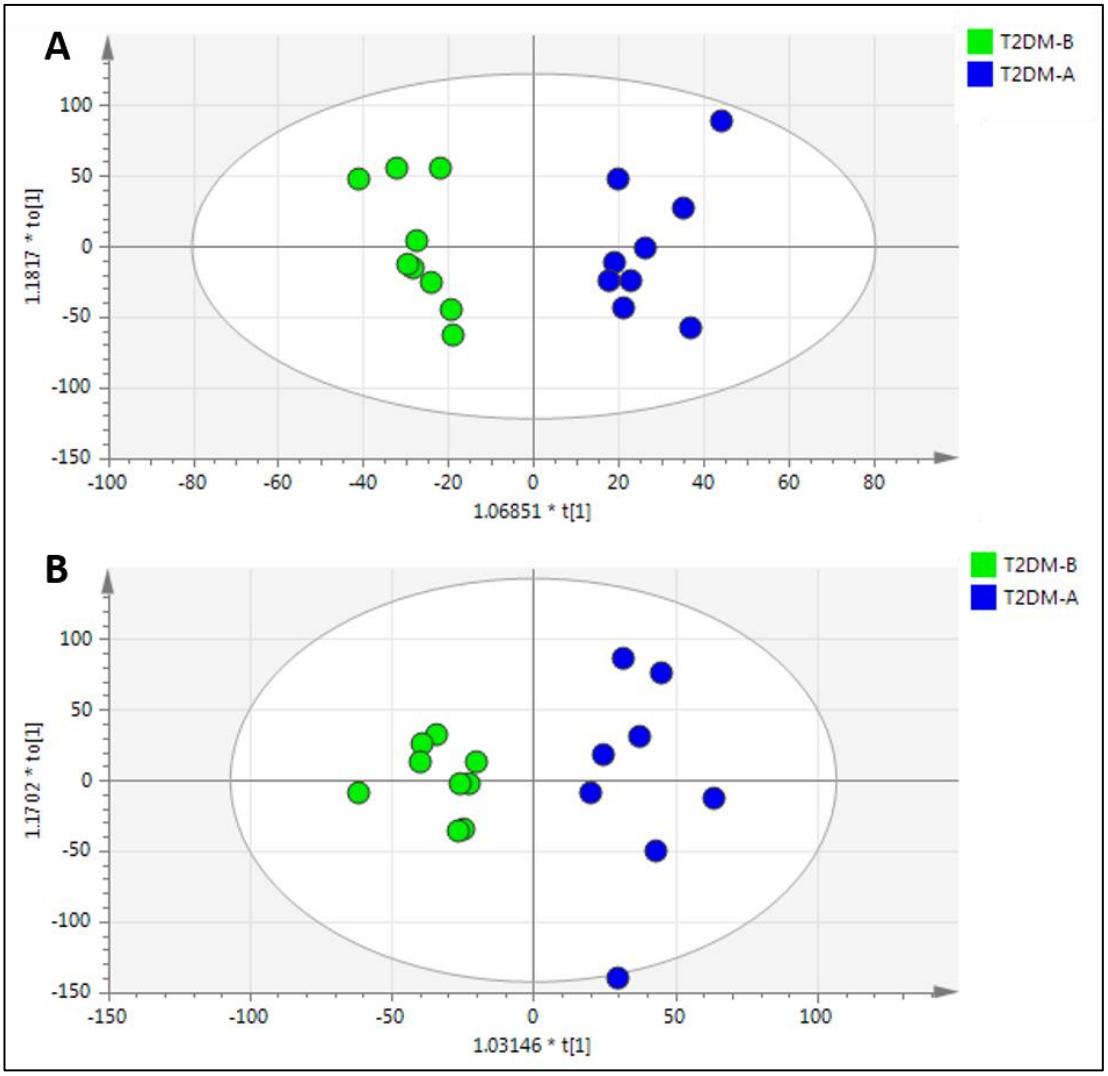

Figure 6.11: OPLS-DA score plots of unidentified features extracted from SIMCA to study the effect of L-carnitine supplement on T2DM patients based on A) fasting pre OGTT samples (R^2X= 0.188, R^2Y=0.923 and Q^2=-0.416) and B) post OGTT plasma samples (R^2X= 0.277, R^2Y=0.887 and Q^2=0.24).

6.5 Conclusion

The LC-MS analysis of T2DM samples using the developed normalisation method was used to investigate the possible lipidomic differences between healthy and T2DM patients, the lipidomic difference between young and old patients recently diagnosed with T2DM and to study the effect of L-carnitine supplement on plasma lipidomic profile of T2DM patients. There was no clear significant separation between the studied groups despite the fact that there is a well-established association between plasma lipid profile and T2DM. This was attributed to either low sample size or small changes that did not pass the statistical threshold. Therefore, larger sample sizes are needed to be able to distinguish the relatively small changes in plasma lipid profiles between the different groups. Also, the lipidomic profile revealed that there is no difference in plasma lipid profile between young and old T2DM patients and this might agree with previous studies that the duration of the disease had a more pronounced effect on the plasma lipid profile of these patients rather than their age. Regards the effect of L-carnitine supplements on T2DM patients no rigid conclusion can be withdrawn, however, it would have been better if the intra-muscular carnitine level was measured at the beginning and throughout the study to truly understand the true effect of oral L-carnitine supplement on T2DM patients. In addition, to obtain better results, it would have been better to analyse tissue samples directly from the skeletal muscle. That would help in understanding the direct effect of these supplement on human skeletal muscles lipidome and fuel selection.

Chapter Seven

Conclusions and future work

7. Conclusions and future work

7.1 Conclusions

7.1.1 Generation of uniformly labelled ^{13}C lipid standards in yeast and bacteria species

In this project, an LC-MS based approach that allows semi-quantification of lipids in complex samples using fully stable isotope-labelled lipid standards was developed. Although the cost and availability of authentic synthesised standards limits the practical usefulness of this approach, an alternative *in vivo* isotopic labelling strategy was evaluated. Multiple optimisation and evaluation steps were conducted to effectively select a microorganism-based source of these labelled standards that could cover the majority of the lipidome in higher eukaryotic species leading the way to comprehensive compound-specific normalisation in quantitative mass spectrometry analysis. First, the lipidome profiles of five different species reported in the literature were investigated and compared including *E. coli* MG1655, spirulina, *S. cerevisiae* CEN.PK 1137D, *S. cerevisiae* BY4741, and *P. pastoris* NCYC 175. Comparison of the lipid profiles of selected organisms shows that there were marked differences in lipid class identified and in the number and the relative amount of the identified lipid species in each class where individual or combinations of species could provide a wide range of standards that cover most of the lipidome of higher eukaryotic samples. Second, an *in vivo* labelling strategy was investigated for each species where a^{13}C-labelled carbon source was used to produce a wide range of labelled lipid standards with the ultimate aim of providing a comprehensive set of ^{13}C-labelled lipids to be used for data correction and quantification in lipidomics analysis. Third, the labelling pattern of these labelled standards was assessed and the efficacy of the

labelling strategy in each species was evaluated. From the outline above, the selected yeast *P. pastoris* grown in controlled meid with one main ^{13}C-labelled carbon source (1%) for 24 h, proved to be the optimum source of isotopically labelled standards that will dilever more common lipids with complex systems such as plasma with high labelling percentage leading the way to comprehensive compound-specific standardisation in quantitative mass spectrometry assays in complex biological samples.

7.1.2 Methods development and validation

The use of a well-established normalisation method for targeted studies based on ^{13}C-labelled internal standards produced by *in vivo* labelling strategy was developed and validated for untargeted lipidomics studies on plasma samples and applied in two clinical untargeted lipidomics studies. First, an extraction protocol was optimised to ensure maximum recovery of lipid species and sufficient sensitivity to facilitate the identification of a wider range of lipids from different classes in a reproducible manner. Second, the optimum amount of ^{13}C-IS mixture was assessed to ensure that the lowest amount of ^{13}C-IS mixture was used, essential to maximise detection of the highest number of ions with minimal or no ion suppression. Following from this initial work, the ^{13}C-IS mixture was used as internal standard introduced at initial stages of plasma samples preparation to evaluate the ability of the optimised ^{13}C-IS mixture in correcting various instrumental variations that could arise in untargeted lipidomics studies (28, 124, 402, 403). Plasma was selected as a model sample matrix because it is usually used as an alternative for blood which is one of the most used biofluids in metabolomics and lipidomics studies (404).

Metabolites and lipids in LC-MS based metabolomics studies are subjected to different sources of variations at multiple stages that could affect the quality of the results and it is very important to correct the effect of these variations. The validated normalisation method was shown to be an effective method in reducing technical and analytical variations introduced during samples preparation and analysis. In addition, this method was able to reduce variations introduced in typical lipidomics large batch analysis (over several days) where the MS response may change from day to day and hence compromise the results. The ^{13}C-IS mixture enables a direct normalisation approach by compound-specific normalisation or an indirect approach based on RT with or without considering chemical similarity (class similarity) that ultimately can used to obtain a more accurate estimate of hundreds of lipid ions identified in samples analysed based on untargeted LC-MS-based lipidomic analysis. Although new interest has risen in evaluating the potential use of these ^{13}C-IS in untargeted lipidomics study, it is the first time that these standards produced by *in vivo* labelling strategy were used comprehensively for normalisation of diverse set of lipids on multiple sets of biological samples. This approach is considered as an efficient alternative for chemically synthesised standards which are limited and expensive or to other normalisations methods that lack the true power for correcting the different source of variations at various stages throughout the study.

Significant challenges had to be overcome during method development and validation. First, an unexpected result demonstrated that the ^{13}C-IS mixture had a little or no effect on correcting analytical variations in short analysis run time (a few hours). This was concluded to be due to the high stability of a short LC-MS run where care was taken in the analytical technique during sample preparation, and stable

chromatography was established with a consistent response of the LC-MS system. Second, the reliability of the whole method was based on the need to correctly identify hundreds of lipid ions, where this was impractical to do manually. Hence the use of LipidSearch^{TM} software was developed to provide a high level of confidence in lipid identity by the use of MS-MS analysis and reference to lipid fragmentation databases. Third, the whole process is manual due to the lack of software that could detect, identify and quantify both unlabelled sample lipids and ^{13}C-labelled lipids in the internal standard mixture when added to the samples. Therefore, due to inability to annotate ^{13}C-labelled lipids, manual curation of ^{13}C datasets was ultimately required to ensure correct annotation.

7.1.3 Clinical applications using the developed and validated normalisation method

The developed normalisation method was used on two clinical lipidomic studies to provide an accurate estimate of the detected and identified lipid ions in those studies. In both studies, the applied normalisation method was expected to decrease systematic and random errors that can be introduced accidentally and unavoidably during the study that could affect the quality of the data.

In chapter five, the developed novel lipidomics method was employed to study intra-tumour heterogeneity in low grade glioma tumour in five patients. The experimental design of this experiment was not ideal because no control samples were available (not possible to take healthy brain tissue) and the number of patients were limited. Despite these limitations, a distinct lipidomic profile was observed between spatially resolved regions of the tumour indicating intra-tumoral heterogeneity that could affect patient stratification, diagnosis and treatment. Also, the degree of intra-tumoral heterogeneity between patients was different. Both observations were

expected to affect treatment output, survival and patient's quality of life before and after treatment and therefore personalised tumour-specific strategies should be considered to accommodate such variations to extend progression-free intervals. In addition, inter and intra-tumour heterogeneity suggests that profiling cancer cell phenotypes from single biopsies to guide therapeutic decision making from heterogeneous tumours may prove challenging especially as heterogeneity could lead to therapeutic resistance or relapse.

In chapter six, the developed novel lipidomics method was employed to study the lipidomic difference between healthy and T2DM patients, the effect of age on the lipidomic profile in patients recently diagnosed with T2DM and to study the effect of L-carnitine supplement on plasma lipidomic profile of T2DM patients. There was no clear significant separation between the studied groups despite the fact that there is a well-established association between plasma lipid profile and T2DM in the scientific literature. This unexpected result can be attributed to either low sample size or to the fact that the changes were small and did not pass the statistical significance threshold. Also, the lipidomic profile revealed that there was no difference in plasma lipid profile between young and old T2DM patients which agrees with previous studies, the duration of the disease had a more pronounced effect on the plasma lipid profile of these patients rather than their age. In addition, oral L-carnitine supplements had no effect on the lipidome profile of T2DM patients. The main limitations on the current study design was the small number of patients who were only males and the poor control over many important factors such as patients' diet and physical activity. A better experimental design can be performed by including

more volunteers of both sexes and more control over their diet and lifestyle throughout the study.

7.2 Future work

In this thesis, lipids were putatively identified by LipidSearch™ based on their fragmentation pattern score which can result in errors due to huge number of lipid isomers. In future work this could be overcome by matching *m/z*, RT and fragmentation pattern with reference to pure authentic standards to confirm the LipiSearch™ identity and to increase the confidence of the obtained results. This improved identification method would also be relevant to the ^{13}C-labelled standards that could be identified in the studied samples and might improve the qualitative and quantitative information discussed in this thesis. In addition, the novel method was used in untargeted analysis but only putatively identified ions were addressed and normalised, it would be advantageous if the effect of untargeted normalisation is done based on selected ^{13}C-ISs identified previously, this will enrich the studies as more ions would be included in the analysis. Furthermore, it would be interesting if we could highlight the main different lipid ions between different regions in each patient included in analysis in chapter five and compare these lipids with other patients and link these ions with other studies in our group regards glioma grade IV (glioblastoma: highly malignant and invasive grade of glioma) in order to expect which ions could be linked to higher grade of the disease or to predict which lipid profile could promote progression to higher grade of the disease.

Also, it would be interesting to compare the hydrophilic metabolites profiles in the selected species and compare between them to investigate which species would be

more beneficial as a source of labelled standards in metabolomics studies as well. Furthermore, to validate and apply that optimum extract in clinical metabolomics studies.

Furthermore, this approach have proven its ability to improve the quality and reproducibility of lipidomics data and have a positive effect on the the qualitative and quantitative description of lipid biomarkers . In addition, the presented approach is a cost efficient alternative to chemical synthesis of labelled lipid standards that can be used in different biological matrices. for clinical and nonclinical use- for example in plant-based lipids or in insects or indeed in microorganisms themselves. Additionally, the studied species can be used as microbial factories to produce valuable labelled chemical intermediates that can be used as standards in targeted or untargetd studies to understand lipid metabolism in different applications.

References

1. E. Fahy, D. Cotter, M. Sud and S. Subramaniam, *Biochimica et Biophysica Acta*, 2011, **1811**, 637-647.
2. E. Fahy, S. Subramaniam, H. A. Brown, C. K. Glass, A. H. Merrill, Jr., R. C. Murphy, C. R. Raetz, D. W. Russell, Y. Seyama, W. Shaw, T. Shimizu, F. Spener, G. van Meer, M. S. VanNieuwenhze, S. H. White, J. L. Witztum and E. A. Dennis, *Journal of Lipid Research*, 2005, **46**, 839-861.
3. K. T, *Journal of Computer Science and Systems Biology*, 2011, **4**, 093-098.
4. G. M. Cooper, *The Cell: A Molecular Approach*, ASM Press, 2 edn., 2000.
5. H. T. McMahon and J. L. Gallop, *Nature*, 2005, **438**, 590-596.
6. J. A. Alberts B, Lewis J. Molecular Biology of the Cell. 4th edition. New York: Garland Science; 2002. The Lipid Bilayer.
7. T. Shemesh, A. Luini, V. Malhotra, K. N. J. Burger and M. M. Kozlov, *Biophysical Journal*, 2003, **85**, 3813-3827.
8. E. E. Kooijman, V. Chupin, N. L. Fuller, M. M. Kozlov, B. de Kruijff, K. N. J. Burger and P. R. Rand, *Biochemistry*, 2005, **44**, 2097-2102.
9. G. van Meer, D. R. Voelker and G. W. Feigenson, *Nature reviews. Molecular cell biology*, 2008, **9**, 112-124.
10. O. Cuvillier, *Biochimica et Biophysica Acta*, 2002, **1585**, 153-162.
11. T. Baumruker, F. Bornancin and A. Billich, *Immunology Letters*, 2005, **96**, 175-185.
12. K. M. Eyster, *Advances in Physiology Education*, 2007, **31**, 5-16.
13. M. P. Wymann, M. Zvelebil and M. Laffargue, *Trends in Pharmacological Sciences*, 2003, **24**, 366-376.
14. T. Hyotylainen, L. Ahonen, P. Poho and M. Oresic, *Biochim Biophys Acta Mol Cell Biol Lipids*, 2017, **1862**, 800-803.
15. F. R. Maxfield and I. Tabas, *Nature*, 2005, **438**, 612-621.
16. R. B. Chan, T. G. Oliveira, E. P. Cortes, L. S. Honig, K. E. Duff, S. A. Small, M. R. Wenk, G. Shui and G. Di Paolo, *Journal of Biological Chemistry*, 2012, **287**, 2678-2688.
17. C. G. Kraegen EW1, Ye JM, Thompson AL, Furler SM., *Exp Clin Endocrinol Diabetes.*, 2001, **109**, 189-201.
18. R. Virmani, A. P. Burke, F. D. Kolodgie and A. Farb, *Journal of Interventional Cardiology*, 2002, **15**, 439-446.
19. Y. J. Geng and P. Libby, *Arteriosclerosis, Thrombosis, and Vascular Biology*, 2002, **22**, 1370-1380.
20. I. Tabas, *Arteriosclerosis, Thrombosis, and Vascular Biology*, 2005, **25**, 2255-2264.
21. D. Lütjohann, S. Meichsner and H. Pettersson, *Clinical Lipidology*, 2012, **7**, 65-78.
22. D. Hanahan and R. A. Weinberg, *Cell*, 2011, **144**, 646-674.
23. S. Beloribi-Djefaflia, S. Vasseur and F. Guillaumond, *Oncogenesis*, 2016, **5**, e189.

24. F. Perrotti, C. Rosa, I. Cicalini, P. Sacchetta, P. Del Boccio, D. Genovesi and D. Pieragostino, *International Journal of Molecular Sciences*, 2016, **17**, 1992.
25. E. Fahy, S. Subramaniam, R. C. Murphy, M. Nishijima, C. R. H. Raetz, T. Shimizu, F. Spener, G. van Meer, M. J. O. Wakelam and E. A. Dennis, *Journal of Lipid Research*, 2009, **50**, S9-S14.
26. O. Fiehn, *Plant Molecular Biology*, 2002, **48**.
27. J. K. Nicholson, J. C. Lindon and E. Holmes, *Xenobiotica*, 1999, **29**, 1181-1189.
28. W. B. Dunn, D. Broadhurst, P. Begley, E. Zelena, S. Francis-McIntyre, N. Anderson, M. Brown, J. D. Knowles, A. Halsall, J. N. Haselden, A. W. Nicholls, I. D. Wilson, D. B. Kell and R. Goodacre, *Nature Protocols*, 2011, **6**, 1060-1083.
29. M. R. Wenk, *Nature Reviews Drug Discovery*, 2005, **4**.
30. R. Smith, A. D. Mathis, D. Ventura and J. T. Prince, *BMC Bioinformatics*, 2014, **15**, 1-14.
31. T. Cajka and O. Fiehn, *Analytical Chemistry*, 2016, **88**, 524-545.
32. L. Li, J. Han, Z. Wang, J. Liu, J. Wei, S. Xiong and Z. Zhao, *International Journal of Molecular Sciences*, 2014, **15**, 10492-10507.
33. K. Dettmer, P. A. Aronov and B. D. Hammock, *Mass Spectrometry Reviews*, 2007, **26**, 51-78.
34. T. Cajka and O. Fiehn, *Trends in Analytical Chemistry*, 2014, **61**, 192-206.
35. A. M. Tsedilin, A. N. Fakhrutdinov, D. B. Eremin, S. S. Zalesskiy, A. O. Chizhov, N. G. Kolotyrkina and V. P. Ananikov, *Mendeleev Communications*, 2015, **25**, 454-456.
36. K. Bingol, *High-throughput*, 2018, **7**, 9.
37. D. P. Downes, J. H. P. Collins, B. Lama, H. Zeng, T. Nguyen, G. Keller, M. Febo and J. R. Long, *Chemphyschem*, 2019, **20**, 216-230.
38. I. Aretz and D. Meierhofer, *International Journal of Molecular Sciences*, 2016, **17**.
39. J. L. Markley, R. Bruschweiler, A. S. Edison, H. R. Eghbalnia, R. Powers, D. Raftery and D. S. Wishart, *Current Opinion in Biotechnology*, 2017, **43**, 34-40.
40. B. Zhou, J. F. Xiao, L. Tuli and H. W. Ressom, *Molecular Biosystems*, 2012, **8**, 470-481.
41. A. Agin, D. Heintz, E. Ruhland, J. M. Chao de la Barca, J. Zumsteg, V. Moal, A. S. Gauchez and I. J. Namer, *Médecine Nucléaire*, 2016, **40**, 4-10.
42. A. D. Watson, *Journal of Lipid Research*, 2006, **47**, 2101-2111.
43. O. L. Knittelfelder, B. P. Weberhofer, T. O. Eichmann, S. D. Kohlwein and G. N. Rechberger, *Journal of Chromatography. B, Analytical Technologies in the Biomedical and Life Sciences*, 2014, **951-952**, 119-128.
44. J. B. Fenn, M. Mann, C. K. Meng, S. F. Wong and C. M. Whitehouse, *Science*, 1989, **246**, 64-71.
45. X. Han and R. W. Gross, *Mass Spectrometry Reviews*, 2005, **24**, 367-412.
46. LAMOND-LAB, *Journal*.
47. T. Yamada, T. Uchikata, S. Sakamoto, Y. Yokoi, E. Fukusaki and T. Bamba, *Journal of Chromatography A*, 2013, **1292**, 211-218.
48. K. Schmelzer, E. Fahy, S. Subramaniam and E. A. Dennis, in *Methods in Enzymology*, Academic Press, 2007, vol. Volume 432, pp. 171-183.
49. X. Han and R. W. Gross, *Mass Spectrometry Reviews*, 2005, **24**, 367-412.

50. K. N. Patel, J. K. Patel, M. P. Patel, G. C. Rajput and H. A. Patel, *Pharmaceutical methods*, 2010, **1**, 2-13.
51. J.-P. Antignac, K. de Wasch, F. Monteau, H. De Brabander, F. Andre and B. Le Bizec, *Analytica Chimica Acta*, 2005, **529**, 129-136.
52. A. Furey, M. Moriarty, V. Bane, B. Kinsella and M. Lehane, *Talanta*, 2013, **115**, 104-122.
53. J. B. German, L. A. Gillies, J. T. Smilowitz, A. M. Zivkovic and S. M. Watkins, *Current Opinion in Lipidology*, 2007, **18**, 66-71.
54. S. S. Bird, V. R. Marur, M. J. Sniatynski, H. K. Greenberg and B. S. Kristal, *Analytical Chemistry*, 2011, **83**, 940-949.
55. Z. Lei, D. V. Huhman and L. W. Sumner, *Journal of Biological Chemistry*, 2011, **286**, 25435-25442.
56. T. Hyotylainen and M. Oresic, *Bioanalysis*, 2016, **8**, 351-364.
57. M. Wang, C. Wang and X. Han, *Mass Spectrometry Reviews*, 2016, DOI: 10.1002/mas.21492, n/a-n/a.
58. C. J. DeLong, P. R. Baker, M. Samuel, Z. Cui and M. J. Thomas, *Journal of Lipid Research*, 2001, **42**, 1959-1968.
59. P. Panuwet, R. E. Hunter, Jr., P. E. D'Souza, X. Chen, S. A. Radford, J. R. Cohen, M. E. Marder, K. Kartavenka, P. B. Ryan and D. B. Barr, *Critical reviews in analytical chemistry*, 2016, **46**, 93-105.
60. S. H. J. Brown, T. W. Mitchell and S. J. Blanksby, *Biochimica et Biophysica Acta (BBA) - Molecular and Cell Biology of Lipids*, 2011, **1811**, 807-817.
61. Y. H. Rustam and G. E. Reid, *Analytical Chemistry*, 2018, **90**, 374-397.
62. B. L. J. Poad, H. T. Pham, M. C. Thomas, J. R. Nealon, J. L. Campbell, T. W. Mitchell and S. J. Blanksby, *Journal of the American Society for Mass Spectrometry*, 2010, **21**, 1989-1999.
63. J. E. Kyle, X. Zhang, K. K. Weitz, M. E. Monroe, Y. M. Ibrahim, R. J. Moore, J. Cha, X. Sun, E. S. Lovelace, J. Wagoner, S. J. Polyak, T. O. Metz, S. K. Dey, R. D. Smith, K. E. Burnum-Johnson and E. S. Baker, *Analyst*, 2016, **141**, 1649-1659.
64. H. T. Pham, T. Ly, A. J. Trevitt, T. W. Mitchell and S. J. Blanksby, *Analytical Chemistry*, 2012, **84**, 7525-7532.
65. J. P. Koelmel, C. Z. Ulmer, C. M. Jones, R. A. Yost and J. A. Bowden, *Biochim Biophys Acta Mol Cell Biol Lipids*, 2017, **1862**, 766-770.
66. H. G. Gika, G. A. Theodoridis, R. S. Plumb and I. D. Wilson, *Journal of Pharmaceutical and Biomedical Analysis*, 2014, **87**, 12-25.
67. E. Werner, J.-F. Heilier, C. Ducruix, E. Ezan, C. Junot and J.-C. Tabet, *Journal of Chromatography B*, 2008, **871**, 143-163.
68. J. P. Koelmel, N. M. Kroeger, C. Z. Ulmer, J. A. Bowden, R. E. Patterson, J. A. Cochran, C. W. W. Beecher, T. J. Garrett and R. A. Yost, *BMC Bioinformatics*, 2017, **18**, 331.
69. J. Hartler, M. Trotzmuller, C. Chitraju, F. Spener, H. C. Kofeler and G. G. Thallinger, *Bioinformatics*, 2011, **27**, 572-577.
70. T. Kind, K. H. Liu, D. Y. Lee, B. DeFelice, J. K. Meissen and O. Fiehn, *Nat Methods*, 2013, **10**, 755-758.
71. R. Taguchi and M. Ishikawa, *Journal of Chromatography A*, 2010, **1217**, 4229-4239.

72. R. Herzog, K. Schuhmann, D. Schwudke, J. L. Sampaio, S. R. Bornstein, M. Schroeder and A. Shevchenko, *PloS One*, 2012, **7**, e29851.
73. K. Yang and X. Han, *Metabolites*, 2011, **1**, 21-40.
74. Z. Lei, D. V. Huhman and L. W. Sumner, *The Journal of biological chemistry*, 2011, **286**, 25435-25442.
75. L. Yuan, D. Zhang, M. Jemal and A.-F. Aubry, *Rapid Communications in Mass Spectrometry*, 2012, **26**, 1465-1474.
76. P. J. Taylor, *Clinical Biochemistry*, 2005, **38**, 328-334.
77. H. Trufelli, P. Palma, G. Famiglini and A. Cappiello, *Mass Spectrometry Reviews*, 2011, **30**, 491-509.
78. K. Becan-McBride, *Journal of Intravenous Nursing*, 1999, **22**, 137-142.
79. M. E. Bollard, E. G. Stanley, J. C. Lindon, J. K. Nicholson and E. Holmes, *NMR in Biomedicine*, 2005, **18**, 143-162.
80. W. M. Ahmed, P. Brinkman, H. Weda, H. H. Knobel, Y. Xu, T. M. Nijsen, R. Goodacre, N. Rattray, T. J. Vink, M. Santonico, G. Pennazza, P. Montuschi, P. J. Sterk and S. J. Fowler, *J Breath Res*, 2018, **13**, 016001.
81. M. Ishikawa, K. Maekawa, K. Saito, Y. Senoo, M. Urata, M. Murayama, Y. Tajima, Y. Kumagai and Y. Saito, *PloS One*, 2014, **9**, e91806.
82. J. M. Weir, G. Wong, C. K. Barlow, M. A. Greeve, A. Kowalczyk, L. Almasy, A. G. Comuzzie, M. C. Mahaney, J. B. Jowett, J. Shaw, J. E. Curran, J. Blangero and P. J. Meikle, *Journal of Lipid Research*, 2013, **54**, 2898-2908.
83. P. K. Cai X, Pajouh SK, Hubbard A, Nomura DK., *Metabolomics*, 2014, **4:131**.
84. M. Lankinen, U. Schwab, M. Kolehmainen, J. Paananen, K. Poutanen, H. Mykkanen, T. Seppanen-Laakso, H. Gylling, M. Uusitupa and M. Oresic, *PloS One*, 2011, **6**, e22646.
85. I. Bondia-Pons, P. Poho, L. Bozzetto, C. Vetrani, L. Patti, A. M. Aura, G. Annuzzi, T. Hyotylainen, A. A. Rivellese and M. Oresic, *Molecular Nutrition & Food Research*, 2014, **58**, 1873-1882.
86. M. Krajcovicova-Kudlackova, R. Simoncic, A. Bederova, E. Grancicova and T. Magalova, *Nahrung*, 1997, **41**, 311-314.
87. M. Lankinen, U. Schwab, A. Erkkila, T. Seppanen-Laakso, M. L. Hannila, H. Mussalo, S. Lehto, M. Uusitupa, H. Gylling and M. Oresic, *PloS One*, 2009, **4**, e5258.
88. S. Krug, G. Kastenmüller, F. Stückler, M. J. Rist, T. Skurk, M. Sailer, J. Raffler, W. Römisch-Margl, J. Adamski, C. Prehn, T. Frank, K.-H. Engel, T. Hofmann, B. Luy, R. Zimmermann, F. Moritz, P. Schmitt-Kopplin, J. Krumsiek, W. Kremer, F. Huber, U. Oeh, F. J. Theis, W. Szymczak, H. Hauner, K. Suhre and H. Daniel, *The FASEB Journal*, 2012, **26**, 2607-2619.
89. K. Kim, C. Mall, S. L. Taylor, S. Hitchcock, C. Zhang, H. I. Wettersten, A. D. Jones, A. Chapman and R. H. Weiss, *PloS One*, 2014, **9**, e86223.
90. E. C. Chua, G. Shui, I. T. Lee, P. Lau, L. C. Tan, S. C. Yeo, B. D. Lam, S. Bulchand, S. A. Summers, K. Puvanendran, S. G. Rozen, M. R. Wenk and J. J. Gooley, *Proceedings of the National Academy of Sciences of the United States of America*, 2013, **110**, 14468-14473.
91. R. Dallmann, A. U. Viola, L. Tarokh, C. Cajochen and S. A. Brown, *Proceedings of the National Academy of Sciences of the United States of America*, 2012, **109**, 2625-2629.

92. J. E. Ang, V. Revell, A. Mann, S. Mantele, D. T. Otway, J. D. Johnston, A. E. Thumser, D. J. Skene and F. Raynaud, *Chronobiology International*, 2012, **29**, 868-881.
93. T. Kasukawa, M. Sugimoto, A. Hida, Y. Minami, M. Mori, S. Honma, K. Honma, K. Mishima, T. Soga and H. R. Ueda, *Proceedings of the National Academy of Sciences of the United States of America*, 2012, **109**, 15036-15041.
94. V. Gonzalez-Covarrubias, A. Dane, T. Hankemeier and R. J. Vreeken, *Metabolomics*, 2013, **9**, 337-348.
95. W. Yang, Y. Chen, C. Xi, R. Zhang, Y. Song, Q. Zhan, X. Bi and Z. Abliz, *Analytical Chemistry*, 2013, **85**, 2606-2610.
96. L. A. Taylor, J. Arends, A. K. Hodina, C. Unger and U. Massing, *Lipids in Health and Disease*, 2007, **6**, 17.
97. A. M. Zivkovic, M. M. Wiest, U. T. Nguyen, R. Davis, S. M. Watkins and J. B. German, *Metabolomics*, 2009, **5**, 507-516.
98. J. Folch, M. Lees and G. H. Sloane Stanley, *Journal of Biological Chemistry*, 1957, **226**, 497-509.
99. E. G. Bligh and W. J. Dyer, *Canadian Journal of Biochemistry and Physiology*, 1959, **37**, 911-917.
100. A. Reis, A. Rudnitskaya, G. J. Blackburn, N. Mohd Fauzi, A. R. Pitt and C. M. Spickett, *Journal of Lipid Research*, 2013, **54**, 1812-1824.
101. R. M. Pellegrino, A. Di Veroli, A. Valeri, L. Goracci and G. Cruciani, *Analytical and Bioanalytical Chemistry*, 2014, **406**, 7937-7948.
102. M. H. Sarafian, M. Gaudin, M. R. Lewis, F.-P. Martin, E. Holmes, J. K. Nicholson and M.-E. Dumas, *Analytical Chemistry*, 2014, **86**, 5766-5774.
103. J. E. Markham, *Methods in Molecular Biology*, 2013, **1009**, 93-101.
104. V. Shulaev and K. D. Chapman, *Biochim Biophys Acta Mol Cell Biol Lipids*, 2017, **1862**, 786-791.
105. D. Broadhurst, R. Goodacre, S. N. Reinke, J. Kuligowski, I. D. Wilson, M. R. Lewis and W. B. Dunn, *Metabolomics*, 2018, **14**, 72.
106. F. F. a. D. Administration, 2001.
107. W. B. Dunn, I. D. Wilson, A. W. Nicholls and D. Broadhurst, *Bioanalysis*, 2012, **4**, 2249-2264.
108. J. J. Pitt, *The Clinical Biochemist Reviews*, 2009, **30**, 19-34.
109. L. Yuan, D. Zhang, M. Jemal and A. F. Aubry, *Rapid Communications in Mass Spectrometry*, 2012, **26**, 1465-1474.
110. F. Gosetti, E. Mazzucco, D. Zampieri and M. C. Gennaro, *Journal of Chromatography A*, 2010, **1217**, 3929-3937.
111. G. S. Ghosh C, Shinde CP, Chakraborty B *J Bioequiv Availab*, 2011, **3**, 122-127.
112. R. King, R. Bonfiglio, C. Fernandez-Metzler, C. Miller-Stein and T. Olah, *Journal of the American Society for Mass Spectrometry*, 2000, **11**, 942-950.
113. T. M. Annesley, *Clinical Chemistry*, 2003, **49**, 1041-1044.
114. H. Redestig, A. Fukushima, H. Stenlund, T. Moritz, M. Arita, K. Saito and M. Kusano, *Analytical Chemistry*, 2009, **81**, 7974-7980.
115. F. M. van der Kloet, I. Bobeldijk, E. R. Verheij and R. H. Jellema, *Journal of Proteome Research*, 2009, **8**, 5132-5141.

116. T. Sangster, H. Major, R. Plumb, A. J. Wilson and I. D. Wilson, *Analyst*, 2006, **131**, 1075-1078.
117. Y. Wu and L. Li, *Journal of Chromatography A*, 2016, **1430**, 80-95.
118. M. Sysi-Aho, M. Katajamaa, L. Yetukuri and M. Orešič, *BMC Bioinformatics*, 2007, **8**, 1-17.
119. M. Rusilowicz, M. Dickinson, A. Charlton, S. O'Keefe and J. Wilson, *Metabolomics : Official journal of the Metabolomic Society*, 2016, **12**, 56-56.
120. R. A. van den Berg, H. C. Hoefsloot, J. A. Westerhuis, A. K. Smilde and M. J. van der Werf, *BMC Genomics*, 2006, **7**, 142.
121. M. Chen, R. S. P. Rao, Y. Zhang, C. X. Zhong and J. J. Thelen, *SpringerPlus*, 2014, **3**, 439.
122. A. M. De Livera, D. A. Dias, D. De Souza, T. Rupasinghe, J. Pyke, D. Tull, U. Roessner, M. McConville and T. P. Speed, *Analytical Chemistry*, 2012, **84**, 10768-10776.
123. *Journal of the American Statistical Association*, 1979, **74**, 829-836.
124. J. A. Kirwan, D. I. Broadhurst, R. L. Davidson and M. R. Viant, *Analytical and Bioanalytical Chemistry*, 2013, **405**, 5147-5157.
125. J. Kuligowski, A. Sanchez-Illana, D. Sanjuan-Herraez, M. Vento and G. Quintas, *Analyst*, 2015, **140**, 7810-7817.
126. C. Brunius, L. Shi and R. Landberg, *Metabolomics*, 2016, **12**, 173.
127. A. Chokkathukalam, D.-H. Kim, M. P. Barrett, R. Breitling and D. J. Creek, *Bioanalysis*, 2014, **6**, 511-524.
128. W. Lu, Y. K. Kwon and J. D. Rabinowitz, *Journal of the American Society for Mass Spectrometry*, 2007, **18**, 898-909.
129. M. R. Mashego, L. Wu, J. C. Van Dam, C. Ras, J. L. Vinke, W. A. Van Winden, W. M. Van Gulik and J. J. Heijnen, *Biotechnology and Bioengineering*, 2004, **85**, 620-628.
130. S. Bijlsma, I. Bobeldijk, E. R. Verheij, R. Ramaker, S. Kochhar, I. A. Macdonald, B. van Ommen and A. K. Smilde, *Analytical Chemistry*, 2006, **78**, 567-574.
131. K. Ekroos, I. V. Chernushevich, K. Simons and A. Shevchenko, *Analytical Chemistry*, 2002, **74**, 941-949.
132. A. Zacarias, D. Bolanowski and A. Bhatnagar, *Analytical Biochemistry*, 2002, **308**, 152-159.
133. X. Han and R. W. Gross, *Analytical Biochemistry*, 2001, **295**, 88-100.
134. D.-H. Kim, F. Achcar, R. Breitling, K. E. Burgess and M. P. Barrett, *Metabolomics*, 2015, **11**, 1721-1732.
135. C. Birkemeyer, A. Luedemann, C. Wagner, A. Erban and J. Kopka, *Trends in Biotechnology*, 2005, **23**, 28-33.
136. L. O. Butler and R. W. Grist, *Journal of General Microbiology*, 1984, **130**, 483-494.
137. A. D. Hegeman, C. F. Schulte, Q. Cui, I. A. Lewis, E. L. Huttlin, H. Eghbalnia, A. C. Harms, E. L. Ulrich, J. L. Markley and M. R. Sussman, *Analytical Chemistry*, 2007, **79**, 6912-6921.
138. K. Li, X. Wang, V. R. Pidatala, C. P. Chang and X. Cao, *Journal of Proteome Research*, 2014, **13**, 5879-5887.
139. X. Luo, S. Zhao, T. Huan, D. Sun, R. M. Friis, M. C. Schultz and L. Li, *Journal of Proteome Research*, 2016, **15**, 1602-1612.

140. S. Neubauer, C. Haberhauer-Troyer, K. Klavins, H. Russmayer, M. G. Steiger, B. Gasser, M. Sauer, D. Mattanovich, S. Hann and G. Koellensperger, *J Sep Sci*, 2012, **35**, 3091-3105.
141. A. de Ghellinck, H. Schaller, V. Laux, M. Haertlein, M. Sferrazza, E. Maréchal, H. Wacklin, J. Jouhet and G. Fragneto, *PloS One*, 2014, **9**, e92999.
142. L. Feldberg, I. Venger, S. Malitsky, I. Rogachev and A. Aharoni, *Analytical Chemistry*, 2009, **81**, 9257-9266.
143. C. Bueschl, B. Kluger, M. Lemmens, G. Adam, G. Wiesenberger, V. Maschietto, A. Marocco, J. Strauss, S. Bödi, G. G. Thallinger, R. Krska and R. Schuhmacher, *Metabolomics*, 2014, **10**, 754-769.
144. B. D. Bennett, E. H. Kimball, M. Gao, R. Osterhout, S. J. Van Dien and J. D. Rabinowitz, *Nature Chemical Biology*, 2009, **5**, 593-599.
145. K. Li, X. Wang, V. R. Pidatala, C.-P. Chang and X. Cao, *Journal of Proteome Research*, 2014, **13**, 5879-5887.
146. P. Giavalisco, K. Kohl, J. Hummel, B. Seiwert and L. Willmitzer, *Analytical Chemistry*, 2009, **81**, 6546-6551.
147. P. Giavalisco, J. Hummel, J. Lisec, A. C. Inostroza, G. Catchpole and L. Willmitzer, *Analytical Chemistry*, 2008, **80**, 9417-9425.
148. S. Schatschneider, S. Abdelrazig, L. Safo, A. M. Henstra, T. Millat, D. H. Kim, K. Winzer, N. P. Minton and D. A. Barrett, *Analytical Chemistry*, 2018, **90**, 4470-4477.
149. R. Guerrasio, C. Haberhauer-Troyer, D. Mattanovich, G. Koellensperger and S. Hann, *Analytical and Bioanalytical Chemistry*, 2014, **406**, 915-922.
150. E. Rampler, C. Coman, G. Hermann, A. Sickmann, R. Ahrends and G. Koellensperger, *Analyst*, 2017, **142**, 1891-1899.
151. D. Weindl, A. Wegner, C. Jäger and K. Hiller, *Journal of Chromatography A*, 2015, **1389**, 112-119.
152. E. Rampler, A. Criscuolo, M. Zeller, Y. El Abiead, H. Schoeny, G. Hermann, E. Sokol, K. Cook, D. A. Peake, B. Delanghe and G. Koellensperger, *Analytical Chemistry*, 2018, **90**, 6494-6501.
153. Y. Wu and L. Li, *Analytical Chemistry*, 2013, **85**, 5755-5763.
154. https://planetorbitrap.com/q-exactive-plus#tab:schematic, (accessed 15/06/2019).
155. E. J. Want, I. D. Wilson, H. Gika, G. Theodoridis, R. S. Plumb, J. Shockcor, E. Holmes and J. K. Nicholson, *Nature Protocols*, 2010, **5**, 1005-1018.
156. H. R. Liang, R. L. Foltz, M. Meng and P. Bennett, *Rapid Communications in Mass Spectrometry*, 2003, **17**, 2815-2821.
157. R. Aebersold and M. Mann, *Nature*, 2003, **422**, 198-207.
158. Y. Shiio and R. Aebersold, *Nature Protocols*, 2006, **1**, 139-145.
159. J. M. Buescher, M. R. Antoniewicz, L. G. Boros, S. C. Burgess, H. Brunengraber, C. B. Clish, R. J. DeBerardinis, O. Feron, C. Frezza, B. Ghesquiere, E. Gottlieb, K. Hiller, R. G. Jones, J. J. Kamphorst, R. G. Kibbey, A. C. Kimmelman, J. W. Locasale, S. Y. Lunt, O. D. K. Maddocks, C. Malloy, C. M. Metallo, E. J. Meuillet, J. Munger, K. Nöh, J. D. Rabinowitz, M. Ralser, U. Sauer, G. Stephanopoulos, J. St-Pierre, D. A. Tennant, C. Wittmann, M. G. Vander Heiden, A. Vazquez, K. Vousden, J. D. Young, N. Zamboni and S.-M. Fendt, *Current Opinion in Biotechnology*, 2015, **34**, 189-201.

160. T. Szyperski, R. W. Glaser, M. Hochuli, J. Fiaux, U. Sauer, J. E. Bailey and K. Wuthrich, *Metab Eng*, 1999, **1**, 189-197.
161. M. R. Antoniewicz, J. K. Kelleher and G. Stephanopoulos, *Analytical Chemistry*, 2011, **83**, 3211-3216.
162. J. Choi, M. T. Grossbach and M. R. Antoniewicz, *Analytical Chemistry*, 2012, **84**, 4628-4632.
163. M. R. Antoniewicz, *Current Opinion in Biotechnology*, 2013, **24**, 48-53.
164. D. J. Creek, A. Jankevics, K. E. Burgess, R. Breitling and M. P. Barrett, *Bioinformatics*, 2012, **28**, 1048-1049.
165. R. A. Scheltema, A. Jankevics, R. C. Jansen, M. A. Swertz and R. Breitling, *Analytical Chemistry*, 2011, **83**, 2786-2793.
166. F. Olivon, G. Grelier, F. Roussi, M. Litaudon and D. Touboul, *Analytical Chemistry*, 2017, **89**, 7836-7840.
167. E. M. Forsberg, T. Huan, D. Rinehart, H. P. Benton, B. Warth, B. Hilmers and G. Siuzdak, *Nature Protocols*, 2018, **13**, 633-651.
168. http://www.nonlinear.com/progenesis/qi/, (accessed 10/06/2019).
169. C. Kuhl, R. Tautenhahn, C. Bottcher, T. R. Larson and S. Neumann, *Analytical Chemistry*, 2012, **84**, 283-289.
170. C. Bueschl, B. Kluger, F. Berthiller, G. Lirk, S. Winkler, R. Krska and R. Schuhmacher, *Bioinformatics*, 2012, **28**, 736-738.
171. E. Melamud, L. Vastag and J. D. Rabinowitz, *Analytical Chemistry*, 2010, **82**, 9818-9826.
172. A. Chokkathukalam, A. Jankevics, D. J. Creek, F. Achcar, M. P. Barrett and R. Breitling, *Bioinformatics*, 2013, **29**, 281-283.
173. N. Zamboni, E. Fischer and U. Sauer, *BMC Bioinformatics*, 2005, **6**, 209-209.
174. C. H. Poskar, J. Huege, C. Krach, M. Franke, Y. Shachar-Hill and B. H. Junker, *BMC Bioinformatics*, 2012, **13**, 295-295.
175. M. Weitzel, K. Nöh, T. Dalman, S. Niedenführ, B. Stute and W. Wiechert, *Bioinformatics (Oxford, England)*, 2013, **29**, 143-145.
176. L.-E. Quek, C. Wittmann, L. K. Nielsen and J. O. Krömer, *Microbial cell factories*, 2009, **8**, 25-25.
177. A. Chokkathukalam, A. Jankevics, D. J. Creek, F. Achcar, M. P. Barrett and R. Breitling, *Bioinformatics (Oxford, England)*, 2013, **29**, 281-283.
178. M. R. Wenk, *Nat Rev Drug Discov*, 2005, **4**, 594-610.
179. A. Lebkuchen, V. M. Carvalho, G. Venturini, J. S. Salgueiro, L. S. Freitas, A. Dellavance, F. C. Martins, G. Lorenzi-Filho, K. H. M. Cardozo and L. F. Drager, *Scientific Reports*, 2018, **8**, 11270.
180. J. Lv, D. Gao, Y. Zhang, D. Wu, L. Shen and X. Wang, *Journal of Cellular and Molecular Medicine*, 2018, **22**, 5155-5159.
181. Y. Chen, Z. Ma, X. Shen, L. Li, J. Zhong, L. S. Min, L. Xu, H. Li, J. Zhang and L. Dai, *BioMed Research International*, 2018, **2018**, 16.
182. J. Lv, L. Zhang, F. Yan and X. Wang, *Clinical and Translational Medicine*, 2018, **7**, 12.
183. H. Zhao, C. Wang, N. Zhao, W. Li, Z. Yang, X. Liu, W. Le and X. Zhang, *Journal of Chromatography. B: Analytical Technologies in the Biomedical and Life Sciences*, 2018, **1081-1082**, 101-108.

184. C. Mesaros, S. H. Lee and I. A. Blair, *Rapid communications in mass spectrometry : RCM*, 2010, **24**, 3237-3247.
185. S. A. Wudy, M. Hartmann and J. Homoki, *Steroids*, 2002, **67**, 851-857.
186. S. D. Chiwocha, S. R. Abrams, S. J. Ambrose, A. J. Cutler, M. Loewen, A. R. Ross and A. R. Kermode, *Plant Journal*, 2003, **35**, 405-417.
187. N. Grankvist, J. D. Watrous, K. A. Lagerborg, Y. Lyutvinskiy, M. Jain and R. Nilsson, *Cell Chem Biol*, 2018, **25**, 1419-1427.e1414.
188. D. J. Creek, B. Nijagal, D. H. Kim, F. Rojas, K. R. Matthews and M. P. Barrett, *Antimicrobial Agents and Chemotherapy*, 2013, **57**, 2768-2779.
189. S. Schatschneider, S. Abdelrazig, L. Safo, A. M. Henstra, T. Millat, D.-H. Kim, K. Winzer, N. P. Minton and D. A. Barrett, *Analytical Chemistry*, 2018, **90**, 4470-4477.
190. C. C. Wu, M. J. MacCoss, K. E. Howell, D. E. Matthews and J. R. Yates, 3rd, *Analytical Chemistry*, 2004, **76**, 4951-4959.
191. D. B. McClatchy, M.-Q. Dong, C. C. Wu, J. D. Venable and J. R. Yates, *Journal of Proteome Research*, 2007, **6**, 2005-2010.
192. L. Wu, M. R. Mashego, J. C. van Dam, A. M. Proell, J. L. Vinke, C. Ras, W. A. van Winden, W. M. van Gulik and J. J. Heijnen, *Analytical Biochemistry*, 2005, **336**, 164-171.
193. M. J. Wood and E. A. Komives, *Journal of Biomolecular NMR*, 1999, **13**, 149-159.
194. S. Yang, J. C. Hoggard, M. E. Lidstrom and R. E. Synovec, *Journal of Chromatography A*, 2013, **1317**, 175-185.
195. P. Giavalisco, Y. Li, A. Matthes, A. Eckhardt, H. M. Hubberten, H. Hesse, S. Segu, J. Hummel, K. Kohl and L. Willmitzer, *Plant Journal*, 2011, **68**, 364-376.
196. M. Katouli, *Iranian journal of microbiology*, 2010, **2**, 59-72.
197. R. A. Darby, S. P. Cartwright, M. V. Dilworth and R. M. Bill, *Methods in Molecular Biology*, 2012, **866**, 11-23.
198. E. M. Hein and H. Hayen, *Metabolites*, 2012, **2**, 254-267.
199. O. Vielhauer, M. Zakhartsev, T. Horn, R. Takors and M. Reuss, *Journal of Chromatography. B: Analytical Technologies in the Biomedical and Life Sciences*, 2011, **879**, 3859-3870.
200. *Cold Spring Harbor Protocols*, 2006, **2006**, pdb.rec8146.
201. C. Verduyn, E. Postma, W. A. Scheffers and J. P. Van Dijken, *Yeast*, 1992, **8**, 501-517.
202. S. Alfenore, M.-L. Délia and P. Strehaiano, *Analytica Chimica Acta*, 2003, **495**, 217-224.
203. V. Lundblad and K. Struhl, *Current Protocols in Molecular Biology*, 2008, **82**, 13.10.11-13.10.14.
204. A. C. Guo, T. Jewison, M. Wilson, Y. Liu, C. Knox, Y. Djoumbou, P. Lo, R. Mandal, R. Krishnamurthy and D. S. Wishart, *Nucleic Acids Research*, 2013, **41**, D625-D630.
205. D. S. Wishart, C. Knox, A. C. Guo, R. Eisner, N. Young, B. Gautam, D. D. Hau, N. Psychogios, E. Dong, S. Bouatra, R. Mandal, I. Sinelnikov, J. Xia, L. Jia, J. A. Cruz, E. Lim, C. A. Sobsey, S. Shrivastava, P. Huang, P. Liu, L. Fang, J. Peng, R. Fradette, D. Cheng, D. Tzur, M. Clements, A. Lewis, A. De Souza, A. Zuniga,

M. Dawe, Y. Xiong, D. Clive, R. Greiner, A. Nazyrova, R. Shaykhutdinov, L. Li, H. J. Vogel and I. Forsythe, *Nucleic Acids Research*, 2009, **37**, D603-610.
206. E. Mileykovskaya and W. Dowhan, *Current Opinion in Microbiology*, 2005, **8**, 135-142.
207. W. Dowhan, E. Mileykovskaya and M. Bogdanov, *Biochimica et Biophysica Acta*, 2004, **1666**, 19-39.
208. D. A. Mannock, R. N. Lewis, R. N. McElhaney, P. E. Harper, D. C. Turner and S. M. Gruner, *European Biophysics Journal*, 2001, **30**, 537-554.
209. B. D. Bennett, J. Yuan, E. H. Kimball and J. D. Rabinowitz, *Nature Protocols*, 2008, **3**, 1299-1311.
210. T. Jewison, C. Knox, V. Neveu, Y. Djoumbou, A. C. Guo, J. Lee, P. Liu, R. Mandal, R. Krishnamurthy, I. Sinelnikov, M. Wilson and D. S. Wishart, *Nucleic Acids Research*, 2012, **40**, D815-820.
211. C. S. Ejsing, J. L. Sampaio, V. Surendranath, E. Duchoslav, K. Ekroos, R. W. Klemm, K. Simons and A. Shevchenko, *Proceedings of the National Academy of Sciences of the United States of America*, 2009, **106**, 2136-2141.
212. Https://Www.Genome.Jp/Kegg-Bin/Show_Pathway?Sce00020., (accessed 01/06/2019).
213. H. Beck, D. Dobritzsch and J. Piškur, *FEMS Yeast Research*, 2008, **8**, 1209-1213.
214. A. Andersson Rasmussen, D. Kandasamy, H. Beck, S. D. Crosby, O. Björnberg, K. D. Schnackerz and J. Piškur, *Eukaryotic cell*, 2014, **13**, 31-42.
215. V. A. Ivashov, K. Grillitsch, H. Koefeler, E. Leitner, D. Baeumlisberger, M. Karas and G. Daum, *Biochimica et Biophysica Acta*, 2013, **1831**, 282-290.
216. K. Grillitsch, P. Tarazona, L. Klug, T. Wriessnegger, G. Zellnig, E. Leitner, I. Feussner and G. Daum, *Biochimica et Biophysica Acta*, 2014, **1838**, 1889-1897.
217. E. Rampler, A. Criscuolo, M. Zeller, Y. El Abiead, H. Schoeny, G. Hermann, E. Sokol, K. Cook, D. A. Peake, B. Delanghe and G. Koellensperger, *Analytical Chemistry*, 2018, **90**, 6494-6501.
218. L. Klug, P. Tarazona, C. Gruber, K. Grillitsch, B. Gasser, M. Trotzmuller, H. Kofeler, E. Leitner, I. Feussner, D. Mattanovich, F. Altmann and G. Daum, *Biochimica et Biophysica Acta*, 2014, **1841**, 215-226.
219. P. Ternes, T. Wobbe, M. Schwarz, S. Albrecht, K. Feussner, I. Riezman, J. M. Cregg, E. Heinz, H. Riezman, I. Feussner and D. Warnecke, *Journal of Biological Chemistry*, 2011, **286**, 11401-11414.
220. C. Rebnegger, T. Vos, A. B. Graf, M. Valli, J. T. Pronk, P. Daran-Lapujade and D. Mattanovich, *Applied and Environmental Microbiology*, 2016, **82**, 4570-4583.
221. L. G. M. Boender, E. A. F. de Hulster, A. J. A. van Maris, P. A. S. Daran-Lapujade and J. T. Pronk, *Applied and Environmental Microbiology*, 2009, **75**, 5607-5614.
222. S. J. Pirt, *Proceedings of the Royal Society of London. Series B: Biological Sciences*, 1965, **163**, 224-231.
223. K. Grillitsch, P. Tarazona, L. Klug, T. Wriessnegger, G. Zellnig, E. Leitner, I. Feussner and G. Daum, *Biochimica et Biophysica Acta (BBA) - Biomembranes*, 2014, **1838**, 1889-1897.

224. H. Chen, Z. Gu, H. Zhang, M. Wang, W. Chen, W. T. Lowther and Y. Q. Chen, *PloS One*, 2013, **8**, e58139-e58139.
225. C. C. Stowers and E. M. Boczko, *Yeast*, 2007, **24**, 533-541.
226. P. K. Herman, *Current Opinion in Microbiology*, 2002, **5**, 602-607.
227. T. Cajka and O. Fiehn, *Trends in analytical chemistry : TRAC*, 2014, **61**, 192-206.
228. L. Xu, X. Wang, Y. Jiao and X. Liu, *Talanta*, 2018, **178**, 287-293.
229. L. Mitsui Knowledge Industry Co., *Journal*, 2015.
230. P. R. a. R. Bevington, D.K. , *Data Reduction and Error Analysis for the Physical Sciences.*, WCB/McGraw-Hill, Boston, 2nd Edition edn., 1992.
231. J. Han, R. M. Danell, J. R. Patel, D. R. Gumerov, C. O. Scarlett, J. P. Speir, C. E. Parker, I. Rusyn, S. Zeisel and C. H. Borchers, *Metabolomics : Official journal of the Metabolomic Society*, 2008, **4**, 128-140.
232. N. L. Kuehnbaum and P. Britz-McKibbin, *Chemical Reviews*, 2013, **113**, 2437-2468.
233. M. R. Lewis, J. T. Pearce, K. Spagou, M. Green, A. C. Dona, A. H. Yuen, M. David, D. J. Berry, K. Chappell, V. Horneffer-van der Sluis, R. Shaw, S. Lovestone, P. Elliott, J. Shockcor, J. C. Lindon, O. Cloarec, Z. Takats, E. Holmes and J. K. Nicholson, *Analytical Chemistry*, 2016, **88**, 9004-9013.
234. S. C. Brown, G. Kruppa and J. L. Dasseux, *Mass Spectrometry Reviews*, 2005, **24**, 223-231.
235. W. B. Dunn, N. J. Bailey and H. E. Johnson, *Analyst*, 2005, **130**, 606-625.
236. I. Surowiec, E. Johansson, H. Stenlund, S. Rantapää-Dahlqvist, S. Bergström, J. Normark and J. Trygg, *Journal of Chromatography A*, 2018, **1568**, 229-234.
237. H. N. B. Moseley, *Computational and structural biotechnology journal*, 2013, **4**, e201301006.
238. D. L. Sackett, *Journal of Chronic Diseases*, 1979, **32**, 51-63.
239. J. R. Swann, K. Spagou, M. Lewis, J. K. Nicholson, D. A. Glei, T. E. Seeman, C. L. Coe, N. Goldman, C. D. Ryff, M. Weinstein and E. Holmes, *Journal of Proteome Research*, 2013, **12**, 3166-3180.
240. K. Contrepois, L. Jiang and M. Snyder, *Molecular & cellular proteomics : MCP*, 2015, **14**, 1684-1695.
241. O. Fiehn, *Plant Molecular Biology*, 2002, **48**, 155-171.
242. P. Yin, A. Peter, H. Franken, X. Zhao, S. S. Neukamm, L. Rosenbaum, M. Lucio, A. Zell, H. U. Haring, G. Xu and R. Lehmann, *Clinical Chemistry*, 2013, **59**, 833-845.
243. W. Wang, H. Zhou, H. Lin, S. Roy, T. A. Shaler, L. R. Hill, S. Norton, P. Kumar, M. Anderle and C. H. Becker, *Analytical Chemistry*, 2003, **75**, 4818-4826.
244. R. A. van den Berg, H. C. J. Hoefsloot, J. A. Westerhuis, A. K. Smilde and M. J. van der Werf, *BMC Genomics*, 2006, **7**, 142-142.
245. M. Nezami Ranjbar, Y. Zhao, M. Tadesse, Y. Wang and H. Ressom, *Evaluation of normalization methods for analysis of LC-MS data*, 2012.
246. M. Chen, R. S. P. Rao, Y. Zhang, C. X. Zhong and J. J. Thelen, *SpringerPlus*, 2014, **3**, 439-439.
247. B. D. Bennett, J. Yuan, E. H. Kimball and J. D. Rabinowitz, *Nature Protocols*, 2008, **3**, 1299-1311.
248. *Journal*.

249. M. M. Koek, R. H. Jellema, J. van der Greef, A. C. Tas and T. Hankemeier, *Metabolomics*, 2011, **7**, 307-328.
250. P. Yin, A. Peter, H. Franken, X. Zhao, S. S. Neukamm, L. Rosenbaum, M. Lucio, A. Zell, H.-U. Häring, G. Xu and R. Lehmann, *Clinical Chemistry*, 2013, **59**, 833-845.
251. D. Rodbard, *Clinical Chemistry*, 1974, **20**, 1255-1270.
252. M. Vinaixa, S. Samino, I. Saez, J. Duran, J. J. Guinovart and O. Yanes, *Metabolites*, 2012, **2**, 775-795.
253. H.-Y. Kim, *Restorative dentistry & endodontics*, 2014, **39**, 329-332.
254. J. Chong, O. Soufan, C. Li, I. Caraus, S. Li, G. Bourque, D. S. Wishart and J. Xia, *Nucleic Acids Research*, 2018, **46**, W486-W494.
255. B. Worley and R. Powers, *Current Metabolomics*, 2013, **1**, 92-107.
256. S.-Y. Wang, C.-H. Kuo and Y. J. Tseng, *Analytical Chemistry*, 2013, **85**, 1037-1046.
257. A. Chokkathukalam, D. H. Kim, M. P. Barrett, R. Breitling and D. J. Creek, *Bioanalysis*, 2014, **6**, 511-524.
258. W. Zhou, S. Yang and P. G. Wang, *Bioanalysis*, 2017, **9**, 1839-1844.
259. A. Tan, I. A. Lévesque, I. M. Lévesque, F. Viel, N. Boudreau and A. Lévesque, *Journal of Chromatography B*, 2011, **879**, 1954-1960.
260. H. Redestig, A. Fukushima, H. Stenlund, T. Moritz, M. Arita, K. Saito and M. Kusano, *Analytical Chemistry*, 2009, **81**, 7974-7980.
261. M. Koivusalo, P. Haimi, L. Heikinheimo, R. Kostiainen and P. Somerharju, *Journal of Lipid Research*, 2001, **42**, 663-672.
262. P. R. Bevington, & Robinson, D. K. , *Data reduction and error analysis for the physical sciences (2nd ed.)*, Boston: WCB/McGraw-Hill.
263. Advanced Chromatography Technologies Ltd., http://www.ace-hplc.com/products/product.aspx?id=2814 (accessed 05/03/2019).
264. P. Jonsson, A. Wuolikainen, E. Thysell, E. Chorell, P. Stattin, P. Wikström and H. Antti, *Metabolomics : Official journal of the Metabolomic Society*, 2015, **11**, 1667-1678.
265. D. A. Cairns, D. Thompson, D. N. Perkins, A. J. Stanley, P. J. Selby and R. E. Banks, *Proteomics*, 2008, **8**, 21-27.
266. I. Conlon and M. Raff, *Cell*, 1999, **96**, 235-244.
267. R. J. DeBerardinis, J. J. Lum, G. Hatzivassiliou and C. B. Thompson, *Cell Metabolism*, 2008, **7**, 11-20.
268. D. E. Bauer, M. H. Harris, D. R. Plas, J. J. Lum, P. S. Hammerman, J. C. Rathmell, J. L. Riley and C. B. Thompson, *FASEB Journal*, 2004, **18**, 1303-1305.
269. F. Baenke, B. Peck, H. Miess and A. Schulze, *Disease Models & Mechanisms*, 2013, **6**, 1353-1363.
270. O. Warburg, *Science*, 1956, **123**, 309-314.
271. V. M. Naifeh J, Treasure Island (FL), StatPearls [Updated 2018 Nov 13]. edn., 2018
272. W. L. McKeehan, *Cell Biology International Reports*, 1982, **6**, 635-650.
273. R. W. Moreadith and A. L. Lehninger, *Journal of Biological Chemistry*, 1984, **259**, 6215-6221.

274. D. I. Benjamin, B. F. Cravatt and D. K. Nomura, *Cell Metabolism*, 2012, **16**, 565-577.
275. L. G. Boros, M. R. Lerner, D. L. Morgan, S. L. Taylor, B. J. Smith, R. G. Postier and D. J. Brackett, *Pancreas*, 2005, **31**, 337-343.
276. A. Carracedo, L. C. Cantley and P. P. Pandolfi, *Nature Reviews: Cancer*, 2013, **13**, 227-232.
277. C. V. Dang, *Cell Cycle*, 2010, **9**, 3884-3886.
278. S. Ray, A. Kassan, A. R. Busija, P. Rangamani and H. H. Patel, *American journal of physiology. Cell physiology*, 2016, **310**, C181-C192.
279. P. L. Yang, in *Viral Pathogenesis* eds. M. G. Katze, M. J. Korth, G. L. Law and N. Nathanson, Academic Press, Boston, Third edn., 2016, DOI: https://doi.org/10.1016/B978-0-12-800964-2.00014-8, pp. 181-198.
280. J. A. Schwartzbaum, J. L. Fisher, K. D. Aldape and M. Wrensch, *Nature Clinical Practice: Neurology*, 2006, **2**, 494-503.
281. M. Gogiashvili, S. Horsch, R. Marchan, K. Gianmoena, C. Cadenas, B. Tanner, S. Naumann, D. Ersova, F. Lippek, J. Rahnenführer, J. T. Andersson, R. Hergenröder, J. Lambert, J. G. Hengstler and K. Edlund, *NMR in Biomedicine*, 2018, **31**, e3862.
282. X. Liu and J. W. Locasale, *EBioMedicine*, 2017, **19**, 4-5.
283. J. Liu, H. Dang and X. W. Wang, *Experimental and Molecular Medicine*, 2018, **50**, e416-e416.
284. T. Okegawa, M. Morimoto, S. Nishizawa, S. Kitazawa, K. Honda, H. Araki, T. Tamura, A. Ando, Y. Satomi, K. Nutahara and T. Hara, *EBioMedicine*, 2017, **19**, 31-38.
285. C. T. Hensley, B. Faubert, Q. Yuan, N. Lev-Cohain, E. Jin, J. Kim, L. Jiang, B. Ko, R. Skelton, L. Loudat, M. Wodzak, C. Klimko, E. McMillan, Y. Butt, M. Ni, D. Oliver, J. Torrealba, C. R. Malloy, K. Kernstine, R. E. Lenkinski and R. J. DeBerardinis, *Cell*, 2016, **164**, 681-694.
286. A. Soeda, A. Hara, T. Kunisada, S. Yoshimura, T. Iwama and D. M. Park, *Scientific Reports*, 2015, **5**, 7979.
287. A. Soeda, A. Inagaki, N. Oka, Y. Ikegame, H. Aoki, S. Yoshimura, S. Nakashima, T. Kunisada and T. Iwama, *Journal of Biological Chemistry*, 2008, **283**, 10958-10966.
288. A. P. Patel, I. Tirosh, J. J. Trombetta, A. K. Shalek, S. M. Gillespie, H. Wakimoto, D. P. Cahill, B. V. Nahed, W. T. Curry, R. L. Martuza, D. N. Louis, O. Rozenblatt-Rosen, M. L. Suva, A. Regev and B. E. Bernstein, *Science*, 2014, **344**, 1396-1401.
289. S. Grande, A. Palma, L. Ricci-Vitiani, A. M. Luciani, M. Buccarelli, M. Biffoni, A. Molinari, A. Calcabrini, E. D'Amore, L. Guidoni, R. Pallini, V. Viti and A. Rosi, *Stem Cells Int*, 2018, **2018**, 3292704.
290. A. R. Anderson, A. M. Weaver, P. T. Cummings and V. Quaranta, *Cell*, 2006, **127**, 905-915.
291. C. Swanton, *Cancer Research*, 2012, **72**, 4875-4882.
292. H. Clevers, *Nature Medicine*, 2011, **17**, 313-319.
293. A. Sottoriva, J. J. Verhoeff, T. Borovski, S. K. McWeeney, L. Naumov, J. P. Medema, P. M. Sloot and L. Vermeulen, *Cancer Research*, 2010, **70**, 46-56.
294. J. P. Medema, *Nature Cell Biology*, 2013, **15**, 338-344.

295. M. Shackleton, E. Quintana, E. R. Fearon and S. J. Morrison, *Cell*, 2009, **138**, 822-829.
296. N. D. Marjanovic, R. A. Weinberg and C. L. Chaffer, *Clinical Chemistry*, 2013, **59**, 168-179.
297. J. J. Keats, M. Chesi, J. B. Egan, V. M. Garbitt, S. E. Palmer, E. Braggio, S. Van Wier, P. R. Blackburn, A. S. Baker, A. Dispenzieri, S. Kumar, S. V. Rajkumar, J. D. Carpten, M. Barrett, R. Fonseca, A. K. Stewart and P. L. Bergsagel, *Blood*, 2012, **120**, 1067-1076.
298. P. J. Campbell, S. Yachida, L. J. Mudie, P. J. Stephens, E. D. Pleasance, L. A. Stebbings, L. A. Morsberger, C. Latimer, S. McLaren, M. L. Lin, D. J. McBride, I. Varela, S. A. Nik-Zainal, C. Leroy, M. Jia, A. Menzies, A. P. Butler, J. W. Teague, C. A. Griffin, J. Burton, H. Swerdlow, M. A. Quail, M. R. Stratton, C. Iacobuzio-Donahue and P. A. Futreal, *Nature*, 2010, **467**, 1109-1113.
299. C. Swanton, J. M. Larkin, M. Gerlinger, A. C. Eklund, M. Howell, G. Stamp, J. Downward, M. Gore, P. A. Futreal, B. Escudier, F. Andre, L. Albiges, B. Beuselinck, S. Oudard, J. Hoffmann, B. Gyorffy, C. J. Torrance, K. A. Boehme, H. Volkmer, L. Toschi, B. Nicke, M. Beck and Z. Szallasi, *Genome Medicine*, 2010, **2**, 53.
300. M. Deininger, E. Buchdunger and B. J. Druker, *Blood*, 2005, **105**, 2640-2653.
301. W. K. Hofmann, M. Komor, B. Wassmann, L. C. Jones, H. Gschaidmeier, D. Hoelzer, H. P. Koeffler and O. G. Ottmann, *Blood*, 2003, **102**, 659-661.
302. N. P. Shah, J. M. Nicoll, B. Nagar, M. E. Gorre, R. L. Paquette, J. Kuriyan and C. L. Sawyers, *Cancer Cell*, 2002, **2**, 117-125.
303. C. Roche-Lestienne, V. Soenen-Cornu, N. Grardel-Duflos, J. L. Lai, N. Philippe, T. Facon, P. Fenaux and C. Preudhomme, *Blood*, 2002, **100**, 1014-1018.
304. C. M. Choi, K. W. Seo, S. J. Jang, Y. M. Oh, T. S. Shim, W. S. Kim, D. S. Lee and S. D. Lee, *Lung Cancer*, 2009, **64**, 66-70.
305. S. L. Carter, A. C. Eklund, I. S. Kohane, L. N. Harris and Z. Szallasi, *Nature Genetics*, 2006, **38**, 1043-1048.
306. A. Walther, R. Houlston and I. Tomlinson, *Gut*, 2008, **57**, 941-950.
307. N. McGranahan, R. A. Burrell, D. Endesfelder, M. R. Novelli and C. Swanton, *EMBO reports*, 2012, **13**, 528-538.
308. G. Poste, *Nature*, 2011, **469**, 156-157.
309. R. D. Beger, *Metabolites*, 2013, **3**, 552-574.
310. E. C. Holland, *Proceedings of the National Academy of Sciences of the United States of America*, 2000, **97**, 6242-6244.
311. E. A. Maher, F. B. Furnari, R. M. Bachoo, D. H. Rowitch, D. N. Louis, W. K. Cavenee and R. A. DePinho, *Genes and Development*, 2001, **15**, 1311-1333.
312. S. Agnihotri, K. E. Burrell, A. Wolf, S. Jalali, C. Hawkins, J. T. Rutka and G. Zadeh, *Archivum Immunologiae et Therapiae Experimentalis*, 2013, **61**, 25-41.
313. P. Wesseling and D. Capper, *Neuropathology and Applied Neurobiology*, 2018, **44**, 139-150.
314. F. Hanif, K. Muzaffar, K. Perveen, S. M. Malhi and S. U. Simjee, *Asian Pacific journal of cancer prevention : APJCP*, **18**, 3-9.
315. C. Kruchko, Q. T. Ostrom, A. Boscia, G. Truitt, H. Gittleman and J. S. Barnholtz-Sloan, *Neuro-Oncology*, 2018, **20**, 1-86.

316. R. Stupp, M. Brada, M. J. van den Bent, J.-C. Tonn and G. Pentheroudakis, *Annals of Oncology*, 2014, **25**, 93-101.
317. M. Diksin, S. J. Smith and R. Rahman, *International Journal of Molecular Sciences*, 2017, **18**, 2342.
318. N. Cancer Genome Atlas Research, D. J. Brat, R. G. W. Verhaak, K. D. Aldape, W. K. A. Yung, S. R. Salama, L. A. D. Cooper, E. Rheinbay, C. R. Miller, M. Vitucci, O. Morozova, A. G. Robertson, H. Noushmehr, P. W. Laird, A. D. Cherniack, R. Akbani, J. T. Huse, G. Ciriello, L. M. Poisson, J. S. Barnholtz-Sloan, M. S. Berger, C. Brennan, R. R. Colen, H. Colman, A. E. Flanders, C. Giannini, M. Grifford, A. Iavarone, R. Jain, I. Joseph, J. Kim, K. Kasaian, T. Mikkelsen, B. A. Murray, B. P. O'Neill, L. Pachter, D. W. Parsons, C. Sougnez, E. P. Sulman, S. R. Vandenberg, E. G. Van Meir, A. von Deimling, H. Zhang, D. Crain, K. Lau, D. Mallery, S. Morris, J. Paulauskis, R. Penny, T. Shelton, M. Sherman, P. Yena, A. Black, J. Bowen, K. Dicostanzo, J. Gastier-Foster, K. M. Leraas, T. M. Lichtenberg, C. R. Pierson, N. C. Ramirez, C. Taylor, S. Weaver, L. Wise, E. Zmuda, T. Davidsen, J. A. Demchok, G. Eley, M. L. Ferguson, C. M. Hutter, K. R. Mills Shaw, B. A. Ozenberger, M. Sheth, H. J. Sofia, R. Tarnuzzer, Z. Wang, L. Yang, J. C. Zenklusen, B. Ayala, J. Baboud, S. Chudamani, M. A. Jensen, J. Liu, T. Pihl, R. Raman, Y. Wan, Y. Wu, A. Ally, J. T. Auman, M. Balasundaram, S. Balu, S. B. Baylin, R. Beroukhim, M. S. Bootwalla, R. Bowlby, C. A. Bristow, D. Brooks, Y. Butterfield, R. Carlsen, S. Carter, L. Chin, A. Chu, E. Chuah, K. Cibulskis, A. Clarke, S. G. Coetzee, N. Dhalla, T. Fennell, S. Fisher, S. Gabriel, G. Getz, R. Gibbs, R. Guin, A. Hadjipanayis, D. N. Hayes, T. Hinoue, K. Hoadley, R. A. Holt, A. P. Hoyle, S. R. Jefferys, S. Jones, C. D. Jones, R. Kucherlapati, P. H. Lai, E. Lander, S. Lee, L. Lichtenstein, Y. Ma, D. T. Maglinte, H. S. Mahadeshwar, M. A. Marra, M. Mayo, S. Meng, M. L. Meyerson, P. A. Mieczkowski, R. A. Moore, L. E. Mose, A. J. Mungall, A. Pantazi, M. Parfenov, P. J. Park, J. S. Parker, C. M. Perou, A. Protopopov, X. Ren, J. Roach, T. S. Sabedot, J. Schein, S. E. Schumacher, J. G. Seidman, S. Seth, H. Shen, J. V. Simons, P. Sipahimalani, M. G. Soloway, X. Song, H. Sun, B. Tabak, A. Tam, D. Tan, J. Tang, N. Thiessen, T. Triche, Jr., D. J. Van Den Berg, U. Veluvolu, S. Waring, D. J. Weisenberger, M. D. Wilkerson, T. Wong, J. Wu, L. Xi, A. W. Xu, L. Yang, T. I. Zack, J. Zhang, B. A. Aksoy, H. Arachchi, C. Benz, B. Bernard, D. Carlin, J. Cho, D. DiCara, S. Frazer, G. N. Fuller, J. Gao, N. Gehlenborg, D. Haussler, D. I. Heiman, L. Iype, A. Jacobsen, Z. Ju, S. Katzman, H. Kim, T. Knijnenburg, R. B. Kreisberg, M. S. Lawrence, W. Lee, K. Leinonen, P. Lin, S. Ling, W. Liu, Y. Liu, Y. Liu, Y. Lu, G. Mills, S. Ng, M. S. Noble, E. Paull, A. Rao, S. Reynolds, G. Saksena, Z. Sanborn, C. Sander, N. Schultz, Y. Senbabaoglu, R. Shen, I. Shmulevich, R. Sinha, J. Stuart, S. O. Sumer, Y. Sun, N. Tasman, B. S. Taylor, D. Voet, N. Weinhold, J. N. Weinstein, D. Yang, K. Yoshihara, S. Zheng, W. Zhang, L. Zou, T. Abel, S. Sadeghi, M. L. Cohen, J. Eschbacher, E. M. Hattab, A. Raghunathan, M. J. Schniederjan, D. Aziz, G. Barnett, W. Barrett, D. D. Bigner, L. Boice, C. Brewer, C. Calatozzolo, B. Campos, C. G. Carlotti, Jr., T. A. Chan, L. Cuppini, E. Curley, S. Cuzzubbo, K. Devine, F. DiMeco, R. Duell, J. B. Elder, A. Fehrenbach, G. Finocchiaro, W. Friedman, J. Fulop, J. Gardner, B. Hermes, C. Herold-Mende, C. Jungk, A. Kendler, N. L. Lehman, E. Lipp, O. Liu, R. Mandt, M. McGraw, R. McLendon,

C. McPherson, L. Neder, P. Nguyen, A. Noss, R. Nunziata, Q. T. Ostrom, C. Palmer, A. Perin, B. Pollo, A. Potapov, O. Potapova, W. K. Rathmell, D. Rotin, L. Scarpace, C. Schilero, K. Senecal, K. Shimmel, V. Shurkhay, S. Sifri, R. Singh, A. E. Sloan, K. Smolenski, S. M. Staugaitis, R. Steele, L. Thorne, D. P. C. Tirapelli, A. Unterberg, M. Vallurupalli, Y. Wang, R. Warnick, F. Williams, Y. Wolinsky, S. Bell, M. Rosenberg, C. Stewart, F. Huang, J. L. Grimsby, A. J. Radenbaugh and J. Zhang, *The New England journal of medicine*, 2015, **372**, 2481-2498.

319. W. Stummer, U. Pichlmeier, T. Meinel, O. D. Wiestler, F. Zanella and H. J. Reulen, *Lancet Oncology*, 2006, **7**, 392-401.
320. N. Sanai, S. Chang and M. S. Berger, *Journal of Neurosurgery*, 2011, **115**, 948-965.
321. J. S. Smith, E. F. Chang, K. R. Lamborn, S. M. Chang, M. D. Prados, S. Cha, T. Tihan, S. Vandenberg, M. W. McDermott and M. S. Berger, *Journal of Clinical Oncology*, 2008, **26**, 1338-1345.
322. A. Lourdusamy, J. Wood, M. Castellanos, R. Grundy, R. Rahman, S. May and S. Smith, *Neuro-Oncology*, 2018, **20**, i16-i17.
323. F. Zaccardi, D. R. Webb, T. Yates and M. J. Davies, *Postgraduate Medical Journal*, 2016, **92**, 63-69.
324. C. C. Thomas and L. H. Philipson, *Medical Clinics of North America*, 2015, **99**, 1-16.
325. N. H. Cho, J. E. Shaw, S. Karuranga, Y. Huang, J. D. da Rocha Fernandes, A. W. Ohlrogge and B. Malanda, *Diabetes Research and Clinical Practice*, 2018, **138**, 271-281.
326. The International Diabetes Federation (IDF), https://www.idf.org/aboutdiabetes/what-is-diabetes/facts-figures.html, accessed on 27/2/2019).
327. The British Diabetic Association operating as Diabetes UK, https://www.diabetes.org.uk/professionals/position-statements-reports/statistics/diabetes-prevalence-2018, (accessed Accessed on 27/2/2019).
328. H. W. Baynest, *Journal of Diabetes & Metabolism*, 2015, **6**, 541.
329. C. T. Carolina Solis-Herrera, Charles Reasner, Ralph A DeFronzo, and Eugenio Cersosimo., ed. A. B. Feingold KR, Boyce A, South Dartmouth
330. M. Stumvoll, B. J. Goldstein and T. W. van Haeften, *Lancet*, 2005, **365**, 1333-1346.
331. H. B. Brewer, Jr., *American Journal of Cardiology*, 1989, **64**, 3g-9g.
332. R. D. Utiger, *Journal*.
333. J. C. Bruning, M. D. Michael, J. N. Winnay, T. Hayashi, D. Horsch, D. Accili, L. J. Goodyear and C. R. Kahn, *Molecular Cell*, 1998, **2**, 559-569.
334. M. D. Michael, R. N. Kulkarni, C. Postic, S. F. Previs, G. I. Shulman, M. A. Magnuson and C. R. Kahn, *Molecular Cell*, 2000, **6**, 87-97.
335. M. Bluher, B. B. Kahn and C. R. Kahn, *Science*, 2003, **299**, 572-574.
336. R. A. DeFronzo, R. Gunnarsson, O. Björkman, M. Olsson and J. Wahren, *The Journal of clinical investigation*, 1985, **76**, 149-155.
337. G. Paolisso, P. A. Tataranni, J. E. Foley, C. Bogardus, B. V. Howard and E. Ravussin, *Diabetologia*, 1995, **38**, 1213-1217.

338. G. Boden, *Diabetes*, 1997, **46**, 3-10.
339. Y. Sako and V. E. Grill, *Endocrinology*, 1990, **127**, 1580-1589.
340. M. L. Elks, *Endocrinology*, 1993, **133**, 208-214.
341. Y. P. Zhou and V. Grill, *Journal of Clinical Endocrinology and Metabolism*, 1995, **80**, 1584-1590.
342. M. Shimabukuro, Y.-T. Zhou, M. Levi and R. H. Unger, *Proceedings of the National Academy of Sciences*, 1998, **95**, 2498-2502.
343. R. Lupi, F. Dotta, L. Marselli, S. Del Guerra, M. Masini, C. Santangelo, G. Patané, U. Boggi, S. Piro, M. Anello, E. Bergamini, F. Mosca, U. Di Mario, S. Del Prato and P. Marchetti, *Evidence that β-Cell Death Is Caspase Mediated, Partially Dependent on Ceramide Pathway, and Bcl-2 Regulated*, 2002, **51**, 1437-1442.
344. M. Cnop, J. C. Hannaert, A. Hoorens, D. L. Eizirik and D. G. Pipeleers, *Diabetes*, 2001, **50**, 1771-1777.
345. A. Dresner, D. Laurent, M. Marcucci, M. E. Griffin, S. Dufour, G. W. Cline, L. A. Slezak, D. K. Andersen, R. S. Hundal, D. L. Rothman, K. F. Petersen and G. I. Shulman, *Journal of Clinical Investigation*, 1999, **103**, 253-259.
346. J. K. Kim, O. Gavrilova, Y. Chen, M. L. Reitman and G. I. Shulman, *Journal of Biological Chemistry*, 2000, **275**, 8456-8460.
347. T. R. Koves, J. R. Ussher, R. C. Noland, D. Slentz, M. Mosedale, O. Ilkayeva, J. Bain, R. Stevens, J. R. Dyck, C. B. Newgard, G. D. Lopaschuk and D. M. Muoio, *Cell Metabolism*, 2008, **7**, 45-56.
348. D. M. Muoio and P. D. Neufer, *Cell Metabolism*, 2012, **15**, 595-605.
349. B. C. Martin, J. H. Warram, A. S. Krolewski, R. N. Bergman, J. S. Soeldner and C. R. Kahn, *Lancet*, 1992, **340**, 925-929.
350. D. G. Carey, A. B. Jenkins, L. V. Campbell, J. Freund and D. J. Chisholm, *Diabetes*, 1996, **45**, 633-638.
351. Y. Miyazaki, A. Mahankali, M. Matsuda, S. Mahankali, J. Hardies, K. Cusi, L. J. Mandarino and R. A. DeFronzo, *Journal of Clinical Endocrinology and Metabolism*, 2002, **87**, 2784-2791.
352. M. C. Alessi, F. Peiretti, P. Morange, M. Henry, G. Nalbone and I. Juhan-Vague, *Diabetes*, 1997, **46**, 860-867.
353. R. A. DeFronzo and E. Ferrannini, *Diabetes Care*, 1991, **14**, 173-194.
354. G. Bonner, *Journal of Cardiovascular Pharmacology*, 1994, **24 Suppl 2**, S39-49.
355. G. Steiner, S. Morita and M. Vranic, *Diabetes*, 1980, **29**, 899-905.
356. E. Moro, P. Gallina, M. Pais, G. Cazzolato, P. Alessandrini and G. Bittolo-Bon, *Metabolism: Clinical and Experimental*, 2003, **52**, 616-619.
357. A. Taniguchi, M. Fukushima, M. Sakai, K. Kataoka, K. Miwa, I. Nagata, K. Doi, K. Tokuyama and Y. Nakai, *Diabetes Care*, 1999, **22**, 2100-2101.
358. A. Taniguchi, M. Fukushima, M. Sakai, K. Kataoka, I. Nagata, K. Doi, H. Arakawa, S. Nagasaka, K. Tokuyama and Y. Nakai, *Metabolism: Clinical and Experimental*, 2000, **49**, 1001-1005.
359. A. Taniguchi, M. Fukushima, M. Sakai, K. Miwa, T. Makita, I. Nagata, S. Nagasaka, K. Doi, T. Okumura, A. Fukuda, H. Kishimoto, T. Fukuda, S. Nakaishi, K. Tokuyama and Y. Nakai, *Diabetes Care*, 2000, **23**, 1766-1769.

360. I. Zavaroni, E. Dall'Aglio, O. Alpi, F. Bruschi, E. Bonora, A. Pezzarossa and U. Butturini, *Atherosclerosis*, 1985, **55**, 259-266.
361. A. Laws, M. L. Stefanick and G. M. Reaven, *Journal of Clinical Endocrinology and Metabolism*, 1989, **69**, 343-347.
362. E. S. Tai, S. C. Emmanuel, S. K. Chew, B. Y. Tan and C. E. Tan, *Diabetes*, 1999, **48**, 1088-1092.
363. S. Fujii, D. Goto, T. Zaman, N. Ishimori, K. Watano, T. Kaneko, H. Okada, M. Makiguchi, T. Nakagawa and A. Kitabatake, *J Atheroscler Thromb*, 1998, **5**, 76-81.
364. I. Martín-Timón, C. Sevillano-Collantes, A. Segura-Galindo and F. J. Del Cañizo-Gómez, *World Journal of Diabetes*, 2014, **5**, 444-470.
365. Y. Zheng, S. H. Ley and F. B. Hu, *Nature Reviews Endocrinology*, 2017, **14**, 88.
366. *Diabetes Care*, 2018, **41**, S13-s27.
367. *Diabetes Care*, 2009, **32**, 1327-1334.
368. P. J. Meikle, G. Wong, C. K. Barlow, J. M. Weir, M. A. Greeve, G. L. MacIntosh, L. Almasy, A. G. Comuzzie, M. C. Mahaney, A. Kowalczyk, I. Haviv, N. Grantham, D. J. Magliano, J. B. M. Jowett, P. Zimmet, J. E. Curran, J. Blangero and J. Shaw, *PloS One*, 2013, **8**, e74341-e74341.
369. E. P. Brass, *Clinical Therapeutics*, 1995, **17**, 176-185; discussion 175.
370. F. B. Stephens, D. Constantin-Teodosiu and P. L. Greenhaff, *The Journal of physiology*, 2007, **581**, 431-444.
371. M. S. Murthy and S. V. Pande, *Proceedings of the National Academy of Sciences of the United States of America*, 1987, **84**, 378-382.
372. M. S. Murthy and S. V. Pande, *Proceedings of the National Academy of Sciences of the United States of America*, 1987, **84**, 378-382.
373. S. V. Pande, *Proceedings of the National Academy of Sciences of the United States of America*, 1975, **72**, 883-887.
374. V. Bezaire, C. R. Bruce, G. J. Heigenhauser, N. N. Tandon, J. F. Glatz, J. J. Luiken, A. Bonen and L. L. Spriet, *American Journal of Physiology: Endocrinology and Metabolism*, 2006, **290**, E509-515.
375. K. F. Woeltje, M. Kuwajima, D. W. Foster and J. D. McGarry, *Journal of Biological Chemistry*, 1987, **262**, 9822-9827.
376. A. Kumari, in *Sweet Biochemistry*, ed. A. Kumari, Academic Press, 2018, DOI: https://doi.org/10.1016/B978-0-12-814453-4.00002-9, pp. 7-11.
377. D. Constantin-Teodosiu, J. I. Carlin, G. Cederblad, R. C. Harris and E. Hultman, *Acta Physiologica Scandinavica*, 1991, **143**, 367-372.
378. S. J. Mihalik, B. H. Goodpaster, D. E. Kelley, D. H. Chace, J. Vockley, F. G. Toledo and J. P. DeLany, *Obesity (Silver Spring)*, 2010, **18**, 1695-1700.
379. B. Capaldo, R. Napoli, P. Di Bonito, G. Albano and L. Sacca, *Diabetes Research and Clinical Practice*, 1991, **14**, 191-195.
380. G. Mingrone, A. V. Greco, E. Capristo, G. Benedetti, A. Giancaterini, A. De Gaetano and G. Gasbarrini, *Journal of the American College of Nutrition*, 1999, **18**, 77-82.
381. F. B. Stephens, D. Constantin-Teodosiu, D. Laithwaite, E. J. Simpson and P. L. Greenhaff, *Journal of Clinical Endocrinology and Metabolism*, 2006, **91**, 5013-5018.

382. B. Rodrigues, D. Seccombe and J. H. McNeill, *Canadian Journal of Physiology and Pharmacology*, 1990, **68**, 1601-1608.
383. A. R. Rahbar, R. Shakerhosseini, N. Saadat, F. Taleban, A. Pordal and B. Gollestan, *European Journal of Clinical Nutrition*, 2005, **59**, 592.
384. L. Hue and H. Taegtmeyer, *American journal of physiology. Endocrinology and metabolism*, 2009, **297**, E578-E591.
385. G. Derosa, A. F. Cicero, A. Gaddi, A. Mugellini, L. Ciccarelli and R. Fogari, *Clinical Therapeutics*, 2003, **25**, 1429-1439.
386. F. B. Stephens, D. Constantin-Teodosiu, D. Laithwaite, E. J. Simpson and P. L. Greenhaff, *FASEB Journal*, 2006, **20**, 377-379.
387. F. B. Stephens, C. E. Evans, D. Constantin-Teodosiu and P. L. Greenhaff, *J Appl Physiol (1985)*, 2007, **102**, 1065-1070.
388. Y. Benjamini and Y. Hochberg, *Journal of the Royal Statistical Society. Series B (Methodological)*, 1995, **57**, 289-300.
389. H. Zhong, C. Fang, Y. Fan, Y. Lu, B. Wen, H. Ren, G. Hou, F. Yang, H. Xie, Z. Jie, Y. Peng, Z. Ye, J. Wu, J. Zi, G. Zhao, J. Chen, X. Bao, Y. Hu, Y. Gao, J. Zhang, H. Yang, J. Wang, L. Madsen, K. Kristiansen, C. Ni, J. Li and S. Liu, *GigaScience*, 2017, **6**, 1-12.
390. M. N. Barber, S. Risis, C. Yang, P. J. Meikle, M. Staples, M. A. Febbraio and C. R. Bruce, *PloS One*, 2012, **7**, e41456.
391. C. Zhu, Q. L. Liang, P. Hu, Y. M. Wang and G. A. Luo, *Talanta*, 2011, **85**, 1711-1720.
392. D. Yu, S. C. Moore, C. E. Matthews, Y.-B. Xiang, X. Zhang, Y.-T. Gao, W. Zheng and X.-O. Shu, *Metabolomics : Official journal of the Metabolomic Society*, 2016, **12**, 3.
393. G. Wong, C. K. Barlow, J. M. Weir, J. B. Jowett, D. J. Magliano, P. Zimmet, J. Shaw and P. J. Meikle, *PloS One*, 2013, **8**, e76577.
394. K. J. J. van Hateren, G. W. D. Landman, N. Kleefstra, S. J. J. Logtenberg, K. H. Groenier, A. M. Kamper, S. T. Houweling and H. J. G. Bilo, *PloS One*, 2009, **4**, e8464-e8464.
395. W. Gunathilake, S. Song, S. Sridharan, D. J. Fernando and I. Idris, *QJM*, 2010, **103**, 881-884.
396. B.-J. Lee, J.-S. Lin, Y.-C. Lin and P.-T. Lin, *Lipids in Health and Disease*, 2016, **15**, 107-107.
397. A. Orzali, F. Donzelli, G. Enzi and F. F. Rubaltelli, *Biology of the Neonate*, 1983, **43**, 186-190.
398. D. Penn and E. Schmidt-Sommerfeld, *Metabolism: Clinical and Experimental*, 1983, **32**, 806-809.
399. L. Cammalleri, M. Vacante, M. Malaguarnera, M. Motta, T. Avitabile and M. Malaguarnera, *The American Journal of Clinical Nutrition*, 2008, **89**, 71-76.
400. A. R. Rahbar, R. Shakerhosseini, N. Saadat, F. Taleban, A. Pordal and B. Gollestan, *European Journal of Clinical Nutrition*, 2005, **59**, 592-596.
401. B. Rodrigues, D. Seccombe and J. H. McNeill, *Canadian Journal of Physiology and Pharmacology*, 1990, **68**, 1601-1608.
402. B. Zhou, J. F. Xiao, L. Tuli and H. W. Ressom, *Molecular Biosystems*, 2012, **8**, 470-481.

403. M. R. Lewis, J. T. M. Pearce, K. Spagou, M. Green, A. C. Dona, A. H. Y. Yuen, M. David, D. J. Berry, K. Chappell, V. Horneffer-van der Sluis, R. Shaw, S. Lovestone, P. Elliott, J. Shockcor, J. C. Lindon, O. Cloarec, Z. Takats, E. Holmes and J. K. Nicholson, *Analytical Chemistry*, 2016, **88**, 9004-9013.
404. M. Suarez-Diez, J. Adam, J. Adamski, S. A. Chasapi, C. Luchinat, A. Peters, C. Prehn, C. Santucci, A. Spyridonidis, G. A. Spyroulias, L. Tenori, R. Wang-Sattler and E. Saccenti, *Journal of Proteome Research*, 2017, **16**, 2547-2559.

Appendix

Table A.1:Lipid ions identified in *P. pastoris* and their ^{13}C-enrichment based on their labelling pattern and the labelling percentage of the fully labelled isotopologues.

Number	Lipid ion ID	Class	Number of carbon atom in the ion	Polarity	Labelling percentage of fully labelled ions	Expected ^{13}C-labelling degree based on the fully labelling percentage obtained
1	Cer(d17:0/16:0)+H	Cer	33	+	0.00	0.00
2	Cer(d17:0/18:0)+H	Cer	35	+	0.00	0.00
3	Cer(d18:0/18:0)+H	Cer	36	+	68.99	98.97
4	Cer(d18:0/18:0)-H	Cer	36	-	74.95	99.20
5	Cer(d18:1/16:0)+H	Cer	34	+	72.16	99.04
6	Cer(d18:1/18:0)+H	Cer	36	+	67.49	98.91
7	Cer(d18:1/28:5)+H	Cer	46	+	59.71	98.89
8	Cer(d18:2/16:0)+H	Cer	34	+	68.10	98.88
9	Cer(d18:2/16:0+O)+H	Cer	34	+	73.76	99.11
10	Cer(d18:2/16:0+O)-H	Cer	34	-	56.83	98.35
11	Cer(d18:2/18:0)+H	Cer	36	+	66.00	98.85
12	Cer(d18:2/18:0+O)+H	Cer	36	+	61.05	98.64
13	Cer(d18:2/18:0+O)-H	Cer	36	-	60.28	98.60
14	Cer(d24:0/18:0+O)+H	Cer	42	+	53.92	98.54
15	Cer(d24:1)-H	Cer	24	-	0.00	0.00
16	CerG1(d18:2/16:0+O)+H	CerG1	40	+	63.71	98.88
17	CerG1(d18:2/18:0+O)+H	CerG1	42	+	59.28	98.76
18	CerG1(d18:2/18:1)+H	CerG1	42	+	63.43	98.92
19	DG(15:0/18:2)+NH_4	DG	36	+	68.15	98.94
20	DG(16:0/14:0)+NH_4	DG	33	+	0.19	82.71
21	DG(16:0/16:0)+H	DG	35	+	0.00	0.00
22	DG(16:0/16:0)+NH_4	DG	35	+	0.05	80.26
23	DG(16:0/17:0)+NH_4	DG	36	+	0.00	0.00
24	DG(16:0/18:1)+NH_4	DG	37	+	66.08	98.89
25	DG(16:1/16:1)+NH_4	DG	35	+	69.35	98.96
26	DG(16:1/18:1)+NH_4	DG	37	+	65.74	98.87
27	DG(16:1/18:2)+NH_4	DG	37	+	66.28	98.89
28	DG(16:1/18:3)+NH_4	DG	37	+	66.51	98.90
29	DG(17:0/18:1)+NH_4	DG	38	+	65.99	98.91
30	DG(17:1/18:1)+NH_4	DG	38	+	65.86	98.91
31	DG(17:1/18:2)+NH_4	DG	38	+	64.67	98.86
32	DG(17:1/18:3)+NH_4	DG	38	+	60.47	98.69
33	DG(18:0/16:0)+H	DG	37	+	0.00	0.00
34	DG(18:0/16:0)+NH_4	DG	37	+	0.03	80.16
35	DG(18:0/16:0)+NH_4	DG	37	+	0.00	0.00
36	DG(18:0/17:0)+NH_4	DG	38	+	0.31	85.87
37	DG(18:0/18:0)+H	DG	39	+	0.00	0.00
38	DG(18:0/18:1)+NH_4	DG	39	+	61.15	98.75
39	DG(18:0/20:0)+NH_4	DG	41	+	0.12	84.84

40	DG(18:1/14:0)+NH_4	DG	35	+	69.65	98.97
41	DG(18:1/18:1)+H	DG	39	+	62.23	98.79
42	DG(18:1/18:1)+NH_4	DG	39	+	65.19	98.91
43	DG(18:1/18:2)+NH_4	DG	39	+	64.55	98.88
44	DG(18:1/19:4)+H	DG	40	+	0.00	0.00
45	DG(18:1/24:0)+NH_4	DG	45	+	56.02	98.72
46	DG(18:2/17:3)+NH_4	DG	38	+	65.96	98.91
47	DG(18:2/18:2)+NH_4	DG	39	+	63.39	98.84
48	DG(18:3/18:2)+H	DG	39	+	0.22	85.51
49	DG(18:3/18:2)+NH_4	DG	39	+	63.43	98.84
50	DG(18:3/18:3)+H	DG	39	+	0.00	0.00
51	DG(18:3/18:3)+NH_4	DG	39	+	61.35	98.76
52	DG(20:1/18:2)+NH_4	DG	41	+	42.30	97.92
53	DG(20:1/18:3)+NH_4	DG	41	+	58.38	98.70
54	DG(37:4)+H	DG	40	+	0.00	0.00
55	dMePE(16:0/18:1)-H	dMePE	41	-	67.25	99.04
56	dMePE(16:0/18:2)-H	dMePE	41	-	66.30	99.00
57	dMePE(16:2/18:2)-H	dMePE	41	-	61.74	98.83
58	dMePE(18:1/18:1)-H	dMePE	43	-	57.62	98.73
59	dMePE(18:1/18:2)-H	dMePE	43	-	59.13	98.79
60	dMePE(18:1/18:3)-H	dMePE	43	-	42.32	98.02
61	dMePE(18:3/18:2)-H	dMePE	43	-	62.63	98.92
62	dMePE(33:2)-H	dMePE	40	-	62.38	98.83
63	dMePE(35:2)-H	dMePE	42	-	27.78	97.00
64	FA(18:2)-H	FA	18	-	81.27	98.85
65	LPC(16:0)+CH_3COO	LPC	24	-	70.67	98.56
66	LPC(16:0)+H	LPC	24	+	75.42	98.83
67	LPC(16:1)+H	LPC	24	+	73.20	98.71
68	LPC(17:1)+H	LPC	25	+	70.65	98.62
69	LPC(18:0)+H	LPC	26	+	75.68	98.93
70	LPC(18:1)+H	LPC	26	+	71.68	98.73
71	LPC(18:2)+H	LPC	26	+	74.85	98.89
72	LPC(18:3)+H	LPC	26	+	71.73	98.73
73	LPC(20:5)+H	LPC	28	+	0.00	0.00
74	LPC(37:6)+H	LPC	45	+	0.00	0.00
75	LPE(16:0)-H	LPE	21	-	77.04	98.77
76	LPE(18:1)-H	LPE	23	-	74.95	98.75
77	LPE(18:2)+H	LPE	23	+	0.00	0.00
78	LPE(18:2)-H	LPE	23	-	73.84	98.69
79	LPE(18:3)+H	LPE	23	+	81.58	99.12
80	LPE(18:3)-H	LPE	23	-	75.42	98.78
81	MG(14:0)+H	MG	17	+	0.00	0.00
82	MG(14:0)+NH_4	MG	17	+	0.00	0.00
83	MG(16:0)+H	MG	19	+	0.00	0.00
84	MG(16:0)+NH_4	MG	19	+	0.00	0.00
85	MG(16:0)+NH_4	MG	19	+	0.00	0.00
86	MG(18:0)+H	MG	21	+	0.00	0.00
87	MG(18:0)+H	MG	21	+	0.00	0.00
88	MG(18:0)+NH_4	MG	21	+	0.00	0.00
89	MG(18:0)+NH_4	MG	21	+	0.00	0.00
90	MG(18:0)+NH_4	MG	21	+	0.00	0.00
91	OAHFA(32:1)-H	OAHFA	32	-	65.32	98.68
92	OAHFA(36:1)-H	OAHFA	36	-	62.48	98.70
93	OAHFA(36:3)-H	OAHFA	36	-	66.16	98.86
94	OAHFA(38:6)-H	OAHFA	38	-	0.00	0.00

95	PA(16:0/18:1)-H	PA	37	-	61.20	98.68
96	PA(16:0/18:2)-H	PA	37	-	71.50	99.10
97	PA(16:0/18:2)-H	PA	37	-	66.79	98.91
98	PA(18:1/18:1)-H	PA	39	-	68.40	99.03
99	PA(18:1/18:2)-H	PA	39	-	68.01	99.02
100	PA(18:3/18:2)-H	PA	39	-	68.09	99.02
101	PC(15:2/18:2)+H	PC	41	+	64.95	98.95
102	PC(16:0/18:1)+H	PC	42	+	59.86	98.79
103	PC(18:1/19:2)+H	PC	45	+	58.22	98.80
104	PC(30:1)+H	PC	38	+	64.31	98.84
105	PC(32:0)+H	PC	40	+	68.47	99.06
106	PC(32:1)+H	PC	40	+	64.98	98.93
107	PC(32:2)+H	PC	40	+	62.62	98.84
108	PC(32:3)+H	PC	40	+	60.84	98.77
109	PC(32:4)+H	PC	40	+	62.52	98.83
110	PC(33:1)+H	PC	41	+	65.17	98.96
111	PC(33:3)+H	PC	41	+	59.94	98.76
112	PC(33:4)+H	PC	41	+	58.93	98.72
113	PC(33:5)+H	PC	41	+	65.64	98.98
114	PC(34:2)+H	PC	42	+	59.62	98.78
115	PC(34:3)+H	PC	42	+	59.50	98.77
116	PC(34:4)+H	PC	42	+	58.66	98.74
117	PC(34:5)+H	PC	42	+	59.42	98.77
118	PC(34:6)+H	PC	42	+	60.85	98.82
119	PC(35:1)+H	PC	43	+	63.66	98.96
120	PC(35:3)+H	PC	43	+	0.00	0.00
121	PC(35:4)+H	PC	43	+	57.08	98.70
122	PC(35:5)+H	PC	43	+	57.43	98.72
123	PC(35:6)+H	PC	43	+	56.04	98.66
124	PC(36:1)+H	PC	44	+	56.15	98.70
125	PC(36:2)+H	PC	44	+	57.38	98.75
126	PC(36:3)+H	PC	44	+	58.42	98.79
127	PC(36:3)+H	PC	44	+	62.65	98.94
128	PC(36:4)+H	PC	44	+	57.91	98.77
129	PC(36:5)+H	PC	44	+	56.81	98.72
130	PC(36:6)+H	PC	44	+	56.12	98.70
131	PC(36:7)+H	PC	44	+	0.00	0.00
132	PC(37:2)+H	PC	45	+	44.07	98.20
133	PC(37:4)+H	PC	45	+	54.74	98.67
134	PC(38:2)+H	PC	46	+	57.23	98.79
135	PC(38:3)+H	PC	46	+	57.06	98.79
136	PC(38:4)+H	PC	46	+	55.96	98.75
137	PC(38:5)+H	PC	46	+	50.57	98.53
138	PC(38:6)+H	PC	46	+	47.08	98.38
139	PE(16:0/16:0)+H	PE	37	+	71.28	99.09
140	PE(16:0/16:1)+H	PE	37	+	64.89	98.84
141	PE(16:0/18:1)+H	PE	39	+	65.37	98.92
142	PE(16:0/18:1)-H	PE	39	-	63.79	98.85
143	PE(16:0/18:3)+H	PE	39	+	65.32	98.91
144	PE(16:0/18:3)-H	PE	39	-	64.04	98.86
145	PE(16:0e)+H	PE	21	+	81.76	99.05
146	PE(16:1/16:1)+H	PE	37	+	64.72	98.83
147	PE(16:1/16:1)-H	PE	37	-	61.63	98.70
148	PE(16:1/18:1)-H	PE	39	-	63.60	98.85
149	PE(16:1/18:3)+H	PE	39	+	64.17	98.87

150	PE(16:1/18:3)-H	PE	39	-	63.03	98.82
151	PE(16:2/18:3)+H	PE	39	+	65.42	98.92
152	PE(17:0/18:1)+H	PE	40	+	58.21	98.66
153	PE(17:1/16:0)-H	PE	38	-	68.55	99.01
154	PE(17:1/18:1)+H	PE	40	+	62.77	98.84
155	PE(17:1/18:1)-H	PE	40	-	62.38	98.83
156	PE(17:1/18:2)+H	PE	40	+	63.00	98.85
157	PE(18:0/18:1)+H	PE	41	+	66.80	99.02
158	PE(18:0/18:1)-H	PE	41	-	66.74	99.02
159	PE(18:0p)+H	PE	23	+	94.42	99.75
160	PE(18:1/18:1)+H	PE	41	+	64.53	98.94
161	PE(18:1/18:1)-H	PE	41	-	63.07	98.88
162	PE(18:1/18:2)+H	PE	41	+	65.17	98.96
163	PE(18:1/18:2)-H	PE	41	-	62.13	98.85
164	PE(18:2/17:2)-H	PE	40	-	61.25	98.78
165	PE(18:2/17:3)+H	PE	40	+	61.95	98.81
166	PE(18:2/17:3)-H	PE	40	-	60.45	98.75
167	PE(18:2/18:2)+H	PE	41	+	64.95	98.95
168	PE(18:2/18:2)-H	PE	41	-	61.74	98.83
169	PE(18:3/18:2)+H	PE	41	+	63.60	98.90
170	PE(18:3/18:2)-H	PE	41	-	59.06	98.72
171	PE(18:3/18:3)+H	PE	41	+	60.89	98.80
172	PE(18:3/18:3)-H	PE	41	-	58.57	98.70
173	PE(32:1e)+H	PE	37	+	91.11	99.75
174	PE(34:0e)+H	PE	39	+	0.00	0.00
175	PE(35:4)+H	PE	40	+	66.58	98.99
176	PE(37:0p)+H	PE	42	+	50.96	98.41
177	PE(37:1p)+H	PE	42	+	62.33	98.88
178	PE(37:2)-H	PE	42	-	27.78	97.00
179	PE(37:5)-H	PE	42	-	25.88	96.83
180	PE(42:2p)+H	PE	47	+	53.74	98.69
181	PE(43:10)+H	PE	48	+	0.00	0.00
182	PE(45:11)+H	PE	50	+	0.00	0.00
183	PE(45:12)+H	PE	50	+	0.00	0.00
184	PE(45:13)+H	PE	50	+	0.00	0.00
185	PE(47:10)+H	PE	52	+	0.00	0.00
186	PE(47:12)+H	PE	52	+	0.00	0.00
187	PE(47:13)+H	PE	52	+	0.00	0.00
188	PG(16:0/18:1)+NH_4	PG	40	+	66.22	98.97
189	PG(16:0/18:1)-H	PG	40	-	69.19	99.08
190	PG(16:0/18:2)+NH_4	PG	40	+	66.72	98.99
191	PG(16:0/18:2)-H	PG	40	-	63.59	98.87
192	PG(16:0/18:3)-H	PG	40	-	65.63	98.95
193	PG(18:1/18:2)-H	PG	42	-	62.58	98.89
194	PG(18:1/18:3)-H	PG	42	-	62.48	98.89
195	PG(18:3/18:2)-H	PG	42	-	62.12	98.87
196	PG(28:0/16:0)+H	PG	50	+	0.00	0.00
197	PG(28:0/18:1)+H	PG	52	+	0.00	0.00
198	PG(28:0/18:2)+H	PG	52	+	0.00	0.00
199	PI(16:0/16:1)+NH_4	PI	41	+	66.56	99.01
200	PI(16:0/16:1)-H	PI	41	-	63.51	98.90
201	PI(16:0/18:1)+H	PI	43	+	61.05	98.86
202	PI(16:0/18:2)+H	PI	43	+	63.66	98.96
203	PI(16:0/18:2)+NH_4	PI	43	+	63.75	98.96
204	PI(16:0/18:2)-H	PI	43	-	60.84	98.85

205	PI(16:0/18:3)+NH_4	PI	43	+	63.54	98.95
206	PI(16:0/18:3)-H	PI	43	-	60.81	98.85
207	PI(16:1/18:3)-H	PI	43	-	59.03	98.78
208	PI(17:0/18:1)-H	PI	44	-	59.21	98.82
209	PI(17:1/16:0)-H	PI	42	-	61.97	98.87
210	PI(17:1/18:1)-H	PI	44	-	59.49	98.83
211	PI(18:0/18:1)+NH_4	PI	45	+	64.18	99.02
212	PI(18:0/18:1)-H	PI	45	-	58.55	98.82
213	PI(18:1/18:1)-H	PI	45	-	59.66	98.86
214	PI(18:1/18:2)-H	PI	45	-	58.60	98.82
215	PI(18:2/18:2)+NH_4	PI	45	+	59.15	98.84
216	PI(18:2/18:2)-H	PI	45	-	58.05	98.80
217	PI(18:3/18:3)+NH_4	PI	45	+	64.73	99.04
218	PI(18:3/18:3)-H	PI	45	-	59.31	98.85
219	PI(36:3)+NH_4	PI	45	+	59.70	98.86
220	PS(16:0/16:1)-H	PS	38	-	48.72	98.13
221	PS(16:0/18:1)+H	PS	40	+	68.79	99.07
222	PS(16:0/18:1)-H	PS	40	-	69.38	99.09
223	PS(16:0/18:2)-H	PS	40	-	62.82	98.84
224	PS(16:0/18:3)-H	PS	40	-	63.38	98.87
225	PS(18:1/18:1)-H	PS	42	-	64.63	98.97
226	PS(18:1/18:2)-H	PS	42	-	70.00	99.15
227	PS(36:1)-H	PS	42	-	1.38	90.31
228	PS(36:4)-H	PS	42	-	0.00	0.00
229	PS(36:4)-H	PS	42	-	0.00	0.00
230	PS(37:3)-H	PS	43	-	0.00	0.00
231	PS(37:4)-H	PS	43	-	0.00	0.00
232	PS(38:1p)-H	PS	44	-	68.99	99.16
233	PS(39:4)-H	PS	45	-	0.00	0.00
234	PS(39:6)-H	PS	45	-	6.45	94.09
235	PS(40:1)-H	PS	46	-	1.05	90.56
236	PS(40:4)-H	PS	46	-	1.11	90.68
237	PS(40:5)-H	PS	46	-	1.06	90.59
238	PS(42:1)-H	PS	48	-	0.00	0.00
239	SM(d41:5)+H	SM	46	+	0.00	0.00
240	So(d17:1)+H	So	17	+	0.00	0.00
241	So(d18:0)+H	So	18	+	84.08	99.04
242	So(d18:1)+H	So	18	+	79.99	98.77
243	So(d20:0)+H	So	20	+	73.85	98.50
244	So(d20:1)+H	So	20	+	78.68	98.81
245	TG(12:0/18:2/18:2)+NH_4	TG	51	+	53.47	98.78
246	TG(12:0/18:2/20:5)+H	TG	53	+	0.00	0.00
247	TG(14:0/18:3/20:4)+H	TG	55	+	0.00	0.00
248	TG(15:0/16:0/18:1)+NH_4	TG	52	+	54.34	98.83
249	TG(15:0/16:0/18:2)+NH_4	TG	52	+	55.17	98.86
250	TG(15:0/16:1/18:3)+NH_4	TG	52	+	50.97	98.71
251	TG(16:0/14:0/16:0)+NH_4	TG	49	+	5.48	94.24
252	TG(16:0/14:0/18:1)+NH_4	TG	51	+	57.73	98.93
253	TG(16:0/14:0/20:4)+H	TG	53	+	0.00	0.00
254	TG(16:0/16:0/16:0)+NH_4	TG	51	+	1.41	91.99
255	TG(16:0/16:0/18:1)+NH_4	TG	53	+	56.21	98.92
256	TG(16:0/16:0/18:3)+H	TG	53	+	0.00	0.00
257	TG(16:0/16:1/18:1)+NH_4	TG	53	+	55.08	98.88
258	TG(16:0/16:1/18:2)+NH_4	TG	53	+	54.90	98.88
259	TG(16:0/17:0/18:1)+NH_4	TG	54	+	54.35	98.88

260	TG(16:0/17:1/18:1)+NH_4	TG	54	+	54.71	98.89
261	TG(16:0/17:1/20:4)+H	TG	56	+	1.02	92.14
262	TG(16:0/18:1/18:1)+NH_4	TG	55	+	54.06	98.89
263	TG(16:0/18:1/20:4)+H	TG	57	+	0.00	0.00
264	TG(16:0/18:2/18:3)+NH_4	TG	55	+	50.82	98.78
265	TG(16:0/20:5/20:5)+H	TG	59	+	0.10	88.96
266	TG(16:1/12:0/18:1)+NH_4	TG	49	+	59.05	98.93
267	TG(16:1/14:0/17:1)+NH_4	TG	50	+	56.16	98.85
268	TG(16:1/14:0/18:1)+NH_4	TG	51	+	57.83	98.93
269	TG(16:1/16:1/16:1)+NH_4	TG	51	+	55.54	98.85
270	TG(16:1/16:1/17:1)+NH_4	TG	52	+	53.89	98.82
271	TG(16:1/16:1/18:2)+NH_4	TG	53	+	54.04	98.85
272	TG(16:1/16:1/18:3)+NH_4	TG	53	+	52.65	98.80
273	TG(16:1/16:2/18:3)+NH_4	TG	53	+	47.29	98.60
274	TG(16:1/17:1/18:1)+NH_4	TG	54	+	54.40	98.88
275	TG(16:1/17:1/18:2)+NH_4	TG	54	+	52.89	98.83
276	TG(16:1/17:3/18:2)+NH_4	TG	54	+	48.34	98.66
277	TG(16:1/17:3/18:3)+NH_4	TG	54	+	46.18	98.58
278	TG(16:1/18:1/18:1)+NH_4	TG	55	+	53.47	98.87
279	TG(16:1/18:1/18:2)+NH_4	TG	55	+	52.73	98.84
280	TG(16:1/18:1/18:3)+H	TG	55	+	0.00	0.00
281	TG(16:1/18:2/18:3)+NH_4	TG	55	+	50.32	98.76
282	TG(16:1/18:2/20:5)+H	TG	57	+	0.00	0.00
283	TG(16:1/18:3/18:3)+NH_4	TG	55	+	48.32	98.69
284	TG(16:2/18:3/18:3)+NH_4	TG	55	+	49.27	98.72
285	TG(17:0/18:1/18:1)+NH_4	TG	56	+	53.25	98.88
286	TG(17:1/17:2/17:2)+NH_4	TG	54	+	50.02	98.73
287	TG(17:4/18:3/21:5)+H	TG	59	+	0.00	0.00
288	TG(18:0/16:0/16:0)+NH_4	TG	53	+	0.33	89.78
289	TG(18:0/16:0/18:0)+NH_4	TG	55	+	0.06	87.50
290	TG(18:0/16:0/18:1)+NH_4	TG	55	+	55.30	98.93
291	TG(18:0/16:1/18:1)+NH_4	TG	55	+	54.06	98.89
292	TG(18:0/18:0/18:0)+NH_4	TG	57	+	0.00	0.00
293	TG(18:0/18:0/18:1)+NH_4	TG	57	+	51.06	98.83
294	TG(18:0/18:1/18:1)+NH_4	TG	57	+	53.09	98.90
295	TG(18:0/18:1/18:2)+NH_4	TG	57	+	52.89	98.89
296	TG(18:0/18:1/20:4)+H	TG	59	+	0.00	0.00
297	TG(18:1/14:0/14:0)+NH_4	TG	49	+	65.05	99.13
298	TG(18:1/17:1/18:1)+NH_4	TG	56	+	52.89	98.87
299	TG(18:1/17:1/18:2)+NH_4	TG	56	+	52.67	98.86
300	TG(18:1/17:1/20:5)+H	TG	58	+	0.81	92.04
301	TG(18:1/18:1/18:2)+NH_4	TG	57	+	52.43	98.87
302	TG(18:1/18:1/19:2)+NH_4	TG	58	+	50.74	98.84
303	TG(18:1/18:1/19:3)+H	TG	58	+	0.00	0.00
304	TG(18:1/18:1/19:5)+NH_4	TG	58	+	0.64	91.66
305	TG(18:1/18:2/18:2)+NH_4	TG	57	+	50.10	98.79
306	TG(18:1/18:2/18:3)+H	TG	57	+	0.00	0.00
307	TG(18:1/18:2/18:3)+NH_4	TG	57	+	49.27	98.77
308	TG(18:1/18:2/20:3)+NH_4	TG	59	+	48.49	98.78
309	TG(18:1/18:2/22:0)+NH_4	TG	61	+	50.57	98.89
310	TG(18:1/18:3/18:3)+H	TG	57	+	0.00	0.00
311	TG(18:1/18:3/19:5)+NH_4	TG	58	+	0.00	0.00
312	TG(18:1/18:3/22:0)+NH_4	TG	61	+	47.34	98.78
313	TG(18:1/18:3/24:0)+NH_4	TG	63	+	45.07	98.74
314	TG(18:1/20:4/22:0)+H	TG	63	+	0.00	0.00

315	TG(18:1/20:4/22:1)+H	TG	63	+	0.00	0.00
316	TG(18:2/17:1/18:2)+NH_4	TG	56	+	50.67	98.79
317	TG(18:2/17:3/17:3)+NH_4	TG	55	+	0.00	0.00
318	TG(18:3/17:1/18:2)+NH_4	TG	56	+	50.09	98.77
319	TG(18:3/17:2/18:2)+NH_4	TG	56	+	47.53	98.68
320	TG(18:3/17:3/17:3)+NH_4	TG	55	+	2.95	93.79
321	TG(18:3/17:3/18:2)+NH_4	TG	56	+	45.19	98.59
322	TG(18:3/17:3/18:3)+NH_4	TG	56	+	42.22	98.47
323	TG(18:3/17:3/20:5)+H	TG	58	+	0.00	0.00
324	TG(18:3/18:2/18:2)+NH_4	TG	57	+	47.59	98.71
325	TG(18:3/18:2/18:2)+NH_4	TG	57	+	1.45	92.84
326	TG(18:3/18:2/18:3)+NH_4	TG	57	+	47.07	98.69
327	TG(18:3/18:3/18:3)+H	TG	57	+	0.00	0.00
328	TG(18:3/18:3/18:3)+NH_4	TG	57	+	45.90	98.64
329	TG(18:3/18:3/20:5)+H	TG	59	+	0.05	87.89
330	TG(18:4/16:1/16:1)+H	TG	53	+	0.00	0.00
331	TG(18:4/16:1/18:3)+H	TG	55	+	0.00	0.00
332	TG(18:4/16:2/18:3)+H	TG	55	+	0.00	0.00
333	TG(18:4/17:1/18:1)+H	TG	56	+	0.13	88.81
334	TG(18:4/17:2/18:3)+H	TG	56	+	0.00	0.00
335	TG(18:4/18:2/18:3)+NH_4	TG	57	+	0.00	0.00
336	TG(18:4/18:3/18:3)+H	TG	57	+	0.00	0.00
337	TG(18:4/18:3/18:3)+NH_4	TG	57	+	0.00	0.00
338	TG(19:0/18:1/18:1)+NH_4	TG	58	+	43.47	98.57
339	TG(19:1/16:0/18:3)+H	TG	56	+	0.00	0.00
340	TG(19:1/18:1/18:1)+NH_4	TG	58	+	46.29	98.68
341	TG(19:1/18:1/18:2)+NH_4	TG	58	+	41.30	98.49
342	TG(19:1/18:1/18:3)+NH_4	TG	58	+	51.67	98.87
343	TG(19:3/18:2/18:3)+NH_4	TG	58	+	0.80	92.02
344	TG(19:4/18:2/18:3)+H	TG	58	+	0.00	0.00
345	TG(19:4/18:3/18:3)+NH_4	TG	58	+	0.00	0.00
346	TG(19:5/18:2/18:3)+H	TG	58	+	0.00	0.00
347	TG(20:0/18:1/18:1)+NH_4	TG	59	+	41.18	98.51
348	TG(20:0/18:1/18:3)+NH_4	TG	59	+	37.58	98.35
349	TG(20:1/18:1/18:1)+NH_4	TG	59	+	0.00	0.00
350	TG(20:1/18:2/18:2)+NH_4	TG	59	+	46.05	98.69
351	TG(20:3/18:2/18:2)+NH_4	TG	59	+	41.89	98.54
352	TG(20:5/17:1/18:2)+H	TG	58	+	0.00	0.00
353	TG(24:3/18:1/18:3)+H	TG	63	+	0.00	0.00
354	TG(24:4/16:0/16:0)+NH_4	TG	59	+	0.00	0.00
355	TG(54:11)+NH_4	TG	57	+	0.00	0.00
356	TG(55:10p)+H	TG	58	+	0.00	0.00
357	TG(55:11)+NH_4	TG	58	+	0.44	91.07

Table A.2: Lipid ions identified by LipidSearch™ in Plasma extract when chloroform was not dried (*n*=3).

#	Lipid ion ID	Class	Ion formula	CalcMz	RT	Peak area ±STD
1	MG(15:2)+NH_4	MG	$C_{18}H_{36}O_4N$	330.2639	1.12	5.41E+07±3.22E+06
2	LPC(20:5)+H	LPC	$C_{28}H_{49}O_7NP$	542.3241	1.14	4.06E+07±3.04E+06
3	LPC(14:0)+H	LPC	$C_{22}H_{47}O_7NP$	468.3085	1.14	3.77E+07±4.04E+06
4	LPC(22:6)+H	LPC	$C_{30}H_{51}O_7NP$	568.3398	1.14	3.34E+07±4.36E+06
5	LPC(17:0)+H	LPC	$C_{25}H_{53}O_7NP$	510.3554	1.14	2.28E+07±1.96E+07
6	LPC(16:1)+H	LPC	$C_{24}H_{49}O_7NP$	494.3241	1.14	6.71E+07±8.01E+06
7	LPC(18:3)+H	LPC	$C_{26}H_{49}O_7NP$	518.3241	1.14	1.19E+08±2.02E+07
8	LPC(20:4)+H	LPC	$C_{28}H_{51}O_7NP$	544.3398	1.15	1.82E+08±3.47E+07
9	LPC(15:0)+H	LPC	$C_{23}H_{49}O_7NP$	482.3241	1.15	2.78E+07±9.05E+06
10	LPC(18:2)+H	LPC	$C_{26}H_{51}O_7NP$	520.3398	1.15	6.17E+08±8.29E+07
11	LPC(16:0)+H	LPC	$C_{24}H_{51}O_7NP$	496.3398	1.15	2.74E+09±8.09E+08
12	LPC(16:0)+CH_3COO	LPC	$C_{26}H_{53}O_9NP$	554.3463	1.16	4.57E+08±1.67E+08
13	LPC(18:1)+H	LPC	$C_{26}H_{53}O_7NP$	522.3554	1.17	3.13E+08±2.40E+08
14	LPC(18:0)+H	LPC	$C_{26}H_{55}O_7NP$	524.3711	1.17	6.30E+08±5.45E+08
15	LPC(18:1)+H	LPC	$C_{26}H_{53}O_7NP$	522.3554	3.56	5.61E+07±9.71E+07
16	LPC(16:1)+H	LPC	$C_{24}H_{49}O_7NP$	494.3241	4.25	9.57E+06±1.90E+06
17	LPC(22:6)+H	LPC	$C_{30}H_{51}O_7NP$	568.3398	4.53	4.82E+06±1.10E+06
18	LPC(18:2)+H	LPC	$C_{26}H_{51}O_7NP$	520.3398	4.67	4.49E+07±2.94E+07
19	LPC(20:4)+H	LPC	$C_{28}H_{51}O_7NP$	544.3398	4.67	3.03E+07±5.85E+06
20	LPC(18:2)+H	LPC	$C_{26}H_{51}O_7NP$	520.3398	4.77	1.05E+08±3.45E+07
21	FA(16:1)-H	FA	$O_2H_{29}C_{16}$	253.2173	5.10	4.55E+08±6.26E+07
22	FA(16:1)-H	FA	$O_2H_{29}C_{16}$	253.2173	5.11	4.46E+08±6.18E+07
23	LPC(20:3)+H	LPC	$C_{28}H_{53}O_7NP$	546.3554	5.23	1.65E+07±7.34E+06
24	LPC(16:0)+H	LPC	$C_{24}H_{51}O_7NP$	496.3398	5.38	7.53E+08±2.15E+08
25	LPC(18:3)+H	LPC	$C_{26}H_{49}O_7NP$	518.3241	5.39	8.75E+07±3.79E+07
26	FA(20:4)-H	FA	$O_2H_{31}C_{20}$	303.2330	5.44	3.41E+08±7.90E+07
27	OAHFA(36:3)-H	OAHFA	$C_{36}H_{63}O_4$	559.4732	5.54	8.59E+06±5.01E+06
28	FA(18:2)-H	FA	$O_2H_{31}C_{18}$	279.2330	5.55	2.52E+09±5.42E+08
29	OAHFA(36:4)-H	OAHFA	$C_{36}H_{61}O_4$	557.4575	5.57	5.14E+06±2.48E+06
30	OAHFA(34:1)-H	OAHFA	$C_{34}H_{63}O_4$	535.4732	5.57	2.58E+07±1.15E+07
31	LPC(18:1)+H	LPC	$C_{26}H_{53}O_7NP$	522.3554	5.61	1.36E+08±5.65E+07
32	LPC(20:4)+H	LPC	$C_{28}H_{51}O_7NP$	544.3398	5.61	1.42E+07±5.00E+06
33	FA(22:5)-H	FA	$O_2H_{33}C_{22}$	329.2486	5.75	4.39E+07±1.09E+07
34	OAHFA(34:2)-H	OAHFA	$C_{34}H_{61}O_4$	533.4575	6.08	1.28E+07±1.67E+06
35	OAHFA(36:3)-H	OAHFA	$C_{36}H_{63}O_4$	559.4732	6.12	2.52E+07±1.94E+06
36	OAHFA(34:0)-H	OAHFA	$C_{34}H_{65}O_4$	537.4888	6.18	1.03E+08±2.27E+07
37	LPC(18:0)+H	LPC	$C_{26}H_{55}O_7NP$	524.3711	6.23	4.10E+08±7.58E+07
38	OAHFA(38:4)-H	OAHFA	$C_{38}H_{65}O_4$	585.4888	6.31	7.22E+06±3.24E+06
39	OAHFA(36:1)-H	OAHFA	$C_{36}H_{67}O_4$	563.5045	6.31	3.31E+07±1.41E+07
40	FA(22:4)-H	FA	$O_2H_{35}C_{22}$	331.2643	6.32	2.13E+07±6.39E+06
41	LPC(20:3)+H	LPC	$C_{28}H_{53}O_7NP$	546.3554	6.38	9.50E+07±8.36E+07
42	LPC(18:0)+H	LPC	$C_{26}H_{55}O_7NP$	524.3711	6.40	5.10E+08±1.86E+08
43	TG(6:0/10:0/17:0)+NH_4	TG	$C_{36}H_{72}O_6N$	614.5354	6.54	3.87E+07±8.74E+06
44	MG(16:1p)+H	MG	$C_{19}H_{37}O_3$	313.2737	6.64	5.38E+07±6.88E+06
45	MG(16:1p)+NH_4	MG	$C_{19}H_{40}O_3N$	330.3003	6.65	5.46E+07±9.00E+06
46	OAHFA(36:2)-H	OAHFA	$C_{36}H_{65}O_4$	561.4888	6.74	4.28E+06±3.07E+06
47	OAHFA(38:2)-H	OAHFA	$C_{38}H_{69}O_4$	589.5201	6.84	8.95E+06±1.92E+06
48	OAHFA(38:2)-H	OAHFA	$C_{38}H_{69}O_4$	589.5201	7.09	6.64E+07±2.18E+07
49	OAHFA(36:2)-H	OAHFA	$C_{36}H_{65}O_4$	561.4888	7.10	2.87E+07±3.58E+06
50	OAHFA(40:3)-H	OAHFA	$C_{40}H_{71}O_4$	615.5358	7.12	1.18E+07±4.70E+05
51	MG(18:0)+H	MG	$C_{21}H_{43}O_4$	359.3156	7.43	8.12E+06±1.25E+06
52	MG(18:0)+NH_4	MG	$C_{21}H_{46}O_4N$	376.3421	7.45	9.17E+06±1.26E+06
53	Cer(d24:1)-H	Cer	$C_{24}H_{46}O_3N$	396.3483	8.01	2.00E+07±2.91E+06
54	TG(8:0/8:0/8:0)+NH_4	TG	$C_{27}H_{54}O_6N$	488.3946	8.22	8.73E+06±3.08E+06
55	SM(d32:1)+H	SM	$C_{37}H_{76}O_6N_2P$	675.5436	8.23	1.66E+08±6.20E+07
56	SM(d34:4)+H	SM	$C_{39}H_{74}O_6N_2P$	697.5279	8.23	2.63E+07±9.04E+06
57	SM(d32:1)+CH_3COO	SM	$C_{39}H_{78}O_8N_2P$	733.5501	8.23	4.91E+07±1.56E+07
58	SM(d36:5)+H	SM	$C_{41}H_{76}O_6N_2P$	723.5436	8.33	4.24E+07±1.37E+07
59	SM(d34:2)+H	SM	$C_{39}H_{78}O_6N_2P$	701.5592	8.33	2.88E+08±1.27E+08
60	SM(d34:2)+CH_3COO	SM	$C_{41}H_{80}O_8N_2P$	759.5658	8.34	8.00E+07±3.07E+07

61	TG(9:0/9:0/9:0)+NH_4	TG	$C_{30}H_{60}O_6N$	530.4415	8.37	2.18E+07±1.86E+06
62	PS(38:3)-H	PS	$C_{44}H_{79}O_{10}NP$	812.5447	8.47	1.09E+07±2.05E+06
63	PC(34:4)+H	PC	$C_{42}H_{77}O_8NP$	754.5381	8.47	5.29E+07±1.16E+07
64	PS(36:1)-H	PS	$C_{42}H_{79}O_{10}NP$	788.5447	8.51	2.71E+07±4.18E+06
65	PC(34:5)+H	PC	$C_{42}H_{75}O_8NP$	752.5225	8.51	2.24E+07±6.14E+06
66	PC(32:2)+H	PC	$C_{40}H_{77}O_8NP$	730.5381	8.51	1.55E+08±3.31E+07
67	SM(d33:1)+CH_3COO	SM	$C_{40}H_{80}O_8N_2P$	747.5658	8.53	3.35E+07±5.04E+06
68	SM(d33:1)+H	SM	$C_{38}H_{78}O_6N_2P$	689.5592	8.53	9.85E+07±2.01E+07
69	PS(39:6)-H	PS	$C_{45}H_{75}O_{10}NP$	820.5134	8.56	2.44E+07±5.37E+06
70	PC(40:8)+H	PC	$C_{48}H_{81}O_8NP$	830.5694	8.57	3.56E+07±1.12E+07
71	PC(38:7)+H	PC	$C_{46}H_{79}O_8NP$	804.5538	8.60	6.34E+07±4.02E+07
72	PS(37:4)-H	PS	$C_{43}H_{75}O_{10}NP$	796.5134	8.62	2.29E+07±6.59E+06
73	PC(38:8)+H	PC	$C_{46}H_{77}O_8NP$	802.5381	8.62	9.36E+07±7.35E+06
74	PC(36:5)+H	PC	$C_{44}H_{79}O_8NP$	780.5538	8.63	7.28E+08±1.69E+08
75	PS(40:4)-H	PS	$C_{46}H_{81}O_{10}NP$	838.5604	8.63	1.31E+08±2.77E+07
76	PC(36:6)+H	PC	$C_{44}H_{77}O_8NP$	778.5381	8.63	7.02E+07±1.15E+07
77	PC(37:6)+H	PC	$C_{45}H_{79}O_8NP$	792.5538	8.63	2.56E+07±5.80E+06
78	PS(35:2)-H	PS	$C_{41}H_{75}O_{10}NP$	772.5134	8.64	2.46E+07±5.66E+06
79	TG(8:0/8:0/10:0)+NH_4	TG	$C_{29}H_{58}O_6N$	516.4259	8.65	8.04E+06±1.69E+06
80	SM(d36:4)+H	SM	$C_{41}H_{78}O_6N_2P$	725.5592	8.66	2.14E+08±2.90E+07
81	PS(38:2)-H	PS	$C_{44}H_{81}O_{10}NP$	814.5604	8.66	9.72E+07±1.53E+07
82	PC(34:3)+H	PC	$C_{42}H_{79}O_8NP$	756.5538	8.66	5.72E+08±1.05E+08
83	PC(35:4)+H	PC	$C_{43}H_{79}O_8NP$	768.5538	8.67	3.90E+07±4.73E+06
84	PS(39:3)-H	PS	$C_{45}H_{81}O_{10}NP$	826.5604	8.67	1.01E+07±3.46E+06
85	PE(17:1/20:4)-H	PE	$C_{42}H_{73}O_8NP$	750.5079	8.71	6.41E+06±1.75E+06
86	PS(37:3)-H	PS	$C_{43}H_{77}O_{10}NP$	798.5291	8.71	1.83E+07±1.98E+06
87	PS(16:0p/23:6)-H	PS	$C_{45}H_{75}O_9NP$	804.5185	8.73	2.27E+07±4.30E+06
88	SM(d18:1/16:0)+CH_3COO	SM	$C_{41}H_{82}O_8N_2P$	761.5814	8.73	5.97E+08±9.44E+07
89	SM(d34:1)+H	SM	$C_{39}H_{80}O_6N_2P$	703.5749	8.73	2.35E+09±4.78E+08
90	PC(34:4)+H	PC	$C_{42}H_{77}O_8NP$	754.5381	8.74	3.43E+07±4.86E+06
91	PE(39:6)-H	PE	$C_{44}H_{75}O_8NP$	776.5236	8.75	1.19E+07±5.22E+06
92	PC(40:9)+H	PC	$C_{48}H_{79}O_8NP$	828.5538	8.76	1.05E+08±1.78E+07
93	PS(18:1p/23:6)-H	PS	$C_{47}H_{77}O_9NP$	830.5341	8.76	6.91E+06±1.96E+06
94	PC(38:6)+H	PC	$C_{46}H_{81}O_8NP$	806.5694	8.77	1.95E+09±2.28E+08
95	PC(32:1)+H	PC	$C_{40}H_{79}O_8NP$	732.5538	8.78	5.13E+08±7.19E+07
96	PS(42:5)-H	PS	$C_{48}H_{83}O_{10}NP$	864.5760	8.78	3.24E+08±4.41E+07
97	PS(36:0)-H	PS	$C_{42}H_{81}O_{10}NP$	790.5604	8.78	9.33E+07±1.61E+07
98	PS(37:1)-H	PS	$C_{43}H_{81}O_{10}NP$	802.5604	8.78	2.36E+07±1.07E+07
99	PI(18:0/20:4)-H	PI	$C_{47}H_{82}O_{13}N_0P$	885.5499	8.79	8.87E+06±2.01E+06
100	SM(d18:0/18:2)+CH_3COO	SM	$C_{43}H_{84}O_8N_2P$	787.5971	8.79	3.76E+07±8.54E+06
101	PC(38:7)+H	PC	$C_{46}H_{79}O_8NP$	804.5538	8.79	2.37E+08±5.72E+07
102	SM(d36:2)+H	SM	$C_{41}H_{82}O_6N_2P$	729.5905	8.79	1.71E+08±2.80E+07
103	PC(40:7)+H	PC	$C_{48}H_{83}O_8NP$	832.5851	8.80	7.99E+07±1.26E+07
104	PC(36:4)+H	PC	$C_{44}H_{81}O_8NP$	782.5694	8.84	5.37E+09±6.67E+08
105	PS(40:3)-H	PS	$C_{46}H_{83}O_{10}NP$	840.5760	8.84	9.49E+08±2.47E+08
106	PC(35:6)+H	PC	$C_{43}H_{75}O_8NP$	764.5225	8.84	3.90E+07±1.08E+07
107	PC(35:3)+H	PC	$C_{43}H_{81}O_8NP$	770.5694	8.84	6.65E+07±1.55E+06
108	PC(34:2)+H	PC	$C_{42}H_{81}O_8NP$	758.5694	8.88	1.06E+10±1.47E+09
109	PS(38:1)-H	PS	$C_{44}H_{83}O_{10}NP$	816.5760	8.89	2.15E+09±3.35E+08
110	PS(38:4p)-H	PS	$C_{44}H_{77}O_9NP$	794.5341	8.89	5.81E+07±1.25E+07
111	PA(27:4/18:2)-H	PA	$C_{48}H_{82}O_8N_0P$	817.5753	8.90	1.08E+09±1.68E+08
112	PS(41:6)-H	PS	$C_{47}H_{79}O_{10}NP$	848.5447	8.91	4.83E+07±9.45E+06
113	PC(16:0/20:5)+H	PC	$C_{44}H_{79}O_8NP$	780.5538	8.91	4.60E+08±3.68E+07
114	PS(36:2p)-H	PS	$C_{42}H_{77}O_9NP$	770.5341	8.91	4.19E+07±8.62E+06
115	PC(17:4/16:0)+H	PC	$C_{41}H_{75}O_8NP$	740.5225	8.92	3.33E+07±6.66E+06
116	PE(16:0/20:4)+H	PE	$C_{41}H_{75}O_8NP$	740.5225	8.92	3.31E+07±6.93E+06
117	PE(16:0/20:4)-H	PE	$C_{41}H_{73}O_8NP$	738.5079	8.92	1.04E+08±3.90E+07
118	SM(d18:1/17:0)+H	SM	$C_{40}H_{82}O_6N_2P$	717.5905	8.92	3.06E+07±6.61E+06
119	PS(42:4)-H	PS	$C_{48}H_{85}O_{10}NP$	866.5917	8.92	3.21E+08±4.89E+07
120	PS(39:4)-H	PS	$C_{45}H_{79}O_{10}NP$	824.5447	8.93	1.59E+08±4.15E+07
121	PC(38:5)+H	PC	$C_{46}H_{83}O_8NP$	808.5851	8.93	1.44E+09±2.28E+08
122	PE(16:0/18:2)-H	PE	$C_{39}H_{73}O_8NP$	714.5079	8.94	9.94E+07±3.20E+07
123	PE(18:1/20:4)-H	PE	$C_{43}H_{75}O_8NP$	764.5236	8.94	7.62E+07±2.63E+07
124	PC(31:2)+H	PC	$C_{39}H_{75}O_8NP$	716.5225	8.95	3.96E+07±1.06E+07
125	PS(37:2)-H	PS	$C_{43}H_{79}O_{10}NP$	800.5447	8.95	1.34E+08±2.89E+07
126	PC(33:1)+H	PC	$C_{41}H_{81}O_8NP$	746.5694	8.96	6.20E+07±7.54E+06
127	PC(18:2/22:6)+H	PC	$C_{48}H_{81}O_8NP$	830.5694	8.97	4.96E+07±5.41E+06
128	PE(18:1/18:2)-H	PE	$C_{41}H_{75}O_8NP$	740.5236	8.98	5.19E+07±2.05E+07

129	PC(36:3)+H	PC	$C_{44}H_{83}O_8NP$	784.5851	8.99	4.45E+09±6.36E+08
130	PS(40:2)-H	PS	$C_{46}H_{85}O_{10}NP$	842.5917	8.99	9.95E+08±1.47E+08
131	PE(16:0p/22:6)-H	PE	$C_{43}H_{73}O_7NP$	746.5130	9.00	6.54E+07±2.90E+07
132	PC(37:4)+H	PC	$C_{45}H_{83}O_8NP$	796.5851	9.01	9.48E+07±2.08E+07
133	PS(40:4e)-H	PS	$C_{46}H_{83}O_9NP$	824.5811	9.02	4.13E+07±8.19E+06
134	PC(36:4p)+H	PC	$C_{44}H_{81}O_7NP$	766.5745	9.02	2.04E+08±1.91E+07
135	PC(35:6p)+H	PC	$C_{43}H_{75}O_7NP$	748.5276	9.03	2.47E+07±6.88E+06
136	PC(16:1p/22:4)+H	PC	$C_{46}H_{83}O_7NP$	792.5902	9.04	8.72E+07±1.09E+07
137	PC(38:6e)+H	PC	$C_{46}H_{83}O_7NP$	792.5902	9.04	8.81E+07±1.18E+07
138	PS(39:1)-H	PS	$C_{45}H_{85}O_{10}NP$	830.5917	9.04	3.54E+07±7.37E+06
139	PC(35:2)+H	PC	$C_{43}H_{83}O_8NP$	772.5851	9.05	1.82E+08±3.55E+07
140	PC(18:2p/16:0)+H	PC	$C_{42}H_{81}O_7NP$	742.5745	9.06	1.04E+08±1.82E+07
141	PS(38:2e)-H	PS	$C_{44}H_{83}O_9NP$	800.5811	9.06	1.96E+07±2.02E+06
142	PC(34:3)+H	PC	$C_{42}H_{79}O_8NP$	756.5538	9.06	2.13E+07±7.89E+05
143	PS(40:3e)-H	PS	$C_{46}H_{85}O_9NP$	826.5967	9.07	6.07E+07±8.59E+06
144	PC(36:4e)+H	PC	$C_{44}H_{83}O_7NP$	768.5902	9.07	3.23E+08±4.42E+07
145	PC(32:0)+H	PC	$C_{40}H_{81}O_8NP$	734.5694	9.08	3.91E+08±5.77E+07
146	PE(16:0p/20:4)+H	PE	$C_{41}H_{75}O_7NP$	724.5276	9.08	2.90E+07±6.36E+06
147	SM(d36:1)+H	SM	$C_{41}H_{84}O_6N_2P$	731.6062	9.09	3.59E+08±4.17E+07
148	SM(d18:1/18:0)+CH_3COO	SM	$C_{43}H_{86}O_8N_2P$	789.6127	9.09	9.45E+07±1.51E+07
149	PE(16:0p/20:4)-H	PE	$C_{41}H_{73}O_7NP$	722.5130	9.09	6.10E+07±2.16E+07
150	PC(38:4p)+H	PC	$C_{46}H_{85}O_7NP$	794.6058	9.10	1.96E+08±2.55E+07
151	PC(34:2e)+H	PC	$C_{42}H_{83}O_7NP$	744.5902	9.10	5.99E+07±5.86E+06
152	PE(18:1p/20:4)+H	PE	$C_{43}H_{77}O_7NP$	750.5432	9.12	3.47E+07±8.72E+06
153	PA(27:4/18:1)-H	PA	$C_{48}H_{84}O_8N_0P$	819.5909	9.12	5.88E+08±1.14E+08
154	PS(44:5)-H	PS	$C_{50}H_{87}O_{10}NP$	892.6073	9.12	1.28E+08±1.95E+07
155	PC(34:1)+H	PC	$C_{42}H_{83}O_8NP$	760.5851	9.12	5.27E+09±6.47E+08
156	PS(38:0)-H	PS	$C_{44}H_{85}O_{10}NP$	818.5917	9.12	1.15E+09±1.60E+08
157	PC(40:6)+H	PC	$C_{48}H_{85}O_8NP$	834.6007	9.12	7.83E+08±8.29E+07
158	PC(42:9)+H	PC	$C_{50}H_{83}O_8NP$	856.5851	9.12	2.25E+07±3.78E+06
159	PE(18:1p/20:4)-H	PE	$C_{43}H_{75}O_7NP$	748.5287	9.12	7.43E+07±3.11E+07
160	PE(16:0p/18:2)-H	PE	$C_{39}H_{73}O_7NP$	698.5130	9.13	2.21E+07±6.89E+06
161	SM(d20:0/18:2)+CH_3COO	SM	$C_{45}H_{88}O_8N_2P$	815.6284	9.15	2.36E+07±4.32E+06
162	SM(d38:2)+H	SM	$C_{43}H_{86}O_6N_2P$	757.6218	9.16	1.05E+08±1.59E+07
163	PE(16:0/18:1)+H	PE	$C_{39}H_{77}O_8NP$	718.5381	9.17	1.90E+07±4.03E+06
164	PS(42:3)-H	PS	$C_{48}H_{87}O_{10}NP$	868.6073	9.18	6.90E+08±9.97E+07
165	PC(38:4)+H	PC	$C_{46}H_{85}O_8NP$	810.6007	9.18	3.42E+09±4.28E+08
166	PC(20:3/20:4)+H	PC	$C_{48}H_{83}O_8NP$	832.5851	9.18	1.13E+08±1.04E+07
167	PC(40:5)+H	PC	$C_{48}H_{87}O_8NP$	836.6164	9.22	4.74E+08±6.69E+07
168	PC(36:2)+H	PC	$C_{44}H_{85}O_8NP$	786.6007	9.22	6.26E+09±1.12E+09
169	PE(18:0/20:4)-H	PE	$C_{43}H_{77}O_8NP$	766.5392	9.22	1.53E+08±5.10E+07
170	PA(29:4/18:2)-H	PA	$C_{50}H_{86}O_8N_0P$	845.6066	9.22	6.77E+08±1.25E+08
171	PS(40:1)-H	PS	$C_{46}H_{87}O_{10}NP$	844.6073	9.22	1.45E+09±3.29E+08
172	Cer(d18:1/18:0+2O)-H	Cer	$C_{36}H_{70}O_5N$	596.5259	9.23	5.72E+07±1.22E+07
173	PC(17:4/18:0)+H	PC	$C_{43}H_{79}O_8NP$	768.5538	9.23	1.16E+08±3.23E+07
174	PC(18:0/20:5)+H	PC	$C_{46}H_{83}O_8NP$	808.5851	9.24	4.00E+08±2.47E+07
175	PE(18:0/18:2)-H	PE	$C_{41}H_{77}O_8NP$	742.5392	9.25	1.37E+08±4.91E+07
176	PC(33:2)+H	PC	$C_{41}H_{79}O_8NP$	744.5538	9.26	1.25E+08±2.63E+07
177	PE(18:0/22:5)-H	PE	$C_{45}H_{79}O_8NP$	792.5549	9.27	1.81E+07±5.30E+06
178	PC(32:1e)+H	PC	$C_{40}H_{81}O_7NP$	718.5745	9.27	4.45E+07±6.44E+06
179	PC(35:1)+H	PC	$C_{43}H_{85}O_8NP$	774.6007	9.29	7.34E+07±1.00E+07
180	DG(14:0/18:2)+NH_4	DG	$C_{35}H_{68}O_5N$	582.5092	9.30	3.06E+07±3.64E+06
181	PC(32:0e)+H	PC	$C_{40}H_{83}O_7NP$	720.5902	9.31	7.56E+07±2.06E+07
182	PC(38:3)+H	PC	$C_{46}H_{87}O_8NP$	812.6164	9.31	2.49E+09±4.41E+08
183	PS(42:2)-H	PS	$C_{48}H_{89}O_{10}NP$	870.6230	9.31	5.52E+08±8.71E+07
184	PE(18:0p/22:6)-H	PE	$C_{45}H_{77}O_7NP$	774.5443	9.33	1.59E+07±4.91E+06
185	PC(34:1e)+H	PC	$C_{42}H_{85}O_7NP$	746.6058	9.34	1.10E+08±2.15E+07
186	DG(18:1/20:5)+NH_4	DG	$C_{41}H_{72}O_5N$	658.5405	9.38	4.12E+07±8.27E+06
187	PE(18:0p/20:4)+H	PE	$C_{43}H_{79}O_7NP$	752.5589	9.39	4.61E+07±1.27E+07
188	DG(16:1/18:2)+NH_4	DG	$C_{37}H_{70}O_5N$	608.5249	9.39	7.96E+07±1.39E+07
189	PE(18:0p/20:4)-H	PE	$C_{43}H_{77}O_7NP$	750.5443	9.39	4.49E+07±1.47E+07
190	PC(38:4e)+H	PC	$C_{46}H_{87}O_7NP$	796.6215	9.39	1.77E+08±4.71E+07
191	PC(40:5e)+H	PC	$C_{48}H_{89}O_7NP$	822.6371	9.40	4.08E+07±1.11E+07
192	PC(40:4)+H	PC	$C_{48}H_{89}O_8NP$	838.6320	9.41	2.26E+08±4.84E+07
193	PS(44:3)-H	PS	$C_{50}H_{91}O_{10}NP$	896.6386	9.41	4.36E+07±1.30E+07
194	PE(18:0p/18:2)-H	PE	$C_{41}H_{77}O_7NP$	726.5443	9.43	2.32E+07±6.57E+06
195	DG(18:2/18:2)+NH_4	DG	$C_{39}H_{72}O_5N$	634.5405	9.43	1.84E+08±3.15E+07
196	SM(d38:1)+H	SM	$C_{43}H_{88}O_6N_2P$	759.6375	9.43	4.77E+08±1.52E+08

197	SM(d22:1/16:0)+CH_3COO	SM	$C_{45}H_{90}O_8N_2P$	817.6440	9.44	1.26E+08±2.43E+07
198	SM(d18:2/22:2)+H	SM	$C_{45}H_{86}O_6N_2P$	781.6218	9.44	4.60E+07±8.58E+06
199	PS(40:0)-H	PS	$C_{46}H_{89}O_{10}NP$	846.6230	9.45	3.32E+08±6.59E+07
200	PC(15:1/18:0)+H	PC	$C_{41}H_{81}O_8NP$	746.5694	9.47	2.62E+07±6.63E+06
201	PE(18:0/18:1)-H	PE	$C_{41}H_{79}O_8NP$	744.5549	9.47	2.08E+07±6.34E+06
202	SM(d18:1/22:1)+H	SM	$C_{45}H_{90}O_6N_2P$	785.6531	9.49	5.96E+08±1.59E+08
203	SM(d42:3)+H	SM	$C_{47}H_{92}O_6N_2P$	811.6688	9.49	5.52E+08±1.49E+08
204	SM(d22:0/20:3)+CH_3COO	SM	$C_{49}H_{94}O_8N_2P$	869.6753	9.49	1.73E+08±3.82E+07
205	SM(d40:2)+CH_3COO	SM	$C_{47}H_{92}O_8N_2P$	843.6597	9.49	1.75E+08±3.49E+07
206	DG(16:0/14:0)+NH_4	DG	$C_{33}H_{68}O_5N$	558.5092	9.50	1.83E+07±4.12E+06
207	SM(d18:2/24:3)+H	SM	$C_{47}H_{88}O_6N_2P$	807.6375	9.50	7.05E+07±2.11E+07
208	SM(d44:6)+H	SM	$C_{49}H_{90}O_6N_2P$	833.6531	9.50	6.74E+07±1.91E+07
209	DG(18:1/14:0)+NH_4	DG	$C_{35}H_{70}O_5N$	584.5249	9.54	8.58E+07±1.29E+07
210	DG(16:1/18:3)+H	DG	$C_{37}H_{65}O_5$	589.4827	9.56	2.51E+07±3.28E+05
211	DG(18:1/20:4)+NH_4	DG	$C_{41}H_{74}O_5N$	660.5562	9.61	5.83E+07±9.12E+06
212	SM(d39:1)+CH_3COO	SM	$C_{46}H_{92}O_8N_2P$	831.6597	9.61	5.16E+07±1.04E+07
213	DG(16:0/18:2)+NH_4	DG	$C_{37}H_{72}O_5N$	610.5405	9.61	3.72E+08±5.43E+07
214	SM(d39:1)+H	SM	$C_{44}H_{90}O_6N_2P$	773.6531	9.62	1.23E+08±2.21E+07
215	DG(18:3/18:2)+H	DG	$C_{39}H_{67}O_5$	615.4983	9.62	1.09E+08±2.25E+06
216	DG(34:3p)+H	DG	$C_{37}H_{67}O_4$	575.5034	9.62	1.80E+07±3.08E+06
217	DG(18:1/20:5)+H	DG	$C_{41}H_{69}O_5$	641.5140	9.65	1.15E+08±2.73E+06
218	SM(d41:2)+H	SM	$C_{46}H_{92}O_6N_2P$	799.6688	9.65	2.11E+08±4.83E+07
219	SM(d18:1/25:4)+H	SM	$C_{48}H_{90}O_6N_2P$	821.6531	9.65	3.29E+07±5.24E+06
220	DG(18:1/18:2)+NH_4	DG	$C_{39}H_{74}O_5N$	636.5562	9.66	3.65E+08±5.87E+07
221	SM(d41:2)+CH_3COO	SM	$C_{48}H_{94}O_8N_2P$	857.6753	9.66	8.57E+07±1.83E+07
222	PC(42:4p)+H	PC	$C_{50}H_{93}O_7NP$	850.6684	9.72	3.00E+07±9.67E+06
223	SM(d44:5)+H	SM	$C_{49}H_{92}O_6N_2P$	835.6688	9.75	2.20E+08±4.71E+07
224	SM(d42:2)+CH_3COO	SM	$C_{49}H_{96}O_8N_2P$	871.6910	9.76	4.58E+08±1.17E+08
225	SM(d22:1/18:0)+CH_3COO	SM	$C_{47}H_{94}O_8N_2P$	845.6753	9.76	3.10E+08±8.44E+07
226	SM(d40:1)+H	SM	$C_{45}H_{92}O_6N_2P$	787.6688	9.76	8.57E+08±1.76E+08
227	SM(d18:1/24:1)+H	SM	$C_{47}H_{94}O_6N_2P$	813.6844	9.77	1.20E+09±2.55E+08
228	SM(d18:1/24:3)+H	SM	$C_{47}H_{90}O_6N_2P$	809.6531	9.77	1.47E+08±2.19E+07
229	CerG1(d40:1)+H	CerG1	$C_{46}H_{90}O_8N$	784.6661	9.78	3.01E+07±5.75E+06
230	PC(44:6e)+H	PC	$C_{52}H_{95}O_7NP$	876.6841	9.78	3.74E+07±8.04E+06
231	DG(16:0/18:3)+H	DG	$C_{37}H_{67}O_5$	591.4983	9.83	3.53E+07±3.85E+06
232	DG(16:0/20:4)+H	DG	$C_{39}H_{69}O_5$	617.5140	9.86	1.46E+08±1.56E+07
233	DG(16:0/18:1)+NH_4	DG	$C_{37}H_{74}O_5N$	612.5562	9.87	3.88E+08±6.95E+07
234	DG(34:2p)+H	DG	$C_{37}H_{69}O_4$	577.5190	9.87	3.41E+07±7.10E+06
235	SM(d43:2)+H	SM	$C_{48}H_{96}O_6N_2P$	827.7001	9.88	3.48E+07±9.93E+06
236	MG(18:2p)+H	MG	$C_{21}H_{39}O_3$	339.2894	9.88	2.12E+07±3.88E+06
237	DG(18:1/20:4)+H	DG	$C_{41}H_{71}O_5$	643.5296	9.89	1.25E+08±1.53E+07
238	DG(18:1/18:1)+NH_4	DG	$C_{39}H_{76}O_5N$	638.5718	9.90	3.36E+08±6.52E+07
239	DG(36:3p)+H	DG	$C_{39}H_{71}O_4$	603.5347	9.91	1.65E+07±3.08E+06
240	SM(d18:1/25:3)+H	SM	$C_{48}H_{92}O_6N_2P$	823.6688	9.93	5.65E+07±1.20E+07
241	SM(d41:1)+H	SM	$C_{46}H_{94}O_6N_2P$	801.6844	9.94	2.49E+08±6.62E+07
242	SM(d41:1)+CH_3COO	SM	$C_{48}H_{96}O_8N_2P$	859.6910	9.95	1.07E+08±2.57E+07
243	PC(42:3p)+H	PC	$C_{50}H_{95}O_7NP$	852.6841	10.07	1.09E+07±1.63E+06
244	CerG1(d42:1)+H	CerG1	$C_{48}H_{94}O_8N$	812.6974	10.11	3.61E+07±7.27E+06
245	SM(d42:1)+H	SM	$C_{47}H_{96}O_6N_2P$	815.7001	10.12	4.71E+08±8.76E+07
246	SM(d44:4)+H	SM	$C_{49}H_{94}O_6N_2P$	837.6844	10.13	9.27E+07±1.42E+07
247	SM(d42:1)+CH_3COO	SM	$C_{49}H_{98}O_8N_2P$	873.7066	10.13	2.03E+08±3.81E+07
248	DG(16:0/20:3)+H	DG	$C_{39}H_{71}O_5$	619.5296	10.19	3.86E+07±1.31E+06
249	DG(18:0/18:1)+NH_4	DG	$C_{39}H_{78}O_5N$	640.5875	10.21	4.91E+07±1.22E+07
250	Cer(d18:1/22:0)-H	Cer	$C_{40}H_{78}O_3N$	620.5987	10.22	9.76E+06±2.33E+06
251	Cer(d18:1/22:0)+H	Cer	$C_{40}H_{80}O_3N$	622.6133	10.22	5.59E+07±1.24E+07
252	Cer(d18:2/24:0)+H	Cer	$C_{42}H_{82}O_3N$	648.6289	10.27	7.94E+07±1.75E+07
253	Cer(d18:2/24:0)-H	Cer	$C_{42}H_{80}O_3N$	646.6144	10.27	1.27E+07±1.91E+06
254	SM(d43:1)+H	SM	$C_{48}H_{98}O_6N_2P$	829.7157	10.30	1.74E+07±4.96E+06
255	Cer(d17:1/24:0)+H	Cer	$C_{41}H_{82}O_3N$	636.6289	10.41	4.63E+07±9.75E+06
256	TG(6:0/14:0/16:0)+NH_4	TG	$C_{39}H_{78}O_6N$	656.5824	10.45	1.23E+07±2.01E+06
257	TG(4:0/16:0/18:1)+NH_4	TG	$C_{41}H_{80}O_6N$	682.5980	10.52	2.06E+07±5.45E+06
258	ChE(20:5)+NH_4	ChE	$C_{47}H_{78}O_2N$	688.6027	10.61	1.09E+07±1.68E+06
259	Cer(d18:1/24:0)-H	Cer	$C_{42}H_{82}O_3N$	648.6300	10.62	2.98E+07±6.29E+06
260	Cer(d18:1/24:0)+H	Cer	$C_{42}H_{84}O_3N$	650.6446	10.62	1.78E+08±3.32E+07
261	TG(16:0/10:0/12:0)+NH_4	TG	$C_{41}H_{82}O_6N$	684.6137	10.82	1.99E+07±2.70E+06
262	TG(8:0/14:0/20:4)+H	TG	$C_{45}H_{79}O_6$	715.5871	10.90	1.38E+07±1.85E+06
263	TG(10:0/12:0/18:1)+NH_4	TG	$C_{43}H_{84}O_6N$	710.6293	10.90	3.17E+07±6.50E+06
264	TG(16:0/8:0/20:5)+H	TG	$C_{47}H_{81}O_6$	741.6028	10.95	1.65E+07±2.21E+06

265	TG(10:0/14:0/18:2)+NH_4	TG	$C_{45}H_{86}O_6N$	736.6450	10.96	3.60E+07±9.66E+06
266	TG(8:0/18:1/18:2)+NH_4	TG	$C_{47}H_{88}O_6N$	762.6606	11.09	3.36E+07±8.23E+06
267	TG(10:0/18:2/18:2)+NH_4	TG	$C_{49}H_{90}O_6N$	788.6763	11.15	3.16E+07±7.99E+06
268	TG(10:0/14:0/18:3)+H	TG	$C_{45}H_{81}O_6$	717.6028	11.26	1.73E+07±3.64E+06
269	TG(12:0/14:0/14:0)+NH_4	TG	$C_{43}H_{86}O_6N$	712.6450	11.26	3.88E+07±8.18E+06
270	TG(12:0/18:2/18:3)+NH_4	TG	$C_{51}H_{92}O_6N$	814.6919	11.31	3.67E+07±8.40E+06
271	TG(10:0/14:0/20:4)+H	TG	$C_{47}H_{83}O_6$	743.6184	11.34	3.09E+07±6.71E+06
272	TG(10:0/14:0/18:1)+NH_4	TG	$C_{45}H_{88}O_6N$	738.6606	11.34	6.97E+07±1.68E+07
273	TG(12:0/14:0/20:5)+H	TG	$C_{49}H_{85}O_6$	769.6341	11.43	4.47E+07±9.51E+06
274	TG(16:0/10:0/18:2)+NH_4	TG	$C_{47}H_{90}O_6N$	764.6763	11.43	1.10E+08±1.69E+07
275	TG(14:0/18:3/18:3)+NH_4	TG	$C_{53}H_{94}O_6N$	840.7076	11.48	4.22E+07±9.83E+06
276	TG(16:1/12:0/18:2)+NH_4	TG	$C_{49}H_{92}O_6N$	790.6919	11.50	1.30E+08±3.17E+07
277	TG(10:0/18:2/20:4)+H	TG	$C_{51}H_{87}O_6$	795.6497	11.53	5.30E+07±9.23E+06
278	TG(12:0/18:2/18:2)+NH_4	TG	$C_{51}H_{94}O_6N$	816.7076	11.66	1.96E+08±4.78E+07
279	TG(12:0/18:2/20:5)+H	TG	$C_{53}H_{89}O_6$	821.6654	11.66	6.88E+07±1.42E+07
280	TG(16:2/18:2/18:3)+NH_4	TG	$C_{55}H_{96}O_6N$	866.7232	11.68	5.02E+07±1.21E+07
281	TG(12:0/14:0/18:3)+H	TG	$C_{47}H_{85}O_6$	745.6341	11.80	3.60E+07±6.27E+06
282	TG(16:0/12:0/14:0)+NH_4	TG	$C_{45}H_{90}O_6N$	740.6763	11.81	1.03E+08±2.70E+07
283	TG(18:4/16:1/18:3)+H	TG	$C_{55}H_{91}O_6$	847.6810	11.84	8.76E+07±1.53E+07
284	TG(12:0/14:0/20:4)+H	TG	$C_{49}H_{87}O_6$	771.6497	11.86	7.80E+07±1.51E+07
285	TG(18:1/12:0/14:0)+NH_4	TG	$C_{47}H_{92}O_6N$	766.6919	11.87	2.50E+08±6.05E+07
286	TG(14:0/18:2/18:3)+NH_4	TG	$C_{53}H_{96}O_6N$	842.7232	11.88	2.73E+08±6.68E+07
287	TG(18:3/18:2/20:5)+H	TG	$C_{59}H_{95}O_6$	899.7123	11.89	8.93E+06±4.83E+06
288	TG(18:3/18:2/20:4)+NH_4	TG	$C_{59}H_{100}O_6N$	918.7545	11.89	7.41E+07±1.93E+07
289	TG(18:3/18:2/18:3)+NH_4	TG	$C_{57}H_{98}O_6N$	892.7389	11.90	6.98E+07±1.62E+07
290	TG(18:4/14:0/16:1)+H	TG	$C_{51}H_{89}O_6$	797.6654	11.98	1.30E+08±2.29E+07
291	TG(16:1/12:0/18:1)+NH_4	TG	$C_{49}H_{94}O_6N$	792.7076	11.99	4.57E+08±9.03E+07
292	TG(18:2/18:2/20:4)+NH_4	TG	$C_{59}H_{102}O_6N$	920.7702	12.03	1.59E+07±6.52E+06
293	TG(16:1/18:2/18:3)+NH_4	TG	$C_{55}H_{98}O_6N$	868.7389	12.04	4.15E+08±9.95E+07
294	TG(16:0/14:0/18:3)+NH_4	TG	$C_{51}H_{96}O_6N$	818.7232	12.07	8.12E+08±1.95E+08
295	TG(18:3/18:3/18:3)+H	TG	$C_{57}H_{93}O_6$	873.6967	12.07	1.07E+08±1.72E+07
296	TG(16:1/14:0/20:5)+H	TG	$C_{53}H_{91}O_6$	823.6810	12.08	2.09E+08±2.92E+07
297	Co(Q10)+NH_4	Co	$C_{59}H_{94}O_4N$	880.7177	12.09	5.22E+07±1.45E+07
298	TG(15:0/18:2/18:3)+NH_4	TG	$C_{54}H_{98}O_6N$	856.7389	12.17	3.45E+07±7.56E+06
299	TG(18:2/18:2/22:6)+NH_4	TG	$C_{61}H_{102}O_6N$	944.7702	12.17	4.14E+07±1.46E+07
300	TG(15:0/12:0/18:1)+NH_4	TG	$C_{48}H_{94}O_6N$	780.7076	12.18	3.61E+07±8.87E+06
301	TG(18:4/16:1/18:2)+H	TG	$C_{55}H_{93}O_6$	849.6967	12.23	2.91E+08±3.16E+07
302	TG(16:1/16:1/18:2)+NH_4	TG	$C_{53}H_{98}O_6N$	844.7389	12.25	1.36E+09±3.22E+08
303	TG(15:0/16:1/16:1)+NH_4	TG	$C_{50}H_{96}O_6N$	806.7232	12.30	6.62E+07±1.61E+07
304	TG(18:3/18:2/18:2)+NH_4	TG	$C_{57}H_{100}O_6N$	894.7545	12.32	4.58E+08±1.59E+08
305	TG(15:0/16:1/18:2)+NH_4	TG	$C_{52}H_{98}O_6N$	832.7389	12.37	9.96E+07±1.96E+07
306	TG(16:0/12:0/18:3)+H	TG	$C_{49}H_{89}O_6$	773.6654	12.44	5.23E+07±6.61E+06
307	TG(16:0/14:0/14:0)+NH_4	TG	$C_{47}H_{94}O_6N$	768.7076	12.45	2.59E+08±5.55E+07
308	TG(16:1/18:2/20:5)+H	TG	$C_{57}H_{95}O_6$	875.7123	12.47	3.73E+08±4.01E+07
309	TG(16:1/18:2/18:2)+NH_4	TG	$C_{55}H_{100}O_6N$	870.7545	12.48	2.11E+09±4.39E+08
310	TG(18:2/18:2/20:4)+NH_4	TG	$C_{59}H_{102}O_6N$	920.7702	12.48	2.82E+08±1.85E+08
311	TG(51:9p)+H	TG	$C_{54}H_{87}O_5$	815.6548	12.50	3.22E+07±3.01E+06
312	TG(16:0/14:0/16:1)+NH_4	TG	$C_{49}H_{96}O_6N$	794.7232	12.51	9.15E+08±1.99E+08
313	TG(18:4/14:0/16:0)+H	TG	$C_{51}H_{91}O_6$	799.6810	12.51	1.64E+08±1.39E+07
314	TG(15:0/18:2/18:2)+NH_4	TG	$C_{54}H_{100}O_6N$	858.7545	12.57	1.38E+08±2.82E+07
315	TG(18:4/16:0/16:1)+H	TG	$C_{53}H_{93}O_6$	825.6967	12.62	3.39E+08±2.67E+07
316	TG(16:1/14:0/18:1)+NH_4	TG	$C_{51}H_{98}O_6N$	820.7389	12.65	2.39E+09±4.43E+08
317	TG(18:1/18:2/22:6)+NH_4	TG	$C_{61}H_{104}O_6N$	946.7858	12.66	9.46E+07±1.96E+07
318	TG(18:1/17:1/18:3)+NH_4	TG	$C_{56}H_{102}O_6N$	884.7702	12.70	7.89E+07±2.91E+07
319	TG(16:0/16:1/18:2)+NH_4	TG	$C_{53}H_{100}O_6N$	846.7545	12.74	4.19E+09±7.62E+08
320	TG(18:2/18:2/18:2)+NH_4	TG	$C_{57}H_{102}O_6N$	896.7702	12.77	1.08E+09±2.02E+08
321	TG(15:0/14:0/16:0)+NH_4	TG	$C_{48}H_{96}O_6N$	782.7232	12.80	4.19E+07±6.82E+06
322	TG(18:1/18:2/20:4)+NH_4	TG	$C_{59}H_{104}O_6N$	922.7858	12.85	4.01E+08±9.12E+07
323	ChE(20:5)+NH_4	ChE	$C_{47}H_{78}O_2N$	688.6027	12.86	1.53E+08±2.08E+07
324	TG(15:0/14:0/18:1)+NH_4	TG	$C_{50}H_{98}O_6N$	808.7389	12.87	1.15E+08±2.20E+07
325	TG(16:0/18:2/18:2)+NH_4	TG	$C_{55}H_{102}O_6N$	872.7702	12.94	6.86E+09±1.24E+09
326	TG(57:12p)+H	TG	$C_{60}H_{93}O_5$	893.7018	12.94	1.94E+08±1.10E+07
327	TG(18:1/18:2/18:2)+NH_4	TG	$C_{57}H_{104}O_6N$	898.7858	13.02	1.83E+09±4.41E+08
328	TG(15:0/16:1/18:1)+NH_4	TG	$C_{52}H_{100}O_6N$	834.7545	13.05	2.81E+08±4.97E+07
329	TG(15:0/18:1/18:2)+NH_4	TG	$C_{54}H_{102}O_6N$	860.7702	13.14	3.23E+08±5.65E+07
330	TG(16:0/18:1/22:6)+NH_4	TG	$C_{59}H_{104}O_6N$	922.7858	13.16	3.08E+08±6.58E+07
331	ChE(18:3)+NH_4	ChE	$C_{45}H_{78}O_2N$	664.6027	13.16	1.18E+08±2.12E+07
332	TG(16:0/14:0/18:3)+H	TG	$C_{51}H_{93}O_6$	801.6967	13.20	8.22E+07±5.75E+06

333	ChE(22:6)+NH_4	ChE	$C_{49}H_{80}O_2N$	714.6184	13.21	1.30E+08±1.86E+07
334	TG(16:0/14:0/16:0)+NH_4	TG	$C_{49}H_{98}O_6N$	796.7389	13.21	6.79E+08±1.31E+08
335	TG(18:1/18:1/22:6)+NH_4	TG	$C_{61}H_{106}O_6N$	948.8015	13.22	9.38E+07±2.84E+07
336	TG(18:1/17:1/18:2)+NH_4	TG	$C_{56}H_{104}O_6N$	886.7858	13.26	1.24E+08±2.66E+07
337	TG(53:9p)+H	TG	$C_{56}H_{91}O_5$	843.6861	13.28	6.32E+07±4.01E+06
338	TG(16:0/14:0/18:1)+NH_4	TG	$C_{51}H_{100}O_6N$	822.7545	13.28	2.86E+09±5.23E+08
339	DG(32:2p)+H	DG	$C_{35}H_{65}O_4$	549.4877	13.33	2.14E+07±2.64E+06
340	TG(55:11e)+H	TG	$C_{58}H_{93}O_5$	869.7018	13.36	1.19E+08±3.94E+06
341	TG(55:10p)+H	TG	$C_{58}H_{93}O_5$	869.7018	13.36	1.20E+08±4.31E+06
342	TG(16:0/18:1/20:4)+NH_4	TG	$C_{57}H_{104}O_6N$	898.7858	13.37	1.16E+09±1.83E+08
343	TG(16:0/16:0/18:2)+NH_4	TG	$C_{53}H_{102}O_6N$	848.7702	13.43	6.76E+09±1.04E+09
344	ChE(20:4)+NH_4	ChE	$C_{47}H_{80}O_2N$	690.6184	13.44	4.68E+08±6.47E+07
345	TG(18:1/18:1/20:4)+NH_4	TG	$C_{59}H_{106}O_6N$	924.8015	13.45	5.16E+08±7.18E+07
346	TG(15:0/16:0/16:0)+NH_4	TG	$C_{50}H_{100}O_6N$	810.7545	13.51	4.28E+07±3.25E+07
347	DG(34:3p)+H	DG	$C_{37}H_{67}O_4$	575.5034	13.52	2.94E+07±8.12E+06
348	TG(16:0/18:1/18:2)+NH_4	TG	$C_{55}H_{104}O_6N$	874.7858	13.56	1.01E+10±1.38E+09
349	DG(36:4p)+H	DG	$C_{39}H_{69}O_4$	601.5190	13.60	1.67E+07±3.80E+06
350	TG(18:1/18:1/18:2)+NH_4	TG	$C_{57}H_{106}O_6N$	900.8015	13.66	1.77E+09±2.37E+08
351	TG(18:1/18:1/22:5)+NH_4	TG	$C_{61}H_{108}O_6N$	950.8171	13.67	5.60E+07±1.88E+07
352	TG(15:0/16:0/18:1)+NH_4	TG	$C_{52}H_{102}O_6N$	836.7702	13.70	2.62E+08±3.46E+07
353	TG(16:0/17:1/18:1)+NH_4	TG	$C_{54}H_{104}O_6N$	862.7858	13.79	3.26E+08±4.97E+07
354	ChE(18:2)+NH_4	ChE	$C_{45}H_{80}O_2N$	666.6184	13.87	1.10E+09±1.80E+08
355	ChE(20:5)+H	ChE	$C_{47}H_{75}O_2$	671.5762	13.89	6.91E+07±3.22E+06
356	TG(17:0/18:1/18:2)+NH_4	TG	$C_{56}H_{106}O_6N$	888.8015	14.03	1.76E+08±3.31E+07
357	ChE(20:3)+NH_4	ChE	$C_{47}H_{82}O_2N$	692.6340	14.04	7.30E+07±9.23E+06
358	TG(53:8p)+H	TG	$C_{56}H_{93}O_5$	845.7018	14.07	2.05E+07±3.39E+06
359	TG(16:0/16:0/16:0)+NH_4	TG	$C_{51}H_{102}O_6N$	824.7702	14.10	1.22E+09±2.42E+08
360	TG(55:9p)+H	TG	$C_{58}H_{95}O_5$	871.7174	14.15	1.13E+08±2.42E+06
361	TG(18:1/18:1/20:3)+NH_4	TG	$C_{59}H_{108}O_6N$	926.8171	14.16	3.28E+08±1.09E+08
362	DG(32:1p)+H	DG	$C_{35}H_{67}O_4$	551.5034	14.16	2.92E+07±4.51E+06
363	TG(16:0/16:0/18:1)+NH_4	TG	$C_{53}H_{104}O_6N$	850.7858	14.19	6.05E+09±9.81E+08
364	DG(34:2p)+H	DG	$C_{37}H_{69}O_4$	577.5190	14.25	6.44E+07±1.01E+07
365	DG(36:3p)+H	DG	$C_{39}H_{71}O_4$	603.5347	14.30	2.49E+07±4.18E+06
366	TG(16:0/18:1/18:1)+NH_4	TG	$C_{55}H_{106}O_6N$	876.8015	14.30	9.93E+09±1.53E+09
367	TG(18:1/18:1/18:3)+H	TG	$C_{57}H_{101}O_6$	881.7593	14.31	8.62E+08±4.05E+07
368	TG(57:10p)+H	TG	$C_{60}H_{97}O_5$	897.7331	14.32	1.87E+08±5.58E+06
369	TG(18:1/18:1/22:4)+NH_4	TG	$C_{61}H_{110}O_6N$	952.8328	14.33	4.39E+07±7.69E+06
370	TG(18:0/18:1/18:2)+NH_4	TG	$C_{57}H_{108}O_6N$	902.8171	14.45	2.01E+09±3.57E+08
371	TG(16:0/16:0/17:0)+NH_4	TG	$C_{52}H_{104}O_6N$	838.7858	14.58	7.52E+07±1.73E+07
372	ChE(16:0)+NH_4	ChE	$C_{43}H_{80}O_2N$	642.6184	14.62	2.27E+07±5.03E+06
373	TG(20:1/18:1/18:2)+NH_4	TG	$C_{59}H_{110}O_6N$	928.8328	14.65	1.49E+08±3.72E+07
374	ChE(18:1)+NH_4	ChE	$C_{45}H_{82}O_2N$	668.6340	14.68	1.71E+08±3.50E+07
375	TG(16:0/17:0/18:1)+NH_4	TG	$C_{54}H_{106}O_6N$	864.8015	14.70	2.22E+08±4.65E+07
376	TG(17:0/18:1/18:1)+NH_4	TG	$C_{56}H_{108}O_6N$	890.8171	14.81	1.65E+08±3.29E+07
377	TG(55:8p)+H	TG	$C_{58}H_{97}O_5$	873.7331	15.15	3.92E+07±6.00E+06
378	TG(18:0/16:0/18:3)+H	TG	$C_{55}H_{101}O_6$	857.7593	15.16	1.78E+08±3.34E+07
379	TG(18:0/16:0/16:0)+NH_4	TG	$C_{53}H_{106}O_6N$	852.8015	15.18	6.15E+08±1.61E+08
380	TG(57:9p)+H	TG	$C_{60}H_{99}O_5$	899.7487	15.27	1.10E+08±1.39E+07
381	TG(18:0/16:0/20:4)+H	TG	$C_{57}H_{103}O_6$	883.7749	15.27	4.61E+08±7.63E+07
382	TG(18:0/16:0/18:1)+NH_4	TG	$C_{55}H_{108}O_6N$	878.8171	15.29	1.78E+09±4.37E+08
383	TG(18:0/18:1/18:1)+NH_4	TG	$C_{57}H_{110}O_6N$	904.8328	15.37	8.41E+08±2.10E+08
384	TG(18:0/18:1/20:4)+H	TG	$C_{59}H_{105}O_6$	909.7906	15.40	2.41E+08±3.94E+07
385	TG(20:1/18:1/18:1)+NH_4	TG	$C_{59}H_{112}O_6N$	930.8484	15.46	6.36E+07±1.46E+07
386	TG(18:0/17:0/18:1)+NH_4	TG	$C_{56}H_{110}O_6N$	892.8328	15.85	2.82E+07±5.38E+06
387	TG(18:0/16:0/20:3)+H	TG	$C_{57}H_{105}O_6$	885.7906	16.43	3.80E+07±8.35E+06
388	TG(18:0/16:0/18:0)+NH_4	TG	$C_{55}H_{110}O_6N$	880.8328	16.43	7.61E+07±1.82E+07
389	TG(18:0/18:0/18:1)+NH_4	TG	$C_{57}H_{112}O_6N$	906.8484	16.51	1.01E+08±2.26E+07
390	TG(18:0/18:1/20:3)+H	TG	$C_{59}H_{107}O_6$	911.8062	16.51	4.84E+07±1.04E+07
391	TG(18:0/18:1/20:1)+NH_4	TG	$C_{59}H_{114}O_6N$	932.8641	16.61	2.82E+07±6.38E+06

Table A.3: Peak area and RT exported by Trace Finder of 48 different adducts of deuterated compounds present in SPLASH®.

Adduct	Precursor Mass	SPLASH (1:10)		SPLASH (1:5)		Extracted-SPLASH (10 µL)		Extracted-SPLASH (20 µL)	
		Peak Area	RT (min)	Peak Area	RT (min)	Peak Area	RT (min)	Peak Area	RT (min)
18:1(d7) Chol Ester ($C_{45}H_{71}D_7O_2$)									
M+3H	220.2217	-	-	-	-	-	-	-	-
M+2H+Na	227.5490	-	-	-	-	6.91E+04	9.96	-	-
M+H+2Na	234.9806	-	-	-	-	-	-	-	-
M+3Na	242.2037	-	-	-	-	-	-	-	-
M+2H	329.8290	-	-	-	-	-	-	-	-
M+H+NH_4	338.3422	4.27E+08	8.01	6.28E+08	8	3.78E+08	8.01	6.40E+08	8.01
M+H+Na	340.8199	-	-	-	-	-	-	-	-
M+H+K	348.8069	-	-	-	-	-	-	-	-
M+ACN+2H	350.3422	-	-	3.42E+04	7.93	3.18E+04	8.58	-	-
M+2Na	351.8109	3.97E+04	11.69	-	-	-	-	1.66E+04	16.12
M+2ACN+2H	370.8555	-	-	-	-	-	-	-	-
M+3ACN+2H	391.3688	-	-	-	-	-	-	-	-
M-H_2O+H	640.6401	-	-	-	-	-	-	-	-
M+H	658.6507	4.30E+05	14.56	1.53E+06	14.59	1.10E+05	14.55	1.98E+05	14.56
M+NH4	675.6772	1.20E+08	14.58	3.01E+08	14.55	4.03E+07	14.55	6.70E+07	14.6
M+Na	680.6326	2.41E+07	14.56	3.81E+07	14.53	1.12E+07	14.55	1.58E+07	14.58
M+CH_3OH+H	690.6769	-	-	-	-	-	-	-	-
M+K	696.6065	9.94E+06	14.56	1.68E+07	14.53	5.80E+06	14.57	7.20E+06	14.6
M+ACN+H	699.6772	-	-	-	-	-	-	-	-
M+2Na-H	702.6145	-	-	3.06E+05	7.57	-	-	4.12E+04	7.59
M+IsoProp+H	718.7087	4.04E+05	14.6	1.28E+06	14.55	-	-	2.89E+05	14.61
M+ACN+Na	721.6591	-	-	-	-	-	-	-	-
M+2K+H	734.5624	-	-	-	-	-	-	8.07E+04	8.78
M+DMSO+H	736.6646	-	-	-	-	-	-	-	-
M+2ACN+H	740.7037	-	-	-	-	-	-	-	-
M+IsoProp+Na+H	741.6985	-	-	-	-	-	-	-	-
2M+H	1316.2940	8.93E+06	9.56	8.51E+06	9.57	7.44E+05	14.57	1.11E+06	9.55
2M+NH_4	1333.3206	8.89E+07	14.58	2.42E+08	14.55	2.40E+07	14.53	4.42E+07	14.58
2M+Na	1338.2760	5.20E+07	14.56	8.32E+07	14.53	2.38E+07	14.57	3.39E+07	14.58
2M+3H_2O+2H	1343.3099	4.23E+04	11.63	4.78E+04	11.63	9.74E+03	4.06	7.75E+03	19.43
2M+K	1354.2499	6.48E+06	14.56	1.18E+07	14.51	3.08E+06	14.53	4.20E+06	14.58
2M+ACN+H	1357.3206	7.95E+06	11.73	2.59E+07	11.65	7.57E+06	11.64	2.62E+06	11.74
2M+ACN+Na	1379.3025	9.23E+04	11.65	2.03E+05	11.66	-	-	2.84E+04	11.73
M-3H	218.2072	-	-	-	-	-	-	-	-
M-2H	327.8144	-	-	-	-	-	-	-	-
M-H_2O-H	638.6250	-	-	-	-	-	-	-	-
M-H	656.6361	-	-	-	-	-	-	-	-
M+Na-2H	678.6180	-	-	6.97E+03	19.93	2.43E+04	6.47	-	-
M+Cl	692.6128	-	-	-	-	-	-	-	-
M+K-2H	694.5920	-	-	-	-	-	-	-	-
M+FA-H	702.6416	-	-	-	-	-	-	-	-
M+Hac-H	716.6572	-	-	-	-	-	-	-	-
M+Br	736.5623	2.78E+05	9.04	1.34E+05	9.03	4.03E+04	10	1.92E+05	8.96
M+TFA-H	770.6290	-	-	-	-	-	-	-	-
2M-H	1314.2795	5.04E+04	8.06	1.43E+04	3.36	-	-	-	-
2M+FA-H	1360.2850	-	-	-	-	-	-	-	-
2M+Hac-H	1374.3006	-	-	-	-	-	-	-	-
3M-H	1973.9374	-	-	-	-	-	-	-	-
Cholesterol (d7) ($C_{27}H_{39}D_7O$)									
M+3H	132.1400	-	-	-	-	-	-	-	-
M+2H+Na	139.4673	-	-	-	-	-	-	-	-
M+H+2Na	146.8989	-	-	-	-	-	-	-	-
M+3Na	154.1219	1.43E+07	0.63	1.77E+06	0.67	1.51E+06	0.63	9.89E+05	0.61
M+2H	197.7063	-	-	-	-	-	-	-	-
M+H+NH_4	206.2196	-	-	-	-	-	-	-	-
M+H+Na	208.6973	-	-	-	-	-	-	-	-

M+H+K	216.6843	-	-	-	-	-	-	-	-
M+ACN+2H	218.2196	-	-	-	-	-	-	-	-
M+2Na	219.6883	-	-	-	-	-	-	-	-
M+2ACN+2H	238.7329	-	-	-	-	-	-	-	-
M+3ACN+2H	259.2461	3.30E+04	11.16	2.15E+04	15.92	2.00E+04	13.63	4.33E+04	8.46
M-H_2O+H	376.3948	1.01E+06	8.94	1.79E+06	8.93	-	-	6.73E+05	8.93
M+H	394.4054	-	-	-	-	-	-	-	-
M+NH_4	411.4319	-	-	-	-	-	-	-	-
M+Na	416.3873	-	-	1.91E+04	15.18	2.28E+04	8.14	-	-
M+CH_3OH+H	426.4316	2.23E+05	10.58	6.46E+05	7.41	1.10E+06	7.78	6.71E+05	7.78
M+K	432.3612	-	-	-	-	-	-	-	-
M+ACN+H	435.4319	-	-	8.56E+04	8.4	-	-	-	-
M+2Na-H	438.3692	-	-	-	-	-	-	-	-
M+IsoProp+H	454.4634	7.24E+06	7.88	1.30E+07	7.87	1.16E+07	7.86	1.11E+07	7.87
M+ACN+Na	457.4138	1.13E+05	5.52	4.20E+05	5.48	2.60E+04	5.33	5.59E+05	5.65
M+2K+H	470.3171	2.27E+04	8.5	2.59E+04	15.54	2.48E+04	14.97	2.02E+04	15.72
M+DMSO+H	472.4193	6.77E+05	7.35	5.93E+05	7.34	8.50E+05	7.34	9.01E+05	7.36
M+2ACN+H	476.4584	-	-	-	-	-	-	-	-
M+IsoProp+Na+H	477.4532	-	-	-	-	-	-	-	-
2M+H	787.8034	-	-	3.90E+04	1.74	-	-	-	-
2M+NH_4	804.8300	-	-	-	-	-	-	-	-
2M+Na	809.7854	-	-	-	-	9.66E+03	4.47	-	-
2M+3H_2O+2H	814.8193	-	-	-	-	-	-	-	-
2M+K	825.7593	1.41E+05	12.74	3.81E+04	12.73	2.77E+04	12.7	2.07E+05	11.29
2M+ACN+H	828.8300	-	-	-	-	-	-	-	-
2M+ACN+Na	850.8119	-	-	-	-	-	-	-	-
M-3H	130.1254	6.27E+04	8.68	-	-	-	-	-	-
M-2H	195.6918	-	-	-	-	-	-	-	-
M-H_2O-H	374.3797	-	-	-	-	-	-	-	-
M-H	392.3908	-	-	-	-	-	-	-	-
M+Na-2H	414.3727	-	-	-	-	-	-	-	-
M+Cl	428.3675	-	-	-	-	-	-	-	-
M+K-2H	430.3467	-	-	-	-	-	-	-	-
M+FA-H	438.3963	-	-	-	-	-	-	-	-
M+Hac-H	452.4119	-	-	-	-	-	-	-	-
M+Br	472.3170	-	-	-	-	-	-	-	-
M+TFA-H	506.3837	-	-	-	-	-	-	8.61E+04	8.17
2M-H	785.7889	-	-	-	-	9.13E+03	2.4	9.32E+03	1.85
2M+FA-H	831.7943	-	-	5.12E+04	16.27	-	-	-	-
2M+Hac-H	845.8100	-	-	-	-	-	-	-	-
3M-H	1181.2015	-	-	-	-	7.69E+03	2.92	8.98E+03	4.04
15:0-18:1(d7) DG ($C_{36}H_{61}D_7O_5$)									
M+3H	196.8572	-	-	-	-	-	-	-	-
M+2H+Na	204.1845	8.86E+03	4.4	6.64E+03	19.29	-	-	1.44E+04	7.53
M+H+2Na	211.6161	-	-	-	-	-	-	-	-
M+3Na	218.8392	-	-	-	-	-	-	-	-
M+2H	294.7822	-	-	-	-	-	-	-	-
M+H+NH_4	303.2955	-	-	-	-	-	-	-	-
M+H+Na	305.7732	-	-	-	-	-	-	-	-
M+H+K	313.7602	-	-	-	-	-	-	-	-
M+ACN+2H	315.2955	-	-	8.94E+03	2.24	-	-	-	-
M+2Na	316.7642	-	-	-	-	-	-	-	-
M+2ACN+2H	335.8088	-	-	-	-	-	-	-	-
M+3ACN+2H	356.3220	-	-	-	-	1.53E+04	19.49	-	-
M-H_2O+H	570.5466	2.95E+08	8.67	3.98E+08	8.67	1.14E+08	8.65	2.64E+08	8.67
M+H	588.5572	1.27E+07	9.71	2.10E+07	9.7	5.08E+06	9.67	1.17E+07	9.72
M+NH_4	605.5837	1.08E+09	9.71	1.63E+09	9.7	5.33E+08	9.69	1.00E+09	9.71
M+Na	610.5391	2.97E+08	9.71	4.36E+08	9.7	1.84E+08	9.69	2.84E+08	9.71
M+CH_3OH+H	620.5834	-	-	-	-	1.72E+05	9.33	1.42E+05	9.37
M+K	626.5130	3.05E+07	9.71	5.09E+07	9.72	2.27E+07	9.69	3.17E+07	9.71
M+ACN+H	629.5837	-	-	-	-	-	-	-	-
M+2Na-H	632.5210	7.89E+05	7.86	-	-	-	-	-	-
M+IsoProp+H	648.6152	7.31E+04	9.79	7.43E+05	9.76	1.06E+05	9.73	2.28E+05	9.74
M+ACN+Na	651.5656	4.41E+04	8.09	-	-	7.62E+04	8.9	1.33E+05	8.91
M+2K+H	664.4689	-	-	-	-	-	-	-	-
M+DMSO+H	666.5711	-	-	-	-	-	-	-	-
M+2ACN+H	670.6102	-	-	8.42E+03	4.75	-	-	-	-

M+IsoProp+Na+H	671.6050	-	-	-	-	-	-	-	-
2M+H	1176.1070	1.42E+04	0.67	6.05E+04	9.79	-	-	-	-
2M+NH_4	1193.1336	-	-	5.70E+05	9.7	1.47E+04	1.39	-	-
2M+Na	1198.0890	1.13E+07	9.71	2.52E+07	9.7	3.85E+06	9.69	9.60E+06	9.69
2M+3H_2O+2H	1203.1229	2.34E+04	5.06	2.38E+04	14.83	-	-	-	-
2M+K	1214.0629	-	-	1.16E+04	1.62	-	-	-	-
2M+ACN+H	1217.1336	3.84E+04	12	4.31E+04	10.68	7.48E+03	4.38	-	-
2M+ACN+Na	1239.1155	-	-	-	-	9.15E+03	4.12	2.36E+04	0.61
M-3H	194.8427	-	-	-	-	-	-	-	-
M-2H	292.7677	-	-	-	-	-	-	-	-
M-H_2O-H	568.5315	-	-	-	-	-	-	-	-
M-H	586.5426	-	-	-	-	-	-	-	-
M+Na-2H	608.5245	-	-	-	-	-	-	-	-
M+Cl	622.5193	4.82E+07	9.7	8.34E+07	9.69	2.83E+07	9.7	4.90E+07	9.7
M+K-2H	624.4985	-	-	-	-	-	-	4.75E+04	9.28
M+FA-H	632.5481	1.29E+06	9.72	2.78E+06	9.69	1.03E+06	9.7	2.04E+06	9.7
M+Hac-H	646.5637	2.85E+08	9.7	4.60E+08	9.69	1.50E+08	9.7	2.74E+08	9.7
M+Br	666.4688	-	-	1.12E+05	17.7	-	-	-	-
M+TFA-H	700.5355	-	-	-	-	5.40E+04	9.15	-	-
2M-H	1174.0925	-	-	-	-	8.81E+03	1.62	-	-
2M+FA-H	1220.0980	-	-	-	-	-	-	-	-
2M+Hac-H	1234.1136	-	-	1.66E+04	5.26	-	-	5.17E+04	17.94
3M-H	1763.6569	-	-	-	-	-	-	-	-
18:1(d7) LPC ($C_{26}H_{45}D_7NO_7P$)									
M+3H	177.1377	3.25E+04	5.44	2.60E+04	16.98	3.35E+04	11.03	3.54E+04	12.73
M+2H+Na	184.4650	-	-	-	-	-	-	-	-
M+H+2Na	191.8966	-	-	-	-	-	-	-	-
M+3Na	199.1197	-	-	-	-	1.85E+04	13.81	1.58E+04	14.08
M+2H	265.2030	-	-	2.44E+04	16.49	5.19E+05	0.88	7.73E+05	0.88
M+H+NH_4	273.7162	-	-	-	-	-	-	-	-
M+H+Na	276.1939	3.76E+06	1.56	1.45E+06	11.82	6.81E+05	10.69	5.20E+05	11.14
M+H+K	284.1809	-	-	-	-	-	-	-	-
M+ACN+2H	285.7162	-	-	-	-	-	-	-	-
M+2Na	287.1849	2.27E+06	7.44	1.59E+06	8.4	6.31E+05	10.69	1.70E+06	7.44
M+2ACN+2H	306.2295	1.74E+05	16.6	1.66E+05	14.78	1.76E+05	6.17	1.18E+05	17.7
M+3ACN+2H	326.7428	-	-	-	-	-	-	-	-
M-H_2O+H	511.3880	3.38E+06	5.61	4.45E+06	5.6	1.32E+06	5.6	3.10E+06	5.62
M+H	529.3986	5.43E+09	5.61	8.40E+09	5.6	1.88E+09	5.61	4.53E+09	5.62
M+NH_4	546.4252	-	-	9.09E+03	2.86	8.01E+04	9.54	-	-
M+Na	551.3806	3.78E+08	5.61	5.84E+08	5.6	1.33E+08	5.61	3.30E+08	5.62
M+CH_3OH+H	561.4248	-	-	7.57E+04	7.83	5.50E+04	9.81	-	-
M+K	567.3545	4.57E+07	5.61	8.07E+07	5.6	1.36E+07	5.6	4.05E+07	5.62
M+ACN+H	570.4252	2.33E+04	6.01	2.23E+04	12.61	3.64E+04	11.89	2.93E+04	11.42
M+2Na-H	573.3625	2.14E+04	12.72	2.70E+04	15.08	2.91E+04	12.15	2.25E+04	16.21
M+IsoProp+H	589.4567	1.18E+07	5.61	5.26E+07	5.6	4.41E+06	5.61	2.26E+07	5.62
M+ACN+Na	592.4071	3.82E+04	11.41	-	-	1.88E+06	5.75	1.75E+06	5.75
M+2K+H	605.3104	-	-	-	-	-	-	-	-
M+DMSO+H	607.4126	5.17E+04	13.95	8.92E+04	16.56	9.23E+04	13.2	6.17E+04	17.09
M+2ACN+H	611.4517	-	-	-	-	1.27E+04	5.92	-	-
M+IsoProp+Na+H	612.4465	-	-	-	-	-	-	-	-
2M+H	1057.7900	2.37E+07	5.61	8.20E+07	5.6	1.41E+06	5.61	1.43E+07	5.62
2M+NH_4	1074.8165	-	-	-	-	-	-	-	-
2M+Na	1079.7719	4.65E+06	5.61	2.07E+07	5.6	6.55E+04	5.6	3.06E+06	5.62
2M+3H_2O+2H	1084.8058	8.52E+03	1.91	-	-	-	-	3.23E+04	11.14
2M+K	1095.7459	3.75E+04	18.63	1.54E+06	5.62	-	-	5.07E+04	5.62
2M+ACN+H	1098.8165	-	-	-	-	-	-	-	-
2M+ACN+Na	1120.7985	-	-	-	-	-	-	7.12E+03	0.32
M-3H	175.1232	-	-	-	-	-	-	-	-
M-2H	263.1884	3.48E+05	12.99	1.46E+05	12.01	3.07E+05	12.01	5.64E+05	15.33
M-H_2O-H	509.3730	-	-	-	-	-	-	-	-
M-H	527.3841	-	-	-	-	-	-	-	-
M+Na-2H	549.3660	-	-	2.61E+05	13.15	3.91E+05	14.84	-	-
M+Cl	563.3608	1.90E+07	5.6	2.60E+07	5.61	7.76E+06	5.6	1.50E+07	5.61
M+K-2H	565.3400	1.26E+05	16.68	6.11E+04	10.52	-	-	5.91E+04	15.79
M+FA-H	573.3896	9.41E+06	5.6	1.29E+07	5.61	3.43E+06	5.6	7.62E+06	5.61
M+Hac-H	587.4052	1.23E+09	5.6	1.81E+09	5.61	4.69E+08	5.6	1.06E+09	5.61
M+Br	607.3102	-	-	-	-	5.61E+04	16.35	1.26E+04	5.05

M+TFA-H	641.3769	6.91E+03	19.95	5.63E+04	14.77	5.19E+04	17.6	-	-
2M-H	1055.7754	8.11E+03	0.72	-	-	-	-	-	-
2M+FA-H	1101.7809	-	-	2.49E+04	5.55	-	-	6.71E+04	17.77
2M+Hac-H	1115.7965	1.33E+07	5.6	2.71E+07	5.61	2.28E+06	5.6	1.02E+07	5.61
3M-H	1586.1813	-	-	-	-	-	-	-	-
18:1(d7) LPE ($C_{23}H_{39}D_7NO_7P$)									
M+3H	163.1221	1.13E+06	0.76	1.24E+06	0.74	5.03E+05	0.75	3.01E+05	0.71
M+2H+Na	170.4494	-	-	-	-	-	-	-	-
M+H+2Na	177.8810	-	-	-	-	-	-	-	-
M+3Na	185.1040	-	-	-	-	-	-	-	-
M+2H	244.1795	-	-	-	-	-	-	-	-
M+H+NH_4	252.6928	-	-	-	-	-	-	-	-
M+H+Na	255.1704	4.65E+05	0.61	2.65E+05	0.63	4.27E+05	0.65	6.71E+05	0.67
M+H+K	263.1574	1.45E+05	8.94	2.46E+04	18.2	-	-	-	-
M+ACN+2H	264.6928	-	-	6.45E+03	19.82	-	-	-	-
M+2Na	266.1614	3.96E+05	12.95	-	-	-	-	4.12E+05	0.63
M+2ACN+2H	285.2060	1.80E+06	8.09	9.65E+05	9.79	1.41E+06	8.86	5.08E+05	9.35
M+3ACN+2H	305.7193	-	-	-	-	-	-	-	-
M-H_2O+H	469.3411	1.63E+06	5.73	2.83E+06	5.73	5.16E+05	5.73	1.10E+06	5.73
M+H	487.3517	7.07E+08	5.73	1.10E+09	5.73	2.60E+08	5.75	5.98E+08	5.73
M+NH4	504.3782	1.39E+04	4.69	1.23E+04	4.58	1.88E+05	4.96	2.33E+05	5.04
M+Na	509.3336	3.38E+07	5.73	4.97E+07	5.73	1.30E+07	5.75	2.94E+07	5.73
M+CH_3OH+H	519.3779	4.96E+04	6.74	2.55E+05	6.86	2.67E+05	6.84	1.25E+06	6.82
M+K	525.3076	1.02E+05	13.82	1.62E+05	5.65	7.43E+04	14.64	5.46E+04	5.87
M+ACN+H	528.3782	-	-	-	-	-	-	-	-
M+2Na-H	531.3156	2.04E+06	5.75	3.03E+06	5.75	9.18E+05	5.77	1.90E+06	5.75
M+IsoProp+H	547.4097	3.33E+05	6.34	1.24E+05	5.73	7.78E+04	8.22	-	-
M+ACN+Na	550.3602	3.25E+04	16.12	3.14E+04	10.7	3.51E+04	8.01	-	-
M+2K+H	563.2634	-	-	-	-	1.68E+06	3.25	1.98E+06	3.25
M+DMSO+H	565.3656	4.89E+05	14.47	5.83E+05	14.95	-	-	2.92E+05	14.65
M+2ACN+H	569.4048	1.76E+04	6.97	4.88E+04	6.8	3.75E+04	6.96	7.44E+04	6.84
M+IsoProp+Na+H	570.3995	2.78E+04	16.96	6.12E+04	10.06	5.27E+04	13.2	1.99E+04	6.92
2M+H	973.6961	3.26E+06	5.73	9.02E+06	5.73	3.03E+05	5.75	2.49E+06	5.73
2M+NH4	990.7226	-	-	-	-	3.04E+04	11.15	6.94E+03	2.47
2M+Na	995.6780	4.79E+05	5.75	1.27E+06	5.75	3.88E+04	5.77	4.49E+05	5.75
2M+3H_2O+2H	1000.7119	-	-	-	-	-	-	-	-
2M+K	1011.6520	-	-	-	-	-	-	8.55E+03	4.52
2M+ACN+H	1014.7226	2.37E+05	9.71	-	-	-	-	9.65E+03	19.65
2M+ACN+Na	1036.7046	-	-	-	-	-	-	-	-
M-3H	161.1075	5.77E+03	1.96	-	-	1.03E+04	4.7	-	-
M-2H	242.1649	-	-	-	-	-	-	-	-
M-H_2O-H	467.3260	-	-	-	-	-	-	-	-
M-H	485.3371	4.03E+08	5.74	6.52E+08	5.74	1.50E+08	5.74	3.42E+08	5.74
M+Na-2H	507.3191	6.15E+05	13.26	4.95E+05	14.69	5.67E+05	13.17	-	-
M+Cl	521.3138	5.13E+04	16.55	5.23E+04	15.13	4.80E+04	13.38	5.51E+04	16.61
M+K-2H	523.2930	-	-	1.67E+05	14.22	2.00E+05	14.01	1.45E+05	16.74
M+FA-H	531.3426	-	-	-	-	8.17E+03	1.71	-	-
M+Hac-H	545.3583	-	-	-	-	-	-	-	-
M+Br	565.2633	5.28E+04	15.35	6.64E+04	9.13	6.60E+04	12.05	4.77E+04	9.15
M+TFA-H	599.3300	1.23E+04	4.49	-	-	-	-	-	-
2M-H	971.6815	1.42E+06	5.74	3.35E+06	5.74	7.78E+04	5.74	9.48E+05	5.74
2M+FA-H	1017.6870	7.79E+03	2.86	-	-	8.64E+03	4.46	-	-
2M+Hac-H	1031.7027	-	-	-	-	-	-	-	-
3M-H	1460.0405	-	-	1.57E+04	2.76	3.16E+04	8.04	-	-
18:1(d7) MG ($C_{21}H_{33}D_7O_4$)									
M+3H	122.1192	-	-	-	-	-	-	-	-
M+2H+Na	129.4465	-	-	-	-	-	-	-	-
M+H+2Na	136.8781	-	-	-	-	-	-	-	-
M+3Na	144.1012	2.37E+06	5.73	3.81E+06	10.44	1.79E+06	8.82	1.41E+06	11.12
M+2H	182.6752	-	-	-	-	-	-	-	-
M+H+NH_4	191.1885	-	-	-	-	-	-	-	-
M+H+Na	193.6662	-	-	-	-	-	-	-	-
M+H+K	201.6532	-	-	-	-	-	-	-	-
M+ACN+2H	203.1885	-	-	-	-	6.79E+03	1.27	-	-
M+2Na	204.6572	-	-	-	-	-	-	-	-
M+2ACN+2H	223.7018	-	-	1.77E+04	17.53	-	-	-	-
M+3ACN+2H	244.2150	7.79E+04	14.64	2.49E+05	14.57	-	-	-	-

M-H_2O+H	346.3326	3.17E+07	9.69	4.62E+07	9.7	1.66E+07	9.69	2.90E+07	9.71
M+H	364.3431	3.05E+07	6.83	2.93E+07	6.82	2.08E+07	6.8	2.70E+07	6.82
M+NH4	381.3697	1.56E+07	6.83	2.45E+07	6.82	6.99E+06	6.82	1.58E+07	6.84
M+Na	386.3251	1.62E+07	6.83	2.16E+07	6.82	6.43E+06	6.82	1.41E+07	6.82
M+CH_3OH+H	396.3694	-	-	-	-	-	-	-	-
M+K	402.2990	1.02E+06	6.83	2.13E+06	6.82	5.75E+05	6.82	1.36E+06	6.82
M+ACN+H	405.3697	1.31E+06	6.55	7.89E+06	6.63	7.87E+06	6.65	8.38E+06	6.69
M+2Na-H	408.3070	5.70E+07	6.91	2.61E+07	6.9	2.81E+07	7.09	3.07E+07	7.11
M+IsoProp+H	424.4012	2.07E+04	4.91	1.36E+04	18.75	-	-	-	-
M+ACN+Na	427.3516	5.91E+05	16.94	1.78E+06	5.96	4.70E+05	17.17	9.00E+05	5.87
M+2K+H	440.2549	-	-	-	-	-	-	-	-
M+DMSO+H	442.3571	-	-	-	-	2.36E+04	14.24	1.88E+04	7.28
M+2ACN+H	446.3962	1.30E+06	6.34	-	-	-	-	-	-
M+IsoProp+Na+H	447.3910	3.03E+05	6.93	1.62E+05	6.92	2.82E+05	7.07	6.55E+05	6.9
2M+H	727.6790	-	-	-	-	-	-	-	-
2M+NH4	744.7056	-	-	-	-	-	-	-	-
2M+Na	749.6610	-	-	2.75E+05	6.82	-	-	1.80E+04	6.86
2M+3H_2O+2H	754.6949	8.84E+05	11.9	4.92E+05	12.08	1.03E+06	11.94	-	-
2M+K	765.6349	-	-	-	-	1.84E+04	18.09	1.97E+04	14.94
2M+ACN+H	768.7056	2.64E+06	12.39	2.41E+06	12.4	3.75E+06	12.38	3.70E+06	12.39
2M+ACN+Na	790.6875	5.28E+04	11.63	3.13E+04	11.55	2.96E+04	11.53	-	-
M-3H	120.1047	-	-	-	-	6.64E+03	4.44	-	-
M-2H	180.6607	-	-	-	-	4.21E+04	14.65	-	-
M-H_2O-H	344.3175	-	-	-	-	-	-	-	-
M-H	362.3286	-	-	-	-	-	-	-	-
M+Na-2H	384.3105	3.22E+06	4.92	3.08E+04	4.88	-	-	1.31E+04	4.93
M+Cl	398.3053	7.63E+07	6.82	1.06E+08	6.83	2.98E+07	6.81	6.41E+07	6.83
M+K-2H	400.2845	-	-	-	-	-	-	-	-
M+FA-H	408.3341	6.59E+06	6.84	1.14E+07	6.83	2.85E+06	6.81	6.43E+06	6.81
M+Hac-H	422.3497	3.54E+08	6.82	4.98E+08	6.83	1.37E+08	6.81	3.02E+08	6.83
M+Br	442.2548	6.79E+06	7.26	7.33E+06	7.19	1.65E+07	7.12	1.97E+07	7.14
M+TFA-H	476.3215	5.03E+04	16.76	6.97E+04	6.79	2.94E+04	7.92	5.14E+04	13.12
2M-H	725.6645	-	-	4.93E+04	13.1	-	-	9.47E+04	7.88
2M+FA-H	771.6699	6.82E+03	0.09	-	-	-	-	-	-
2M+Hac-H	785.6856	-	-	-	-	-	-	-	-
3M-H	1091.0149	-	-	-	-	9.12E+03	2.4	-	-
15:0-18:1(d7) PA (Na Salt) ($C_{36}H_{61}D_7NaO_8P$)									
M+3H	223.5127	-	-	-	-	-	-	-	-
M+2H+Na	230.8400	-	-	-	-	-	-	-	-
M+H+2Na	238.2716	-	-	-	-	-	-	-	-
M+3Na	245.4946	-	-	-	-	-	-	-	-
M+2H	334.7654	-	-	-	-	-	-	-	-
M+H+NH_4	343.2787	8.32E+04	1.93	-	-	-	-	-	-
M+H+Na	345.7564	-	-	-	-	-	-	-	-
M+H+K	353.7433	-	-	-	-	-	-	-	-
M+ACN+2H	355.2787	-	-	-	-	-	-	-	-
M+2Na	356.7473	-	-	-	-	-	-	-	-
M+2ACN+2H	375.7919	-	-	-	-	-	-	-	-
M+3ACN+2H	396.3052	7.31E+04	9.41	1.82E+05	9.36	1.12E+05	8.92	-	-
M-H_2O+H	650.5129	-	-	3.48E+04	7.87	-	-	2.47E+04	7.8
M+H	668.5235	4.62E+05	9.09	1.15E+06	9.17	7.00E+04	9.13	1.33E+06	9.14
M+NH_4	685.5500	3.67E+07	9.13	1.31E+08	9.14	4.09E+07	9.07	1.32E+08	9.12
M+Na	690.5054	1.68E+06	9.15	2.77E+07	9.19	6.20E+06	9.37	1.35E+07	9.31
M+CH_3OH+H	700.5497	1.25E+05	7.12	1.03E+05	7.15	2.16E+04	16.07	8.72E+04	8.69
M+K	706.4794	-	-	1.74E+05	9.53	-	-	9.69E+04	8.91
M+ACN+H	709.5500	-	-	2.16E+05	9.06	3.65E+05	8.99	1.23E+05	8.82
M+2Na-H	712.4874	-	-	2.12E+06	9.57	5.22E+05	7.05	4.25E+05	9.59
M+IsoProp+H	728.5815	7.77E+04	8.69	4.93E+04	8.72	5.63E+04	15.31	1.34E+05	8.69
M+ACN+Na	731.5320	-	-	-	-	-	-	1.57E+04	6.02
M+2K+H	744.4352	2.30E+04	16.25	2.16E+04	5.98	5.29E+04	4.76	-	-
M+DMSO+H	746.5374	-	-	8.01E+03	3.84	-	-	-	-
M+2ACN+H	750.5766	-	-	-	-	-	-	-	-
M+IsoProp+Na+H	751.5713	1.61E+05	7.27	2.25E+05	7.28	5.57E+04	7.26	1.51E+05	7.28
2M+H	1336.0397	1.61E+04	1.78	-	-	-	-	1.51E+04	18.56
2M+NH_4	1353.0662	-	-	-	-	8.10E+03	19.71	9.61E+03	6.21
2M+Na	1358.0216	-	-	-	-	-	-	1.53E+04	4.79
2M+3H_2O+2H	1363.0555	-	-	2.44E+04	18.6	-	-	-	-

2M+K	1373.9956	3.70E+04	6.76	-	-	9.69E+03	1.27	-	-
2M+ACN+H	1377.0662	8.20E+03	19.56	1.82E+04	18.28	-	-	-	-
2M+ACN+Na	1399.0482	3.81E+04	5.31	8.92E+03	2.71	1.73E+04	7.86	-	-
M-3H	221.4981	-	-	-	-	-	-	-	-
M-2H	332.7508	-	-	-	-	-	-	-	-
M-H_2O-H	648.4978	3.73E+04	8.55	-	-	-	-	-	-
M-H	666.5089	2.98E+07	9.25	9.79E+07	9.18	2.79E+07	9.1	7.11E+07	9.09
M+Na-2H	688.4909	-	-	-	-	-	-	-	-
M+Cl	702.4856	6.70E+04	14.74	1.27E+06	9.3	4.64E+04	9.29	7.95E+05	9.28
M+K-2H	704.4648	-	-	-	-	-	-	-	-
M+FA-H	712.5144	8.98E+04	8.31	8.18E+04	8.3	4.60E+04	7.25	-	-
M+Hac-H	726.5301	1.79E+06	8.51	3.40E+06	8.5	5.99E+05	8.49	1.63E+06	8.51
M+Br	746.4351	-	-	-	-	-	-	7.59E+03	3.75
M+TFA-H	780.5018	-	-	-	-	-	-	-	-
2M-H	1334.0251	-	-	-	-	8.91E+03	0.89	-	-
2M+FA-H	1380.0306	-	-	-	-	-	-	-	-
2M+Hac-H	1394.0463	-	-	-	-	-	-	-	-
3M-H	2003.5559	-	-	-	-	-	-	-	-
15:0-18:1(d7) PC ($C_{41}H_{73}D_7NO_8P$)									
M+3H	251.8757	-	-	-	-	-	-	-	-
M+2H+Na	259.2030	9.00E+05	13.61	1.69E+06	13.69	9.53E+05	12.49	7.77E+05	13.66
M+H+2Na	266.6346	-	-	-	-	-	-	-	-
M+3Na	273.8577	-	-	-	-	1.21E+05	8.99	-	-
M+2H	377.3100	-	-	-	-	1.60E+06	2.47	2.82E+04	2.51
M+H+NH_4	385.8232	-	-	-	-	-	-	-	-
M+H+Na	388.3009	-	-	-	-	-	-	-	-
M+H+K	396.2879	1.22E+05	8.81	-	-	-	-	-	-
M+ACN+2H	397.8232	-	-	-	-	-	-	-	-
M+2Na	399.2919	1.45E+04	1.41	6.05E+04	8.89	-	-	-	-
M+2ACN+2H	418.3365	2.44E+06	5.31	2.63E+04	5.48	8.28E+05	2.49	9.27E+04	6.11
M+3ACN+2H	438.8498	-	-	-	-	-	-	-	-
M-H_2O+H	735.6021	-	-	-	-	-	-	-	-
M+H	753.6126	1.90E+10	8.99	2.40E+10	8.99	9.82E+09	8.98	1.77E+10	8.99
M+NH_4	770.6392	-	-	1.19E+05	9.15	-	-	9.84E+04	7.63
M+Na	775.5946	1.06E+09	8.98	1.17E+09	9.06	7.95E+08	8.99	1.06E+09	8.99
M+CH_3OH+H	785.6388	-	-	-	-	-	-	-	-
M+K	791.5685	1.20E+08	9.05	1.41E+08	9.02	8.51E+07	8.99	1.19E+08	8.99
M+ACN+H	794.6392	-	-	-	-	-	-	-	-
M+2Na-H	797.5765	-	-	-	-	4.70E+04	0.53	-	-
M+IsoProp+H	813.6707	2.07E+08	8.98	2.52E+08	8.95	1.42E+08	8.98	1.98E+08	8.97
M+ACN+Na	816.6211	-	-	-	-	-	-	-	-
M+2K+H	829.5244	-	-	2.89E+05	9.14	1.85E+05	9.01	1.04E+04	4.03
M+DMSO+H	831.6266	-	-	-	-	-	-	-	-
M+2ACN+H	835.6657	-	-	-	-	-	-	-	-
M+IsoProp+Na+H	836.6605	-	-	-	-	-	-	-	-
2M+H	1506.2180	-	-	-	-	-	-	-	-
2M+NH_4	1523.2445	-	-	-	-	-	-	-	-
2M+Na	1528.1999	-	-	-	-	-	-	-	-
2M+3H_2O+2H	1533.2338	-	-	-	-	-	-	-	-
2M+K	1544.1739	-	-	-	-	-	-	-	-
2M+ACN+H	1547.2445	-	-	-	-	-	-	-	-
2M+ACN+Na	1569.2265	-	-	-	-	-	-	-	-
M-3H	249.8612	-	-	-	-	-	-	2.64E+04	5.95
M-2H	375.2954	8.65E+05	2.49	-	-	-	-	8.67E+05	4.91
M-H_2O-H	733.5870	-	-	-	-	-	-	7.00E+03	3.65
M-H	751.5981	-	-	-	-	4.94E+04	11.14	2.45E+05	8.92
M+Na-2H	773.5800	4.30E+04	13.31	3.51E+05	8.94	-	-	-	-
M+Cl	787.5748	1.46E+08	9	1.66E+08	9.01	9.90E+07	8.99	1.34E+08	8.98
M+K-2H	789.5540	-	-	-	-	-	-	-	-
M+FA-H	797.6036	3.90E+07	9	4.74E+07	8.99	2.18E+07	8.99	3.52E+07	8.98
M+Hac-H	811.6192	3.59E+09	8.99	4.48E+09	8.98	1.87E+09	8.99	3.28E+09	8.98
M+Br	831.5242	-	-	7.81E+04	9.26	-	-	7.28E+04	9.22
M+TFA-H	865.5909	2.81E+04	6.4	-	-	-	-	-	-
2M-H	1504.2034	-	-	-	-	-	-	-	-
2M+FA-H	1550.2089	-	-	-	-	-	-	-	-
2M+Hac-H	1564.2246	-	-	-	-	-	-	-	-
3M-H	2258.8233	-	-	-	-	-	-	-	-

15:0-18:1(d7) PE ($C_{38}H_{67}D_7NO_8P$)									
M+3H	237.8601	-	-	-	-	-	-	-	-
M+2H+Na	245.1874	1.80E+07	15.95	6.06E+06	13.68	1.78E+07	14.93	4.88E+06	14.06
M+H+2Na	252.6190	-	-	-	-	-	-	-	-
M+3Na	259.8420	-	-	-	-	-	-	-	-
M+2H	356.2865	4.71E+06	6.11	7.39E+06	5.82	6.79E+06	6.06	5.77E+06	6.06
M+H+NH_4	364.7998	-	-	-	-	1.52E+04	16.58	-	-
M+H+Na	367.2774	-	-	-	-	-	-	-	-
M+H+K	375.2644	-	-	-	-	-	-	-	-
M+ACN+2H	376.7998	-	-	-	-	-	-	-	-
M+2Na	378.2684	6.54E+05	13.12	1.51E+06	13.5	9.71E+05	14.95	3.60E+05	16.77
M+2ACN+2H	397.3130	-	-	7.19E+04	8.74	-	-	8.55E+04	9.59
M+3ACN+2H	417.8263	-	-	-	-	-	-	-	-
M-H_2O+H	693.5551	-	-	-	-	-	-	-	-
M+H	711.5657	4.85E+08	9.05	6.49E+08	9.04	2.62E+08	9.03	4.63E+08	9.05
M+NH_4	728.5922	3.65E+05	7.67	1.79E+05	8.12	4.19E+05	7.78	4.22E+05	7.8
M+Na	733.5476	3.58E+07	9.05	4.59E+07	9.06	2.51E+07	9.05	3.71E+07	9.06
M+CH_3OH+H	743.5919	-	-	-	-	-	-	-	-
M+K	749.5216	7.76E+05	9.11	9.07E+05	9.08	7.07E+05	9.05	1.20E+06	9.06
M+ACN+H	752.5922	-	-	9.52E+04	8.78	-	-	8.51E+04	7.93
M+2Na-H	755.5296	5.92E+05	6.28	6.38E+05	6.17	5.28E+05	6.34	1.56E+06	6.25
M+IsoProp+H	771.6237	-	-	1.48E+05	9.1	-	-	-	-
M+ACN+Na	774.5742	-	-	-	-	-	-	-	-
M+2K+H	787.4774	-	-	-	-	-	-	-	-
M+DMSO+H	789.5796	-	-	1.53E+04	6	-	-	-	-
M+2ACN+H	793.6188	-	-	-	-	-	-	-	-
M+IsoProp+Na+H	794.6135	-	-	-	-	5.03E+05	9.47	1.53E+05	9.35
2M+H	1422.1241	1.51E+06	9.05	7.03E+06	9.04	2.41E+05	9.01	2.38E+06	9.05
2M+NH_4	1439.1506	-	-	-	-	-	-	-	-
2M+Na	1444.1060	-	-	1.93E+05	9.15	2.59E+04	18.87	1.16E+05	9.12
2M+3H_2O+2H	1449.1399	8.83E+03	0.26	3.40E+04	14.87	-	-	-	-
2M+K	1460.0800	-	-	-	-	-	-	-	-
2M+ACN+H	1463.1506	-	-	-	-	7.92E+03	19.81	-	-
2M+ACN+Na	1485.1326	-	-	9.62E+03	3.35	8.14E+03	19.59	-	-
M-3H	235.8455	-	-	-	-	-	-	-	-
M-2H	354.2719	-	-	-	-	3.49E+05	8.51	1.43E+05	5.95
M-H_2O-H	691.5400	-	-	-	-	-	-	-	-
M-H	709.5511	3.25E+08	9.04	4.90E+08	9.03	1.52E+08	9.04	3.20E+08	9.04
M+Na-2H	731.5331	5.87E+04	12.19	6.65E+04	16.78	6.96E+04	15.81	-	-
M+Cl	745.5278	-	-	-	-	-	-	-	-
M+K-2H	747.5070	3.75E+06	7.03	3.72E+06	7.04	8.63E+06	7.1	8.94E+06	7.08
M+FA-H	755.5566	-	-	-	-	-	-	-	-
M+Hac-H	769.5723	-	-	-	-	-	-	-	-
M+Br	789.4773	-	-	-	-	-	-	-	-
M+TFA-H	823.5440	-	-	-	-	-	-	-	-
2M-H	1420.1095	1.96E+05	9.02	1.43E+06	9.03	-	-	6.95E+05	9.04
2M+FA-H	1466.1150	-	-	2.17E+04	18.76	-	-	-	-
2M+Hac-H	1480.1307	-	-	-	-	-	-	-	-
3M-H	2132.6825	-	-	-	-	-	-	-	-
15:0-18:1(d7) PG (Na Salt) ($C_{39}H_{67}D_7NaO_{10}P$)									
M+3H	248.1916	-	-	-	-	-	-	-	-
M+2H+Na	255.5189	-	-	-	-	-	-	-	-
M+H+2Na	262.9505	-	-	-	-	-	-	-	-
M+3Na	270.1735	-	-	-	-	-	-	-	-
M+2H	371.7838	-	-	-	-	-	-	-	-
M+H+NH_4	380.2970	1.24E+04	2.21	1.26E+04	3.31	4.33E+04	5.48	9.33E+03	4.13
M+H+Na	382.7747	-	-	-	-	-	-	-	-
M+H+K	390.7617	-	-	8.41E+03	3.78	-	-	-	-
M+ACN+2H	392.2970	-	-	-	-	6.22E+03	3.48	3.16E+04	14.56
M+2Na	393.7657	-	-	-	-	-	-	-	-
M+2ACN+2H	412.8103	-	-	-	-	1.02E+04	5.15	-	-
M+3ACN+2H	433.3236	-	-	-	-	-	-	-	-
M-H_2O+H	724.5497	6.26E+04	8.71	1.23E+05	8.65	-	-	1.40E+05	8.65
M+H	742.5603	1.28E+08	8.67	1.69E+08	8.67	4.86E+07	8.65	1.17E+08	8.67
M+NH_4	759.5868	1.48E+09	8.67	1.90E+09	8.67	5.90E+08	8.65	1.32E+09	8.67
M+Na	764.5422	1.53E+08	8.67	1.69E+08	8.67	8.41E+07	8.65	1.46E+08	8.67
M+CH_3OH+H	774.5865	6.87E+07	8.99	7.63E+07	9.04	5.23E+07	8.99	6.90E+07	9.01

M+K	780.5161	-	-	-	-	-	-	-	-
M+ACN+H	783.5868	-	-	-	-	-	-	-	-
M+2Na-H	786.5241	1.02E+07	8.69	9.86E+06	8.7	9.87E+06	8.67	1.12E+07	8.67
M+IsoProp+H	802.6183	6.84E+06	8.67	1.94E+07	8.67	1.04E+06	8.67	5.52E+06	8.67
M+ACN+Na	805.5688	-	-	-	-	-	-	-	-
M+2K+H	818.4720	-	-	-	-	-	-	3.74E+05	6.21
M+DMSO+H	820.5742	-	-	-	-	-	-	-	-
M+2ACN+H	824.6134	-	-	-	-	-	-	-	-
M+IsoProp+Na+H	825.6081	-	-	-	-	1.43E+04	7.05	-	-
2M+H	1484.1132	5.10E+06	8.67	9.21E+06	8.67	7.54E+05	8.65	4.96E+06	8.67
2M+NH_4	1501.1398	-	-	-	-	-	-	-	-
2M+Na	1506.0952	-	-	-	-	-	-	-	-
2M+3H_2O+2H	1511.1291	-	-	-	-	-	-	-	-
2M+K	1522.0691	-	-	-	-	-	-	-	-
2M+ACN+H	1525.1398	-	-	-	-	-	-	-	-
2M+ACN+Na	1547.1217	-	-	-	-	-	-	-	-
M-3H	246.1771	-	-	-	-	-	-	-	-
M-2H	369.7692	-	-	-	-	-	-	-	-
M-H_2O-H	722.5346	-	-	-	-	-	-	-	-
M-H	740.5457	1.89E+09	8.67	2.88E+09	8.66	7.76E+08	8.66	1.66E+09	8.66
M+Na-2H	762.5277	-	-	1.35E+04	4.47	-	-	-	-
M+Cl	776.5224	1.05E+05	9.1	1.06E+05	8.69	-	-	7.59E+04	9.13
M+K-2H	778.5016	-	-	-	-	-	-	-	-
M+FA-H	786.5512	-	-	-	-	-	-	-	-
M+Hac-H	800.5668	-	-	-	-	-	-	-	-
M+Br	820.4719	-	-	-	-	-	-	-	-
M+TFA-H	854.5386	-	-	-	-	-	-	-	-
2M-H	1482.0987	1.61E+07	8.67	3.29E+07	8.66	2.99E+06	8.66	1.15E+07	8.66
2M+FA-H	1528.1042	-	-	-	-	-	-	-	-
2M+Hac-H	1542.1198	-	-	-	-	-	-	-	-
3M-H	2225.6662	-	-	-	-	-	-	-	-
15:0-18:1(d7) PI (NH4 Salt) ($C_{42}H_{75}D_7NO_{13}P$)									
M+3H	277.5303	-	-	-	-	-	-	-	-
M+2H+Na	284.8576	-	-	-	-	-	-	-	-
M+H+2Na	292.2892	-	-	-	-	-	-	-	-
M+3Na	299.5122	-	-	-	-	-	-	-	-
M+2H	415.7918	-	-	-	-	-	-	-	-
M+H+NH_4	424.3051	7.14E+05	5.99	5.54E+05	6.04	2.78E+05	7.61	2.06E+05	7.63
M+H+Na	426.7828	-	-	-	-	-	-	-	-
M+H+K	434.7697	-	-	-	-	-	-	-	-
M+ACN+2H	436.3051	2.41E+05	5.27	7.90E+04	4.85	6.85E+04	4.4	5.84E+04	5.12
M+2Na	437.7737	-	-	-	-	-	-	-	-
M+2ACN+2H	456.8183	-	-	-	-	-	-	-	-
M+3ACN+2H	477.3316	2.02E+05	7.86	7.50E+05	7.85	3.59E+05	7.89	2.12E+05	7.97
M-H_2O+H	812.5657	6.68E+06	5.61	1.54E+07	5.6	4.45E+06	8.82	5.87E+06	8.84
M+H	830.5763	3.78E+07	8.58	5.39E+07	8.57	8.77E+06	8.58	2.44E+07	8.58
M+NH_4	847.6029	2.68E+08	8.58	3.72E+08	8.57	6.43E+07	8.58	1.68E+08	8.58
M+Na	852.5582	4.39E+07	8.58	5.33E+07	8.57	1.30E+07	8.58	3.04E+07	8.58
M+CH_3OH+H	862.6025	8.30E+03	1.48	8.27E+03	4.15	-	-	-	-
M+K	868.5322	1.72E+05	8.69	2.85E+05	8.72	7.61E+04	8.71	3.68E+05	8.74
M+ACN+H	871.6029	2.90E+04	8.24	1.72E+05	8.19	6.89E+04	9.58	8.46E+04	8.14
M+2Na-H	874.5402	4.66E+06	8.58	4.82E+06	8.57	1.81E+06	8.56	3.64E+06	8.58
M+IsoProp+H	890.6344	2.21E+04	6.41	-	-	4.17E+04	6.32	-	-
M+ACN+Na	893.5848	7.87E+05	8.18	1.06E+06	8.19	1.43E+06	8.22	1.17E+06	8.16
M+2K+H	906.4881	-	-	-	-	-	-	1.36E+04	18.73
M+DMSO+H	908.5902	-	-	8.30E+03	4.25	2.95E+04	13.07	-	-
M+2ACN+H	912.6294	3.95E+04	5.78	3.48E+04	13.64	-	-	1.95E+04	13.68
M+IsoProp+Na+H	913.6241	1.52E+04	4.44	1.61E+04	4.77	1.56E+04	7.05	2.53E+04	5.5
2M+H	1660.1453	-	-	-	-	-	-	-	-
2M+NH_4	1677.1719	-	-	-	-	-	-	-	-
2M+Na	1682.1273	-	-	-	-	-	-	-	-
2M+3H_2O+2H	1687.1612	-	-	-	-	-	-	-	-
2M+K	1698.1012	-	-	-	-	-	-	-	-
2M+ACN+H	1701.1719	-	-	-	-	-	-	-	-
2M+ACN+Na	1723.1538	-	-	-	-	-	-	-	-
M-3H	275.5157	-	-	-	-	-	-	-	-
M-2H	413.7772	-	-	-	-	-	-	-	-

M-H_2O-H	810.5506	4.45E+04	18.38	-	-	5.28E+04	17.49	-	-
M-H	828.5618	3.83E+08	8.57	6.08E+08	8.56	9.54E+07	8.57	2.51E+08	8.57
M+Na-2H	850.5437	-	-	-	-	5.95E+04	8.68	-	-
M+Cl	864.5384	-	-	-	-	-	-	8.63E+03	2.83
M+K-2H	866.5176	-	-	-	-	-	-	-	-
M+FA-H	874.5672	-	-	-	-	5.60E+04	14.01	-	-
M+Hac-H	888.5829	-	-	-	-	-	-	-	-
M+Br	908.4879	-	-	-	-	-	-	-	-
M+TFA-H	942.5546	-	-	2.66E+04	8.24	-	-	-	-
2M-H	1658.1308	-	-	-	-	-	-	-	-
2M+FA-H	1704.1363	-	-	-	-	-	-	-	-
2M+Hac-H	1718.1519	-	-	-	-	-	-	-	-
3M-H	2489.7144	-	-	-	-	-	-	-	-
15:0-18:1(d7) PS (Na Salt) ($C_{39}H_{66}D_7NNaO_{10}P$)									
M+3H	252.5234	-	-	-	-	-	-	-	-
M+2H+Na	259.8507	-	-	-	-	-	-	-	-
M+H+2Na	267.2823	-	-	-	-	-	-	-	-
M+3Na	274.5053	-	-	-	-	-	-	-	-
M+2H	378.2814	-	-	-	-	9.90E+03	2.47	9.85E+03	18.54
M+H+NH_4	386.7947	-	-	-	-	-	-	-	-
M+H+Na	389.2724	5.77E+04	9.82	4.88E+04	5.06	1.60E+04	0.79	1.76E+04	3.11
M+H+K	397.2593	7.59E+05	13.44	9.14E+05	12.96	3.27E+05	13.29	7.40E+05	8.44
M+ACN+2H	398.7947	-	-	-	-	-	-	-	-
M+2Na	400.2633	-	-	-	-	-	-	-	-
M+2ACN+2H	419.3079	-	-	-	-	-	-	-	-
M+3ACN+2H	439.8212	-	-	-	-	-	-	-	-
M-H_2O+H	737.5449	1.34E+06	9.39	9.34E+05	9.4	1.66E+07	9.41	1.58E+07	9.4
M+H	755.5555	5.90E+07	8.77	1.29E+08	8.76	1.87E+07	8.81	7.26E+07	8.76
M+NH_4	772.5821	1.26E+08	8.98	1.43E+08	8.99	8.56E+07	8.98	1.27E+08	8.99
M+Na	777.5375	6.28E+06	8.77	1.14E+07	8.76	2.76E+06	8.82	8.45E+06	8.76
M+CH_3OH+H	787.5817	-	-	-	-	1.35E+05	12.23	7.67E+04	12.22
M+K	793.5114	1.45E+05	9.15	9.11E+04	9.19	2.86E+04	10.65	1.45E+05	9.61
M+ACN+H	796.5821	-	-	8.02E+03	0.32	-	-	-	-
M+2Na-H	799.5194	1.67E+05	9.35	6.56E+05	8.76	7.15E+04	8.73	5.31E+05	8.74
M+IsoProp+H	815.6136	-	-	-	-	-	-	-	-
M+ACN+Na	818.5640	-	-	2.19E+04	12.99	-	-	-	-
M+2K+H	831.4673	4.26E+05	9.97	2.31E+06	9.91	7.59E+05	9.88	3.38E+06	9.89
M+DMSO+H	833.5695	-	-	-	-	-	-	1.80E+04	6.86
M+2ACN+H	837.6086	6.19E+05	8.94	1.96E+05	9.17	-	-	7.36E+03	0.46
M+IsoProp+Na+H	838.6033	-	-	-	-	-	-	-	-
2M+H	1510.1037	-	-	-	-	-	-	-	-
2M+NH_4	1527.1303	-	-	-	-	-	-	-	-
2M+Na	1532.0857	-	-	-	-	-	-	-	-
2M+3H_2O+2H	1537.1196	-	-	-	-	-	-	-	-
2M+K	1548.0596	-	-	-	-	-	-	-	-
2M+ACN+H	1551.1303	-	-	-	-	-	-	-	-
2M+ACN+Na	1573.1122	-	-	-	-	-	-	-	-
M-3H	250.5088	-	-	-	-	-	-	-	-
M-2H	376.2668	-	-	-	-	-	-	-	-
M-H_2O-H	735.5298	-	-	1.29E+04	4.82	-	-	-	-
M-H	753.5410	7.65E+07	8.76	1.69E+08	8.73	2.37E+07	8.82	8.12E+07	8.75
M+Na-2H	775.5229	3.82E+06	8.76	7.55E+06	8.73	1.33E+06	8.83	4.84E+06	8.75
M+Cl	789.5176	-	-	5.30E+04	10.67	7.78E+03	2.12	8.04E+04	8.92
M+K-2H	791.4968	5.18E+04	9.47	1.04E+05	9.26	-	-	-	-
M+FA-H	799.5464	-	-	-	-	-	-	1.21E+04	19.11
M+Hac-H	813.5621	-	-	-	-	-	-	5.11E+04	18.09
M+Br	833.4671	-	-	-	-	-	-	-	-
M+TFA-H	867.5338	-	-	-	-	7.24E+04	8.99	-	-
2M-H	1508.0892	-	-	-	-	-	-	-	-
2M+FA-H	1554.0947	-	-	-	-	-	-	-	-
2M+Hac-H	1568.1103	-	-	-	-	-	-	-	-
3M-H	2264.6520	-	-	-	-	-	-	-	-
d18:1-18:1(d9) SM ($C_{41}H_{72}D_9N_2O_6P$)									
M+3H	246.8869	-	-	-	-	-	-	-	-
M+2H+Na	254.2142	-	-	7.44E+03	5.16	-	-	-	-
M+H+2Na	261.6458	-	-	-	-	-	-	-	-
M+3Na	268.8688	-	-	2.17E+05	10.53	-	-	-	-

M+2H	369.8267	-	-	-	-	-	-	-	-
M+H+NH_4	378.3399	1.28E+06	5.86	9.58E+05	5.43	4.27E+06	5.6	2.18E+06	5.48
M+H+Na	380.8176	-	-	-	-	-	-	-	-
M+H+K	388.8046	-	-	-	-	-	-	-	-
M+ACN+2H	390.3399	1.57E+04	5.99	-	-	8.51E+03	6.77	-	-
M+2Na	391.8086	-	-	-	-	-	-	-	-
M+2ACN+2H	410.8532	-	-	-	-	-	-	-	-
M+3ACN+2H	431.3665	4.21E+06	6.77	6.63E+04	6.73	3.08E+04	6.57	-	-
M-H_2O+H	720.6355	1.14E+05	9.41	1.10E+05	9.36	1.74E+06	9.3	1.99E+06	9.35
M+H	738.6460	4.09E+09	8.83	5.73E+09	8.82	1.59E+09	8.82	3.61E+09	8.82
M+NH_4	755.6726	-	-	-	-	-	-	-	-
M+Na	760.6280	3.77E+08	8.83	4.74E+08	8.83	1.89E+08	8.82	3.51E+08	8.82
M+CH_3OH+H	770.6723	-	-	-	-	-	-	-	-
M+K	776.6019	3.08E+07	8.83	4.18E+07	8.83	1.42E+07	8.82	2.74E+07	8.82
M+ACN+H	779.6726	-	-	-	-	-	-	-	-
M+2Na-H	782.6099	-	-	-	-	-	-	-	-
M+IsoProp+H	798.7041	2.93E+07	8.83	4.82E+07	8.82	8.39E+06	8.82	2.69E+07	8.82
M+ACN+Na	801.6545	1.17E+04	4.15	2.05E+05	0.55	-	-	1.42E+04	4.87
M+2K+H	814.5578	-	-	-	-	-	-	-	-
M+DMSO+H	816.6600	-	-	-	-	-	-	-	-
M+2ACN+H	820.6991	-	-	-	-	-	-	6.18E+04	10.84
M+IsoProp+Na+H	821.6939	-	-	-	-	-	-	-	-
2M+H	1476.2848	1.90E+07	8.83	4.61E+07	8.82	1.75E+06	8.82	1.41E+07	8.82
2M+NH_4	1493.3114	-	-	1.10E+05	10.66	3.57E+04	18.85	-	-
2M+Na	1498.2668	9.98E+04	8.81	-	-	-	-	5.46E+05	8.8
2M+3H_2O+2H	1503.3007	-	-	-	-	-	-	-	-
2M+K	1514.2407	-	-	-	-	-	-	-	-
2M+ACN+H	1517.3114	-	-	-	-	-	-	-	-
2M+ACN+Na	1539.2933	-	-	-	-	-	-	-	-
M-3H	244.8723	-	-	-	-	-	-	-	-
M-2H	367.8121	-	-	-	-	-	-	-	-
M-H_2O-H	718.6204	4.64E+04	13.96	-	-	-	-	-	-
M-H	736.6315	-	-	-	-	-	-	-	-
M+Na-2H	758.6134	5.11E+04	8.74	-	-	5.11E+05	8.68	8.26E+04	8.68
M+Cl	772.6082	6.17E+07	8.84	8.04E+07	8.83	3.39E+07	8.82	5.23E+07	8.83
M+K-2H	774.5874	-	-	4.92E+04	10.31	-	-	-	-
M+FA-H	782.6370	1.36E+07	8.84	2.04E+07	8.83	5.63E+06	8.82	1.29E+07	8.83
M+Hac-H	796.6526	1.08E+09	8.84	1.51E+09	8.83	4.64E+08	8.82	9.51E+08	8.83
M+Br	816.5577	-	-	-	-	-	-	-	-
M+TFA-H	850.6244	-	-	-	-	-	-	-	-
2M-H	1474.2703	4.34E+06	10.78	1.55E+06	10.77	-	-	3.43E+06	10.71
2M+FA-H	1520.2757	-	-	-	-	-	-	-	-
2M+Hac-H	1534.2914	-	-	-	-	-	-	-	-
3M-H	2213.9236	-	-	-	-	-	-	-	-
15:0-18:1(d7)-15:0 TAG ($C_{51}H_{89}D_7O_6$)									
M+3H	271.5952	-	-	-	-	-	-	-	-
M+2H+Na	278.9225	-	-	-	-	-	-	-	-
M+H+2Na	286.3542	-	-	-	-	-	-	-	-
M+3Na	293.5772	-	-	-	-	-	-	-	-
M+2H	406.8892	-	-	-	-	-	-	-	-
M+H+NH_4	415.4025	-	-	-	-	-	-	-	-
M+H+Na	417.8802	-	-	-	-	-	-	-	-
M+H+K	425.8672	-	-	-	-	-	-	-	-
M+ACN+2H	427.4025	-	-	1.44E+04	6.99	-	-	-	-
M+2Na	428.8712	-	-	-	-	-	-	-	-
M+2ACN+2H	447.9158	-	-	-	-	-	-	-	-
M+3ACN+2H	468.4290	-	-	-	-	-	-	-	-
M-H_2O+H	794.7606	-	-	-	-	-	-	-	-
M+H	812.7712	2.71E+06	13.15	4.22E+06	13.2	6.54E+05	13.14	2.87E+06	13.17
M+NH_4	829.7977	5.77E+09	13.17	8.61E+09	13.16	2.10E+09	13.16	4.59E+09	13.17
M+Na	834.7531	9.95E+08	13.17	1.26E+09	13.16	5.21E+08	13.16	8.90E+08	13.17
M+CH_3OH+H	844.7974	-	-	-	-	-	-	-	-
M+K	850.7270	1.97E+08	13.17	2.53E+08	13.16	1.12E+08	13.16	1.74E+08	13.17
M+ACN+H	853.7977	2.10E+05	15.05	-	-	8.51E+04	14.97	-	-
M+2Na-H	856.7350	3.23E+04	0.59	2.02E+04	17.38	-	-	1.22E+04	18.85
M+IsoProp+H	872.8292	2.75E+08	13.17	3.54E+08	13.16	1.42E+08	13.16	2.33E+08	13.17
M+ACN+Na	875.7796	1.51E+05	12.98	-	-	1.01E+06	13.01	1.16E+06	12.98

M+2K+H	888.6829	1.38E+04	18.73	-	-	-	-	-	-
M+DMSO+H	890.7851	-	-	1.24E+04	2.75	-	-	-	-
M+2ACN+H	894.8242	-	-	-	-	7.25E+04	15.08	2.30E+04	15.05
M+IsoProp+Na+H	895.8190	-	-	-	-	-	-	-	-
2M+H	1624.5350	-	-	-	-	-	-	-	-
2M+NH_4	1641.5616	-	-	-	-	-	-	-	-
2M+Na	1646.5170	-	-	-	-	-	-	-	-
2M+3H_2O+2H	1651.5509	-	-	-	-	-	-	-	-
2M+K	1662.4909	-	-	-	-	-	-	-	-
2M+ACN+H	1665.5616	-	-	-	-	-	-	-	-
2M+ACN+Na	1687.5435	-	-	-	-	-	-	-	-
M-3H	269.5807	-	-	-	-	-	-	-	-
M-2H	404.8747	-	-	-	-	-	-	-	-
M-H_2O-H	792.7455	-	-	-	-	7.36E+04	12.16	-	-
M-H	810.7566	9.45E+05	11.78	2.06E+05	11.77	8.29E+05	11.76	1.50E+06	11.77
M+Na-2H	832.7385	7.87E+03	1.81	1.13E+04	0.91	9.79E+03	3.55	-	-
M+Cl	846.7333	2.76E+05	13.16	1.05E+06	13.14	-	-	4.94E+04	13.18
M+K-2H	848.7125	-	-	9.07E+03	3.42	-	-	-	-
M+FA-H	856.7621	-	-	-	-	4.56E+04	9.72	5.97E+04	9.73
M+Hac-H	870.7777	7.64E+03	2.94	-	-	-	-	-	-
M+Br	890.6828	-	-	-	-	8.80E+03	0.43	-	-
M+TFA-H	924.7495	-	-	-	-	1.65E+04	0.62	7.70E+03	0.95
2M-H	1622.5205	-	-	-	-	-	-	-	-
2M+FA-H	1668.5260	-	-	-	-	-	-	-	-
2M+Hac-H	1682.5416	-	-	-	-	-	-	-	-
3M-H	2436.2989	-	-	-	-	-	-	-	-

Table A.4: Number of identified lipid ions by LipidSearch™ in samples extracted from patient # 1 analysed with and without ^{13}C-IS mixture.

Sample	Number of identified lipid ions	
	Samples extracted without ^{13}C-IS	**Samples extracted with ^{13}C-IS**
2.1A	300	173
2.1B	314	188
2.1C	274	166
2.1D	358	290
2.1E	347	260
2.2A	299	202
2.2B	246	138
2.2C	314	206
2.2D	345	228
2.2E	300	201
2.3A	281	166
2.3B	297	187
2.3C	339	196
2.3D	293	186
2.3E	329	212
2.4A	330	244
2.4B	349	250
2.4C	383	277
2.4D	298	207
2.4E	342	243
Average	**317**	211

Table A.5: Number of identified lipid ions by LipidSearch™ in control plasma samples (healthy subjects before and after OGTT) extracted and analysed with and without ^{13}C-IS mixture.

Patients codes	**Number of identified lipid ions**	
	Samples extracted without ^{13}C-IS	**Samples extracted with ^{13}C-IS**
RA2D43 Pre OGTT	307	200
RA2D43 Post OGTT	287	203
RJYPFA Pre OGTT	214	158
RJYPFA Post OGTT	257	158
6PD4YF Pre OGTT	289	208
6PD4YF Post OGTT	285	207
NQ2A3R Pre OGTT	273	166
NQ2A3R Post OGTT	270	184
56PG2N Pre OGTT	321	218
56PG2N Post OGTT	291	221
NF5783 Pre OGTT	261	167
NF5783 Post OGTT	259	167
P258CP Pre OGTT	269	197
P258CP Post OGTT	284	186
TKPGBX Pre OGTT	275	183
TKPGBX Post OGTT	266	186
VJXH3W Pre OGTT	268	179
VJXH3W Post OGTT	274	182
Average	**275**	**187**

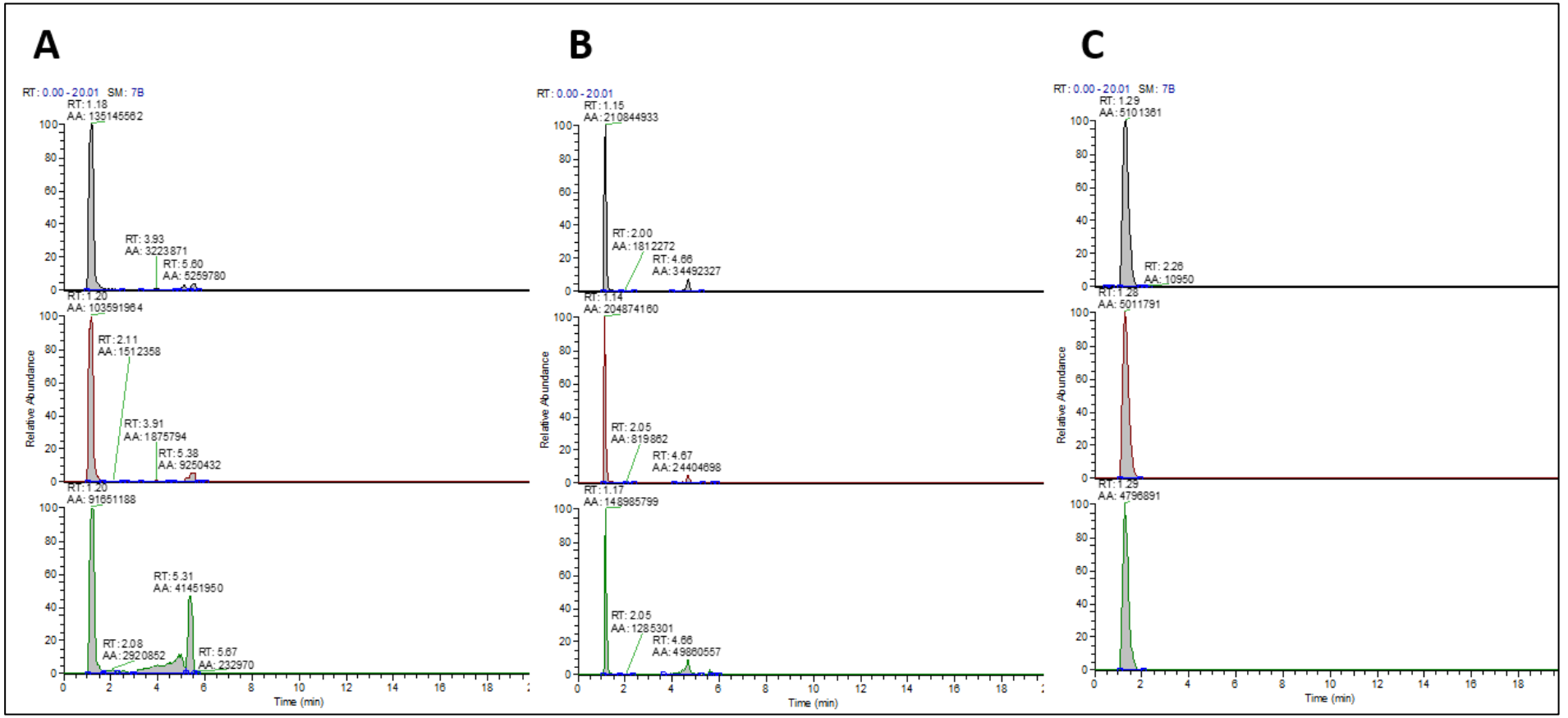

Figure A.1: The effect of chloroform on the detection of A) LPC(18:3)+H (*m/z* 518.3241), B) LPC(20:4)+H (*m/z* 544.3397) putatively identified by LipidSearch™ in positive mode in three replicates of plasma extract and C) represents the chloroform peak detected in negative mode (*m/z* 116.9071).

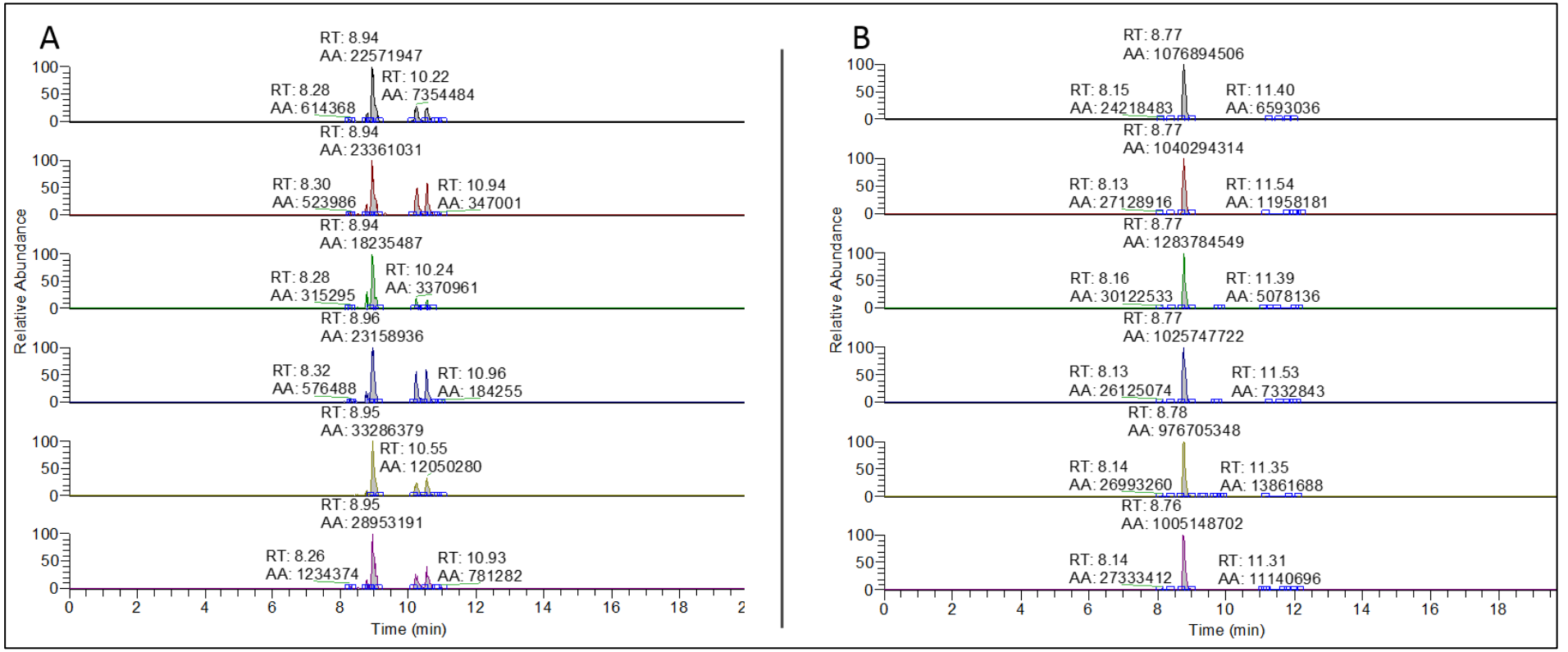

Figure A.2: Extracted ion chromatogram of A) unlabelled form detected at *m/z* of 740.5236, B) labelled matched form detected at *m/z* of 781.6589 of PE(16:0/20:4)+H detected in mice plasma samples extracted in the presence of ^{13}C-IS

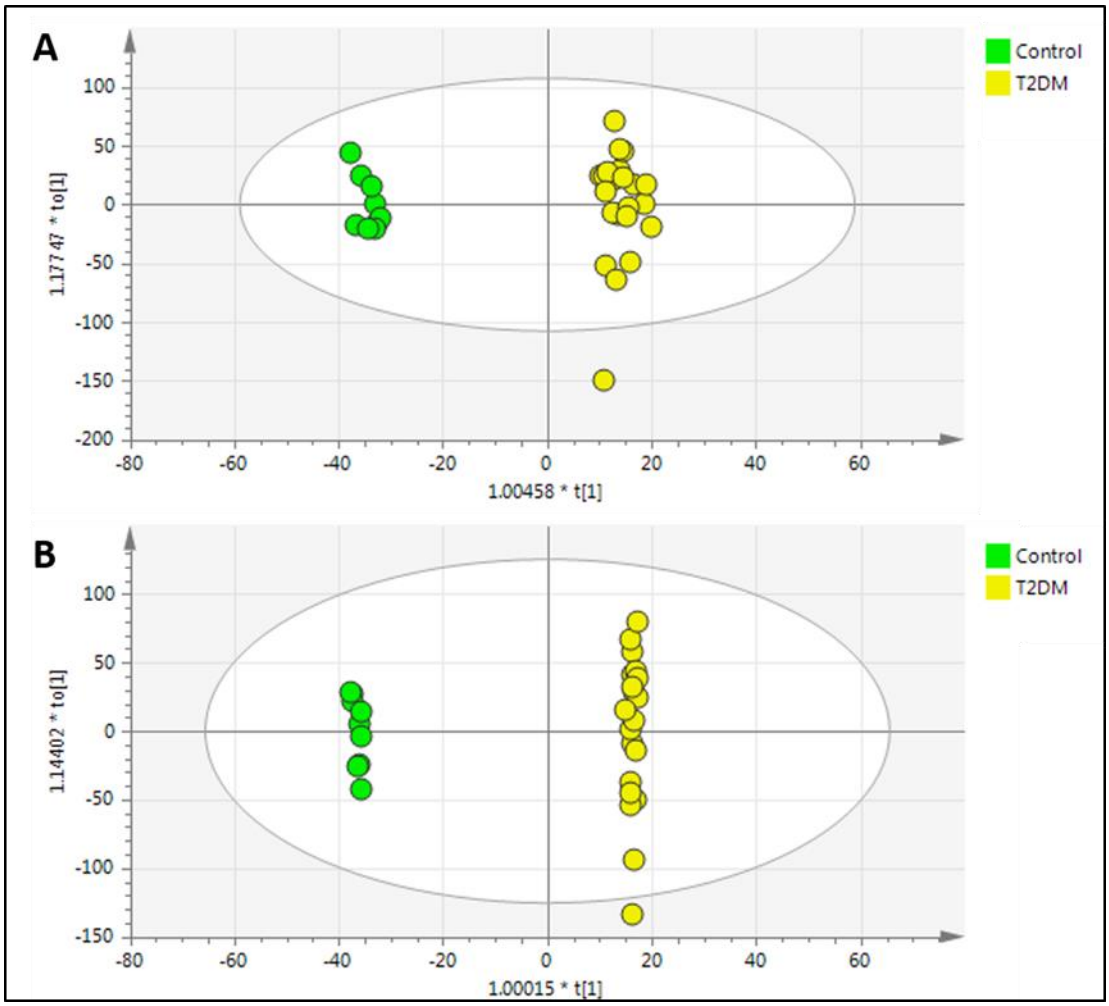

Figure A.3: Multivariate analysis of untargeted lipidomics profile of control group (*n*=9) vs patients diagnosed with T2DM (*n*=22) based on A) fasting plasma level using supervised OPLS-DA score plot with R^2X= 0.311, R^2Y=0.987 and Q^2=0.281, B) 2h after OGTT using supervised OPLS-DA score plots with R^2X= 0.471, R^2Y=0.999 and Q^2=0.382.

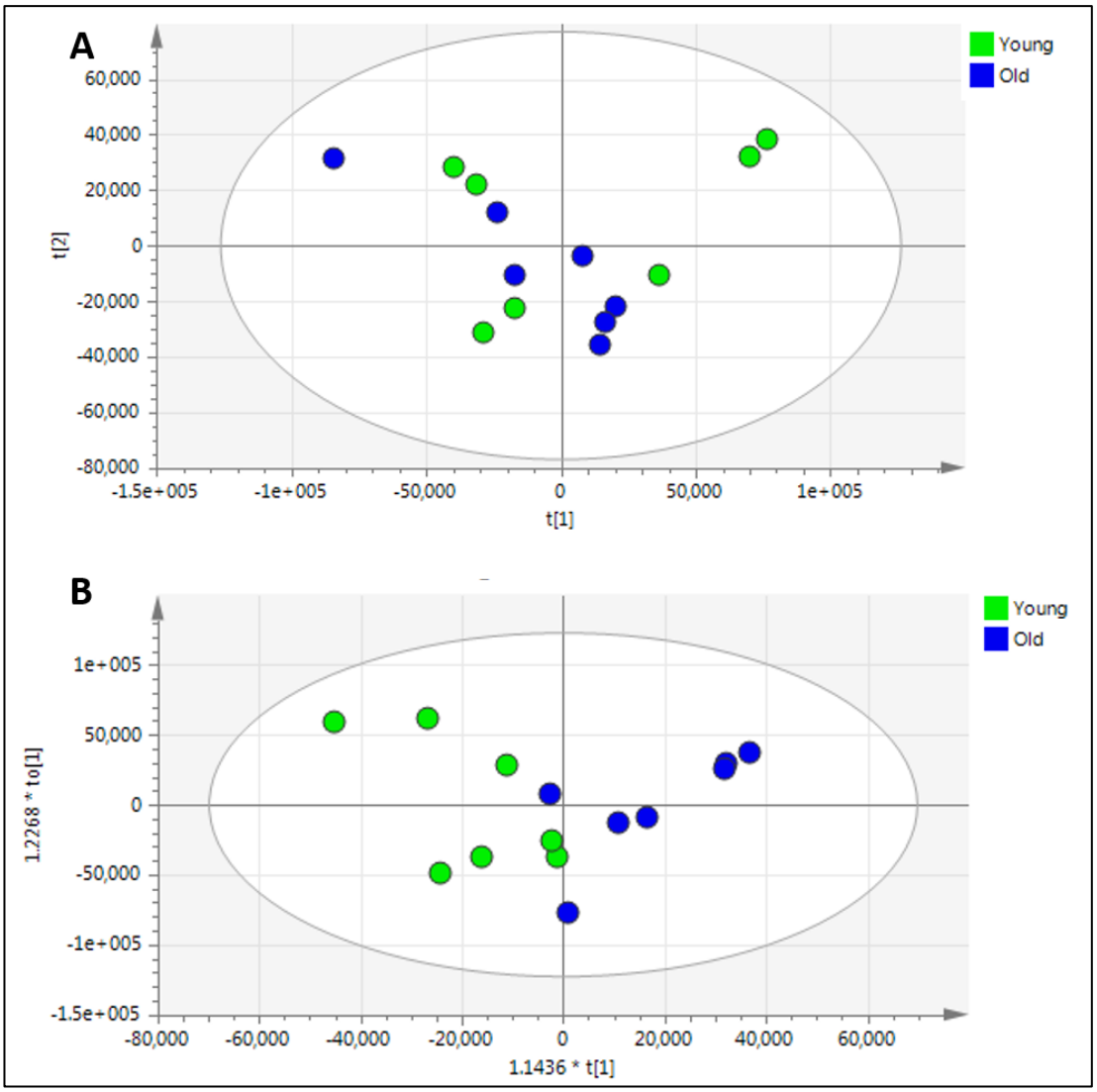

Figure A.4: Multivariate analysis of untargeted lipidomics profile of young T2DM patients (<50 years old, *n*=7) vs old T2DM patients (>70 years old, *n*=7) based on fasting plasma level using A) unsupervised PCA score plot with R^2= 0.608 and Q^2=0.408, B) supervised OPLS-DA score plots with R^2X= 0.556, R^2Y=0.609 and Q^2=-0.134.